COAL SEAM GAS ASSOCIATIONS IN THE HUNTLY, OHAI AND GREYMOUTH REGIONS, NEW ZEALAND.

A thesis submitted in partial fulfillment of the requirements
for the degree of
Master of Science in geology
at the University of Canterbury
by

Caroline I Butland

Department of Geological Sciences,
University of Canterbury, Christchurch, New Zealand

June 2006

Frontispiece

Mangapiko (Waikato Basin) at dawn

Nothing in life is worthy of great anxiety

Plato

Abstract

Coal seam gas has been recognised as a new, potential energy resource in New Zealand. Exploration and assessment programmes carried out by various companies have evaluated the resource and indicated that this unconventional gas may form a part of New Zealand's future energy supply. This study has delineated some of the controls between coal properties and gas content in coal seams in selected New Zealand locations.

Four coal cores, one from Huntly (Eocene), two from Ohai (Cretaceous) and one from Greymouth (Cretaceous), have been sampled and analysed in terms of gas content and coal properties. Methods used include proximate, sulphur and calorifc value analyses; ash constituent determination; rank assessment; macroscopic analysis; mineralogical analysis; maceral analysis; and gas analyses (desorption, adsorption, gas quality and gas isotopes).

Coal cores varied in rank from sub-bituminous B-A (Huntly); sub-bituminous C-A (Ohai); and high volatile bituminous A (Greymouth). All locations contained high vitrinite content (~85 %) with overall relatively low mineral matter observed in most samples. Mineral matter consisted of both detrital grains (quartz in matrix material) and infilling pores and fractures (clays in fusinite pores; carbonates in fractures). Average gas contents were 1.6 m^3/t in the Huntly core, 4.7 m^3/t in the Ohai cores, and 2.35 m^3/t in the Greymouth core. The Ohai core contained more gas and was more saturated than the other cores. Carbon isotopes indicated that the Ohai gas composition was more mature, containing heavier ^{13}C isotopes than either the Huntly or Greymouth gas samples. This indicates the gas was derived from a mixed biogenic and thermogenic source. The Huntly and Greymouth gases appear to be derived from a biogenic (by CO_2 reduction) source.

The ash yield proved to be the dominant control on gas volume in all locations when the ash yield was above 10 %. Below 10 % the amount of gas variation is unrelated to ash yield. Although organic content had some influence on gas volume, associations were basin and /or rank dependant. In the Huntly core total gas content and structured vitrinite increased together. Although this relationship did not appear in the other cores, in the Ohai SC3 core lost gas and fusinite are associated with each other, while desmocollinite (unstructured vitrinite) correlated positively with residual gas in the Greymouth core. Although it is generally accepted that higher rank coals will have higher adsorption capacities, this was not seen in this data set. Although the lowest rank coal (Huntly) contains the lowest adsorption capacity, the highest adsorption capacity was not seen in the highest rank coal (Greymouth), but in the Ohai coal instead.

The Ohai core acted like a higher rank coal with respect to the Greymouth coal, in terms of adsorption capacity, isotopic signatures and gas volume. Two hypothesis can be used to explain these results: (1) That a thermogenically derived gas migrated from down-dip of the SC3 and SC1 drill holes and saturated the section. (2) Rank measurements (e.g. proximate analyses) have a fairly wide variance in both the Greymouth and Ohai coal cores, thus it maybe feasible that the Ohai cores may be higher rank coal than the Greymouth coal core. Although the second hypothesis may explain the adsorption capacity, isotopic signatures and the gas volume, when the data is plotted on a Suggate rank curve, the Ohai coal core is clearly lower rank than the Greymouth core. Thus, pending additional data, the first hypothesis is favoured.

Table of Contents

List of Figures

Chapter Four: Gas associations

Chapter Five: Discussion

List of Tables

Acknowledgements

There are several people who deserve a mention, as without them this thesis would have been a lot harder to do.

Firstly, I would like to thank Tim Moore (Solid Energy) for coming up with such a great, new innovative line of research, and to providing HEAPS of valuable feedback, ideas and support. (And who listened to numerous anecdotes about my cat). I would also like to thank Tim for providing me with work, and more invaluably, with work experience. It was great to get out there and get dirty, and get drillers to lift heavy things for me! And to also realise that I actually like doing what I am doing! I would also like to thank Steve Weaver, my other supervisor, who was great support and encouragement.

Thanks to Solid Energy (in particular Grant Gillard and Carlos Galceran) who provided me with a job, experience, a work space and lots of printing and photocopying (more than they know!). Both Grant and Carlos were great for helping out with GIS stuff, and it was also lots of fun working with them for un-related thesis stuff too.

Thank you to Technology in New Zealand and Solid Energy for giving me a scholarship, and opportunities to gain experience, and also to Orion Energy who also gave me a research scholarship and helped keep down the student loan…a bit!

A big thank you to Jane Newman and Nick Moore (Newman Energy Research) who trained me up to do my petrography and kept me company while point counting. This thesis would not have been the same without you, and without the 'special' company of Jet, Titus and Spot. Also a big thank you to Nigel Newman (CRL Energy) who gave me lots of help regarding mineral matter, and more importantly was a life saver when dealing with the LTA.

A thank you too, to all the technicians, especially Rob Speirs who kept me company when grinding coal and was always there to lend a hand or help me find bits and pieces, and to Steven Brown for showing me how to prepare my XRD slides, and to Sacha for just having a chat. Also to Anekant for helping me with formatting problems and showing me his cat photos. And I must not forget the amazing Pat Roberts who was a whiz when dealing with all my queries and problems about scholarships and Canterprise.

Thanks to all my friends and office mates (Liv, Amy, Jo, Kim, Darryn, Andy, Carl, Miles, Francie, Tennille, Mitch, Scott, Joyce, Katie, Emma, Hamish, Sam and I hope I haven't forgotten anyone), my aikido mates (especially Kerry and Yuko) and my family (John, Corinna, Mum, Dad and Cleo the Cat, although she forgot me when I went back home) for helping me keep sane. Mum and Dad, thanks for sending me food parcels, especially the ones with chocolate in them.

The biggest thanks goes out to my husband Shawn. "THANKS." Without him this thesis would not have been as enjoyable. Thank you for helping me out with tedious lab work, and keeping me calm when I started to stress. Thank you for keeping me company while grinding copious amounts of coal, and putting up with me travelling a lot and being away a lot. Even though you were busy with your own study you always had time to help me when I needed it, even if it was just to keep me relaxed. I suppose I owe you one now! And thanks to Cian, for being what you are, a really cool cat.

Chapter One

Introduction

1.1 Introduction

The occurrence of methane in coal seams has long been known, with gas explosions first being documented in 1810 in the United States and 1845 in France (Flores, 1998). Since the late 20th Century, there has been emphasis on coal seam gas as a potential energy source. This has lead to several countries including the United States, the United Kingdom, Canada, Australia, China and India, carrying out active exploration programmes (Hayton et al., 2004). As a result of this exploration there are many basins (mainly in the United States) which are now producing significant amounts of coal seam gas (CSG). Early CSG models emphasized the importance of thermogenic gas but in the last 5 years low rank deposits have also been shown to be economically significant, most notably with the successful development of the Powder River Basin as a CSG play (Ayers, 2002).

The overseas development of CSG plays in low rank coal deposits has lead to exploration of basins of similar rank in New Zealand. Assessment of New Zealand's CSG resources began in the 1980s (Thorburn, 1983), although it faced a slow start (Manhire and Hayton, 2003). With the recent decline of gas resources in the Maui gas field (Sherwood et al., 2003), renewed activity in CSG exploration has occurred. Currently New Zealand does not have any commercially producing CSG wells but there have been a number of companies

working on exploration and research, assessing the size and nature of potential resources (Moore and Twombly, 2006; Moore and Butland, 2005; Moore et al., 2002a; Twombly et al., 2004; Cave, 2002).

The Huntly, Ohai and Greymouth basins all contain coal measures with ranks ranging from subbituminous to bituminous. Coal seams from the Huntly, Ohai and Greymouth basins contain significant amounts of CSG. These basins have had only limited amounts of research conducted in relation to their gas content, and the relationship with other geological and coal parameters (such as maceral composition, mineral matter and proximate analyses). This study will attempt to determine controls on gas variability from these selected New Zealand CSG reservoirs, as well as establish some fundamental knowledge regarding types of mineralisation in New Zealand coals, maceral composition and the relationship to gas volume.

1.2 Objective of study

The objective of this study is to determine whether organic or inorganic composition play a more important role in controlling gas variation. Thus, three sites in New Zealand have been selected (Huntly, Greymouth and Ohai).

In order to accomplish this objective, the study has three aims:

1. Characterise the organic and inorganic composition using four cores, one from each of the basins except for the Ohai coalfield from which two cores were available,
2. Correlate the organic and inorganic composition with gas content and quantity, and
3. Develop a model which explains the relative contributions organic and inorganic composition have to gas content and gas variation.

The objective will be met through a combination of different analytical methodologies. Organic composition will be assessed using an optical petrographic analysis, whereas the inorganic components will be assessed using XRF, XRD, proximate (moisture, volatile matter, ash yield, fixed carbon and calorific value) analyses as well as supporting optical petrographic analysis. Gas content will be characterised using desorption and adsorption isotherms, carbon-methane isotopes and gas composition analyses. Simple statistics will be applied to look for significant correlations and associations between these parameters.

1.3 What is coal seam gas?

1.3.1 Introduction

Coal seam gas, also known as coal seam methane, coalbed methane and coal seam natural gas, develops naturally within coal beds and associated sediments as part of the burial and coalification process. Unlike

conventional reservoirs where the gas exists in a free state in the pores between sediment grains, CSG exists in a near liquid-like state, because of the physical **sorption** process (Yee et al., 1993). During coalification hydrocarbons are released along with nitrogen, carbon dioxide and water. A significant proportion of the gas is stored by physical sorption, trapped within the coal seam or associated sediments through van der Waals forces (a weak intermolecular force), onto the organic matter in coal (Fig. 1.1).

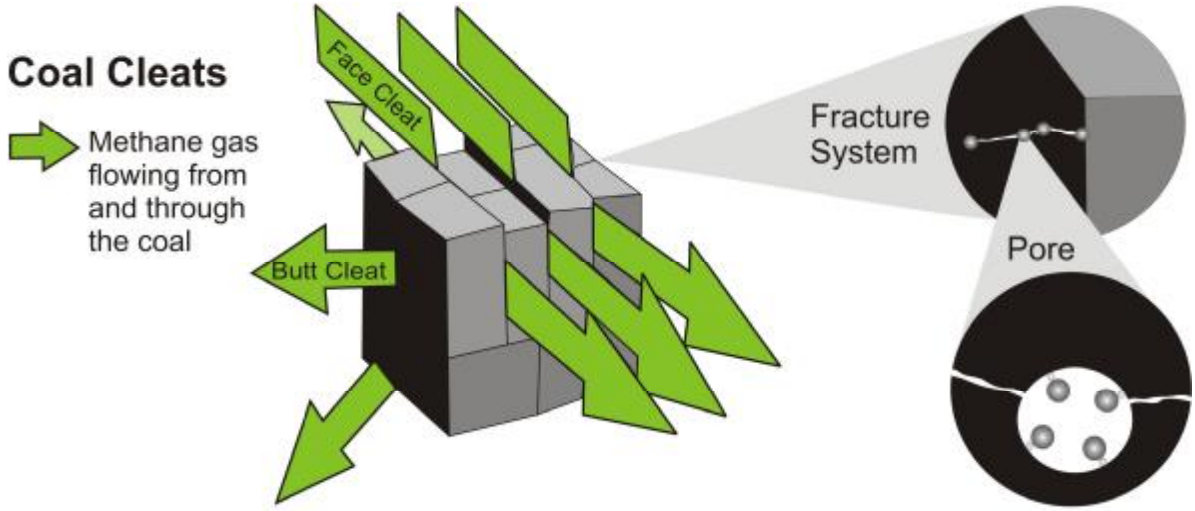

Figure 1.1: Gas in coal is mainly held in pores and cleats, with van der Waals forces.

In coal, the gas is mainly held in pores and cleats (closely spaced jointing). There have been four mechanisms proposed for the storage of gas in coal: 1) as a free gas compressed in pore spaces, 2) Condensed as a solid or liquid, 3) dissolved in the coal structure, and 4) adsorbed on the internal surfaces (Crosdale et al., 1998). Studies of gas flow show the gas in coal must diffuse through the micropore structure of the matrix, until it reaches a cleat (Gamson et al., 1996). The relationship of coal seam structure and gas flow behaviour can be demonstrated as a dual porosity model of macropores (cleats) and micropores. The gas flow through the coal can be viewed as a three-stage process (Crosdale at al., 1998, Fig. 1.2): (i) gas desorbs off the internal surfaces. This leads to (ii) gas diffusion through the coal matrix, where the gas travels through the micropores to the large pores. Unlike flow through the cleat system (stage three), which is pressure driven, flow through the matrix is concentration driven and can be modelled using Fick's law of diffusitivity. Finally (iii) free flow (Darcy's law, which groups pore size, shape, distribution and connectivity as one parameter: permeability) where gas flows through large pores out of the coal system, as a response to a pressure change. (Gamson et al., 1996; Busch et al., 2004).

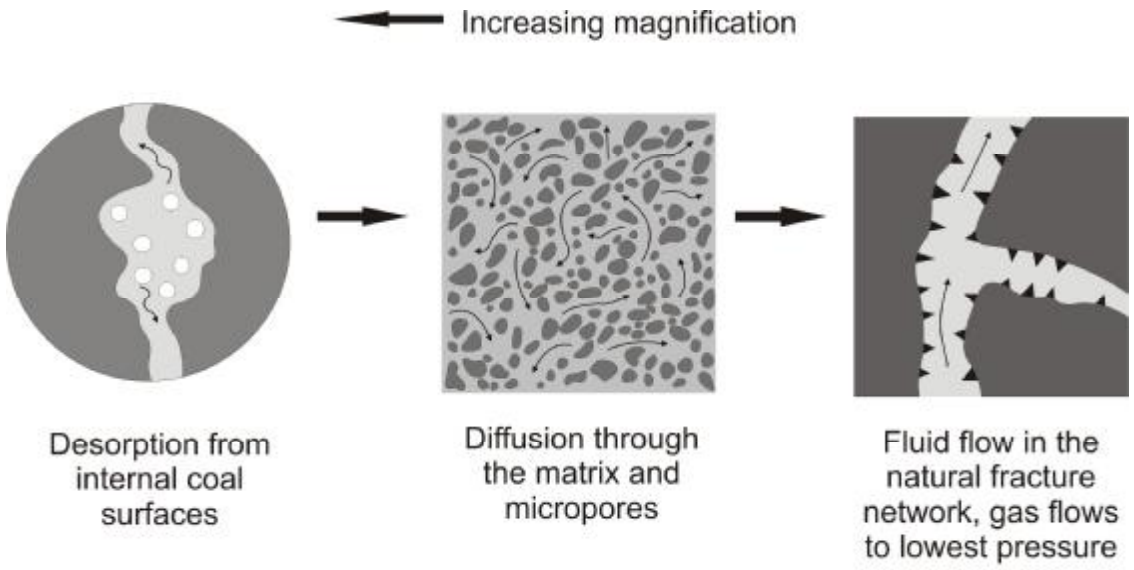

Figure 1.2: Model of methane flow through coal showing desorption, diffusion and Darcy flow.

1.3.2 Coal Seam Gas Composition

Coal seam gas consists of various hydrocarbons in different proportions, as well as small quantities of nitrogen, oxygen, hydrogen and helium. CH_4 is the dominant component of coal seam gas, followed by CO_2 and heavier hydrocarbons (Rice, 1993; Clayton, 1998). There are a number of controlling factors which determine the proportions of gas in the coal seam. These include:

1. Thermal maturity of the coal,
2. H/C (elemental composition) of macerals present, and
3. the mechanism of gas generation (thermogenic vs. biogenic).

The carbon isotopic composition of coal seam gas has a large amount of variation. The controls over the coal seam gas isotopic variation are the same as which determine the proportion of gas in the seam: process of formation; thermal maturation, and maceral composition (Clayton, 1998; Whiticar, 1996). Whiticar et al., (1986) developed the often reproduced diagram illustrating gas generation mechanisms (see Figure 3.26). The diagram combines $\delta^{13}C$ and δD values, and although hydrogen isotopes do not exhibit a clear maturity dependency, they provide information on depositional environment and therefore pathway of formation. As methane becomes enriched in deuterium (more positive δD values) and the heavy isotope $\delta^{13}C$ (more positive $\delta^{13}C$ values) with increasing maturation (Rice, 1993), the source for gas generation changes from biogenic to thermogenic.

Coal seam gas generation is controlled by two distinct processes: biogenic and thermogenic generation. Biogenic gas comprises mainly methane and CO_2 which have been produced by the decomposition of organic

material by micro-organisms, commonly in peat swamps. There are a number of requirements needed to produce significant proportions of gas, and these include an anoxic environment, low sulphate concentrations, low temperatures, abundant organic material, high pH values, adequate pore space and rapid sedimentation (Rice, 1993). Biogenic gas generation is available from two distinct pathways: methyl-type fermentation (primary) and CO_2 reduction (secondary). Secondary biogenic gases are different from primary biogenic gases in that the bacteria involved are introduced into the coal seams after burial and coalification. This is often from the influence of the recharge of meteoric waters moving through permeable coal beds, with the waters introducing metabolic activity of bacteria (Scott, 2002). Secondary biogenic gas can form in coals of any rank, while primary biogenic gas forms early in the burial history of lower rank coal.

Thermogenic gases form at the higher pressures and temperatures associated with increasing coalification. At ranks higher than high-volatile bituminous coals, devolatilisation occurs with coals becoming enriched in carbon and expelling volatile matter. Methane, CO_2 and water are the by products of this reaction (Rice, 1993).

Thermogenic gas generation can form without deep burial. Gurba and Weber (2001) have observed igneous activity in the Gunnedah Basin, which has produced in an increase of rank in local coal. This has lead to large areas of coal generating thermogenic gas, as the intrusion has resulted in a move towards the thermogenic gas generation window. Ayers (2002) has noted that although most coal seams are self sourcing reservoirs, many contain a mixture of different types of gas. Coal seams may contain any combination of the following: self sourced or migrated thermogenic gas; primary biogenic gas; secondary biogenic gas. Ayers (2002) compares two end member coal seam gas producing basins: the San Juan Basin and the Powder River Basin. The Powder River Basin contains low rank coal (sub-bituminous C-B) and methyl-type fermented biogenic gas. The San Juan Basin, however, is much more variable. It can be broken into four regions all containing bituminous coal, ranging from high-volatile A to low volatile bituminous coal. Each region contains a different blend of gas, with regions 1a-c containing thermogenic gas with a high biogenic component, and regions 2 and 3 containing early stage and migrated thermogenic gas. Different gas mixtures can be a result of number of parameters, including structural history, which will determine the thermal maturation patterns of the basin, and hydrology, which promotes the migration of secondary biogenic gases into the coal seam.

1.4 General Geology

1.4.1 The Waikato Region

The Waikato coal region comprises several distinct coal areas, from Drury, 30km south of Auckland, to Mangapehi, 20km south of Te Kuiti, in the north of the North Island, New Zealand. There are thirteen coal

areas in total, and their boundaries are based on major seam discontinuities, usually at major fault zones. See Edbrooke et al. (1999) for a comprehensive delineation of the coal basins. The general geology is illustrated in Figure 1.3.

The general structural style of the Waikato coalfield is dominated by block faulting (Hall, 2003, Gillard and Trumm, 2002). This faulting has resulted in a regional north-westerly dip of 5-15° for the Tertiary sequence with vertical to steeply dipping normal faults (Gillard and Trumm, 2002). Two main fault sets dominate the region: a north-northwest trending fault set which runs parallel to the Waipa Fault (a major basement structure) active in the early Cenozoic, and a northeast to north-northeast trending fault set, originally thought to be related to the ongoing Kaikoura Orogeny. The latter set tends to offset the north trending set, which has resulted in the sector boundaries of the coalfield (Barry et al., 1994). Hall (2003) and Hall et al., (2006) demonstrated that fault displacement in the Waikato region post-dates the deposition of the coal measures, contrary to previous studies (for example Kear and Schofield, 1978; Kirk et al. 1988; Barry et al. 1994), with fault movement commencing around 36-35 Ma and continuing to approximately 30 Ma.

Waikato Coalfield stratigraphy was initially defined in 1864 by Ferdinand Hochstetter (cited in Edbrooke et al., 1994) and since then has undergone many revisions. Kear and Schofield (1959) revised the nomenclature, and subsequent publications have uniformly adopted their usage. Two major stratigraphic groups are recognised in the Waikato Coal Region (Table 1.1):

a) The Tauranga Group: Late Miocene to Recent.
b) The Te Kuiti Group, which contain the Waikato Coal Measures: Late Eocene to Oligiocene in age.

Table 1.1 Stratigraphy of the Waikato coal region.

Group	Formation	Member	Age
Tauranga Group			Pleistocene to Recent
Te Kuiti Group	Mangakotuku Formation	Whaingaroa Siltstone	Miocene to Pleistocene
		Glen Massey Formation	
		Mangakotuku Siltstone	
		Pukemiro Sandstone	
		Glen Afton Claystone	
	Waikato Coal Measures		Late Eocene to Oligocene

The Waikato Coal Measures are the basal formation of the transgressive Te Kuiti Group, and rest on an undulating erosion surface which cuts deeply weathered and indurated Mesozoic basement rocks, and grades upwards into shallow marine formations (Whaingaroa Siltstone, Glen Massey Formation) (Edbrooke et al., 1999; Kirk et al., 1988). The Waikato Coal Measures are mid-to late Eocene in age in the Huntly coalfield, and become younger in both north and south directions.

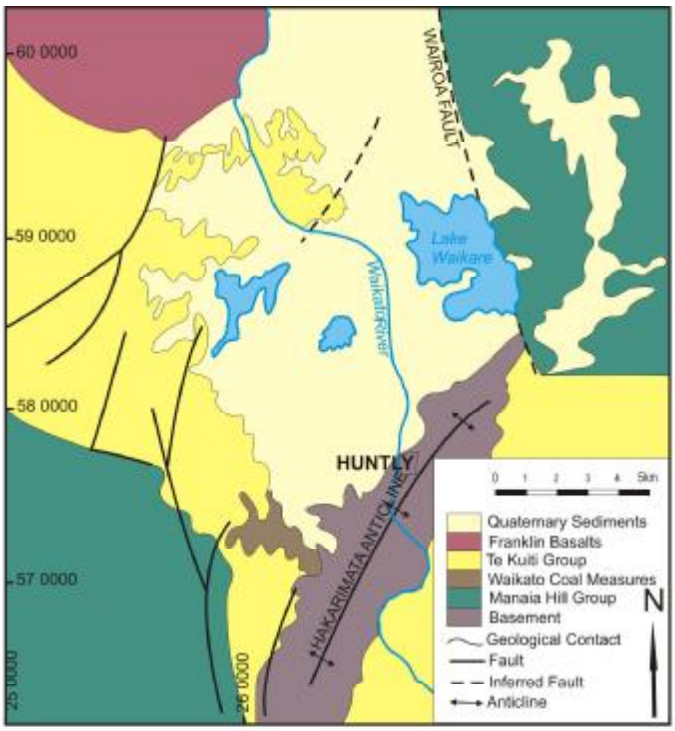

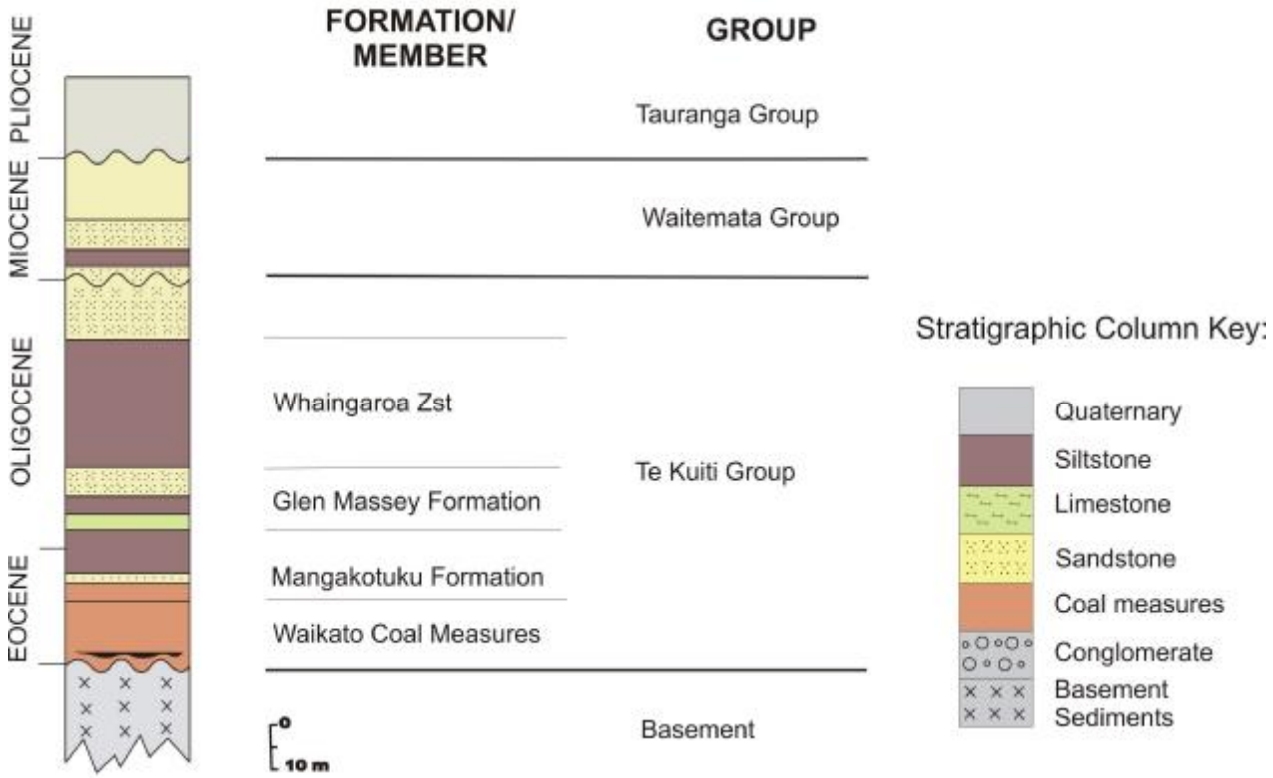

Figure 1.3:Geologic map and stratigraphic column for the Huntly region. Map uses NZMG (1949) co-ordinate system. For greater detail of stratigraphic units see Hall, (2003) and Edbrooke et al., (1994).

The coal measures were mainly deposited and preserved in a north-northwest trending valley system, 30 km by 200 km, which was coaxial with the major Mesozoic movement on the Waipa Fault (Kirk et al, 1988). The Waikato Coal Measures contain eight significant coal seams: four in the northern region and four in the southern region. Depth to seams through the region varies considerably from 2 m to 550 m + (Edbrooke, 1999). Ferm et al. (2000) have produced a pictorial guide to the classification of the coal measure sediments in the North Waikato coal region.

The Huntly coalfield extends almost 20km in a north, northwest direction from the township of Huntly, and encompasses an area of up to 140 km^2 (Kirk et al., 1988). The Huntly coalfield is dominated by the presence of the Kupakupa and the Renown seams, both of economic importance. The Kupakupa seam occurs at or near the base of the coal measures, and typically varies from 3 to12 m thick, although it exceeds 20 m in the Huntly region, where it converges with the overlying Renown seam. The Renown seam is less extensive and thinner than the Kupakupa seam, and seam splitting is more common. Newman et al., (1997) examined the petrography and geochemistry of the Kupakupa seam.

Two main depositional environments controlled the accumulation of sediments, and the influence that these settings exerted can be seen in two distinct, subregions of the coalfield (Edbrooke et al., 1994). The northern region was dominated by an inland alluvial plain setting and was bounded by hills and was not influenced by marine sedimentation until the marginal marine sediments of the Mangakotuku Formation were laid above the coal measures. In the southern region the coal measures accumulated in a coastal plain setting strongly influenced by marine sediments, in particular at the end of coal measure deposition.

Gas characteristics of the Waikato coalfield have also been documented (Moore nad Twombly, 2006; Twombly et al., 2004) with particular reference to four commercially producing US basins. Adsorption isotherm data have been published from the Huntly area, however associations between coal properties and gas characteristics have yet to be determined.

1.4.2 The Ohai Region

The Ohai coalfield is situated at the south of the South Island, approximately 80 km north west of Invercargill. The coalfield lies in an east-west trending fault bounded depression, known as the Ohai or Birchwood-Wairio depression, which separates the Takutimu and Longwood mountain ranges. The coalfield extends for approximately 100 km^2, and has been extensively mapped by the New Zealand Geological Survey (Sykes, 1988) and by Bowen (1964, Fig. 1.4).

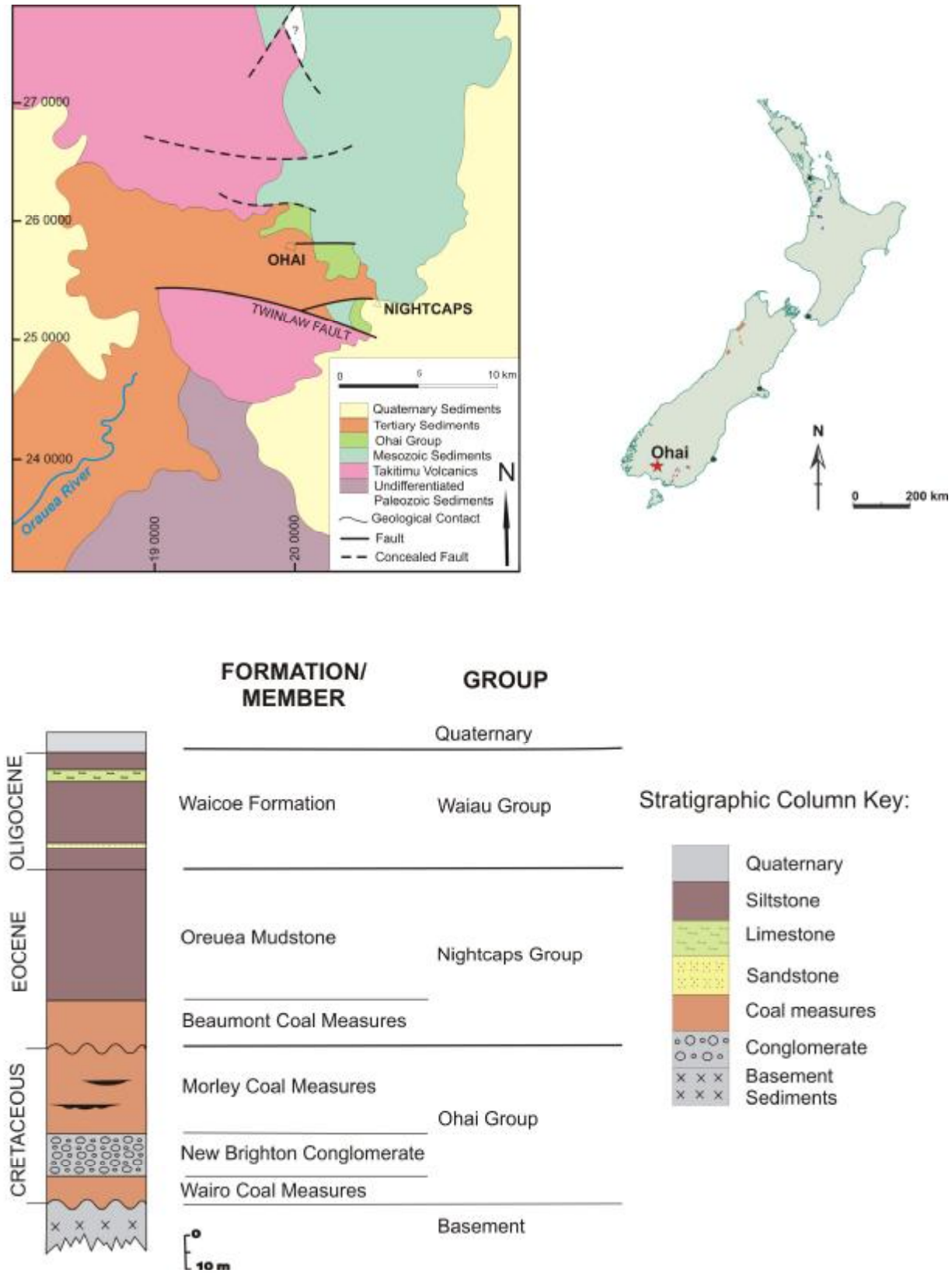

Figure 1.4: Geologic map and stratigraphic column for the Ohai region. Map uses NZMG (1949) co-ordinate system. For greater detail of stratigraphic units see Shearer (1992).

Bowen (1964) and Bowman et al., (1987) interpreted the structural nature of the Ohai region. A north-south structural trend dominates the Ohai region. The area is further divisible into three north-south trending belts, which from west to east comprise the Tertiary sediments of the Waiau Basin; the Permo-Carboniferous volcanics and intrusives of the Taktimu-Longwood Divide; and the Triassic sediments which help form the south-west limb of the Southland Syncline. Within the Takitimu volcanics lies the fault bounded Ohai basin. The Ohai Basin, prominent because of its east-west trend and Cretaceous age sediments, contains coal measure sediments which form the north-eastern limb of a major syncline, the axis which lies 2 km south-west of the town of Birchwood. Additional folds in the coalfield trend to the north-west and follow a dominant Cretaceous structural trend (Warnes, 1990). Major faults in the area are parallel to the north-east trend of folding, whereas minor faults seem randomly orientated. Faulting and folding are believed to be contemporaneous with sedimentation (Warnes, 1990).

The stratigraphy has been defined by Bowen (1964). Two major groups are recognised (Table 1.2):

a) The Nightcaps Group of Mid Eocene to Early Oligocene (Bortonian-Whaingaroan) age. The Nightcaps Group unconformably overlies the Ohai Group.
b) The Ohai Group of Late Cretaceous (Piripauan-Haumaurian) age, which contains the Morley Coal Measures.

Table 1.2: Stratigraphy of the Ohai coalfield, based on Bowen (1964). Source: Warnes, 1990.

Group	Formation	Age
Nightcaps Group	Orauea Mudstone	Eocene
	Beaumont Coal Measures	
Ohai Group	New Brighton Conglomerate	Late Cretaceous
	Wairo Coal Measures	
	Basement	Triassic to Carboniferous

The Morley Coal Measures are the most economically important formation in the Ohai coalfield. The Morley Coal Measures lie conformably above the New Brighton Conglomerate, although it has been suggested that the conformable contact may not extend through the whole of the coalfield (Bowen, 1964). Lithologies in the coal measures range from clay to boulder conglomerate. Areas contiguous to coal seams show prominent occurrences of carbonaceous mud, siltstone and sandstone. There are six coal horizons recognized but these cannot be referred to as discrete seams as they undergo splitting and thinning throughout the coalfield. These coal seams vary with a maximum thickness of 30m. The maximum indicated thickness of the coal measures is 270 m, (Sherwood et al., 1992). The estimates of Sherwood et al. (1992) are considered similar to Sykes (1988), and more accurate than Bowen (1964), as palynological age control was introduced.

The Morley Coal Measures were deposited in an intermontane basin. An alluvial environment gave rise to three interrelated depositional environments: a sandy, braided river system; a well-drained flood plain

environment; and poorly drained, peat-accumulating backswamps. Depositional models have been suggested by Sykes (1985) and Shearer (1992). Sykes (1985) incorporates sandstone and coal petrography as well as geochemistry to his interpretations. Shearer (1992) focussed on integrating sedimentology, coal chemistry, coal petrography and palynology to delineate the depositional environments for both the Morley and Beamont coal measures.

Of all the basins in New Zealand, the Ohai coalfield has had the most work conducted on it for CSG. For example, in the 1980s a New Zealand joint venture company, Southgas, formed and investigated the potential for methane extraction of deep coal from the Ohai coalfield. Preliminary data on desorption of methane were gathered and discussed in a government report (Thorburn, 1983). Isotopic composition of South Island natural gas has also been briefly studied, and determined that gas from the Ohai coalfield originated from a low-maturity microbial source (Lyon and Giggenbach, 1994). Adsorption and desorption data has been commonly collected, however only a limited amount of these data has been published (Manhire and Hayton, 2003; Pope at al., 2004; Moore and Butland, 2005).

1.4.2 The Greymouth Region

The Greymouth coalfield is situated on the West Coast of the South Island, 10 km north of the town of Greymouth (Fig. 1.5). It occupies an area of 200 km^2 at the southern end of the Paparoa Ranges, west of the Alpine Fault. Both the southern and the eastern margins are defined by the Grey River, whereas the western margin extends offshore into the Tasman Sea. The Greymouth coalfield was first discovered by Thomas Brunner in 1848. Gage (1952) and Nathan (1978) conducted detailed geological surveys of the Greymouth region, followed by a comprehensive basin study by Nathan et al.(1986).

The Greymouth coalfield is part of the West Coast Basin and Range tectonic unit, which is one of four that dominate all of the west coast regions of New Zealand. The West Coast Basin and Range Province is dominated by a north-northeast structural trend, which developed from Late Cenozoic block faulting. This region is tectonically unstable, and this is characterized by subsidence in small fault bounded basins. The north-northeast fault pattern has controlled sedimentation over the last 80 million years as well as the orientation of several Late Cretaceous to Pliocene sedimentary basins (Nathan, 1986). Individual faults have been reactivated in response to changing stress regimes (Laird, 1968, 1972).

Coal measure sedimentation began in the Late Cretaceous, and was restricted to four fault-bounded basins. The Paparoa Coal Measures, the main coal measure found in the Greymouth coalfield, were deposited from the Late Cretaceous to Paleocene in the Paparoa trough, one of the four fault-bounded basins.

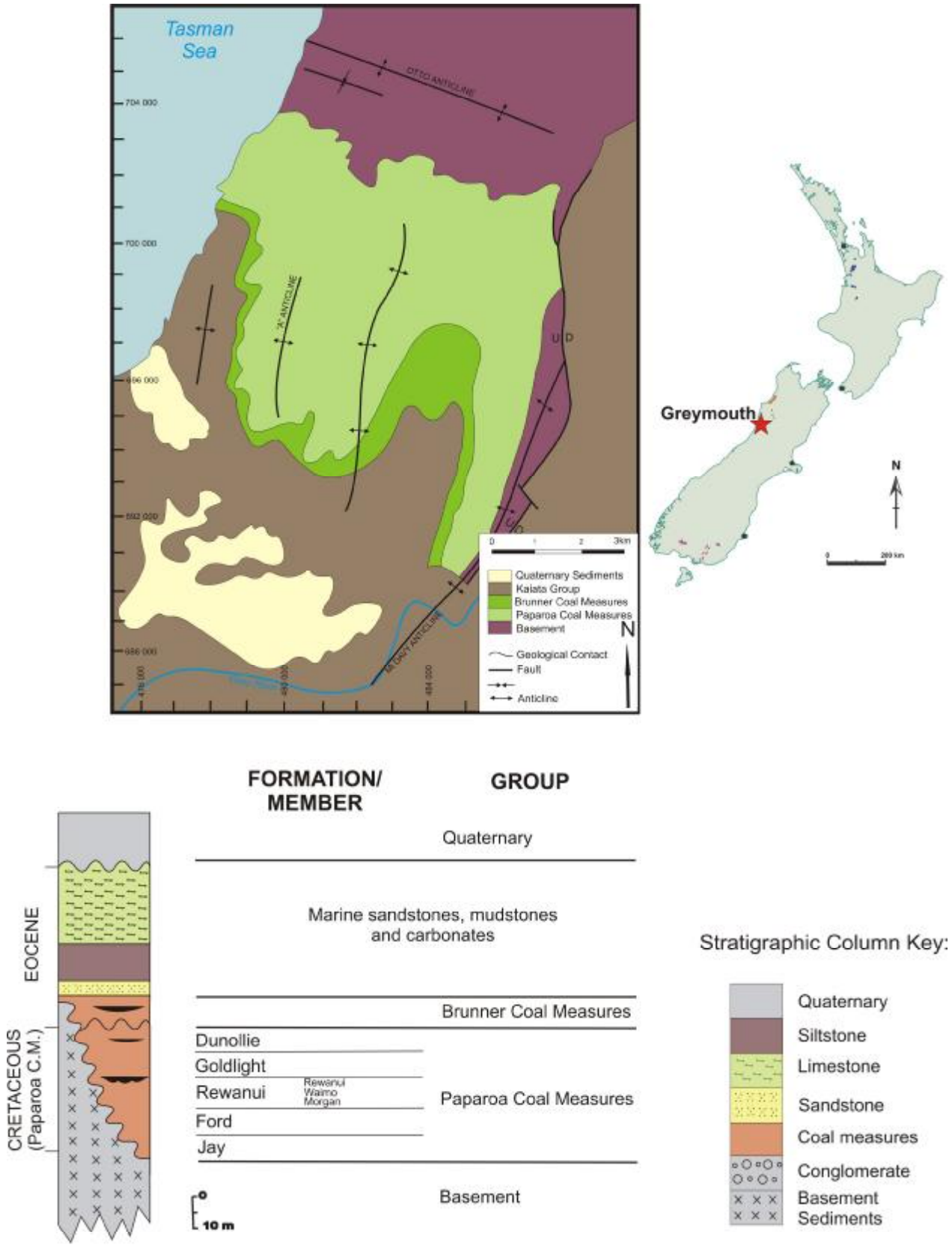

Figure 1.5: Geologic map and stratigraphic column for the Greymouth region. Map uses NZMG 1949 co-ordinate system. For greater detail of stratigraphic units see Nathan (1986).

Formations and units in the Greymouth coalfield and adjacent areas have undergone various name and sequence reclassification changes in the past. Gage (1952), Nathan (1978,) and Nathan et al. (1986) all defined and revised the nomenclature, but the terms this study has adopted is based on works by Ward (1997) (Table 1.3).

Table 1.3: Stratigraphy of the Greymouth coal region.

Group	Formation	Member	Age
Brunner coal measures			Mid-Late Eocene
Paparoa coal measures	Dunollie		Paleocene to Late Cretaceous
	Goldlight	Rewanui	
	Rewanui	Waimo	
	Ford	Morgan	
	Jay		
Greenland Group			Ordovician

The Paparoa Coal Measures are mined extensively in the Greymouth coalfield. They lie unconformably on the mid-Cretaceous Pororari Group rocks, and concordantly beneath the Brunner Coal Measures. The basin extends for 60 km in a north-south trend, although the maximum width of the basin does not exceed 12 km. There are five main formations, with the coal horizons being the Dunollie Formation, and Rewanui and Morgan Members of the Rewanui Formation. The Rewanui Member contains the most extensively mined seam in the Paparoa Coal Measures (Ward, 1997). Coal properties of the Paparoa Coal Measures have been studied extensively, from petrographic analysis, palynology and mineral matter and trace element geochemistry (Newman, 1997; Moore, 1995, 1996; Ferm and Moore, 1997; Ward, 1997; Li, 2002; Li et al., 2001a, 2001b, 2005; Moore et al. 2005, 2006; Moore and Butland, 2005).

Newman (1985, 1987) interpreted the paleoenvironments of the Paparoa Coal Measures. Thick, extensive coal seams were deposited in fluviodeltaic lake margins during periods of transgression and regression of the lake. Syndepositional faulting confined the high energy fluvial environment and protected peat accumulation. In the south-west corner thick coal developed as the region was isolated from fluvial activity and exposed to lesser amounts of subsidence. Depositional controls were also examined by Sherwood et al. (1992), who concluded that the same depositional conditions controlled the Paparoa Coal Measures delineated by Newman (1985, 1987). Palaeotemperatures during burial and coalification were interpreted by Kamp et al. (1999) using fission track and vitrinite reflectance. Maximum paleotemperatures were found to exceed 85ºC throughout the whole coalfield, reaching a peak of 180 ºC along the axis of the former basin.

Beamish et al. (1996) examined the methane sorption capacity of upper Cretaceous coals from the Greymouth coalfield. The adsorption isotherm suggested that the maximum sorption capacity passes through a minimum in the medium volatile bituminous rank. Beamish et al. (1998) contrasted methane sorption

properties of New Zealand and Australian coals and found that New Zealand coals had a lower adsorption capacity because of decreased microporosity from the presence of volatile components blocking the micropore structure.

Chapter Two
Methodology

To characterise the four cores from the different locations a series of analytical techniques were adopted. Macroscopic analysis was carried out on all cores to determine textural character. Geochemical analyses were completed on all samples, and consisted of moisture, ash, volatile matter, fixed carbon, sulphur and calorific value (Table 2.1). Some of these data were used to construct a Suggate plot, and in turn used to differentiate rank and type differences. Subsplits of samples (8 for Huntly, 13 for Ohai and 10 for Greymouth) were taken for mineralogical analysis. Ash constituents were determined on all available samples (33 for Huntly, 27 for Ohai and 19 for Greymouth). Subsplits of samples were also taken for crushed particulate pellets (8 for Huntly, 12 for Ohai and 8 for Greymouth). In addition nine blocks for the Greymouth coal field were also examined to determine modes of occurrence of mineral matter. Finally, gas analyses consisted of desorption measurements (lost gas, residual gas, measured gas and total gas), gas isotopes, gas quality and adsorption isotherms (Table 2.1).

2.1 Macroscopic Analyses

2.1.1 Coal Type

The type of coal that is produced from peat is controlled by a variety of parameters including the type of the original plant material, the geochemical conditions affecting the plant material during peat deposition, and the final level of maturation of the coal. Coal type, or the visual appearance, varies systematically within a seam

Table 2.1: Analyses completed on samples- geochemical and organic

ID			Geochemical Analyses									Organic Analyses		
Basin	Drillhole ID	Canister	Moisture	Ash	Volatile Matter	Fixed Carbon	Sulphur	Calorific Value	XRD	XRF	Suggate rank	Coal Type	Maceral Point count	Block pellet
Huntly	TW1	9	√	√	√	√	√	√		√	√	√		
Huntly	TW1	10	√	√	√	√	√	√	√	√	√	√	√	
Huntly	TW1	11	√	√	√	√	√	√	√	√	√	√	√	
Huntly	TW1	12						√		√				
Huntly	TW1	13	√	√	√	√	√	√		√	√	√		
Huntly	TW1	14	√	√	√	√	√	√		√	√	√		
Huntly	TW1	15	√	√	√	√	√	√		√	√	√		
Huntly	TW1	16	√	√	√	√	√	√		√	√	√		
Huntly	TW1	17	√	√	√	√	√	√		√	√	√		
Huntly	TW1	18	√	√	√	√	√	√		√	√	√		
Huntly	TW1	19	√	√	√	√	√	√	√	√	√	√	√	
Huntly	TW1	20	√	√	√	√	√	√		√	√	√		
Huntly	TW1	21	√	√	√	√	√	√	√	√	√	√	√	
Huntly	TW1	22	√	√	√	√	√	√		√	√	√		
Huntly	TW1	23						√		√				
Huntly	TW1	24	√	√	√	√	√	√		√	√	√		
Huntly	TW1	25	√	√	√	√	√	√		√	√	√		
Huntly	TW1	26	√	√	√	√	√	√		√	√	√		
Huntly	TW1	27	√	√	√	√	√	√		√	√	√		
Huntly	TW1	28	√	√	√	√	√	√	√	√	√	√	√	
Huntly	TW1	29	√	√	√	√	√	√		√	√	√		
Huntly	TW1	30	√	√	√	√	√	√		√	√	√		
Huntly	TW1	31	√	√	√	√	√	√		√	√	√		
Huntly	TW1	32	√	√	√	√	√	√	√	√	√	√	√	
Huntly	TW1	33	√	√	√	√	√	√		√	√	√		
Huntly	TW1	34						√		√				
Huntly	TW1	35	√	√	√	√	√	√		√	√	√		
Huntly	TW1	36	√	√	√	√	√	√		√	√	√		
Huntly	TW1	37	√	√	√	√	√	√	√	√	√	√	√	

Table 2.1 (continued): Analyses completed on samples- geochemical and organic.

Huntly	TW1	38	√	√	√	√	√	√		√	√	√		
Huntly	TW1	39	√	√	√	√	√	√		√	√	√		
Huntly	TW1	40						√		√				
Huntly	TW1	41	√	√	√	√	√	√		√	√	√		
Huntly	TW1	42	√	√	√	√	√	√		√	√	√		
Huntly	TW1	43	√	√	√	√	√	√	√	√	√	√	√	
Huntly	TW1	44	√	√	√	√	√	√		√	√	√		
Huntly	TW1	45	√	√	√	√	√	√		√	√	√		
Greymouth	944	16	√	√	√	√	√	√	√	√	√	√	√	
Greymouth	944	1	√	√	√	√	√	√		√	√	√		
Greymouth	944	2	√	√	√	√	√	√		√	√	√		√
Greymouth	944	3	√	√	√	√	√	√		√	√	√		
Greymouth	944	4	√	√	√	√	√	√		√	√	√		
Greymouth	944	5	√	√	√	√	√	√	√	√	√	√	√	√
Greymouth	944	6	√	√	√	√	√	√	√	√	√	√	√	√
Greymouth	944	7	√	√	√	√	√	√			√	√		
Greymouth	944	8	√	√	√	√	√	√			√	√		
Greymouth	944	9	√	√	√	√	√	√		√	√	√		
Greymouth	944	10	√	√	√	√	√	√		√	√	√		
Greymouth	944	11	√	√	√	√	√	√		√	√	√		
Greymouth	944	12	√	√	√	√	√	√		√	√	√		
Greymouth	944	13	√	√	√	√	√	√	√	√	√	√	√	√
Greymouth	944	14	√	√	√	√	√	√			√	√		
Greymouth	944	15	√	√	√	√	√	√	√	√	√	√	√	√
Greymouth	944	17	√	√	√	√	√	√		√	√	√		
Greymouth	944	18	√	√	√	√	√	√		√	√	√		
Greymouth	944	19	√	√	√	√	√	√		√	√	√		√
Greymouth	944	20	√	√	√	√	√	√	√	√	√	√	√	√
Greymouth	944	21	√	√	√	√	√	√	√	√	√	√	√	√
Greymouth	944	22	√	√	√	√	√	√			√	√		
Greymouth	944	23	√	√	√	√	√	√			√	√		√
Greymouth	944	24	√	√	√	√	√	√		√	√	√		
Ohai	SC3	SC3-1	√	√	√	√	√	√	√	√	√	√	√	
Ohai	SC3	SC3-2	√	√	√	√	√	√		√	√	√		

Table 2.1 (continued): Analyses completed on samples- geochemical and organic.

Ohai	SC3	SC3-3	√	√	√	√	√	√	√	√	√	√	√	
Ohai	SC3	SC3-4	√	√	√	√	√	√		√	√	√		
Ohai	SC3	SC3-5	√	√	√	√	√	√		√	√	√		
Ohai	SC3	SC3-6	√	√	√	√	√	√		√	√	√		
Ohai	SC3	SC3-7	√	√	√	√	√	√	√	√	√	√	√	
Ohai	SC3	SC3-8	√	√	√	√	√	√		√	√	√		
Ohai	SC3	SC3-9	√	√	√	√	√	√	√	√	√	√	√	
Ohai	SC3	SC3-10	√	√	√	√	√	√		√	√	√		
Ohai	SC3	SC3-11	√	√	√	√	√	√		√	√	√		
Ohai	SC3	SC3-12	√	√	√	√	√	√	√	√	√	√	√	
Ohai	SC3	SC3-13	√	√	√	√	√	√	√	√	√	√	√	
Ohai	SC3	SC3-14	√	√	√	√	√	√		√	√	√		
Ohai	SC3	SC3-15	√	√	√	√	√	√	√	√	√	√	√	
Ohai	SC3	SC3-16	√	√	√	√	√	√		√	√	√		
Ohai	SC3	SC3-17	√	√	√	√	√	√	√	√	√	√	√	
Ohai	SC3	SC3-18	√	√	√	√	√	√		√	√	√		
Ohai	SC1	SC1-1	√	√	√	√	√	√		√	√	√		
Ohai	SC1	SC1-2								√				
Ohai	SC1	SC1-3	√	√	√	√	√	√	√	√	√	√	√	
Ohai	SC1	SC1-4							√					
Ohai	SC1	SC1-5	√	√	√	√	√	√		√	√	√		
Ohai	SC1	SC1-6	√	√	√	√	√	√		√	√	√		
Ohai	SC1	SC1-7	√	√	√	√	√	√		√	√	√		
Ohai	SC1	SC1-8	√	√	√	√	√	√	√	√	√	√	√	
Ohai	SC1	SC1-9	√	√	√	√	√	√		√	√	√		
Ohai	SC1	SC1-10	√	√	√	√	√	√	√	√	√	√	√	
Ohai	SC1	SC1-11	√	√	√	√	√	√	√	√	√	√	√	

Table 2.1: Analyses completed on samples- gas analyses.

ID			Gas Analyses							
Basin	Drillhole ID	Canister	Measured gas	Residual gas	Lost gas	Total gas	Adsorption*	Saturation	Gas quality*	Gas isotopes*
Huntly	TW1	9	√	√	√	√		√		
Huntly	TW1	10	√	√	√	√		√		
Huntly	TW1	11	√	√	√	√		√		
Huntly	TW1	12	√	√	√	√		√		
Huntly	TW1	13	√	√	√	√		√		
Huntly	TW1	14	√	√	√	√		√		
Huntly	TW1	15	√	√	√	√		√		
Huntly	TW1	16	√	√	√	√		√		
Huntly	TW1	17	√	√	√	√		√		
Huntly	TW1	18	√	√	√	√		√		
Huntly	TW1	19	√	√	√	√		√		
Huntly	TW1	20	√	√	√	√		√		
Huntly	TW1	21	√	√	√	√		√		
Huntly	TW1	22	√	√	√	√		√		
Huntly	TW1	23	√	√	√	√		√		
Huntly	TW1	24	√	√	√	√		√		
Huntly	TW1	25	√	√	√	√		√		
Huntly	TW1	26	√	√	√	√		√		
Huntly	TW1	27	√	√	√	√	√	√	√	√
Huntly	TW1	28	√	√	√	√		√		
Huntly	TW1	29	√	√	√	√		√		
Huntly	TW1	30	√	√	√	√		√		
Huntly	TW1	31	√	√	√	√		√		
Huntly	TW1	32	√	√	√	√		√		
Huntly	TW1	33	√	√	√	√		√		
Huntly	TW1	34	√	√	√	√		√		
Huntly	TW1	35	√	√	√	√		√		
Huntly	TW1	36	√	√	√	√		√		
Huntly	TW1	37	√	√	√	√		√		
Huntly	TW1	38	√	√	√	√		√		
Huntly	TW1	39	√	√	√	√		√		
Huntly	TW1	40	√	√	√	√		√		
Huntly	TW1	41	√	√	√	√		√		
Huntly	TW1	42	√	√	√	√		√		
Huntly	TW1	43	√	√	√	√		√		
Huntly	TW1	44	√	√	√	√		√		
Huntly	TW1	45	√	√	√	√		√		
Greymouth	944	16	√	√	√	√		√		
Greymouth	944	1	√	√	√	√		√		
Greymouth	944	2	√	√	√	√		√		
Greymouth	944	3	√	√	√	√	√	√	√	√
Greymouth	944	4	√	√	√	√		√		
Greymouth	944	5	√	√	√	√		√		
Greymouth	944	6	√	√	√	√		√		
Greymouth	944	7	√	√	√	√		√		

Table 2.1 (continued): Analyses completed on samples- gas analyses.

Greymouth	944	8	√	√	√	√		√		
Greymouth	944	9	√	√	√	√		√		
Greymouth	944	10	√	√	√	√		√		
Greymouth	944	11	√	√	√	√		√		
Greymouth	944	12	√	√	√	√		√		
Greymouth	944	13	√	√	√	√		√		
Greymouth	944	14	√	√	√	√		√		
Greymouth	944	15	√	√	√	√	√	√	√	√
Greymouth	944	17	√	√	√	√		√		
Greymouth	944	18	√	√	√	√		√		
Greymouth	944	19	√	√	√	√		√		
Greymouth	944	20	√	√	√	√		√		
Greymouth	944	21	√	√	√	√		√		
Greymouth	944	22	√	√	√	√		√		
Greymouth	944	23	√	√	√	√		√		
Greymouth	944	24	√	√	√	√		√		
Ohai	SC3	SC3-1	√	√	√	√		√		
Ohai	SC3	SC3-2	√	√	√	√		√		
Ohai	SC3	SC3-3	√	√	√	√		√		
Ohai	SC3	SC3-4	√	√	√	√		√		
Ohai	SC3	SC3-5	√	√	√	√		√		
Ohai	SC3	SC3-6	√	√	√	√		√		
Ohai	SC3	SC3-7	√	√	√	√		√		
Ohai	SC3	SC3-8	√	√	√	√		√		
Ohai	SC3	SC3-9	√	√	√	√		√		
Ohai	SC3	SC3-10	√	√	√	√		√		
Ohai	SC3	SC3-11	√	√	√	√		√		
Ohai	SC3	SC3-12	√	√	√	√		√		
Ohai	SC3	SC3-13	√	√	√	√		√		
Ohai	SC3	SC3-14	√	√	√	√		√		
Ohai	SC3	SC3-15	√	√	√	√	√	√	√	√
Ohai	SC3	SC3-16	√	√	√	√		√		
Ohai	SC3	SC3-17	√	√	√	√		√		
Ohai	SC3	SC3-18	√	√	√	√		√		
Ohai	SC1	SC1-1	√	√	√	√		√		
Ohai	SC1	SC1-2	√	√	√	√		√		
Ohai	SC1	SC1-3	√	√	√	√		√		
Ohai	SC1	SC1-4	√	√	√	√		√		
Ohai	SC1	SC1-5	√	√	√	√		√		
Ohai	SC1	SC1-6	√	√	√	√		√		
Ohai	SC1	SC1-7	√	√	√	√		√		
Ohai	SC1	SC1-8	√	√	√	√		√		
Ohai	SC1	SC1-9	√	√	√	√		√		
Ohai	SC1	SC1-10	√	√	√	√		√		
Ohai	SC1	SC1-11	√	√	√	√		√		

* Data on composite intervals or represents entire hole.

(Esterle and Ferm, 1986; Moore, 1996). Macroscopic analysis of coal core is conducted to quantify its visual character. The visual character of coal gives clues to how it may behave in regards to gas flow properties.

There are a number of different macroscopic classification schemes for coal. The earliest scheme was defined by Stopes (1919) who described vitrain, clarain, fusain and durain. Since this initial classification, there have been a number of other classification schemes which are beyond the scope of this study to discuss. However the reader is directed to Davis (1978), Taylor et al. (1998), and Schopf (1960) among others. This study uses the classification scheme described in Shearer and Moore (1994) and Moore et al. (1993, 2006). This methodology divides the coal into two broad categories: matrix and plant parts (i.e. vitrain). The matrix is described on the basis of its lustre (dull or bright) and the proportion and size of the vitrain bands (≥ 1 mm).

2.1.2 Macroscopic Point Count Analyses

A macroscopic point count quantifies the amount and size (if measured) of vitrain in the coal seam. A point count is **representative** of the coal core, because only a portion of the core is counted. All four drill cores in this study were macroscopically point counted.

Drill cores were split roughly in half, mostly along cleat boundaries using a hammer or chisel. A standard string is used, with points divided out every 1 cm. The string is laid over the split core, and material (matrix versus vitrain) that lies beneath a marked point is recorded. When vitrain was counted, the thickness perpendicular to bedding was also recorded (in millimetres).

Point counts are made on an entire coal core, and tallied by either canister interval (~ 50 cm) or by ply interval (coal type). Coal type boundaries may cross canister boundaries. After coal types are tallied, each canister is assigned a coal type based on the point count. The coal types assigned are as follows (see also Ferm et al., 2000).

- Bright lustre, non-banded
- Vitrain is greater than 20 %, by volume
- Vitrain is less than 20%, by volume
- Dull lustre coal
- Carbonaceous mudstone

2.2 Sampling

Each drill site used slightly different methods in recording coal intervals and plies. Figures 2.1 to 2.4 illustrate the different numbering systems used in each drill hole.

The Huntly core used a straightforward system, numbering the canisters from 9 to 45, in numerical order, for both proximate and gas analyses.

The Ohai core used two systems. Gas data were analysed with the coal in canister intervals of approximately 0.50 m in thickness. The canister intervals were numbered from X1 to X34 for the SC3 drill hole, and A1 to A19 for the SC1 drill hole. These were not always in numerical order. Some of these canister intervals were then combined to produce ply intervals, from SC3-1 to SC3-18 for the SC3 drill hole, and from SC1-1 to SC1-11 for the SC1 drill hole. Proximate analyses were undertaken on ply intervals.

The Greymouth core also used two numbering systems. Gas data were analysed with the coal in canister intervals of approximately 0.50 m. These canister intervals were numbered from 1 to 24. Some of these intervals were then split because of differences in coal type, creating a new system from 1 to 27. Proximate analyses were undertaken on the intervals from 1 to 27, however these intervals vary slightly from the coal type intervals.

Because the four drill cores contain a large number of canister and ply intervals, it was not feasible to test and sample each interval for petrological composites and mineralogy, because of time and funding constraints. To overcome this problem a selected number of samples were chosen. They were selected to represent the main geochemical and coal type signatures found within each core, as well as to represent the variability present in each core. The criteria for selecting these samples were:

1. Suggate plot position: samples that occur along isorank lines, and samples that had wide spread along the average type line,
2. Stratigraphic position: a spread of samples from throughout the drill core,
3. Coal type: a sample of all different coal types present,
4. Ash content: a range of both high and low ash yields,
5. Gas content: a range of both high and low total gas volumes.

The selected samples for petrological and mineralogical analysis are illustrated in Table 2.2, along with their defining characteristics. Figure 2.5 illustrates the selected samples in a stratigraphic position, along with coal type. Selected samples for the Huntly core are canisters 10, 11, 19, 21, 28, 32, 37, 43; for the Ohai SC3 core are SC3-1, SC3-3, SC3-7, SC3-9, SC3-12, SC3-13, SC3-15, SC3-15; for the Ohai SC1 core are SC1-3, SC1-8, SC1-10, SC1-11; and for the Greymouth core 16, 5, 6, 13, 15, 20, 21.

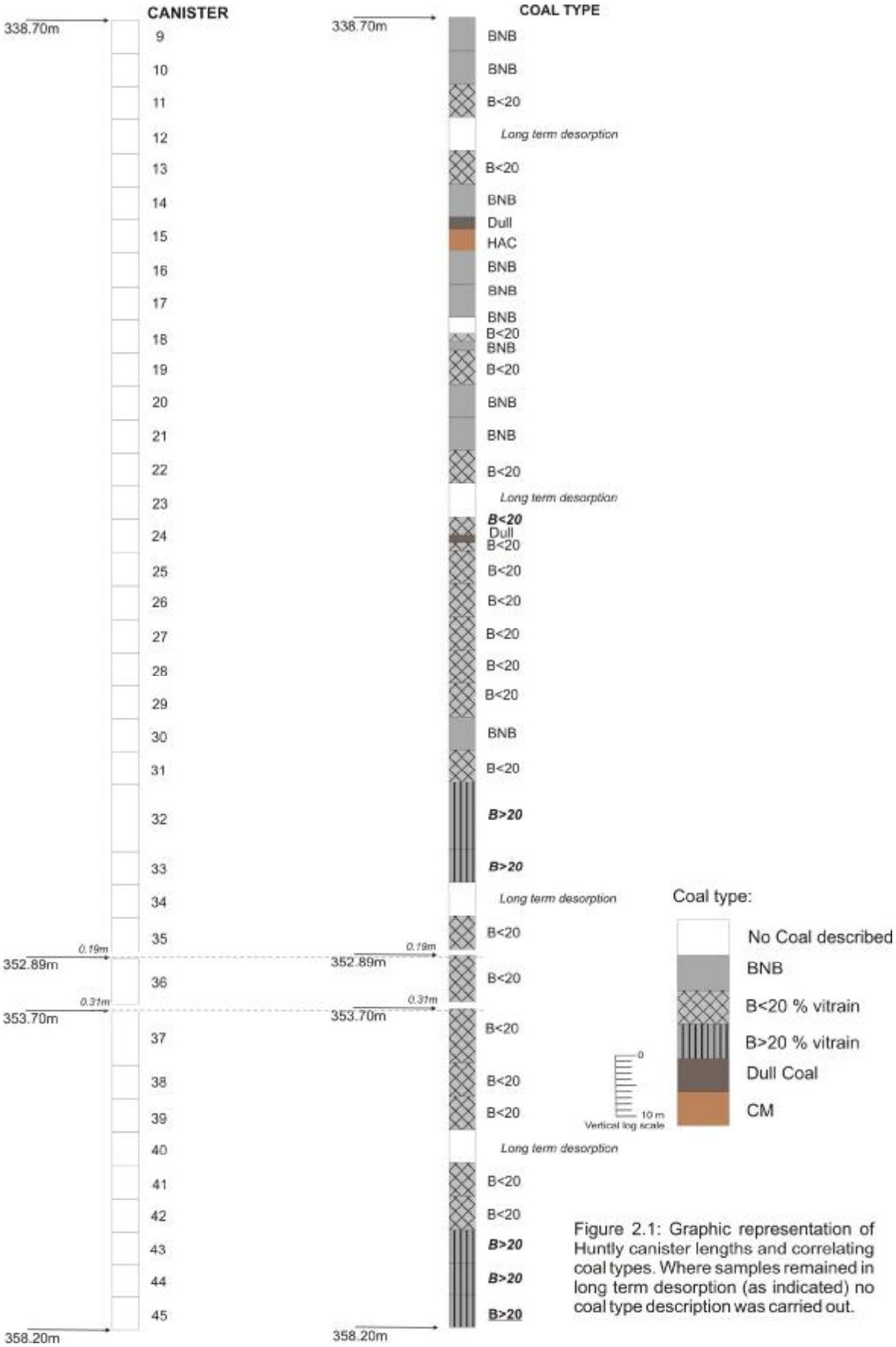

Figure 2.1: Graphic representation of Huntly canister lengths and correlating coal types. Where samples remained in long term desorption (as indicated) no coal type description was carried out.

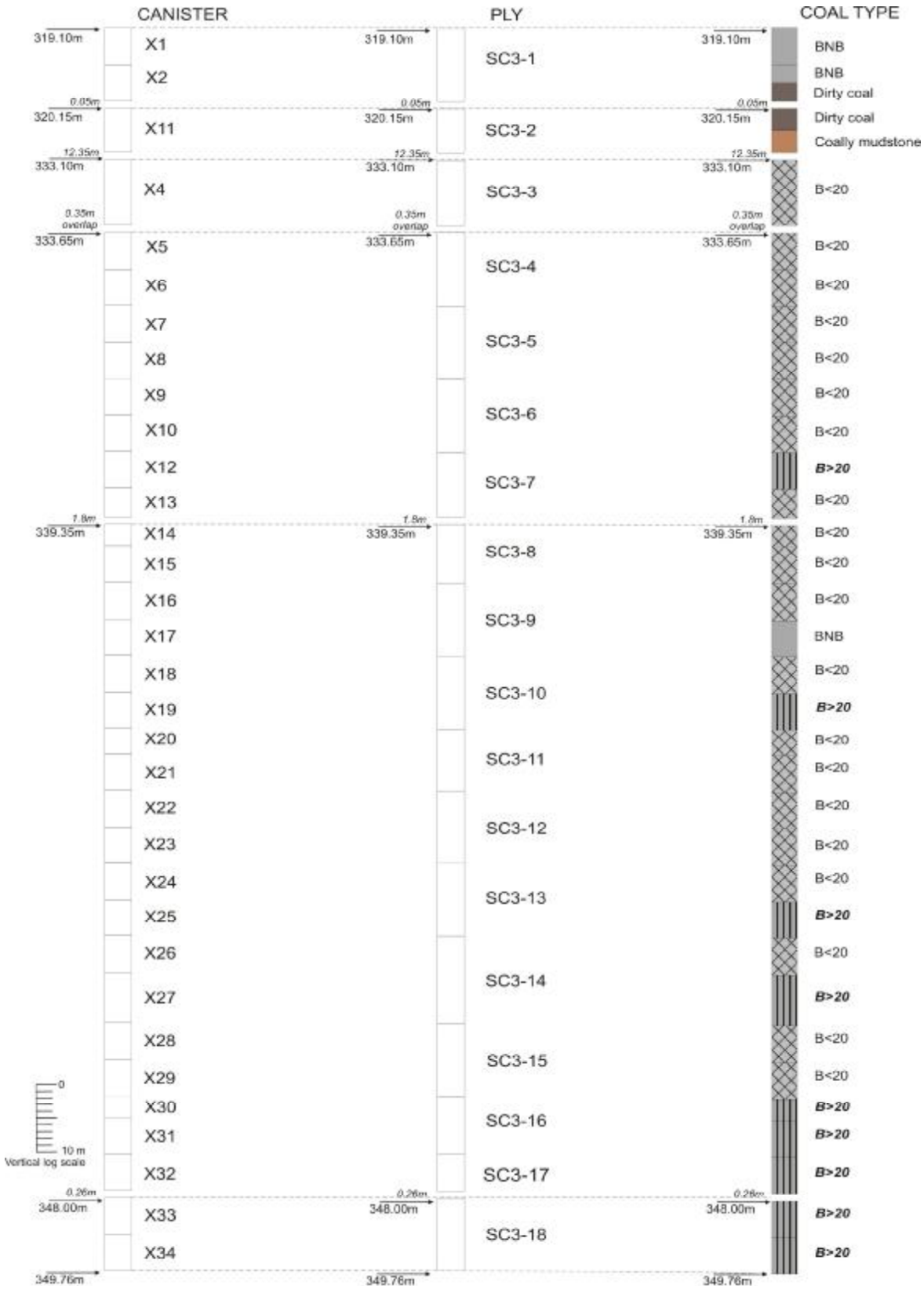

Figure 2.2: Graphic representation of Ohai SC3 canister intervals and correlating ply intervals and coal type. Coal types include BNB= bright, non-banded; B<20 = bright vitrain less than 20% ; B>20= bright, vitrain greater than 20% ; Dull ; CM = carbonaceous mudstone

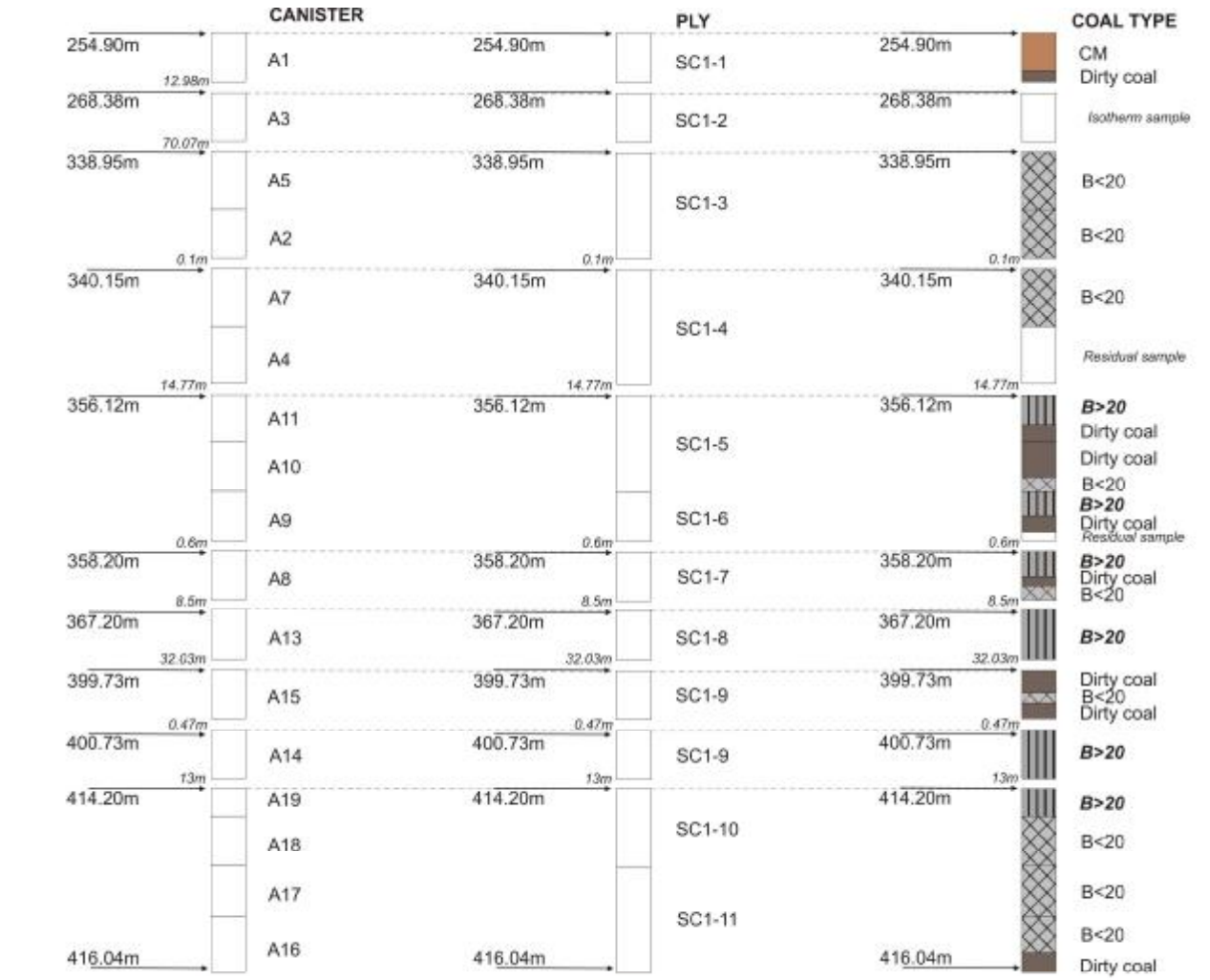

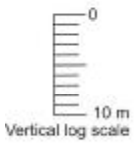

Figure 2.3: Graphic representation of Ohai SC1 canister lengths and correlating coal types. Where samples remained in long term desorption, or were taken for residual gas sampling (as indicated) no coal type description was carried out.

No Coal described

BNB; bright non-banded

B<20 % vitrain

B>20 % vitrain

Dull/dirty Coal

CM; carbonaceous mudstone

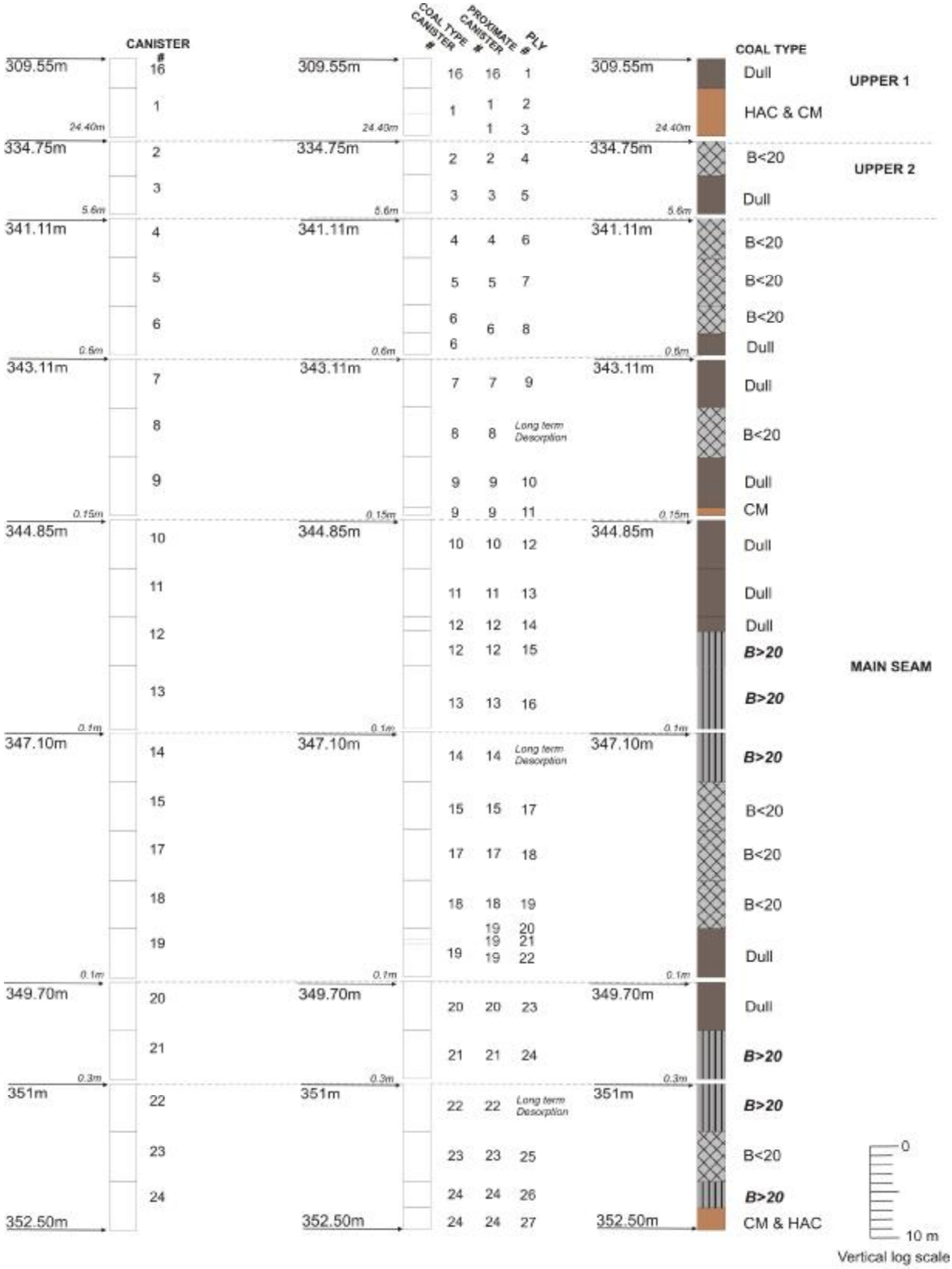

Figure 2.4: Graphic representation of Greymouth canister and ply intervals and correlating coal types. Long term desorption samples were taken out from 'ply' intervals, and these were logged for coal type at a later date. Coal types include: BNB = bright, non-banded ;B<20=bright vitrain less than 20% ;B>20=bright, vitrain greater than 20% ;Dull ;HAC=high ash coal ; CM=carbonaceous mudstone .

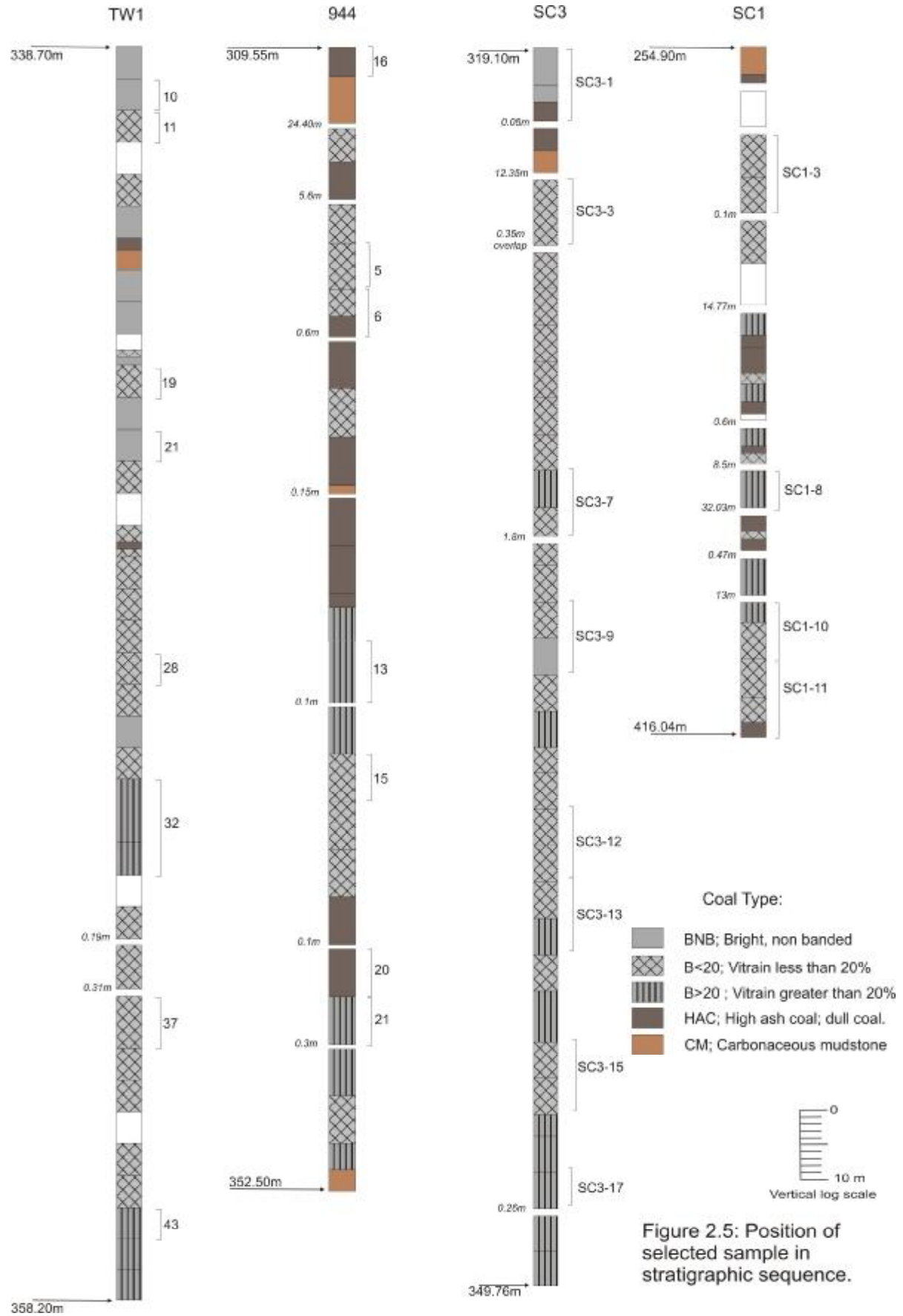

Figure 2.5: Position of selected sample in stratigraphic sequence.

Table 2.2: Properties of samples selected for petrological and mineralogical analysis.

Location	Coal type	Ash content (aa)	VM (dmmSf)	CV (dmmSf)	Position in strat column*	Outlier/ middle of group*	Measured gas m3/t	Total gas m3/t
Huntly								
10	BNB	3.8%	42.2	30.2	T	R	1.1	1.4
11	B<20	2.9%	47.7	30.8	T	R	1.0	1.3
19	B<20	1.6%	45.0	30.2	MT	R	0.6	1.4
21	BNB	3.0%	44.6	30.3	MT	R	0.9	1.3
28	B<20	3.4%	41.2	29.8	M	R	1.0	1.4
32	B>20	2.1%	44.9	30.6	M	R	1.0	1.7
37	B<20	1.5%	41.8	29.9	MB	R	1.2	1.9
43	B>20	1.2%	43.5	31.2	B	R	0.5	1.7
Ohai SC3								
SC3-1	**BNB**/dull	14.4%	42.23	32.10	T	O	3.2	4.4
SC3-3	B>20	1.8%	45.13	31.95	T	O	3.9	4.7
SC3-7	**B<20**/B>20	1.6%	43.04	31.66	M	R	4.1	4.9
SC3-9	B>20/BNB	1.3%	42.85	31.56	M	R	4.5	5.3
SC3-12	**B>20**	1.2%	43.45	31.46	M	R	3.6	4.5
SC3-13	B>20/B<20	1.5%	43.95	31.58	B	R	4.6	5.5
SC3-15	B>20	1.5%	44.00	31.55	B	R	4.8	5.7
SC3-17	B<20	2.1%	42.09	31.61	B	R	4.9	5.8
Ohai SC1								
SC1-3	B<20	4.5%	43.46	31.81	T	R	3.2	4.3
SC1-8	B>20	13.1%	41.22	32.26	M	O	4.3	5.0
SC1-10	B>20/**B<20**	4.9%	43.51	32.13	B	R	5.4	6.3
SC1-11	**B<20**/dull	12.4%	47.12	33.07	B	O	5.0	5.6
Greymouth								
16	dull	2.3%	40.83	33.49	T	O	2.89	3.70
5	B<20	2.5%	43.11	34.14	MT	R	2.12	3.21
6	B<20/Dull	0.7%	44.78	33.97	MT	O	1.37	2.21
13	B>20	4.3%	42.93	34.2	MB	R	1.81	2.32
15	B<20	5.3%	43.52	34.32	MB	R	1.13	1.77
20	Dull	7.0%	42.08	33.96	B	R	1.03	1.57
21	B>20	13.6%	42.99	34.33	B	R	1.85	2.32

* T = Top; MT = Mid top; M = Middle; MB = Mid bottom; B = Base; O = Outlier; R = Representative.

2.3 Coal Geochemistry

2.3.1 Proximate analyses

Proximate analyses were conducted to give an indication of changes of geochemistry within and between coal cores. In this study proximate analyses were performed: moisture, volatile matter, ash, fixed carbon. In addition both sulphur and calorific value analyses were also carried out. These analyses were determined

using ASTM D3173 for moisture (American Standards for Testing and Materials [ASTM], 2003), ASTM 3175 for volatile matter (ASTM, 2002), ASTM D3174 for ash yield (ASTM, 2004a), ASTM D4239 for sulphur (ASTM, 2004b) and ASTM D5865 for calorific value (ASTM, 2004c). Corrections were applied to compensate for non-organic impurities so that one coal can be compared directly with another coal (Ward, 1984, Appendix B).

2.3.2 Ash Constituents

Ash constituents were determined using X-Ray fluorescence (XRF) analysis. The procedure follows the ASTM D4326-01 standard (ASTM, 2004d), where the coal is first combusted at 815°C to a constant weight. The residual ash is then fused with lithium tetraborate to form a pellet which is irradiated by a high energy X-ray beam. The X-rays of the atom which are fluoresced upon absorption of the incident rays are dispersed, and the intensities are measured at selected wavelengths. All elements are determined as the element, and reported as the oxide (G. Murray, pers. comm., CRL energy Ltd, 2005)

2.3.3 Mineralogy

In order to determine the mineralogy within and between the coal core, 27 samples were selected for X-Ray diffractometry (XRD) analysis (see Table 2.2). As XRD analysis requires a powder residue of the mineral matter, coal samples were oxidised using a low temperature asher (LTA). The LTA 302 Low Temperature Ashing machine was used following similar operating conditions to those described by Newman (1988). The LTA has two vacuum chambers and each chamber held between one and two samples simultaneously, with oxidation taking between 14-48 hours to complete. The temperature in the ashing chambers was approximately 170°C.

Samples were ground to -1mm then powdered using a ring mill, before being placed in the LTA. The amount of powder was determined using the ash yield from the proximate analyses and the relationship of 1% ash equating to 0.01 grams of ash residue.

The slides of residual ash from the LTA were analysed for mineral occurrences on a Philips PW 1720 X-Ray diffractometer (XRD) in the Department of Geological Sciences, University of Canterbury. Because of the uncertainty of soluble minerals present in the samples, a pre-XRD preparation trial was undertaken using both alcohol and distilled water in the preparation process. Soluble material in the LTA residue can lead to synthetic compounds forming during or after oxidation of coal samples in the LTA process. This can obscure mineral patterns in the XRD analysis with high background noise and additional mineral peaks forming from the soluble compounds. (Newman, 1988; Sykes, 1985). The trial showed two additional peaks in the samples prepared with alcohol, whereas the water prepared sample lacked these additional peaks and had lower

background scatter, emphasising the mineral peaks present. Therefore, the water preparation technique was adopted for this study.

Preparation of samples involved LTA residue being placed in an agate mortar. Distilled water was added, the sample was washed and left for a few minutes for the particles to settle out of suspension. Once settled, water was removed with a pipette, and the washing process was repeated. The slurry was then ground, and then transferred to a glass slide and left to dry, before being analysed.

A Rietveld based interpretation method was used to determine the identity of the crystalline material (Li et al., 1999; Ward et al., 2001; Ward 2002). The Rietveld method calculates a profile of each mineral, which is generated from its crystal structure. Mineral percentages are determined when the sum of all calculated patterns are fitted to the XRD profile in a mutli-mineral sample using statistical analyses (Ward et al., 2001; Ward 2002). The mineral matter can either occur as discrete mineral grains or bound in the organic material.

2.4 Suggate Rank

2.4.1 Introduction

Broad chemical differences are routinely observed in coal. These differences are the result from two main causes: type difference (the nature of the original peat set before or directly after initial burial); and rank difference (the effects from the geological conditions that peat is subjected to, mainly progressive burial) (Suggate and Dickinson, 2004). Suggate's rank scale, based on the type variation and the rank difference, was revised in 2000 and is known as Rank (S_r) or Suggate Rank. Suggate rank uses either proximate analyses of calorific value and volatile matter (CV-VM axes) or ultimate analyses of carbon and hydrogen (O/C and H/C ratios) to follow the maturation path of coal.

Suggate's diagram contains several important features (Fig. 2.6). The first is a line of progressive coalification of 'average type' coal, called the average type line. This line is based on a theoretical coal with an average type starting chemistry, that is, the coal is not hydrogen enriched. Killops et al. (1998) defined this line as the maturation path of lignin. The second important feature is the New Zealand Coal band. A coal band represents a distribution of analytical points for a related group of coal (often of a similar location and age). The band generalises the metamorphic process in the peat to meta-anthracite range, and acts as an analogous maturation path for the kerogens (Suggate, 1998). The New Zealand coal band is based on coals that are Late Cretaceous to Cenozoic in age. They have medium to high H/C ratios, and have high vitrinite-huminite contents (87-93%), with liptinite (5-11%) exceeding inertinite content (1-6%) (Suggate, 1998). The high hydrogen content in New Zealand coals, compared with an average type coal, leads to a coal band that is elevated from the average type line. The New Zealand coal band also shows a full range of coal ranks from

lignite to semi-anthracite. The final feature of a Suggate plot are the isorank lines. Suggate (2000) has provided isorank lines initially derived from Late Cretaceous and Tertiary coal sequences. These lines radiate out from the average type line on a 45° angle, and movement along this line, away from the average type line, represents type differences in coal. The Suggate plot representatively illustrates differences in coal that are both type related (movement along isorank lines) and rank related (movement along the average type line).

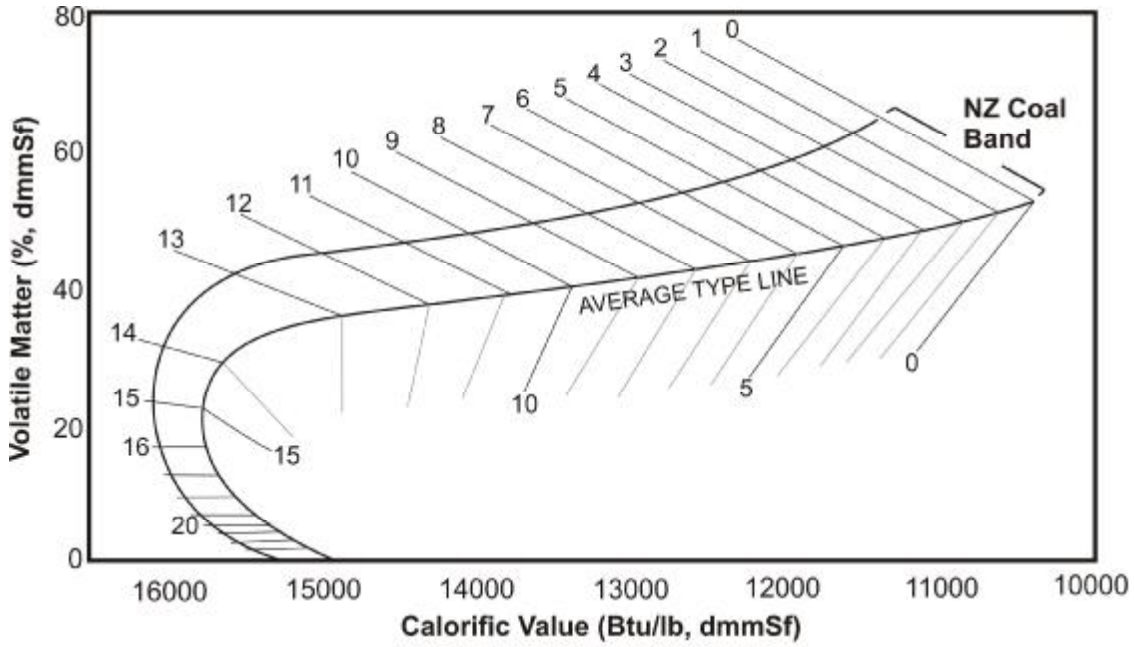

Figure 2.6: Suggate plot showing the New Zealand coal band, Suggate number and the average type line; a line of progressive coalification for an 'average' type coal.

2.4.2 Construction of Suggate Plot

The Suggate plot was used to differentiate between type differences and rank differences, by comparing calorific value (Btu/lb) with volatile matter. The purpose was to isolate appropriate samples for further analyses (see Section 2.2).

Suggate (1959) observed that New Zealand coals which had high total organic sulphur contents also had high volatile matter and calorific values present, compared with coals which had a low total organic sulphur content at a similar rank. To eliminate effects from the sulphur and mineral matter, data must be corrected to an organic basis independent of moisture, mineral matter and sulphur (dmmSf). Mineral matter and sulphur both affect the burning properties of the coal, which influences the calorific value, used to determine the Suggate rank. Suggate (1959) recommended a correction factor of 1.1, based on averaged data from across New Zealand coalfields. Correction formulas used are given below:

$$\text{Volatile Matter (dmmSf)} = \frac{100\,(VM - 0.1A - 0.55S}{100-1.1A-S} \quad \text{(all dry basis)}$$

$$\text{Calorific Value (dmmSf)} = \frac{100(CV-0.095S)}{100-1.1A-S} \quad \text{(all dry basis; CV in MJ/Kg)}$$

Where S = sulphur and A=Ash.

After data are corrected, diagrams can be produced on volatile matter and calorific value axes. The average type line can also be plotted on the axes to help correlate ASTM rank with Suggate rank (S_r). Preliminary analyses found that coals with ash yield in excess of 12% caused variation that was not purely the result of rank. To overcome this, only samples with ash yield less than 12% were initially plotted. Although it is important to minimise error influences on data, such as high ash content, ash-related anomalies do not cause major variance in rank.

2.5 Petrographic Analysis

2.5.1 Introduction

Coal is composed of various microscopic components termed macerals. Stopes (1935) first defined macerals, as an analogy to minerals of inorganic rocks. Unlike minerals, which have specific chemical and physical signatures, macerals vary widely in their chemical composition and physical properties. However, studies on pure maceral components have helped determine standard chemical and physical properties (Stach et al., 1982)

Coal macerals are classified into three groups based on their physical appearance, chemical characteristics and biological affinities:

1. Vitrinite
2. Liptinite
3. Inertinite

These maceral groups are further subdivided into macerals and the macerals recognised in this study are summarised in Table 2.3.

The International Commission on Coal and Organic Petrography (ICCP) has developed standard rules for coal petrography that state the description of macerals shall correspond to their appearance in incident light using oil immersion with magnifications between 250x and 400x (Stach et al., 1982).

Selected samples (as discussed in Section 2.2) were analysed petrographically using polished particulate mounts under reflected light using a Zeiss UMSP50 incident light microscope, at 400x magnification with oil immersion. Block samples were also analysed qualitatively for the Greymouth core. Block samples were not collected from the Huntly and Ohai cores.

Table 2.3: Summary of maceral groups identified in this study.

Maceral Group	Maceral	Origin
Vitrinite	Telocollinite –in cell walls	Stems, roots, leaves, bark, wood
	-in bands	
	-in large areas	
	Desmocollinite	
	Vitrodetrinite	
Liptinite	Sporinite	Spores, pollen, cuticular material, Resin, algae
	Cutinite	
	Resinite	
	Suberinite	
	Liptodetrinite	
Inertinite	Semi-fusinite	Fossil charcoal (most materials Inert during coking process)
	Fusinite	
	Scelrotinite	
	Inertodetrinite	

2.5.2 Coal particulate pellet preparation.

Coal was ground to 1mm, then subsplit to approximately 20 grams and dried in a 40°C oven for one hour, to remove excess moisture. The coal was then mixed with epoxy resin and hardener at a ratio of 5:1. Plastic moulds were lubricated with vaseline and labelled. The coal resin mix was then transferred to the plastic moulds, where they sat in a ~20°C room for an hour to set. The pellets were then placed back in the 40°C oven for at least eight hours, to finish the curing process, before being polished.

2.5.3 Coal block pellet preparation

Coal blocks were cut to approximately 4 cm x 3 cm rectangles using a diamond edged rock saw. Because the coal was hard, reinforcing to avoid breakage and splitting was not needed. Samples were then dried in a 40°C oven overnight, to remove excess moisture. Samples were then placed in a silicone block mould, and epoxy resin was poured into the bottom of the mould. Weights were placed on top to stop the coal from floating. When the resin set, a second resin pour was conducted, covering the coal and label. The pellets were left over night in a 20°C room to set and cure, before being polished (Pontolillo and Stanton, 1992).

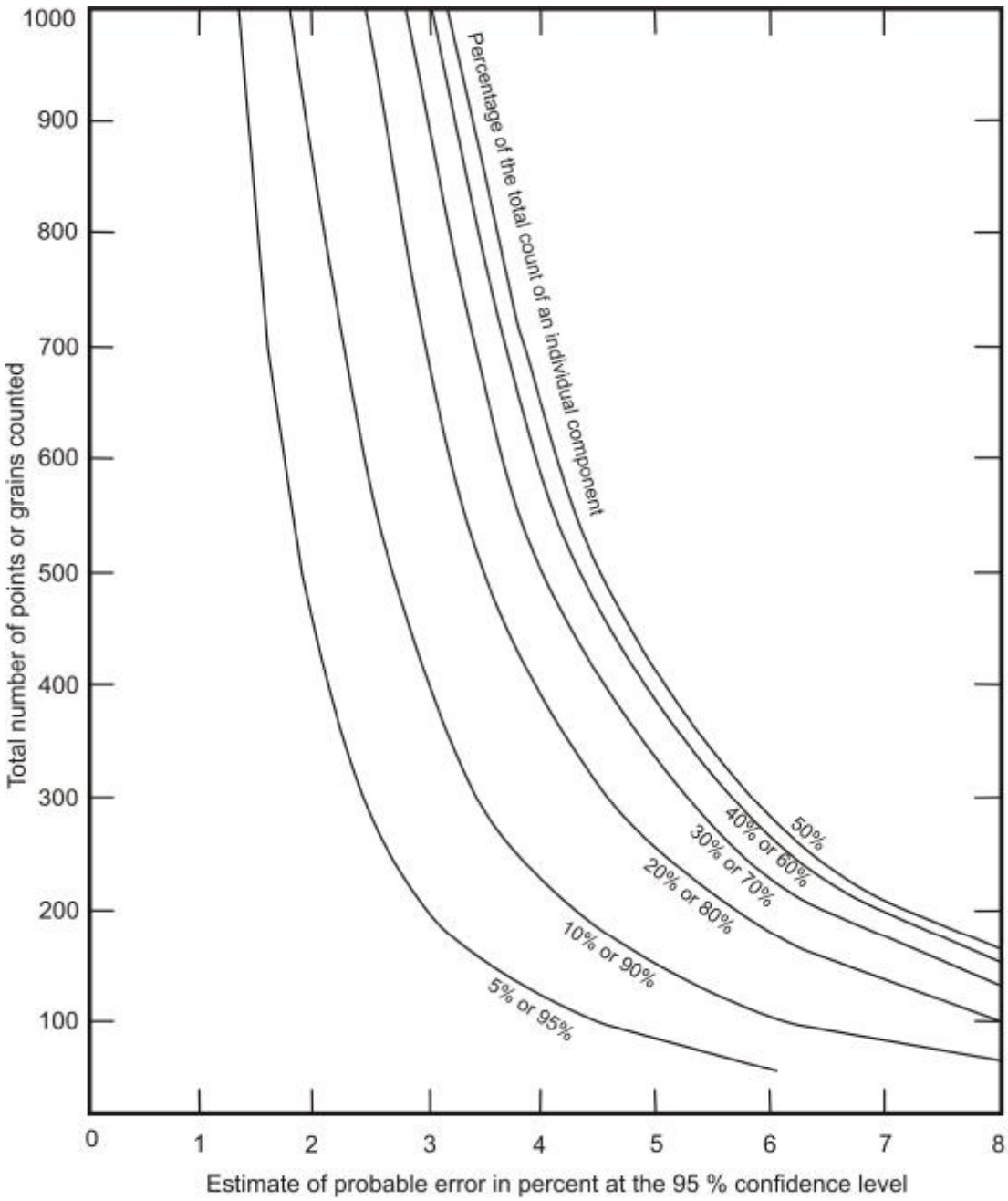

Figure 2.7: Curves illustrating the probable error in percent at the 95 % confidence level, related to the number of points counted. The uncertainty for 500 counts is listed below in the table. Source: J. Newman, pers. comm. Newman energy research, 2005.

VOLUME PERCENT OF COMPONENT	'UNCERTAINTY' VALUE, 500 COUNTS
2% or 98%	±1%
5% or 95%	±2%
10% or 90%	±3%
20% or 80%	±4%
40% or 60%	±4.5%
50%	±4.5%

2.5.4 Microscopic analytical method

Macerals and inorganic material are quantified by a random sample of 500 grains following procedures set out in ASTM Standard D2799 (ASTM, 2005a). Maceral analyses were conducted on a total of twenty-eight samples across all four cores (8 from Huntly, 8 from Ohai SC3, 4 from Ohai SC1, and 8 from Greymouth). A grid was set up using a computer programme called 'Digimax', with 1mm line spacings. Every component that lands on the predetermined point is recorded. Unlike bulk chemistry, which consumes the whole coal and therefore represents the chemistry precisely, microscopic analyses (point count) can only approximate actual proportions as 500 grains is only a small proportion of the total sample. No grain is counted twice.

Point counts are usually limited to 500 readings because the advantage of making additional counts rapidly decreases (Fig. 2.7). In order to obtain 500 counts, two petrographic pellets were constructed for each sample.

Fourteen different macerals were identified as mentioned above, along with five major types of mineral matter; clays, carbonates, sulphides (pyrite), iron oxides and quartz. The telocollinite maceral was divided into three macerals to represent the form it was observed as: 1. in cellular material; 2. in bands 20 – 100 microns thick; and 3. in large homogeneous areas.

2.6 Gas Data

Five types of tests or calculations were carried out on samples from each drillhole, in order to determine information about coal bed gas:

1. Desorption analysis (lost, residual, measured and total gas);
2. Adsorption analysis;
3. Saturation calculations;
4. Gas quality analysis;
5. Stable isotope analysis.

2.6.1 Desorption Analysis

Desorption was measured using methods outlined in Moore et al. (2004) and Moore and Butland (2005) (Figs. 2.8 and 2.9).

The coal sample is immediately sealed in a canister after retrieval from the drill hole, and immediately placed into on site water baths at reservoir temperature. The coal bed gas emission (predominantly methane) is bled into a manometer (Fig. 2.10). Measurements are taken every 15 minutes until gas volume reaches below 10 ml, where the time interval is doubled. The time interval is gradually decreased until desorption is minimal. Ambient temperature and barometric pressure are also recorded at each reading. Finally the sample is air

dried and weighed. The gas yield is calculated and expressed in cubic metres of gas per tonne of coal. This method fails to account for any free gas that may have escaped from open fractures before the sample was sealed in a canister (Bodden and Ehrlich, 1998).

The measured gas is obtained by recording the volume of gas that desorbs from the coal in a set amount of time. Lost gas is gas that has been expelled between the end of coring and the start of the desorption measurements (Diamond and Schatzel, 1998). This is calculated using a trend line analysis of measured gas values. Residual gas is gas that remains in the coal after a critically low desorption rate is reached. This was originally thought to be a result of slow diffusion rates (Diamond and Schatzel, 1998). However, it has been suggested that it is a result of gas remaining in equilibrium under 1 atmospheric pressure, in the desorption canister (Levine, 1992). The residual gas can be determined by crushing the sample in a ring mill with a special desorption apparatus attached (Diamond et al., 2001). The total gas is determined by calculating the lost gas, measured gas and residual gas values in a coal interval.

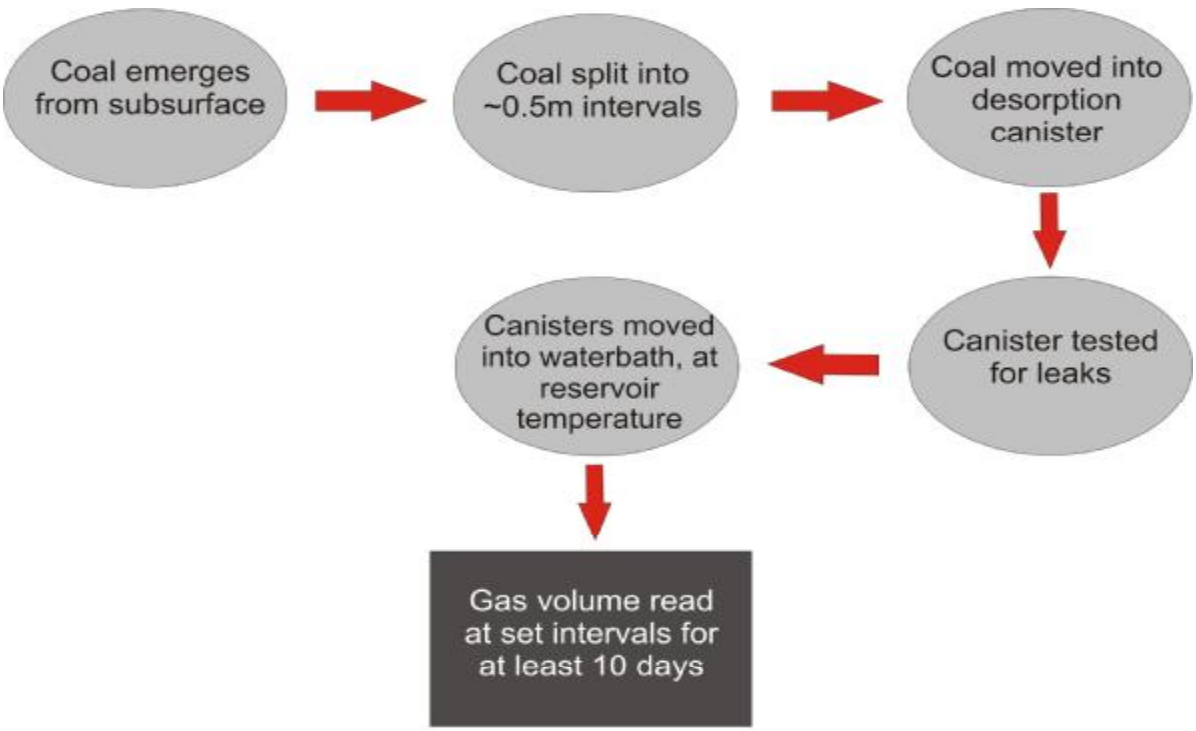

Figure 2.8: Flow chart of procedure used in gas desorption measurements.

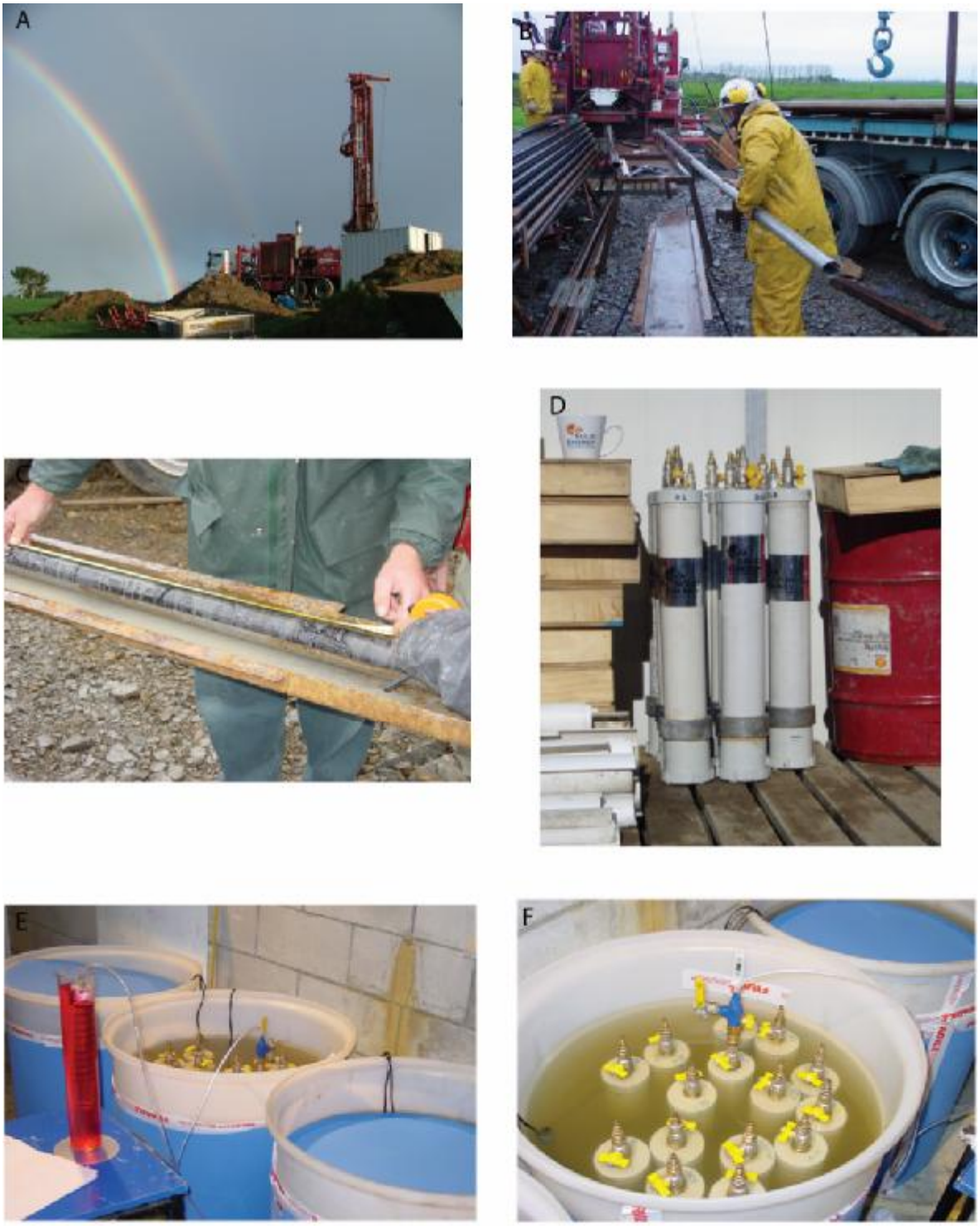

Figures 2.9 A-F: The process involved in collecting samples for gas desorption. A: Drill rig in action, Huntly; B: Core run emerges from sub-surface; C: Description of core; D: Canisters used for gas desorption; E: Apparatus used for gas desorption; F: Canisters desorbing in water bath, which is kept at reservoir temperature.

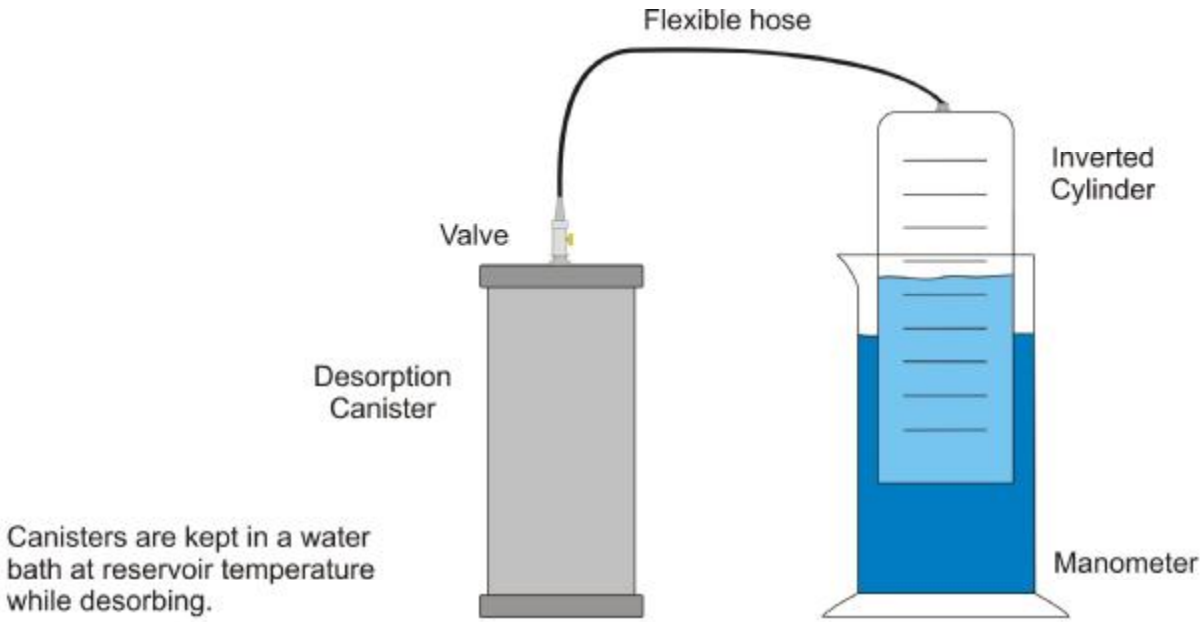

Figure 2.10: Example of gas desorption equipment used. Modified from Diamond and Schatzel (1998).

2.6.2 Adsorption Analysis

To measure the gas holding capacity of the coal, adsorption isotherms are used. Adsorption isotherms can be modelled using a variety of methods based on different theories. The extended Langmuir model (Langmuir, 1981 in: Clarkson and Bustin 2000; Laxminarayana and Crosdale, 1999; Bromhal et al., 2005) is most commonly used for the prediction of gas adsorption on coal. The Langmuir parameters required for pure component isotherms can be used to predict adsorbed volumes for gases of a mixed composition (Clarkson and Bustin, 2000). The Langmuir isotherm is based on two-parameters, P_L and V_L, and models a multi-component adsorption isotherm using the Langmuir equation: $V_A=V_L*P_H/(P_L+P_H)$. The Langmuir volume, V_L, represents the physical monolayer adsorption capacity of the coal, while the Langmuir pressure, P_L, is a mathematical value which is equal to the pressure at half the Langmuir volume, which may yield information on the heterogeneity of the pores (Laxminarayana and Crosdale, 1999). P_H represents the hydrostatic pressure.

Methane adsorption isotherms were determined by Energy Resources Consulting Pty Ltd, formally Coalseam Gas Research Institute. The process involved two steps: sampling and methane isotherm determination (Crosdale, 2004; Crosdale, 2003a; Crosdale 2003b). In order to determine methane adsorption isotherms, a gravimetric technique using nine pressure steps (up to a maximum pressure of 8 MPa) was used. Analysis was executed as close as possible to the reservoir temperature of the coal.

Sampling involved core being stored at - 10°C until processed. The core was initially crushed to less than 4mm, then sub-sampled to obtain between 200-250g of coal. The whole thickness of the coal was sampled to get a representative sample. The sample was then crushed to < 0.212 mm and bought to an equilibrium moist state. Equilibrium moisture content, ash yield and helium density were determined prior to methane adsorption analysis.

Adsorption isotherm 'bombs' were weighed, evacuated, and weighed again. The equilibrium moist coal was placed in the bombs, and the bombs were weighed, evacuated, and weighed a second time. Helium was introduced into the bombs, and the bombs were weighed at helium pressures of approximately 1, 2, 3 and 4 MPa; these data are used to calculate the free volume of the bombs and consequently the helium density of the coal. The bombs are evacuated and weighed again. A fixed volume of methane was introduced into the bomb and the pressure was monitored to the nearest 1 kPa until there was no change of pressure for a period of at least one hour. The bomb was weighed. The last stage of methane introduction was repeated for each pressure step.

The results were tabulated and presented graphically as isotherms. Isotherm results were calculated to standardized conditions of 20°C and 1 atmosphere (101.3 kPa) pressure, and indicate the maximum holding capacity of the coal.

2.6.3 Saturation levels

Saturation of the coal is calculated using a combination of desorption and adsorption data. Saturation indicates how much gas the coal holds relative to its maximum holding capacity.

Because each location has only one adsorption isotherm, the downhole saturation content is calculated on the assumption that the holding capacity is constant throughout the drill hole. Two steps are involved in the calculation of saturation:

1) Calculation of the adsorption gas value at a set pressure;
2) Calculation of saturation.

Step one involves the following inputs and calculations:

a) Input sample depth, D_S

b) Calculation of hydrostatic pressure, P_H (in MPa):

i) D_S * constant 0.096 = pressure (in atm)

ii) pressure * constant 0.101325 = hydrostatic pressure, P_H

c) Calculation of adsorption value, V_A (in m^3/t) using Langmuir coefficients V_L and P_L, at a set pressure P_H:

i) $V_A = V_L * P_H / (P_H + P_L)$

Step two involves the following inputs and calculations:

a) Calculation of saturation, as a percentage of the holding capacity V_A:

i) $1-((V_A-V_D)/V_A)$

where V_A is the adsorption value, and V_D is the desorption value, that is total gas, at a specific depth.

2.6.4 Gas Quality

Gas quality was determined from the collection of gas samples from coal filled canisters. The gas was analysed for CH_4, CO_2, C_2H_4, C_2H_6, H_2, N_2, and O_2. Samples were collected on site, as gas canisters were being desorbed. Canisters used for gas quality were left unread from measured gas readings to allow gas to accumulate. In some cases, because of minimal gas volumes, composite gas measurements were taken from several canisters, to obtain high enough gas volumes to analyse gas quality. High quality Teflon bags with a single polypropylene fitting and shut-off value, and a rubber hose were used to collect gas samples from the coal core. A rubber hose was attached to the end of the canister being read, with the other end fixed to a Teflon bag. Gas was fed into the Teflon bag by opening the canister valve and feeding through the gas which had desorbed (G. Gillard, pers. comm. Solid Energy NZ Ltd, 2006). Analyses were made using a gas chromatograph with ppm detection limits for minor hydrocarbons, and 0.5% precision limits for N_2, O_2 and CH_4. Three corrections were then applied to the raw results: removal of Ar, air (O_2 and N_2 using a N_2/O_2 ratio) and remaining N_2, all assumed to be products of air contamination (Pope, 2005).

2.6.5 Stable Isotopes

Stable Isotopes were analysed by Geological and Nuclear Sciences, in Lower Hutt, New Zealand. Sample and analysis proceedings are given in Lyon, (2004), but are also briefly explained here. A sample of gas was admitted to a gas chromatograph where CH_4 was separated from CO_2 and other gases. Methane was oxidized by reaction of CH_4 with copper oxide at 800°C to form CO_2 and H_2O for stable isotope analysis. For δ^2H (=δD) analysis, H_2O from oxidation of CH_4 was collected and transferred to a tube containing zinc. The tube was sealed, heated to 500°C to reduce H_2O to H_2 for stable isotope analysis.

The isotope ratios were measured using standard mass spectrometer procedures (Lyon, 2004) and reported as deviations from internationally recognize standards as $\delta^{13}C$ and δ^2H values in parts per thousand ($^0/_{00}$). Analytical precision for $\delta^{13}C$ is ~± 0.2 $^0/_{00,}$ and for δ^2H ~± 5 $^0/_{00.}$

Chapter Three

Results

3.1 Coal type distribution

All locations had coal with two predominant matrix lustres: bright and dull. Within each of these lustre types, there were variable amounts of vitrain bands ranging from essentially no bands ('non-banded') to greater than 20% vitrain bands These coal types are were also found by Ferm et al. (2000) and Ferm and Moore (1997) in the Huntly and Greymouth coalfields respectively. The vitrain percentages were quantitatively determined and the results are given in Appendix C.

The predominant coal types in the Huntly core were bright non-banded (24 %) and bright coal with less than 20 % vitrain bands (54 %). At the centre of the seam and near the base of the seam the coal type changed to greater than 20 % vitrain banded (Fig. 2.5).

The Greymouth core is highly variable in terms of coal type (Fig. 2.5). Unlike the Huntly core which was predominantly coal with a bright lustre matrix, the Greymouth core has multiple dull coal/high ash layers throughout (these account for 34 % of the core). Bright coal with greater than 20 % vitrain is found near the centre and at the base of the seam. Interestingly, the Greymouth coal contains no bright, non banded material.

Compared with the Huntly and Greymouth cores, the Ohai SC3 core contains the most banded coal (82 % of the core). Again, bright coal with greater than 20 % vitrain bands resided at the base of the seam, as well as throughout the centre of the column (Fig. 2.5). The SC1 column has dull coal (23 %) scattered throughout the banded material (Fig. 2.5).

3.2 Geochemistry and Mineralogy

3.2.1 Proximate analyses

Proximate analyses (moisture, volatile matter, ash yield, fixed carbon), as well as sulphur and calorific value, are displayed in Appendix D. Figure 3.1 shows the average values for volatile matter (daf), ash yield (db), sulphur (daf), and calorific value (daf). Of note are the large standard deviations in the volatile matter. The volatile matter also shows considerable downhole variation in each of the four cores (Fig. 3.2). In order to assess the rank of the coal, volatile matter has been combined with calorific value to help determine true rank changes from coal type changes (see Chapter sections 2.4 and 3.3.)

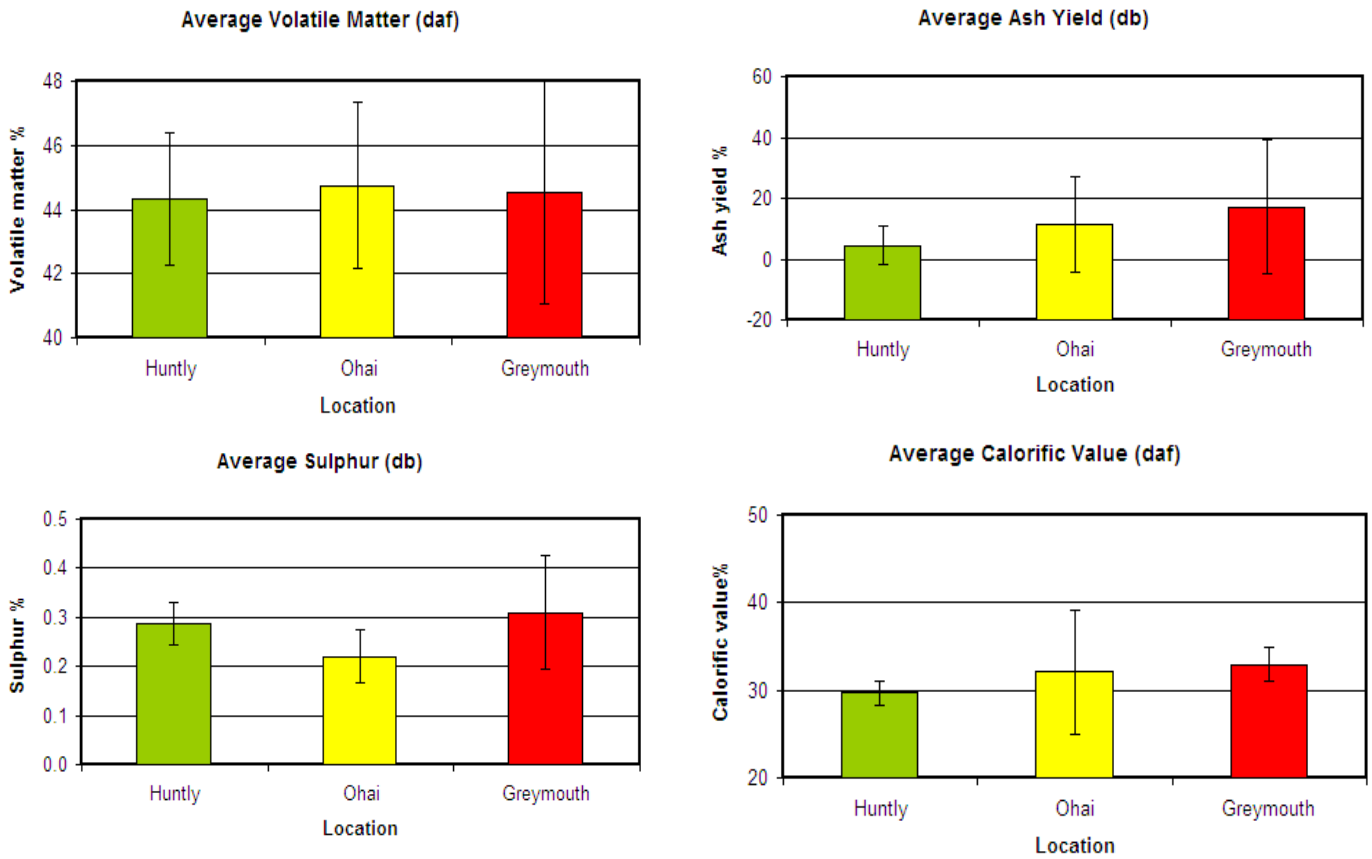

Figure 3.1: Average values for volatile matter, ash yield, sulphur and calorific value, in the Huntly, Ohai and Greymouth cores. Bars on graphs represent standard deviation of data.

Ash yield (db) ranges from 1.1% to 36.4% in the Huntly core samples; from 1.3% to 44.7% in the Ohai SC3 core samples and 1.4% to 75.5% in the Greymouth core samples. However it should be noted that ash yield is on average low in all three areas (Appendix D). The Ohai SC1 core has the highest ash yield, ranging from 5.2% to 55%. This is because multiple high ash layers are present. Average ash yields in both the Huntly and Ohai SC3 coals are very low when partings are removed from the dataset (3.6% and 1.8 % respectively).

3.2.2 Introduction to mineral matter

Although ash yield is commonly used to estimate the inorganic proportion in coal, because of the high temperatures of the technique, some minerals are volatised. However, a low temperature plasma asher (LTA) can be used, and this preserves mineral matter relatively untouched. Mineral matter is the term used to describe all the inorganic components found in coal. Mineral matter can consist of three different constituents: dissolved salts and other soluble material in the pore water, inorganic components dispersed with the organic compounds, and discrete organic particles (minerals, both crystalline and non-crystalline) (Ward, 2002). This study has used a variety of methods to look at the inorganic components (petrography, XRF and XRD analysis).

Generally clays make up approximately 60 – 80 % of total mineral matter in coals. The most common clays found are kaolinite, illite and sericite (white mica). Clays can occur in two forms; either as fine dispersed material, or as a kaolin-coal tonstein, however, no tonsteins were observed in any of the drill cores. In the three locations studied, kaolinite and illite are the only clays identified in this study through XRD analysis. Illite refers to a degraded form of muscovite / hydrous mica group of minerals, and is present in trace amounts in the Greymouth area. Because of the preparation method used for XRD analysis, the term illite will also represent muscovite (Newman, 1988). Illite was also observed by Shearer (1992) in the Morley Coal Measures, Ohai. Illite has been found in coals with marine roofs, while kaolinite is associated with non-marine influenced coals (Taylor, 1998). Ohai, Greymouth and coal from the northern Waikato basin all had very little marine influence, which explains the dominance of kaolinite. Although coal from the southern Waikato subregion formed in a coastal environment and was subjected to marine influence, mineral matter is low and no illite was observed. The lack of illite observed may be the result of poor crystallinity of the mineral, which would make it impossible to be identified under XRD analysis (Newman, 1988).

Clays are either detrital in origin, or form as a secondary mineral from aqueous solutions. Clays were often observed infilling pore spaces using optical microscopy, particularly in semi-fusinite and fusinite macerals. Under the microscope the clay family tend to have no surface reflection and have shallow internal reflections. Crystal boundaries are often present, and they appear translucent, which arises from the platyness of the mineral (J. Newman, pers. comm., Newman energy research, 2005).

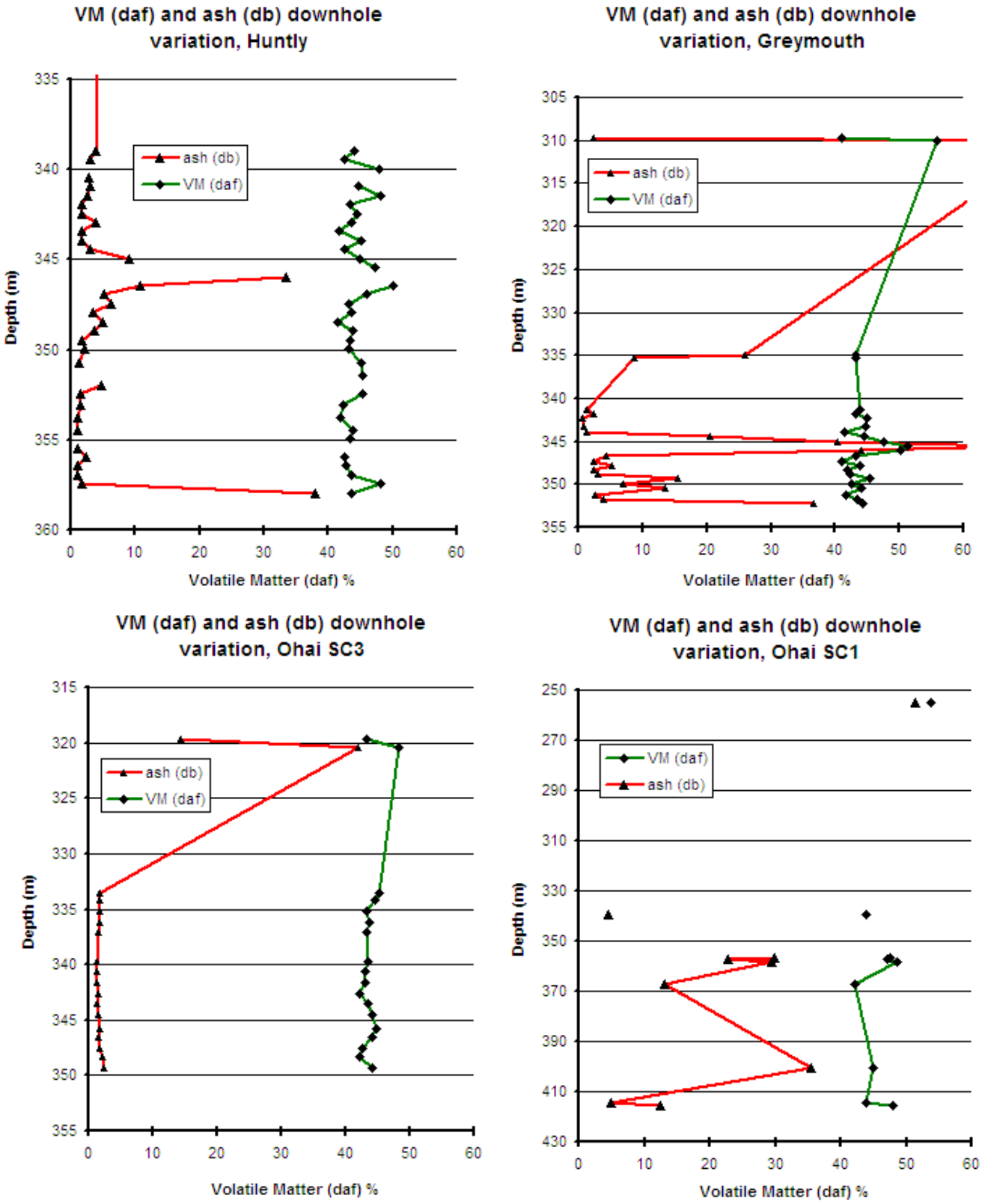

Figure 3.2: Down hole variation of ash yield (db) and volatile matter (daf) in Huntly, Ohai SC3 and SC1, and Greymouth cores, depth from surface.

Quartz is the most important of the oxide minerals, and is mostly introduced at peat stage. Clastic quartz grains are bought into the peat by water or air. Quartz is common throughout all locations studied and is normally the dominant mineral, only locally exceeded by kaolinite in a few places. Under the microscope quartz is observed dispersed throughout the desmocollinite, and has surface reflections and deeper internal reflections.

There tends to be two groups of carbonates, a syngenetic (early formed) group, comprising siderite and dolomite, and a secondary, late stage group comprising calcite and ankerite. The secondary carbonates will fill cracks, fractures and fissures during coalification, which was observed in all locations.

3.2.3 Ash constituents

Ash constituents are displayed in Appendix E. Major elements are reported as the simplest oxide, except for Mn, which has been reported as Mn_3O_4, because of lab procedures (G. Murray, pers. comm., CRL Energy Ltd, 2006). Figure 3.3 shows the average ash constituents found in each location.

Ash constituents from the Huntly core show some interesting trends. SiO_2 and Al_2O_3 contents are high mid seam (SiO_2 ~25-58 %; Al_2O_3 ~20-30 %), with SiO_2 also high near the roof of the seam (~41-58 %). CaO steadily increases to mid seam, where levels decrease rapidly (relative to the rise in SiO_2 and Al_2O_3). This increase in SiO_2 and Al_2O_3 and decrease in CaO occurs at the same place as a high ash layer occurs. SO_3 is relatively high throughout the seam (~15-25 %), except where it declines mid seam. Fe_2O_3 maintains relatively constant levels throughout the first half of the seam (~6 %), with concentrations decreasing mid seam (~3 %), then increasing at the base of the seam (~ 10%). The small seam split which occurs around canister 36 is noted by a decrease in SiO_2 and Al_2O_3, and a large rise in CaO content (Fig. 3.4).

Ash constituents for the Ohai SC3 core show SiO_2 levels highest in the top rider seam (~60 %), compared with the main coal seam. In the main coal seam the SiO_2 content also decreases towards the base. However, Al_2O_3, MgO and Fe_2O_3 are constant throughout the main seam. CaO increases towards the base of the seam. CaO content is much higher in the main coal seam (~20-30 %) than in seam one (0.77-4.19 %, Fig. 3.5). SiO_2 and Al_2O_3 contents in the Ohai SC1 core are highest mid seam (SiO_2 ~70 %; Al_2O_3 ~30%), while Fe_2O_3 levels fluctuate heavily (0.92-18.76 %, Fig. 3.6).

High levels of SiO_2 (mean value 70.21 %) dominate the Greymouth core (Fig. 3.7). Although SiO_2 concentrations fluctuate throughout the seam, there is a general increase towards the base. K_2O content is highest at the roof of the seam (~2 %), but peaks again mid seam (~4 %). Fe_2O_3 content varies throughout the core, with peaks both near the roof and mid seam. TiO_2 is fairly consistent through the profile in small quantities, whereas SO_3 levels are nominal.

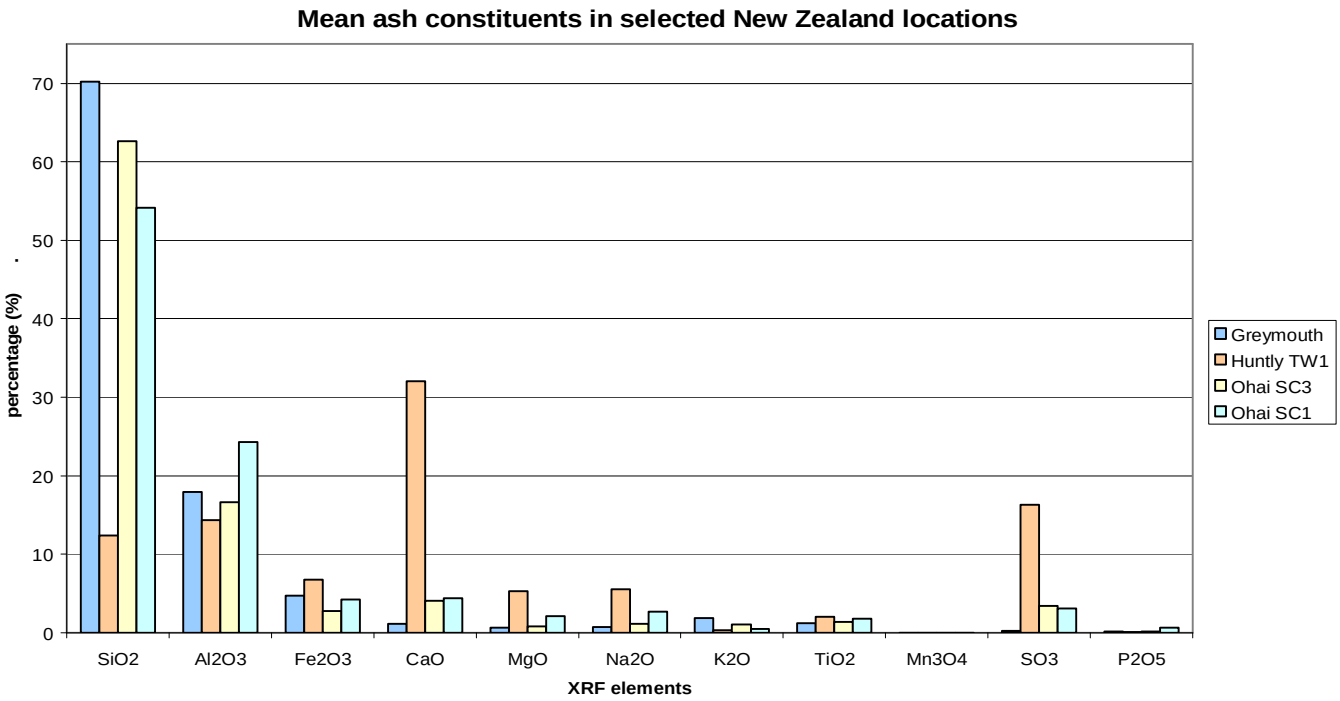

Figure 3.3: Mean values of ash constituents for Huntly, Ohai SC3, Ohai SC1 and Greymouth drill cores.

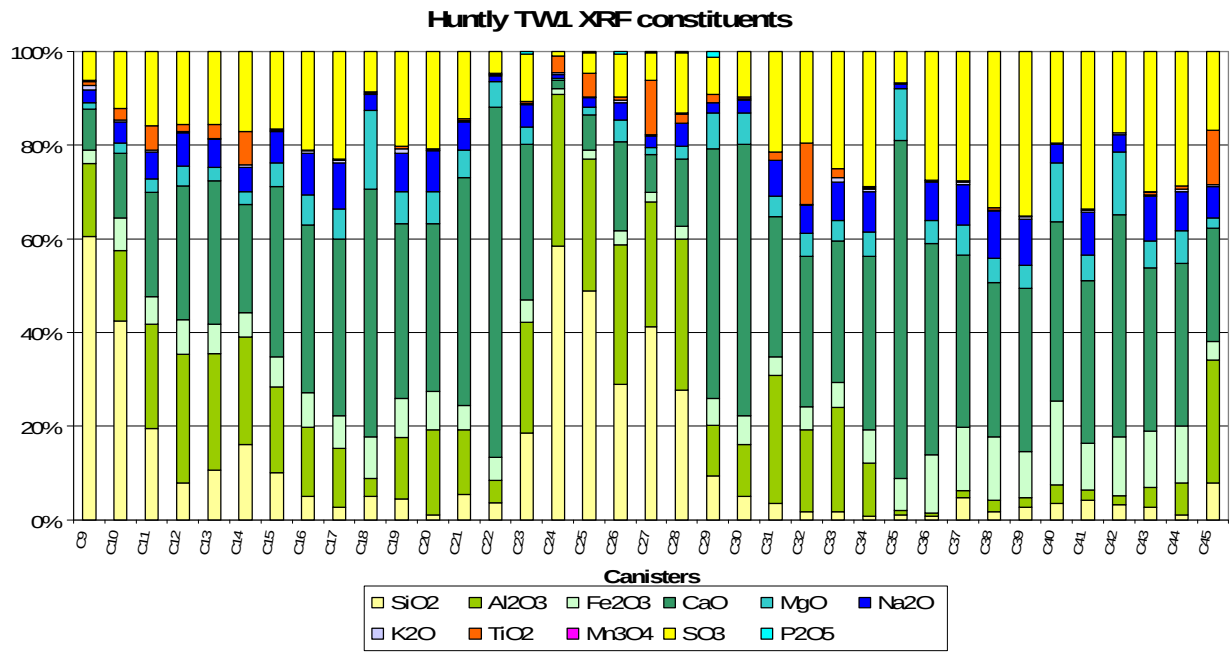

Figure 3.4: Percentage of ash constituents, by canister intervals (x-axis), in the Huntly drill core.

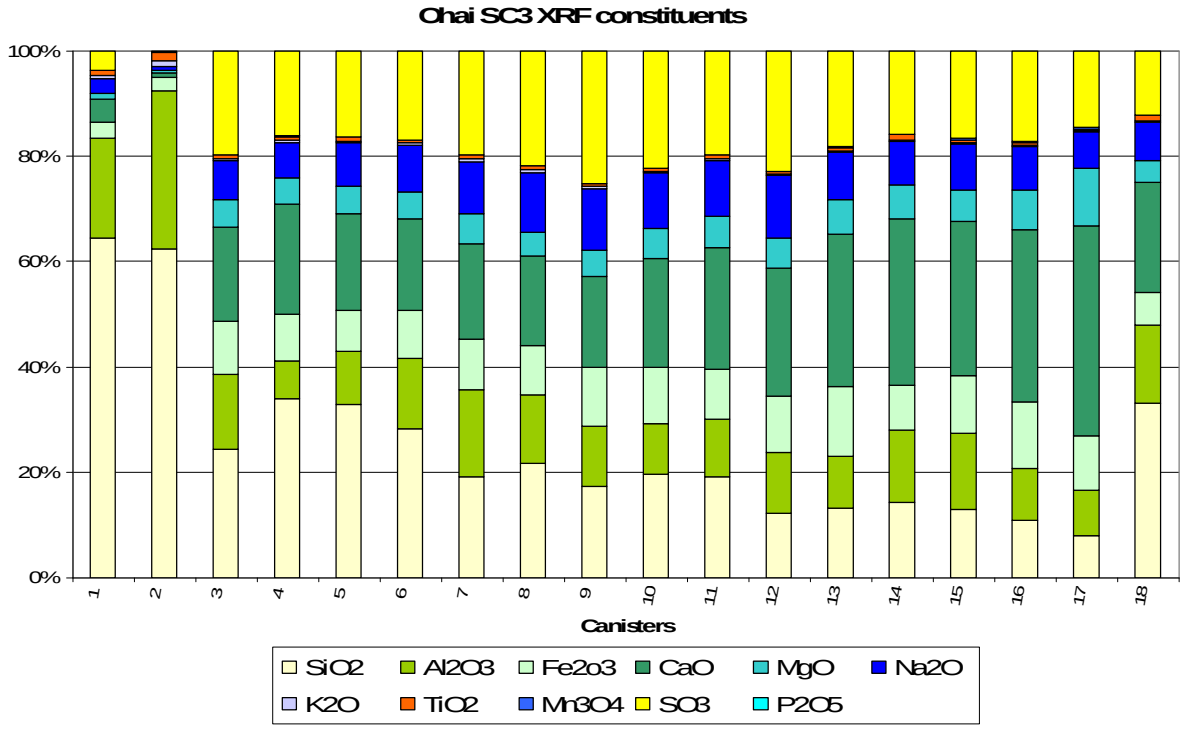

Figure 3.5: Percentage of ash constituents, by canister interval, in the Ohai SC3 drill core.

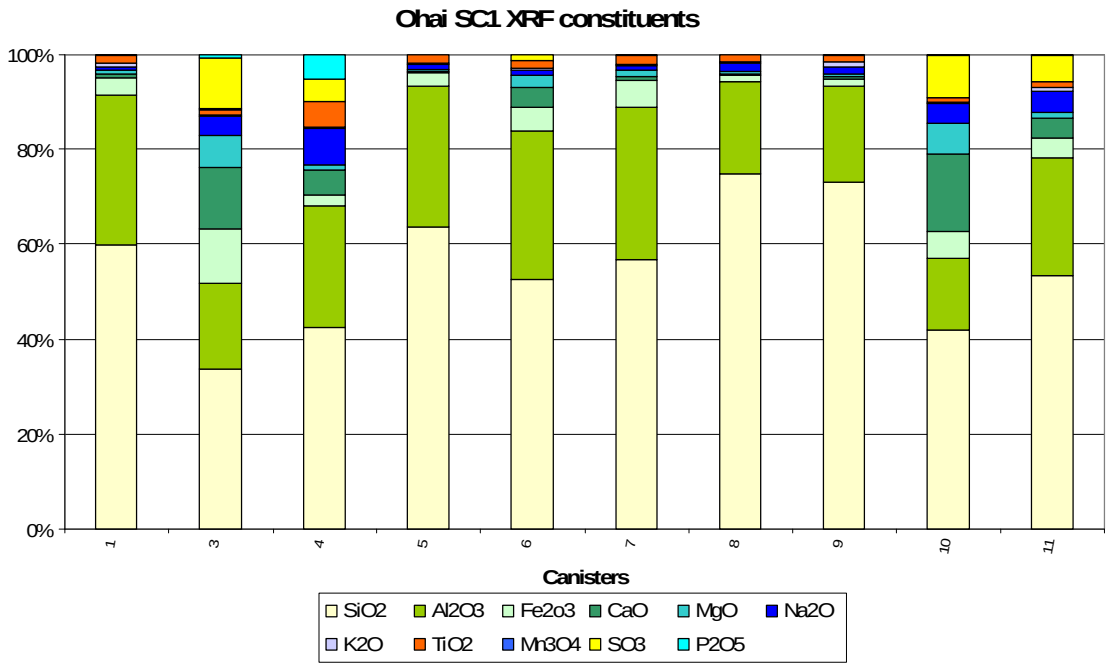

Figure 3.6: Percentage of ash constituents, by canister interval, in the Ohai SC1 drill core.

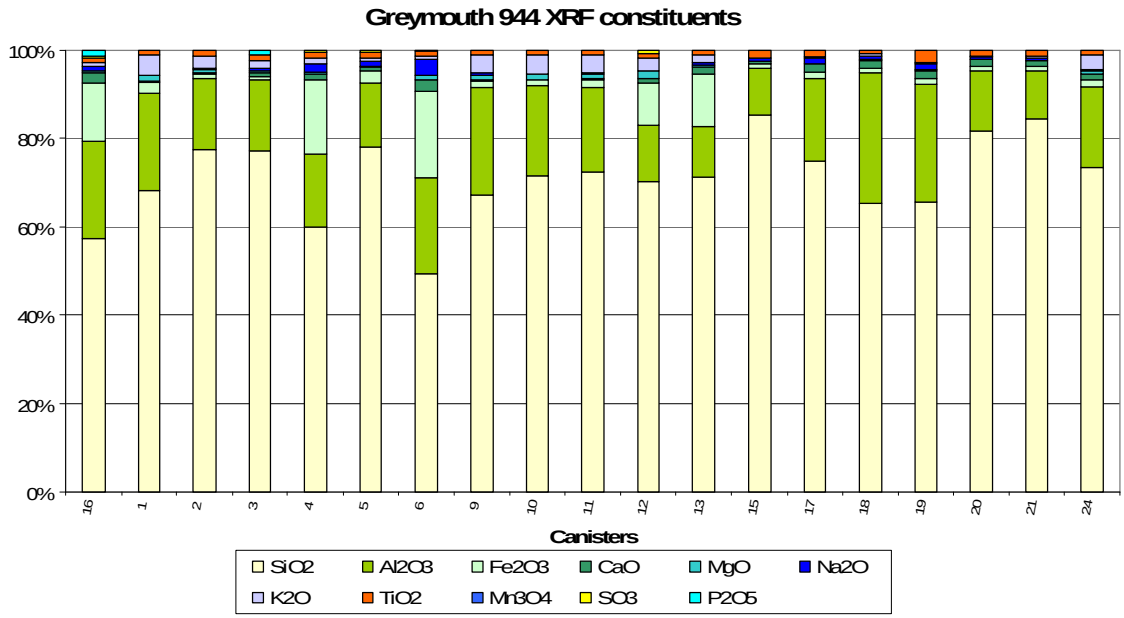

Figure 3.7: Percentage of ash constituents, by canister interval, in the Greymouth 944 drill core.

Ash constituents do not add up to 100% in all plies (Table 3.1). This is because there is a considerable portion (nearly up to 10% in some plies) of other elements present. Whole coal elemental scans using pressed coal pellets showed significant portions of Sr , along with smaller amounts of Zn, Ni, Cu, Ba, and Ce.

Table 3.1: Total of major elements plus loss on ignition, XRF analysis.

Location	Low (%)	Mean (%)	Std
Huntly	90.87	96.61	3.36
Ohai SC1	95.6	98.63	1.74
Ohai SC3	95.72	97.28	1.57
Greymouth	96.43	100.28	1.98

3.2.3 Mineralogy

Thirty-one samples were processed for X-Ray diffraction (XRD): ten samples from the Greymouth 944 coal core, 5 samples from The Ohai SC1 coal core, 9 samples from the Ohai SC3 coal core and 8 samples from the Huntly TW1 coal core. Tables 3.2 and 3.3 summarises the minerals identified and the relative quantities of the minerals present, along with minerals recorded from the samples in the microscopic analysis. Figure 3.8 delineates the average mineral matter content and type found in each location, while Figure 3.9 shows the mineralogy in each ply.

Quartz and kaolinite were the most common inorganic components found in the Huntly coal core. Quartz ranged from nil occurrence to 95 %, whereas kaolinite ranged from nil occurrence to 100 %. The carbonates

calcite and ankerite were also present in one sample, with calcite being the dominant carbonate (75%). Three plies showed no minerals present; in the microscopic analysis they also yielded no minerals.

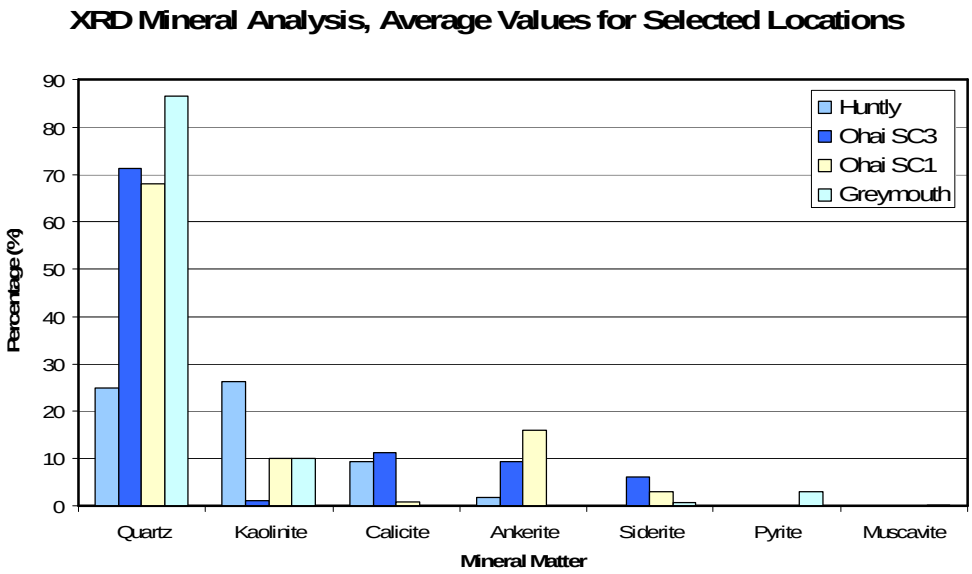

Figure 3.8: Percentage of average XRD mineral matter in the Huntly, Ohai and Greymouth cores.

Quartz, kaolinite, calcite, ankerite, and siderite dominate the Ohai SC3 coal core. Quartz ranges from 100 % in one ply to just 20 % in another. Kaolinite either occurs with quartz (or in one case with quartz and calcite) in modest amounts (5 – 20 %), or not at all. The carbonates calcite, ankerite and siderite are present in many plies, and are in fact only absent from plies nearer to the roof of the seam. Their quantities range from 5 – 50 %. Ohai SC1 shows similar minerals present. The carbonate siderite makes an appearance in one of the plies, which is dominated by ankerite (40%). Apart from this ply, quartz is the dominant mineral, making up as much as 90 % of the mineral matter in one ply. Previous research on the Morley Coal Measures (Shearer, 1992; Sykes, 1985) also supports the general occurrence of quartz, kaolinite, calcite and siderite. However, the work of Shearer (1992) and Sykes (1985) shows a generally wider assemblage of minerals. These additional minerals include dolomite, rutile, illite and pyrite.

The most common mineral found in the Greymouth coal core was quartz, ranging from 75 – 95 %. Kaolinite was the second most abundant mineral, present in every sample tested, ranging from 5 – 20 %. The carbonate mineral siderite was present in two plies, as was the sulphide pyrite. Trace amounts of muscovite were also present in two plies. Previous research on the mineral matter in the Greymouth coals (Paparoa Coal Measures) by Li (2002) also found the same minerals. However, Li's (2002) work show a broader range of minerals present including illite and smectite from the clay family; calcite and ankerite from the carbonate family; and trace amounts of minerals such as gypsum, apatite, halite and sylvite. Crocoite, an unusual mode of occurrence for lead in coal, was also identified (Li et al., 1999, 2001a).

Table 3.2: Mineral occurrences in selected samples, from XRD analysis.
see Fig. 2.5 for sample locations.

Huntly	Quartz	Kaolinite	Calcite	Ankerite	Siderite	Pyrite	Muscovite
c10	√	√					
c11	√	√					
c19	√	√					
c21	√		√	√			
c28		√					
c32							
c37							
c43							
Ohai SC3							
c1	√	√					
c3	√	√					
c7	√		√	√	√		
c9	√						
c12	√		√	√	√		
c13	√		√	√	√		
c15	√		√	√	√		
c17	√		√	√	√		
c15 x28	√	√	√				
Greymouth							
c16	√	√			√		
c5	√	√			√	√	
c6	√	√					
c6p8	√	√				√	
c13	√	√				√	√
c13p17	√	√					
c15	√	√					
c20	√	√					
c20	√	√					
c21	√	√					√
Ohai SC1							
c3	√	√		√	√		
c4	√	√	√				
c8	√	√					
c10	√	√		√			
c11	√	√					

Table 3.3: Mineral percentages in selected samples, from XRD analysis.
see Fig. 2.5 for sample locations.

Huntly	Quartz	Kaolinite	Calcite	Ankerite	Siderite	Pyrite	Muscovite
c10	95	5	0	0	0	0	0
c11	45	55	0	0	0	0	0
c19	50	50	0	0	0	0	0
c21	10	0	75	15	0	0	0
c28	0	100	0	0	0	0	0
c32	0	0	0	0	0	0	0
c37	0	0	0	0	0	0	0
c43	0	0	0	0	0	0	0
Ohai SC3							
c1	95	5	0	0	0	0	0
c3	95	5	0	0	0	0	0
c7	85	0	5	5	5	0	0
c9	100	0	0	0	0	0	0
c12	60	0	10	15	15	0	0
c13	45	0	25	10	20	0	0
c15	70	0	15	5	10	0	0
c17	20	0	35	40	5	0	0
c15 x28	20	30	50	0	0	0	0
Greymouth							
c16	80	15	0	0	5	0	0
c5	80	10	0	0	1	10	0
c6	95	5	0	0	0	0	0
c6p8	75	15	0	0	0	10	0
c13	85	5	0	0	0	10	1
c13p17	95	5	0	0	0	0	0
c15	80	20	0	0	0	0	0
c20	90	10	0	0	0	0	0
c20	95	5	0	0	0	0	0
c21	90	10	0	0	0	0	1
Ohai SC1							
c3	25	10	0	40	15	0	0
c4	85	10	5	0	0	0	0
c8	90	10	0	0	0	0	0
c10	55	5	0	40	0	0	0
c11	85	15	0	0	0	0	0

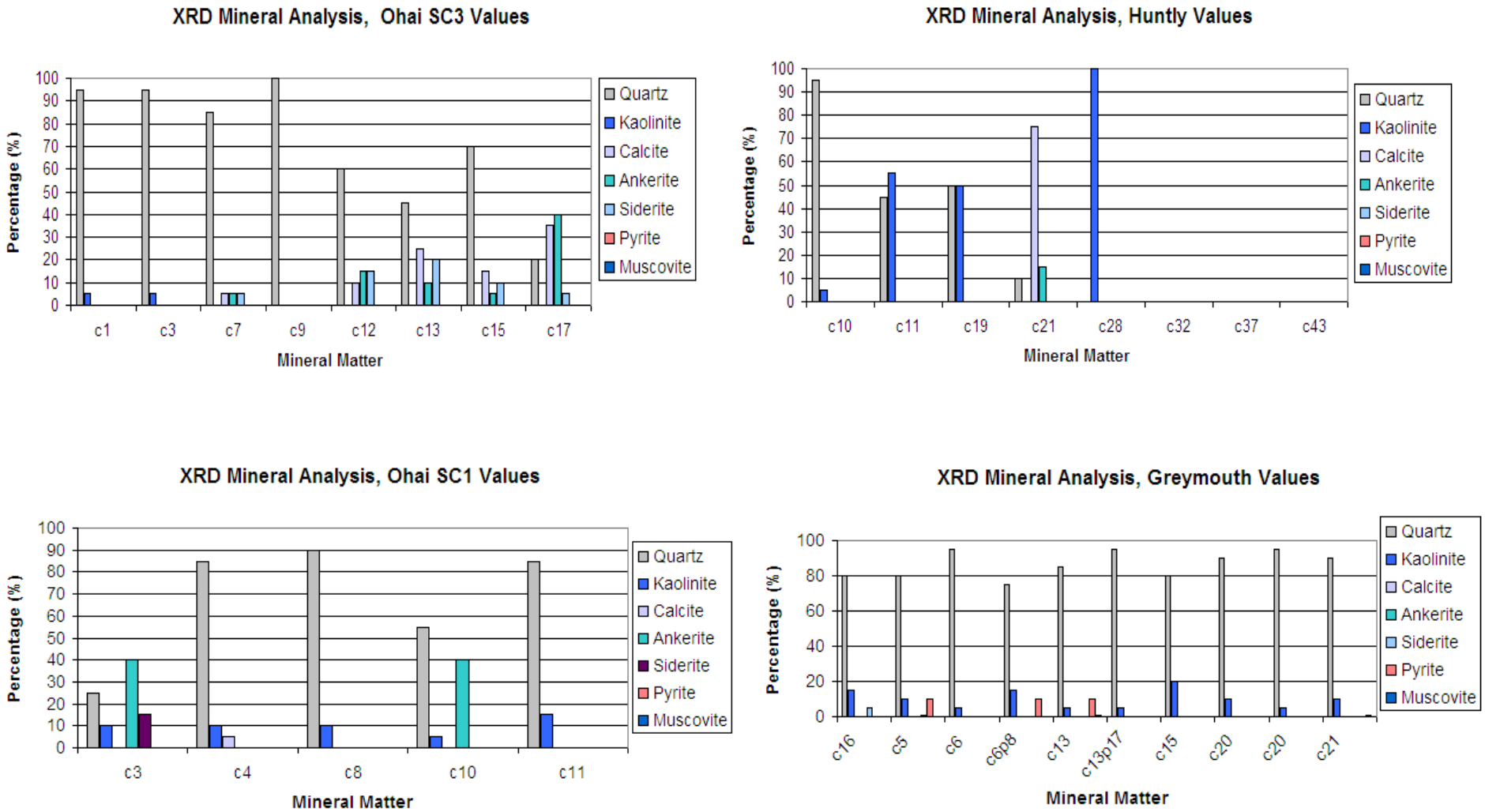

Figure 3.9: Percentage of XRD mineral matter in each canister, for Huntly, Ohai and Greymouth cores. Canister/sample intervals are shown on the x –axis, see Fig. 2.5 for exact locations of sample intervals.

3.3 Rank and Suggate Rank

Rank of a coal can be estimated using volatile matter (ASTM D388, 2005b). Using this system, the Huntly coal would be classed as sub-bituminous B-A, Ohai coal as sub-bituminous C-A, and Greymouth coal high volatile bituminous A (Fig. 3.10). In all cases in-seam variation of volatile matter, and thus "rank", can be noted (Fig. 3.2). This variation is most likely a result of type changes rather than true rank differences. To differentiate between rank and type changes all samples were plotted using a Suggate plot (Suggate, 1959). The relationship between Suggate rank and ASTM rank classification is shown in Table 3.4.

When plotted on a Suggate curve (Fig. 3.11) type changes spread out along isorank lines, while rank changes spread out along the **average type line**. Average Suggate rank values are given in Table 3.5. It is important to note that the rank from all three locations is different and distinct, as illustrated in the Suggate plot. The Suggate plot shows sample variation along the isorank lines. This means that variation in the volatile matter and calorific value are from type changes, not rank changes. Although slight variation is also seen along the average type line, especially in the Greymouth core, these rank differences do not cross into the Ohai rank range. Hence, we have three distinct ranked coals.

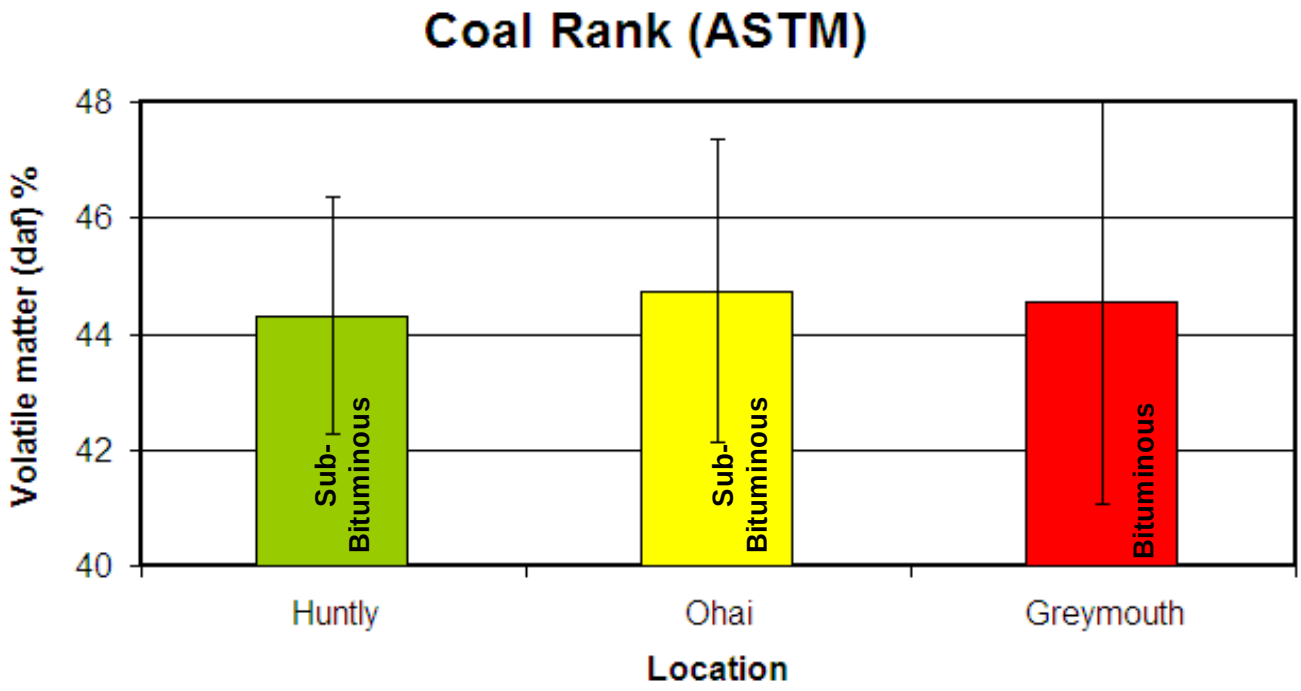

Figure 3.10: American Society for Testing and Materials (ASTM) rank classification, based on volatile matter (daf), for Huntly, Ohai and Greymouth cores.

Table 3.4; Approximate rank correlations between Suggate rank and ASTM[a] rank.

ASTM Rank	Suggate Rank
Lignite B and A	0.5 – 4.0
Sub-bituminous C, B and A[b]	4.0 – 8.0
High volatile bituminous C[b], B and A	7.0 – 14.0
Medium volatile bituminous	14.0 – 15.3
Low volatile bituminous	15.3 – 16.7
Semi-anthracite	16.7 – 19.8
Anthracite	19.8 – 27.0
Meta-anthracite	> 27

[a] Because ASTM rank classification is for industrial purposes exact correlation is not possible.
[b] The ASTM classification allows overlap between sub-bituminous A and high volatile bituminous C.

Table 3.5: Average Suggate rank values, by location.

Location	Suggate Rank
Huntly	5.7
Ohai SC1	8.6
Ohai SC3	8.3
Greymouth	10.5

3.4 Organic petrology

3.4.1 Particulate Mounts

Overall, there were only a few petrographic differences between cores for all locations (Table 3.6). Total vitrinite content ranged from 85.6% for the Ohai SC1 core to 86.9% for the Ohai SC3 core. Liptinites ranged from a high of 9.5% in Ohai SC1, to 6.6% in Ohai SC3. Total inertinite ranged from 4.7% in the Huntly core to 6.4% in the Ohai SC3 core. Ohai SC1 had the highest mineral matter content (3.4%) followed by Greymouth (1.7%). Although all locations had similar total vitrinite contents, Huntly had the least telocollinite. This telocollinite contained 9.3% cell telocollinite, compared with approximately 2% found in the other cores (Fig. 3.12). Figures 3.13 to 3.20 show the maceral composition for each sample studied in each location. Main differences between locations are described below. Figures 3.21 to 3.23 show photomicrographs of macerals and mineral matter viewed under the microscope.

Samples from the Huntly core had high concentrations of cell telocollinite, especially in samples TW1 c19, c28, c32 and c37. There was an average of nearly 10% cell telocollinite, compared with under 3% in both Greymouth and Ohai cores. Large telocollinite was low in the Huntly area, relative to the other locations studied. Huntly had only 12% large telocollinite, while all other regions contained on average over ~20% of large telocollinite.

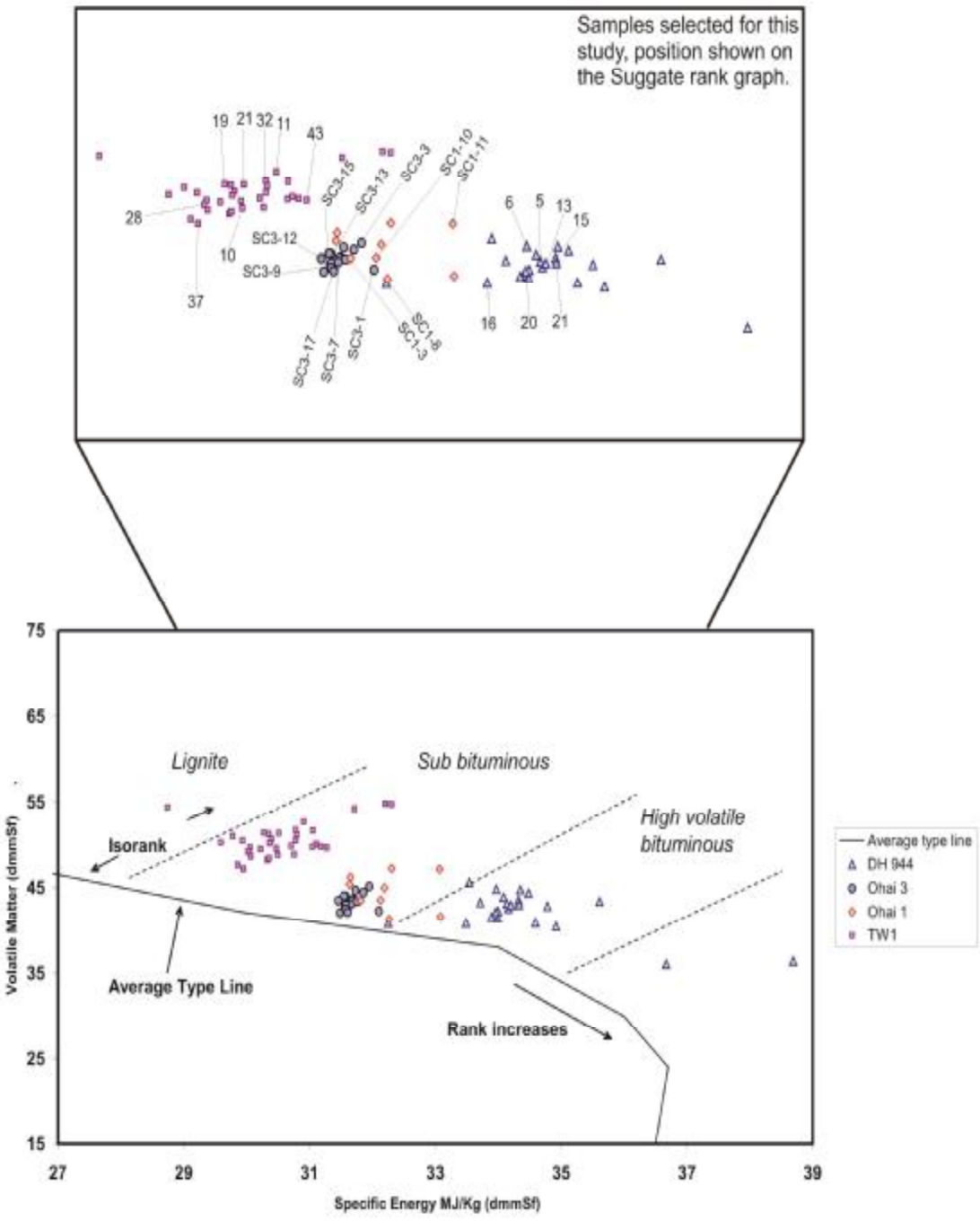

Figure 3.11: Suggate rank graph for Greymouth, Ohai and Huntly samples. Suggate rank is determined by the volatile matter (dmmSf) on the y-axis and the calorific value (dmmSf) on the x-axis. Rank variation occurs along the average type line, while coal type variation occurs along the isorank lines. Samples selected for petrographic and mineralogical analysis are outlined in the top figure.

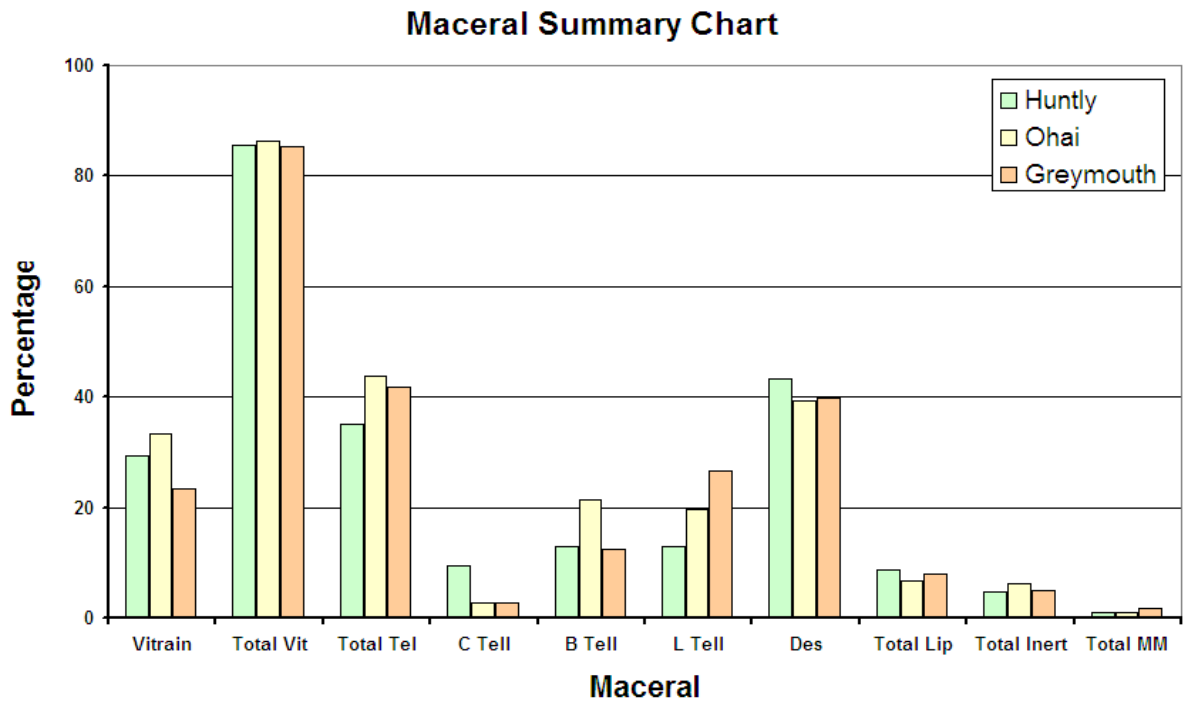

Figure 3.12: Average maceral contents in the Huntly, Ohai and Greymouth cores.

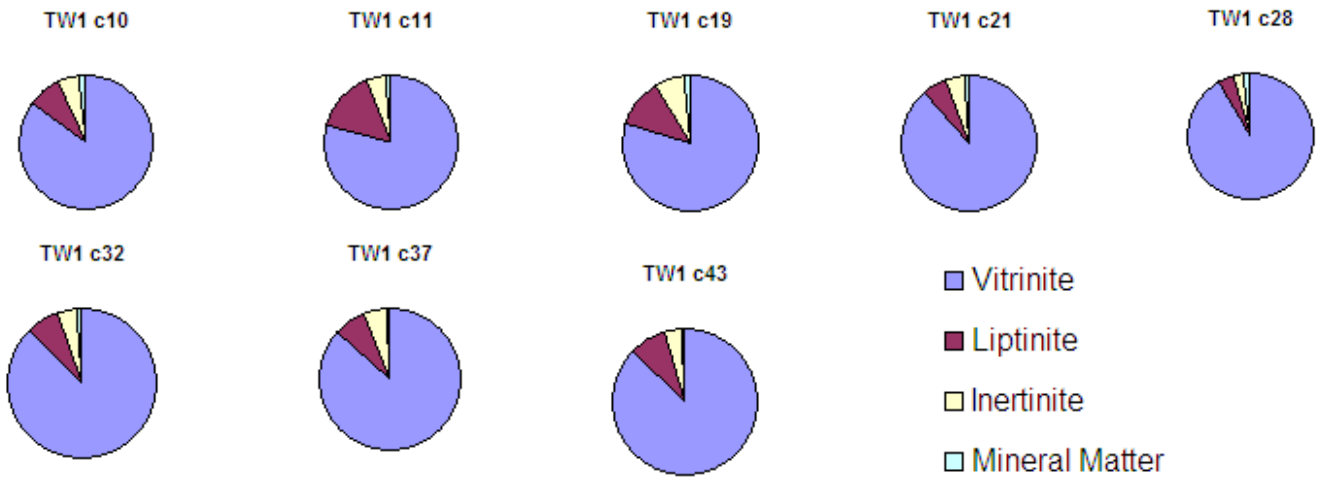

Figure 3.13: Huntly pie graphs showing proportion of maceral groups in each canister interval.

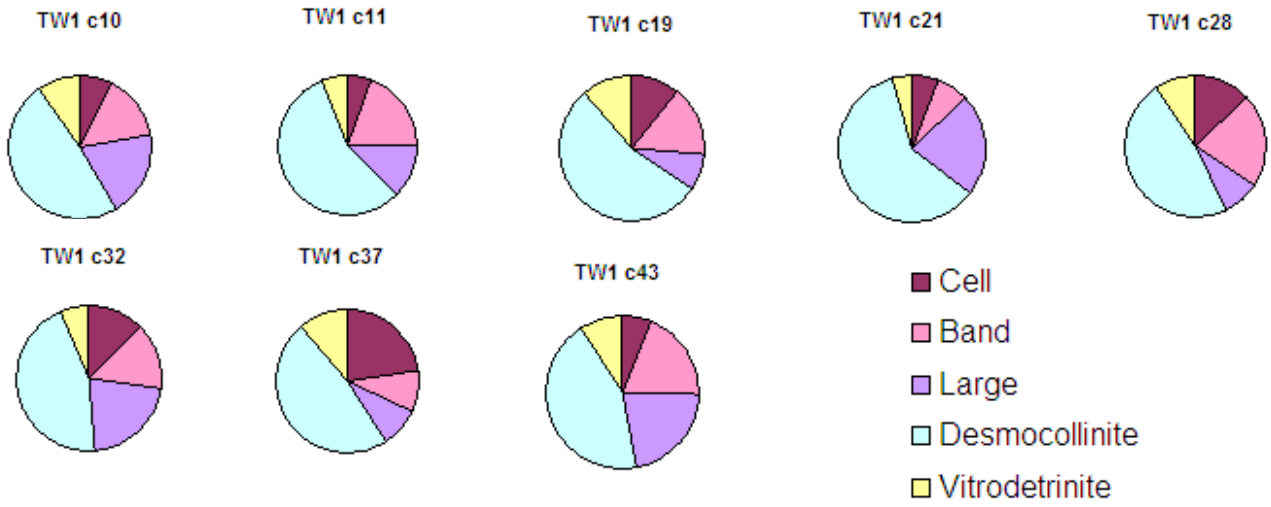

Figure 3.14: Huntly pie graphs showing proportion of vitrinite macerals in each canister interval

Samples from the Ohai SC1 core had higher mineral matter concentrations than all of the other areas, whereas SC3 had very low mineral matter content. Both Ohai locations showed high inertinites. SC1 had a high large telocollinite content (~32%). The maceral composition in SC3 was consistent throughout all the samples, both in terms of main maceral groups and in the vitrinite macerals. The biggest variable in SC3 was the amount of desmocollinite compared to large telocollinite, although desmocollinite was always the more dominant vitrinite maceral.

The Greymouth core showed a lot of variety in terms of maceral composition. Samples c15, c20 and c21 had high mineral matter content. Sample c21 also lacked inertinite. Most samples had high desmocollinite concentrations, excluding c16, c20 and c21. Samples c16 and c20 had low values of vitrodetrinite.

Figure 3.15: Ohai SC3 pie graphs showing proportion of maceral groups in each canister interval.

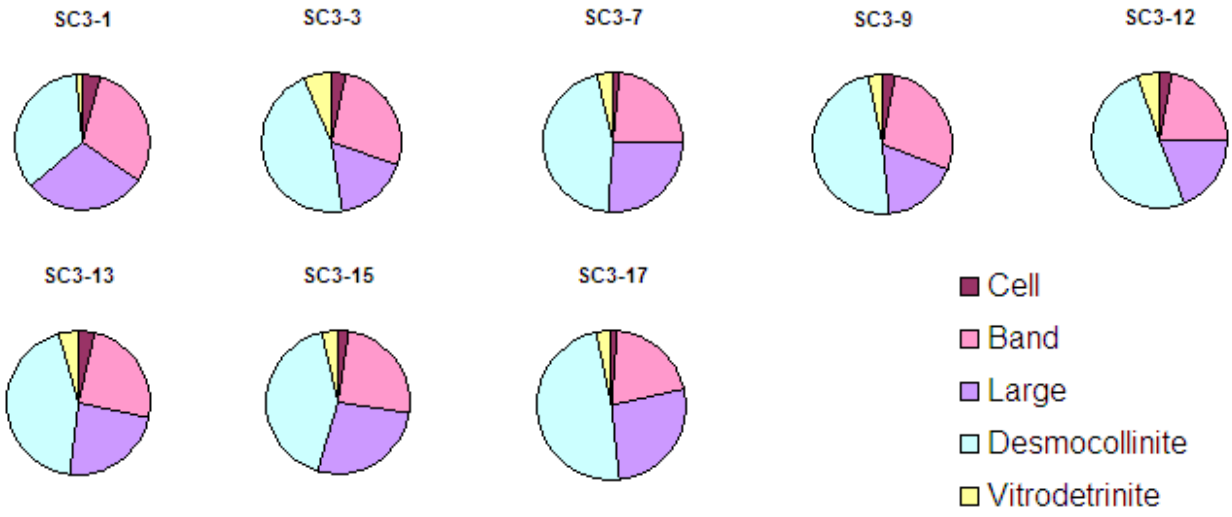

Figure 3.16: Ohai SC3 pie graphs showing proportion of proportion of vitrinite macerals in each canister interval

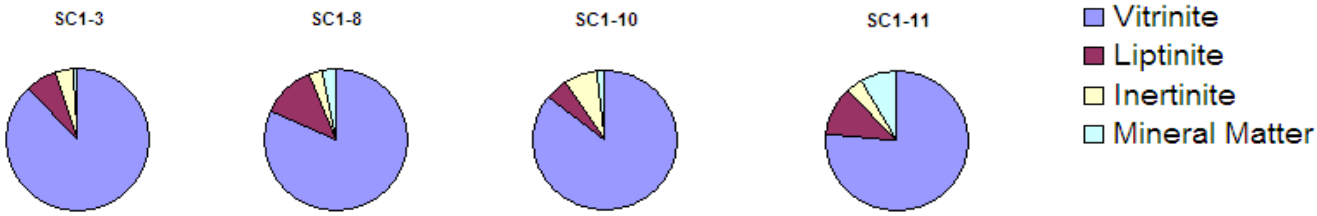

Figure 3.17: Ohai SC1 pie graphs showing proportion of maceral groups in each canister interval.

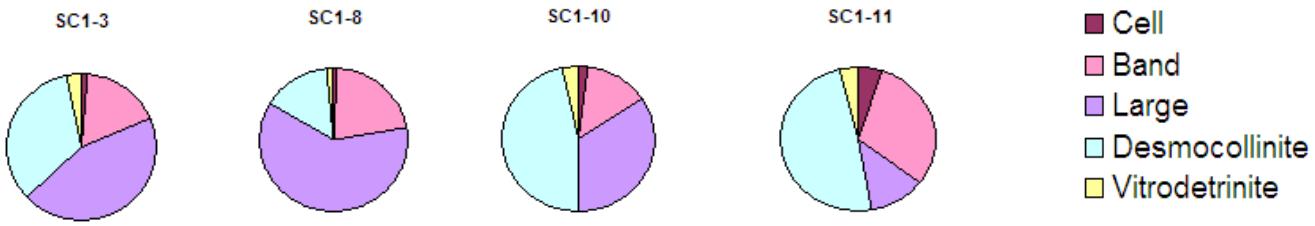

Figure 3.18: Ohai SC1 pie graphs showing proportion of proportion of vitrinite macerals in each canister interval

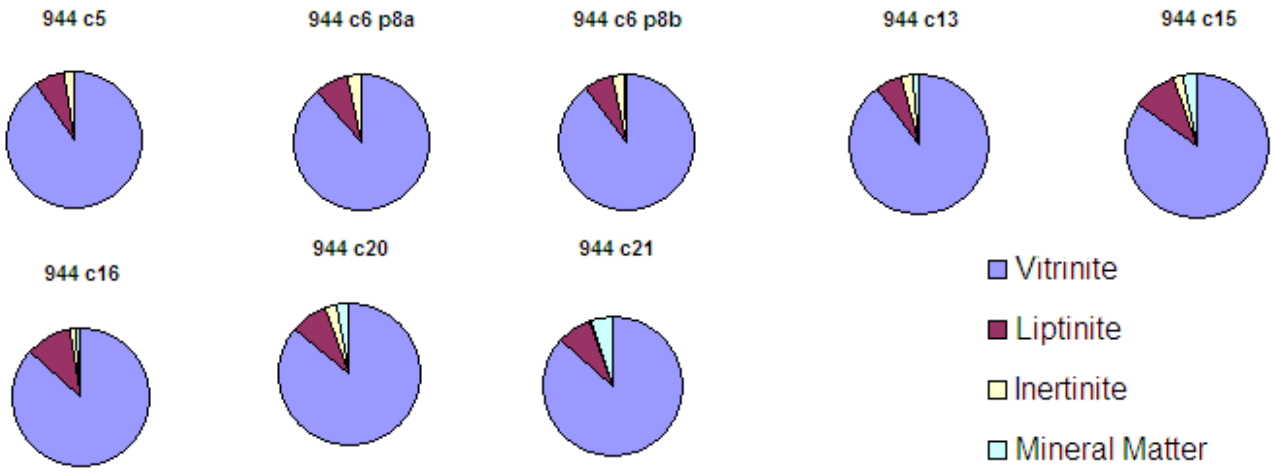

Figure 3.19: Greymouth pie graphs showing proportion of maceral groups in each canister interval.

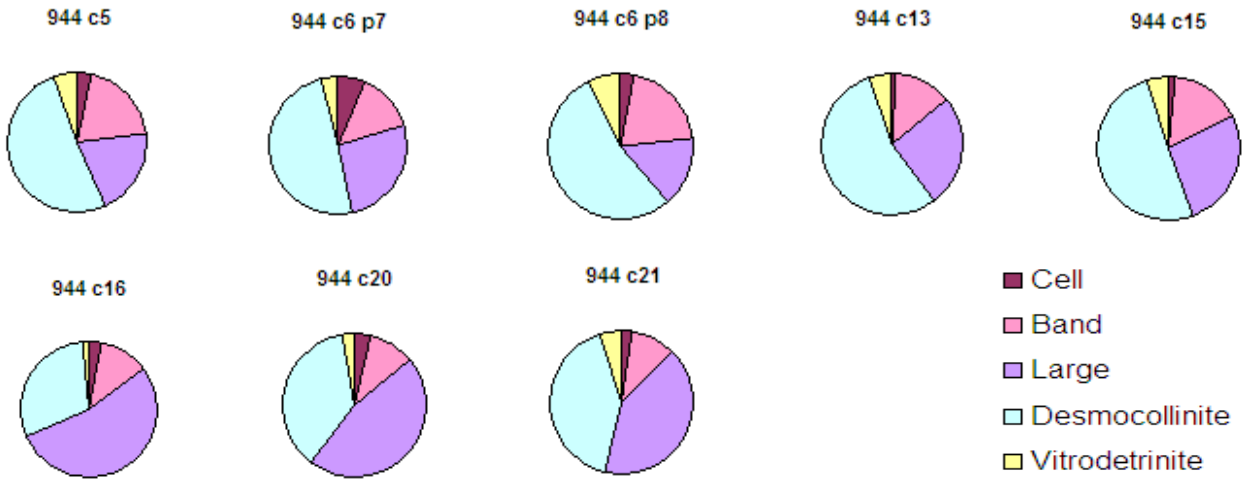

Figure 3.20: Ohai SC1 pie graphs showing proportion of proportion of vitrinite macerals in each canister interval

3.4.2 Block Mounts

Petrographic observations of the Greymouth block samples were described qualitatively to identify mineral matter present, and modes of occurrence (Table 3.7). Mineral matter was observed both infilling pore spaces and fractures (clays, carbonates and occasional pyrite) as well as detrital grains dispersed in the matrix (quartz, and occasional clay and pyrite).

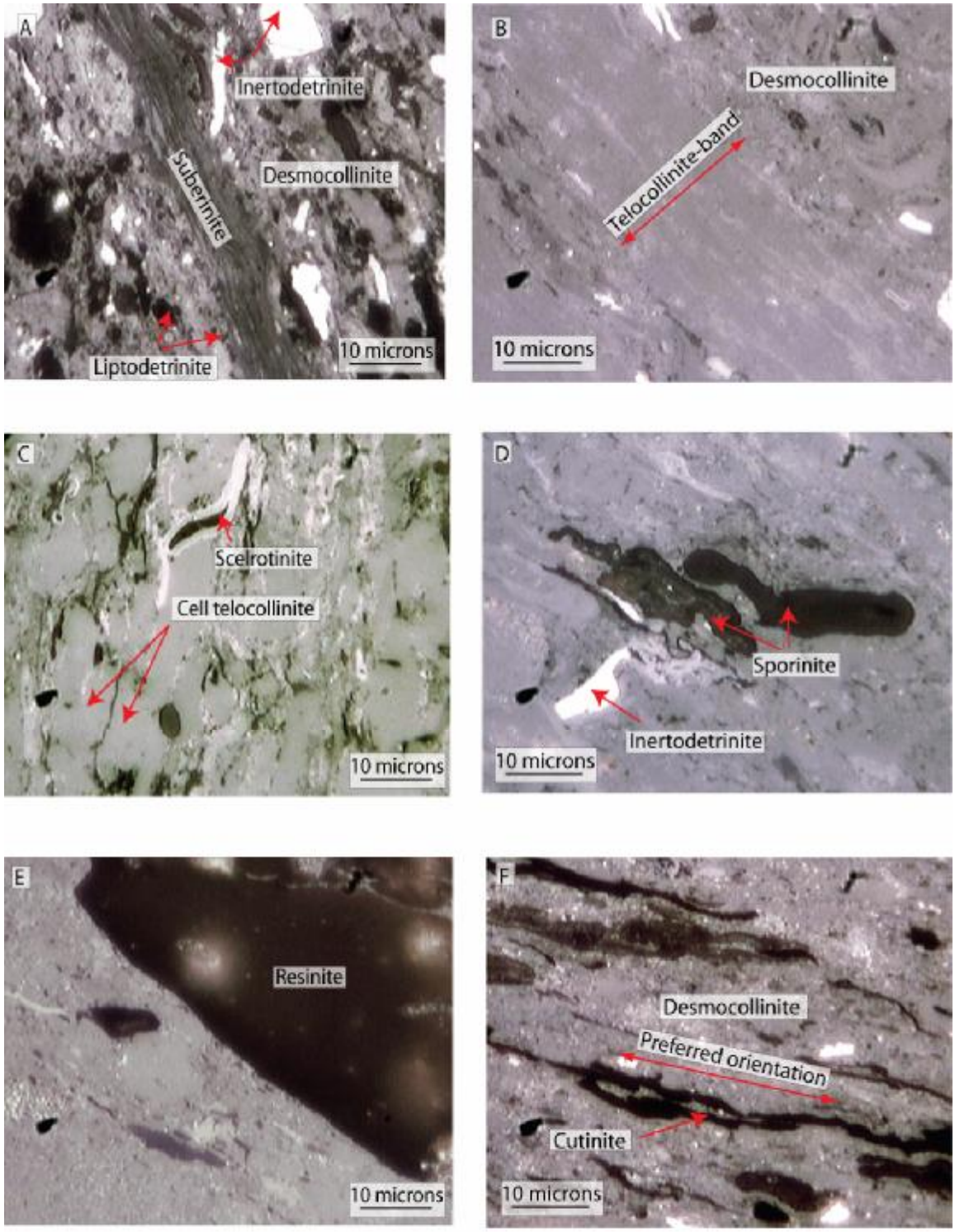

Figure 3.21: Examples of common macerals found in block and particulate mounts, in petrographic study of Huntly, Ohai and Greymouth samples. This figure concentrates on macerals of the vitrinite and liptinite groups. (A) Ohai sample SC1-8; (B) Ohai sample SC3-17; (C) Huntly sample TW1-19; (D) Ohai sample SC3-13; (E) Huntly sample TW1-11; (F) Greymouth sample 944-23, (Table 3.7).

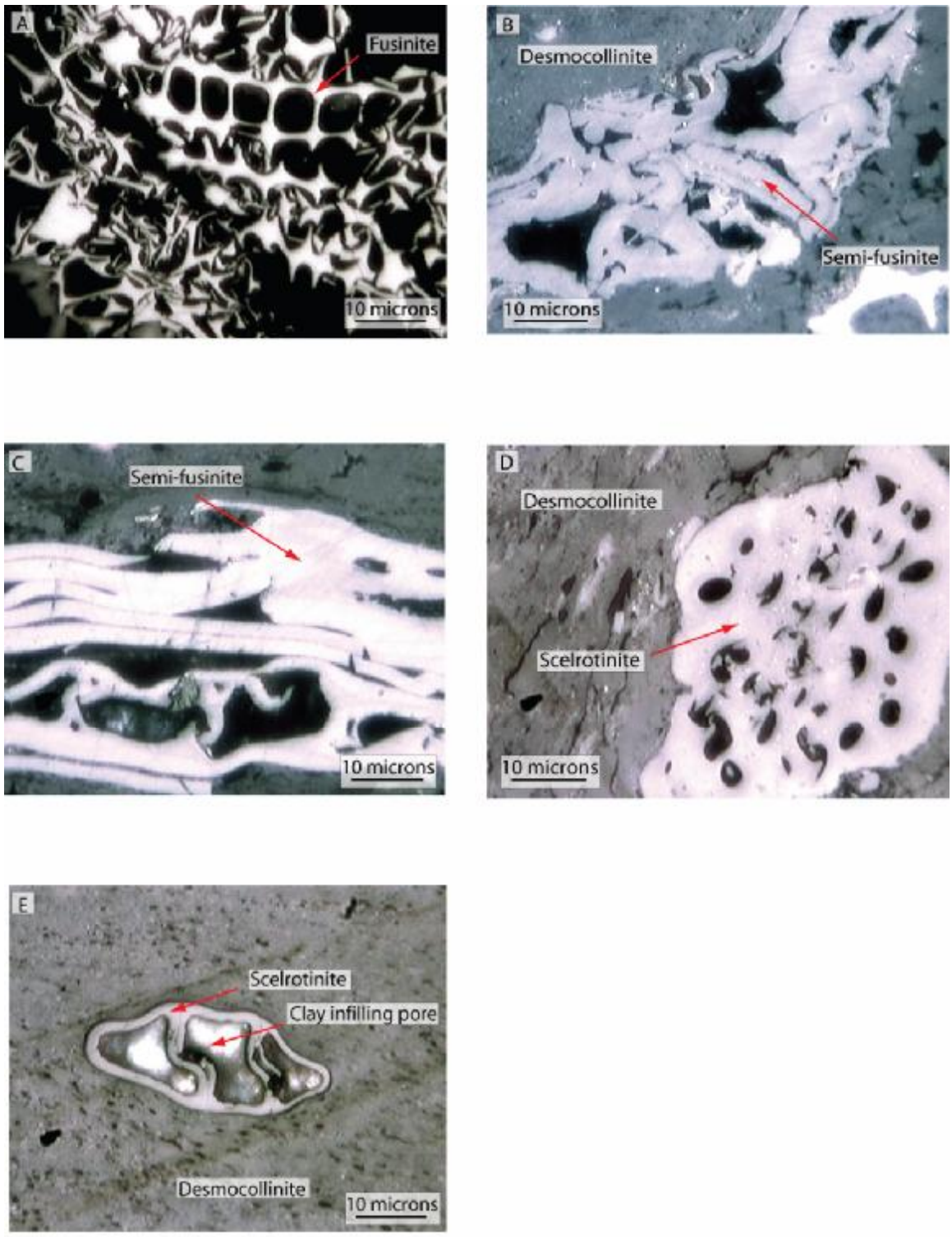

Figure 3.22: Examples of common macerals found in block and particulate mounts, in petrographic study of Huntly, Ohai and Greymouth samples. This figure concentrates on macerals of the inertinite groups. (A) Ohai sample SC3-15; (B) Greymouth sample 944-15; (C) Greymouth sample 944-20; (D) Huntly sample TW1-19; (E) Huntly sample TW1-11.

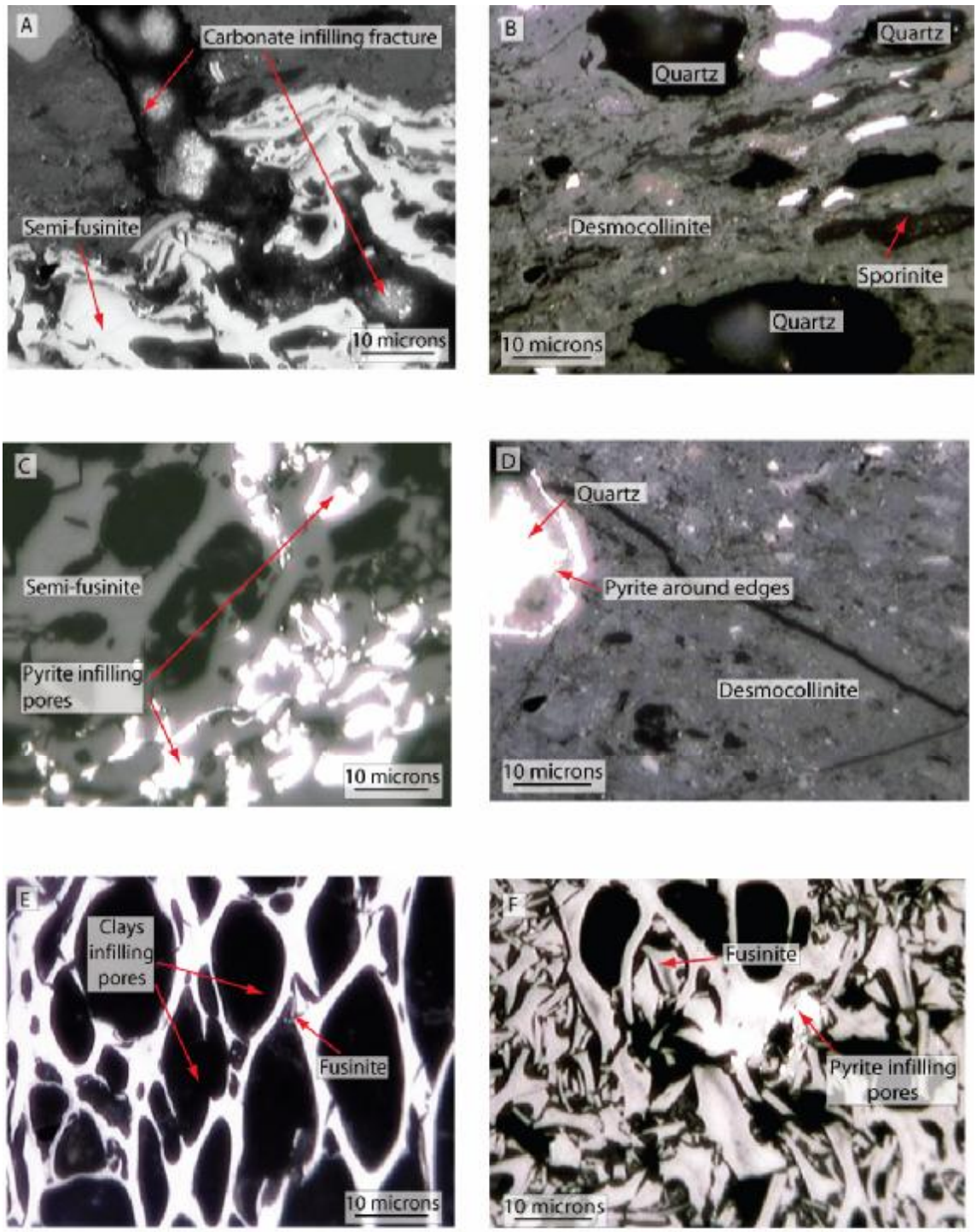

Figure 3.23: Examples of common macerals found in block and particulate mounts, in petrographic study of Huntly, Ohai and Greymouth samples. This figure concentrates on the modes of occurance of mineral matter. (A) Greymouth sample 944-13; (B) Greymouth sample 944-20; (C) Greymouth sample 944-13; (D) Greymouth sample 944-13; (E) Greymouth sample 944-15; (F) Greymouth sample 944-15.

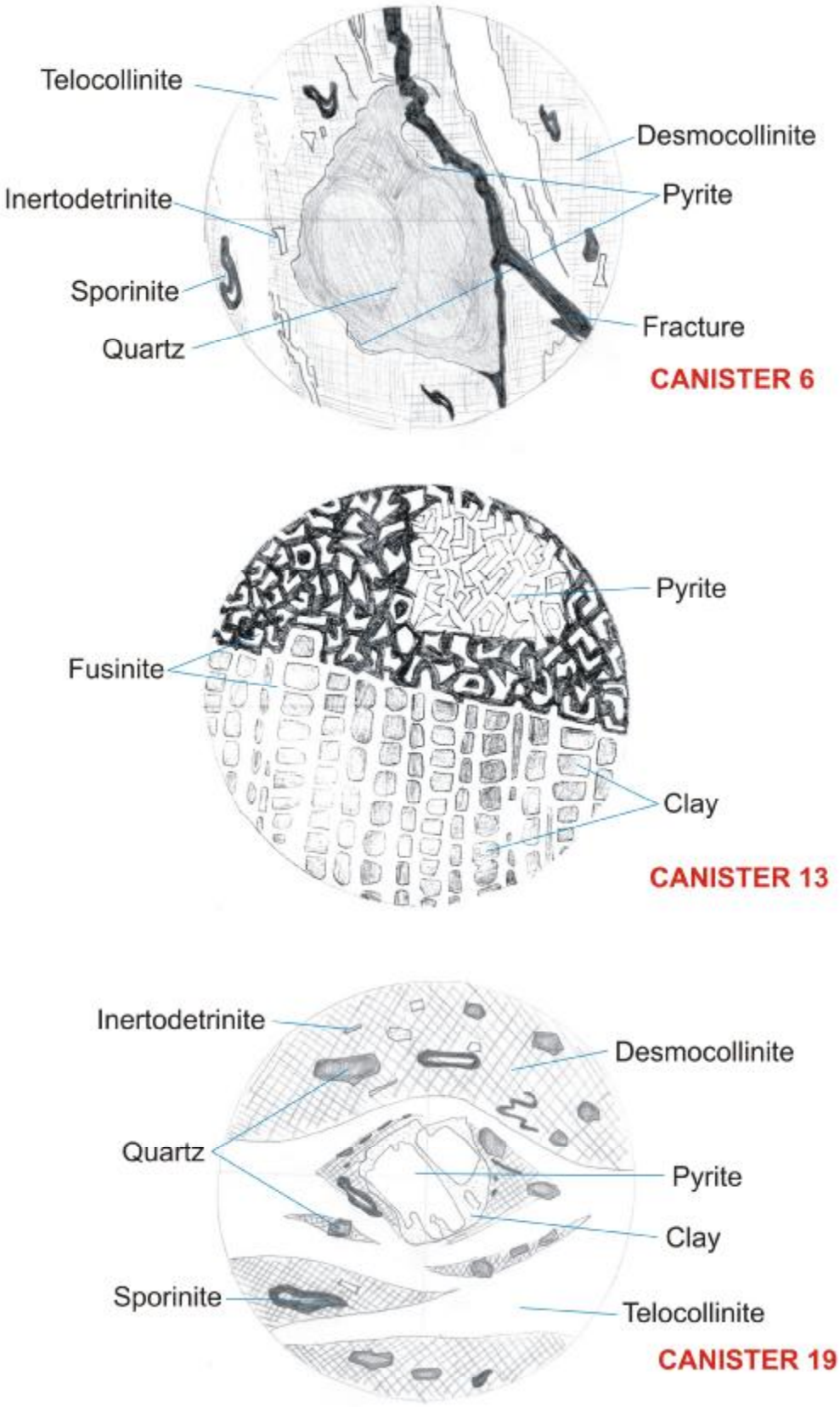

Figure 3.24: Sketches of canister 6, canister 13 and canister block mounts. See Table 3.7 for explanations.

Table 3.6: Percentages of maceral concentrations in selected samples.

	Vitrinite					Liptinite						Inertinite				Mineral matter					Total	Total	Total	Total
Sample	C Tell	B Tell	L Tell	Des	V-d	Spor	Cu	Res	L-d	Sub	Fl	S-Fus	Fus	I-d	Scel	Pyr	Qtz	clay	Cbn	Fe-O	**Vit**	**Lip**	**Int**	**MM**
944 c5	3	17	17	45	5	1	3	1	2	0	0	1	1	2	1	0	0	0	0	0	87	7	6	0
944 c6 p8 A	6	12	21	42	3	1	4	0	2	0	0	2	1	2	2	0	1	0	0	0	85	8	7	1
944 c6 p8 B	3	18	13	47	6	0	2	0	4	0	0	2	1	2	1	0	0	0	0	0	87	7	5	1
944 c13	1	12	22	48	4	1	0	1	4	0	0	2	1	3	0	0	1	0	0	0	87	6	6	1
944 c15	1	13	22	42	4	1	2	2	2	3	0	1	1	2	0	0	2	1	0	0	83	10	4	3
944 c16	3	10	44	26	1	1	1	1	3	5	0	1	1	3	0	0	0	0	0	0	83	11	5	1
944 c20	3	9	39	31	2	1	1	2	3	1	0	1	2	1	1	0	2	0	0	0	84	8	6	2
944 c21	2	9	35	36	4	2	1	1	2	2	0	1	0	0	1	0	3	1	0	0	85	8	2	5
mean=	**2.8**	**12.4**	**26.6**	**39.7**	**3.7**	**1.0**	**1.6**	**1.1**	**2.7**	**1.5**	**0.0**	**1.2**	**1.1**	**1.8**	**0.9**	**0.0**	**1.2**	**0.3**	**0.1**	**0.0**	**85.3**	**8.0**	**5.1**	**1.7**
stddev=	*1.4*	*3.3*	*10.3*	*7.6*	*1.5*	*0.4*	*1.0*	*0.6*	*0.9*	*1.5*	*0.1*	*0.5*	*0.5*	*0.8*	*0.5*	*0.1*	*1.1*	*0.3*	*0.1*	*0.1*	*1.7*	*1.5*	*1.3*	*1.4*
TW1 c10	7	13	16	41	8	1	1	1	5	0	0	1	0	3	1	0	0	1	0	0	85	8	6	1
TW1 c11	5	15	10	44	5	1	1	3	10	1	0	1	0	1	2	0	0	0	0	1	79	15	5	1
TW1 c19	9	12	6	43	9	1	0	2	9	0	0	1	0	3	3	0	0	0	1	0	79	12	7	1
TW1 c21	5	6	20	54	4	1	0	1	3	1	0	0	0	3	1	0	0	0	1	0	88	6	5	1
TW1 c28	12	19	8	44	9	1	0	1	2	0	0	0	0	2	0	0	0	1	0	0	92	4	2	1
TW1 c32	12	13	18	40	6	1	1	1	5	0	0	0	0	3	2	0	0	0	0	0	87	8	4	1
TW1 c37	20	8	8	41	10	1	3	0	4	0	0	0	0	4	1	0	0	0	0	0	86	8	5	0
TW1 c43	6	17	18	38	8	1	3	0	4	1	0	0	0	2	2	0	0	0	0	0	87	9	4	0
mean=	**9.3**	**12.9**	**12.9**	**43.2**	**7.2**	**0.9**	**1.2**	**1.1**	**5.1**	**0.5**	**0.1**	**0.4**	**0.1**	**2.6**	**1.6**	**0.0**	**0.1**	**0.4**	**0.3**	**0.2**	**85.6**	**8.8**	**4.7**	**1.0**
stddev=	*4.7*	*4.0*	*5.2*	*4.4*	*2.0*	*0.2*	*1.1*	*0.9*	*2.5*	*0.3*	*0.1*	*0.5*	*0.1*	*0.8*	*0.8*	*0.1*	*0.1*	*0.4*	*0.3*	*0.3*	*4.2*	*3.3*	*1.3*	*0.4*
SC3-1	4	24	23	27	1	2	2	1	3	3	0	3	1	1	0	0	3	1	0	0	79	12	5	4
SC3-3	3	24	15	41	6	0	2	0	2	1	0	1	2	1	0	0	0	0	0	0	89	6	5	0
SC3-7	2	20	22	39	3	1	3	0	1	2	0	2	2	3	1	0	0	0	0	0	84	7	8	0
SC3-9	3	25	16	44	3	0	2	0	1	1	0	1	1	2	1	0	0	0	0	0	91	4	5	0
SC3-12	3	19	16	45	4	1	1	0	3	1	0	1	1	3	2	0	0	0	0	0	88	6	6	0
SC3-13	3	21	20	38	4	0	1	0	3	4	0	1	1	1	2	0	0	0	0	0	86	8	5	0
SC3-15	2	21	23	37	3	2	1	0	1	1	0	3	2	3	0	0	0	1	0	0	86	6	7	1
SC3-17	1	18	22	43	2	1	0	0	2	1	0	3	2	3	1	0	0	0	0	0	86	4	9	1
mean=	**2.7**	**21.5**	**19.6**	**39.2**	**3.3**	**1.0**	**1.6**	**0.2**	**2.0**	**1.8**	**0.0**	**1.8**	**1.5**	**2.1**	**0.9**	**0.0**	**0.5**	**0.2**	**0.1**	**0.0**	**86.2**	**6.6**	**6.3**	**0.9**
stddev=	*0.8*	*2.4*	*3.1*	*5.2*	*1.3*	*0.7*	*0.9*	*0.3*	*0.8*	*1.2*	*0.0*	*0.9*	*0.5*	*0.8*	*0.5*	*0.0*	*1.0*	*0.3*	*0.1*	*0.0*	*3.4*	*2.4*	*1.5*	*1.2*
SC1-3	1	15	39	30	3	1	1	1	3	2	0	1	1	1	1	0	0	0	0	0	88	8	4	1
SC1-8	1	18	50	13	1	1	1	4	4	3	0	1	1	1	1	0	2	1	0	0	82	12	3	3
SC1-10	2	11	29	40	3	1	0	0	3	1	0	2	3	2	1	0	0	0	1	0	86	5	8	1
SC1-11	4	23	9	38	3	0	3	1	4	3	0	1	1	0	1	0	2	7	0	0	76	12	4	8
mean=	**2.0**	**16.8**	**31.6**	**30.1**	**2.2**	**1.0**	**1.3**	**1.3**	**3.6**	**1.9**	**0.0**	**1.1**	**1.5**	**1.0**	**1.0**	**0.0**	**1.0**	**2.0**	**0.2**	**0.1**	**82.8**	**9.2**	**4.7**	**3.4**
stddev=	*1.2*	*4.2*	*15.0*	*10.7*	*0.8*	*0.4*	*1.2*	*1.4*	*0.7*	*0.9*	*0.0*	*0.4*	*1.0*	*0.7*	*0.2*	*0.0*	*0.7*	*2.7*	*0.3*	*0.1*	*4.3*	*2.8*	*1.8*	*3.0*

Table 3.7: Summary of Greymouth Block samples

ID	Description	Dominant Mineralisation	Dominant mode of occurrence	Coal type	Ash %	Measured gas (m^3/t)	Residual gas (m^3/t)	Lost gas (m^3/t)	Total gas (m^3/t)
2	Canister two contains a large (2 cm in hand specimen) vitrain band. The band of telocollinite is homogeneous, but not featureless, with arrays of pre-existing material running N-S in the sample. There are also fracture systems present, with only one fracture mineralised. Desmocollinite has a dissolved appearance, with very little maceral matter in the desmocollinite. Small portions of pyrite are present, and clay is abundant, filling in remnants of cell wall material.	Clays	Infilling pores	B<20	25.9	1.83	0.26	0.05	2.14
5	Canister five is heavily banded, with telocollinite being the dominant maceral. The telocollinite is heterogeneous, with smaller pieces of inertodetrinite and liptodetrinite scattered throughout. The desmocollinite has liptinites scattered throughout, but inertinites are scarce. Liptonites are predominantly sporinites, resinites and long bands of cutinites that can be followed for a distance. Clays are seen to be infilling some fractures, and are also observed infilling pore spaces in a large piece of fusinite. Scelrotinite does not have pores infilled with clay. Detrital quartz is also observed.	Clays	Infilling pores and fractures	B<20	2.5	2.12	1.04	0.05	3.21
6	Canister six contains bands. Telocollinite is homogeneous and structureless. Desmocollinite contains Sporinite and bands of Cutinite, all aligned in a single orientation. Semi-fusinite does not have many intact spore spaces. A few pore spaces are infilled with clay, but many are not. Detrital quartz grains are present. One quartz grain was observed with pyrite mineralised on the quartz grain boundaries (see Fig 3.24). fractures are also present, with slight mineralisation (slight surface reflections present) in zones along the fracture.	Clays	Detrital	B<20	0.7	1.37	0.77	0.07	2.21
13	Canister thirteen contains multiple thick bands of homogeneous telocollinite. The desmocollinite contains abundant pieces if inertodetrinite, as well as liptodetrinites, Sporinite and Cutinite. Cutinite bands can be followed for some distance, and show orientation, although smaller desmocollinite components are not as obviously aligned. The desmocollinite has a greater abundance of the inertinite group compared with other block mounts. Pore spaces in semi-fusinite and fusinites show both mineralisation and free pore spaces. A large fusinite field was observed, with clay mineralisation in some of the pore spaces, and pyrite mineralisation around broken fragments of fusinite (Fig 3.24).	Clays and pyrite	Infilling pores	B>20	4.3	1.81	0.45	0.06	2.31
15	Canister fifteen contains bands of homogeneous, structureless telocollinite. Desmocollinite contains liptodetrinites, sporinites, cutinites, ineryo0detrinites, fusinites and semi-fusinites. Pore spaces in fusinites and semi-fusinites are predominantly mineralised, as are fractures. Often the whole length of the fracture is not mineralised; it is possible that parts of the fracture are new due to the drying out process, and developed along the previous fracture lines / planes of weakness. Where fractures bisect fusinites or semifusinites pore spaces and the fracture zones are mineralised	Clays and carbonates	Infilling pores and fractures	B<20	5.3	1.13	0.60	0.04	1.77
19	Canister nineteen is banded with hetrogeneous telocollinite, with remnants of structure observed in the mid section, possibly old pore spaces. Smaller telocollinite bands are also found dispersed throughout the desmocollinite. The desmocollinite has a moderate amount of liptinites and inertinites, as well as moderate amounts of resinites (including fluorinite) not observed in other samples. The desmocolloinite also contains moderate amounts of detrital quartz grains. Although there is a slight infilling of pore spaces, and slight mineralization of fracture systems, the mineral matter is dominated by detrital quartz grains. Fig 3.24 shows a detrital pyrite fragment surrounded by quartz grains. The structure around the pyrite suggests that the pyrite was early forming, as the desmocollinite and telocollinite form an augen-like lens around the grain.	Quartz	Detrital	Dull	15.6	1.96	0.54	0.07	2.57
20	Canister twenty has the same appearance and characteristics of canister nineteen. It is dominated with detrital quartz grains, however mineralisation is also apparent in fractures, and clays infill pore spaces in fusinite grains.	Quartz	Detrital	dull	7.0	1.03	0.45	0.09	1.57
21	Canister twenty-one contains a thick, 1 cm (in hand specimen) band of homogeneous, structureless telocollinite. The desmocollinite is similar to the desmocollinite found in canisters nineteen and twenty, although there is not as much macerals from the inertinite group present. Clay was observed occasionally infilling pore spaces.	Quartz	Detrital	B>20	13.6	1.85	0.43	0.04	2.32
23	Banded telocollinite is present, with multiple, small scale bands present throughout the desmocollinite. Large fusinite and semi-fusinite macerals wre present, with a slight infilling of pore spaces with clay. Detrital quartz grains are also present. This sample showed a strong orientation, with sporinites, cutinites, liptodetrinites, semi-fusinites and fusinites all aligned in a single direction.	Quartz	Detrital	B>20	4.0	1.56	0.41	0.05	2.02

3.5 Gas quantity, quality and type

3.5.1 Adsorption

Isotherm results are calculated to standardised conditions of 20°C and 1 atmospheric pressure. Graphs are calculated using the Langmuir equation $V_A = V_{L*}P_H/(P_H + P_L)$, where P_H is the hydrostatic pressure, and V_L and P_L are the Langmuir coefficients. The graph is calculated using dry ash free (daf) Langmuir coefficients, to eliminate the effect of the ash yield when comparing the holding capacities. The isotherms do not reflect the assumed trend of increasing holding capacities with an increase in coal rank, as the Ohai isotherms contain a higher holding capacity than the higher ranked Greymouth isotherm.

Table 3.8: Langmuir coefficients for the studied areas

Location	Analysis temp (°C)	P_L		V_L	
Huntly	23.8	aa	4.10	aa	10.59
		daf	4.10	daf	12.46
Ohai	24	aa	3.73	aa	11.15
		daf	3.73	daf	14.47
Greymouth	25	aa	7.45	aa	20.63
		daf	7.45	daf	24.67

The Langmuir coefficients V_L (volume) and P_L (pressure) are shown in Table 3.8 for both as received (aa) and dry ash free (daf). Tables 3.9 and 3.10 summarise the holding capacity for each location at three different pressures; 2 MPa, 4 MPa and 8 MPa (both aa and daf). The pressure is a hydrostatic pressure, which is approximately proportional to depth in New Zealand. Hence, 4 MPa is equivalent to 400 m depth. Adsorption isotherms show the Greymouth isotherm nearly 50% greater than the Huntly isotherm at 2 MPa, whereas both Ohai isotherms act independently of each other. Ohai A is more than twice as high as the Greymouth isotherm, while the Ohai B isotherm is just above the Huntly curve. However, at 8 MPa, both Ohai isotherms show greater holding capacity than both the Greymouth and the Huntly isotherms. At this pressure all isotherms have levelled out towards an asymptote, with only 1 m^3/t of methane between Ohai B, Greymouth and Huntly, respectively. Ohai A holds approximately 3 m^3/t more gas than Ohai B (Fig. 3.25).

Table 3.9: Adsorption capacity, given as gas content (m^3/t), for different pressures (as analysed).

Location	Pressure		
	2 MPa	4 MPa	8 MPa
Huntly	3.47	5.23	7.00
Ohai A	3.89	5.77	7.60
Ohai B	4.37	7.21	10.68
Greymouth	3.80	6.02	8.50

Table 3.10: Adsorption capacity, given as gas content (m^3/t), for different pressures (dry, ash free).

Location	Pressure		
	2 MPa	4 MPa	8 MPa
Huntly	4.08	6.15	8.23
Ohai A	5.05	7.49	9.87
Ohai B	12.02	13.21	13.89
Greymouth	7.08	8.58	9.60

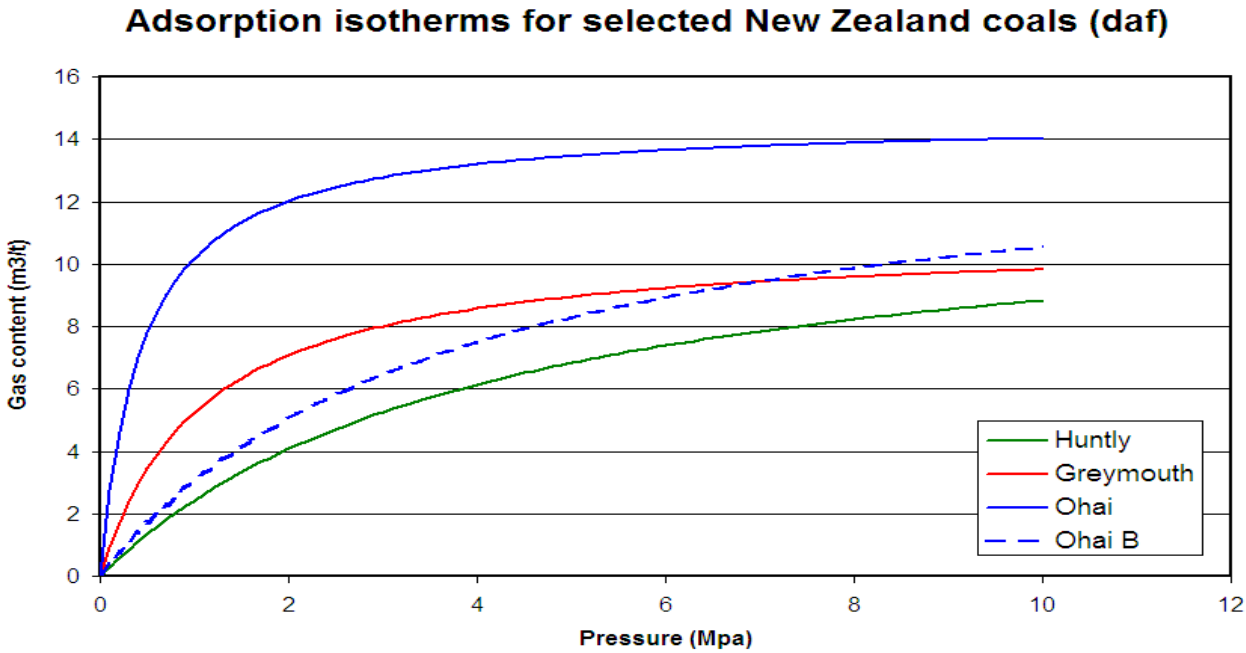

Figure 3.25: Adsorption isotherms for the studied regions, New Zealand. All have been calculated using daf (dry, ash free) Langmuir coefficients to eliminate ash influence, for comparison.

3.5.2 Desorption

Gas volumes (m^3/ton of coal) for each location are given in Appendix G. Total gas comprises lost, measured and residual proportions. The average total gas values for the Huntly, Ohai and Greymouth cores are 1.6 m^3/ton (std = 0.24, n = 37); 4.7 m^3/ton (std = 0.89, n = 29); 2.35 m^3/ton (std = 0.75, n = 24) respectively (Fig. 3.26).

Total gas measurements plotted against depth are depicted in Figure 3.27. All locations show significant downhole variation in gas content (Table 3.11). Huntly contains 57% of variation in gas volume, Ohai contains 48% variation, while Greymouth shows the largest range, with 82% variation in total gas volume.

Table 3.11: Variation in total gas volumes, for the Huntly, Ohai and Greymouth samples.

Location	Gas Variation	Lowest Desorption (m^3/t)	Highest Desorption (m^3/t)
Huntly	57%	0.9	2.1
Ohai	48%	3.0	5.8
Greymouth	82%	0.7	3.7

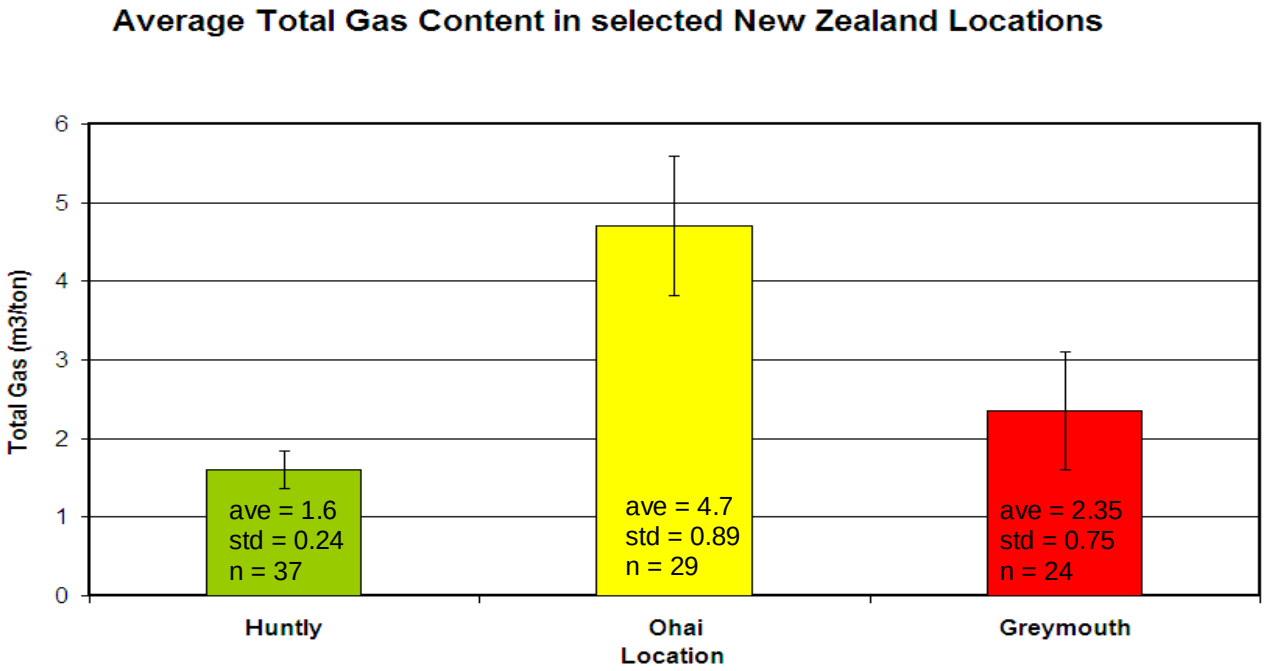

Figure 3.26: Average values, with standard deviation bars, of total gas content (m3/t) in the studied locations, New Zealand.

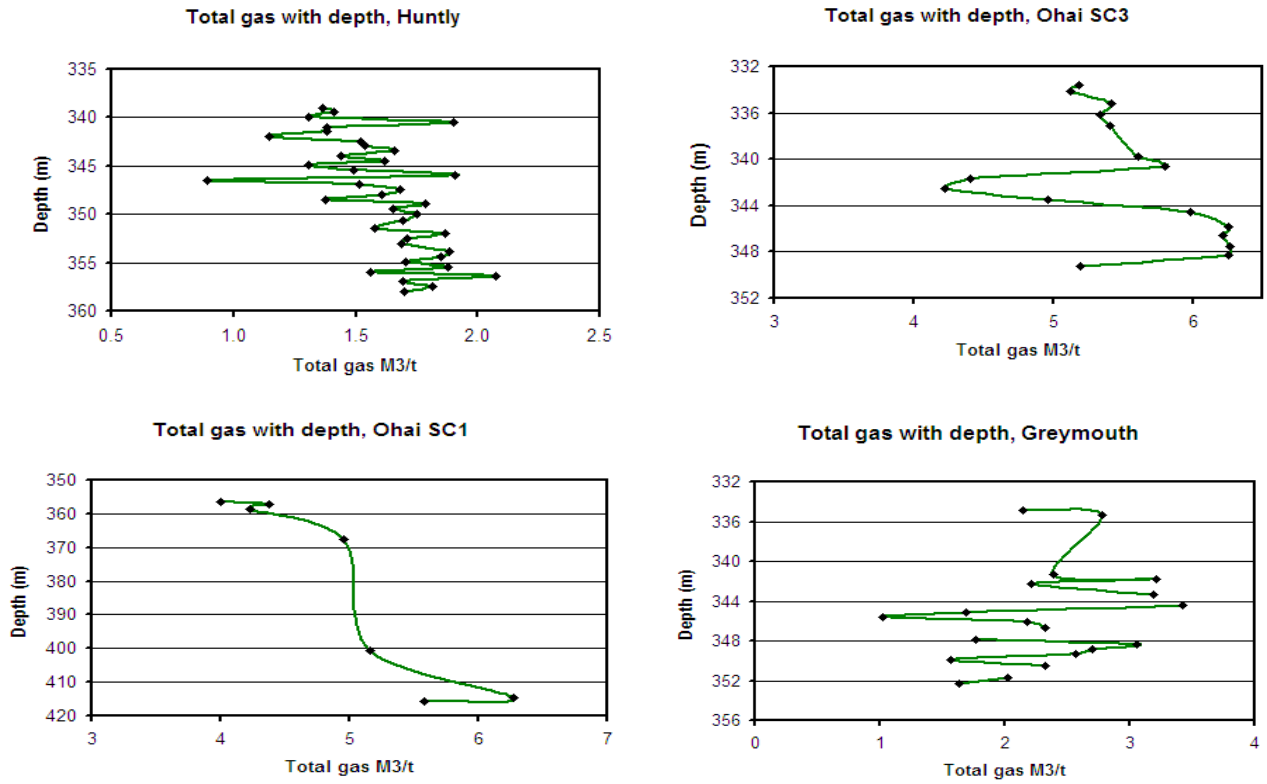

Figure 3.27: Down-hole total gas variation, in the Huntly, Ohai and Greymouth cores. Depths are from surface.

3.5.3 Gas Saturation

Gas saturation data are given in Appendix I. The Huntly core has a saturation yield ranging from 18.3 - 42.7%; the Ohai SC1 core ranges from 55.8 – 98.8%; the Ohai SC3 core has saturation yield ranging from 47.7 – 90.8%; the Greymouth from 12.7 – 70.2%. The Ohai cores contain the highest saturated coals. They also contain the highest desorbed gas volumes, a function of the high saturation content.

3.5.4 Gas Isotopes

Isotopic signatures of δD and $\delta^{13}C$ were determined from various sources (Table 3.12, Fig. 3.28). Huntly contains the lightest $\delta^{13}C$ and δD values, pointing to a secondary biogenically sourced gas, from CO_2 reduction. Greymouth has heavier $\delta^{13}C$ and δD isotopes, as expected from a higher ranked coal, and these also fall into a CO_2 reduced, biogenic gas source. As the Ohai coal falls mid way in between the Huntly and the Greymouth coal, in terms of thermal maturity or rank, one would expect the isotopic signatures to also fall in between the Huntly and Greymouth gas isotopes. However, this is not the case, the gas isotopes from the Ohai core are more mature, and plot as heavier $\delta^{13}C$ and δD values. The source of the Ohai gas plots from a biogenic / transitional (that is, trending towards thermogenic) origin.

Table 3.12: Gas isotope values, for the Huntly, Ohia and Greymouth samples. Greymouth and Huntly values are from unpublished Solid Energy NZ Ltd. data or laboratory.

Location	δD (per mil)	$\delta^{13}C$ (per mil)	References
Ohai	-206.0	-58.70	Lyon and Giggenbach, 1994
Greymouth 944	-210.0	-63.40	GNS Science
Greymouth 944	-246.0	-61.60	GNS Science
Greymouth (other)	-230.0	-59.30	GNS Science
Huntly TW1	-225.0	-65.50	GNS Science
Huntly (other)	-216.0	-65.70	Rafter, Canada
Huntly (other)	-204.0	-67.60	Rafter, Canada
Huntly (other)	-209.7	-65.88	Geoscience Australia
Huntly (other)	-210.6	-65.77	Geoscience Australia
Huntly (other)	-206.4	-65.71	Geoscience Australia
Huntly (other)	-206.5	-65.50	Geoscience Australia

3.5.5 Gas Quality

Gas quality analyses are shown in Table 3.13 reported with O_2, N_2 and air free corrections. The Huntly core has 96.4 % CH_4, the Ohai cores have 92.79 and 95.59 % CH_4, and Greymouth has the lowest CH_4 content, of 89.16%.

Table 3.13: Gas quality data, corrected for free air, O_2 and N_2.(n=1 for Huntly and Greymouth; n=2 for Ohai).

Gas		Location			
		Huntly	Ohai		Greymouth
CH_4	%	96.40	92.79	95.59	89.16
CO_2	%	3.54	6.63	4.01	6.88
C_2H_4	ppm	0.00	0.00	0.00	0.00
C_2H_6	ppm	611.41	2661.65	3683.88	0.04
H_2	%	0.00	3154.48	340.08	0.00
O_2	%	0.00	0.00	0.00	0.00
N_2	%	0.00	0.00	0.00	0.00

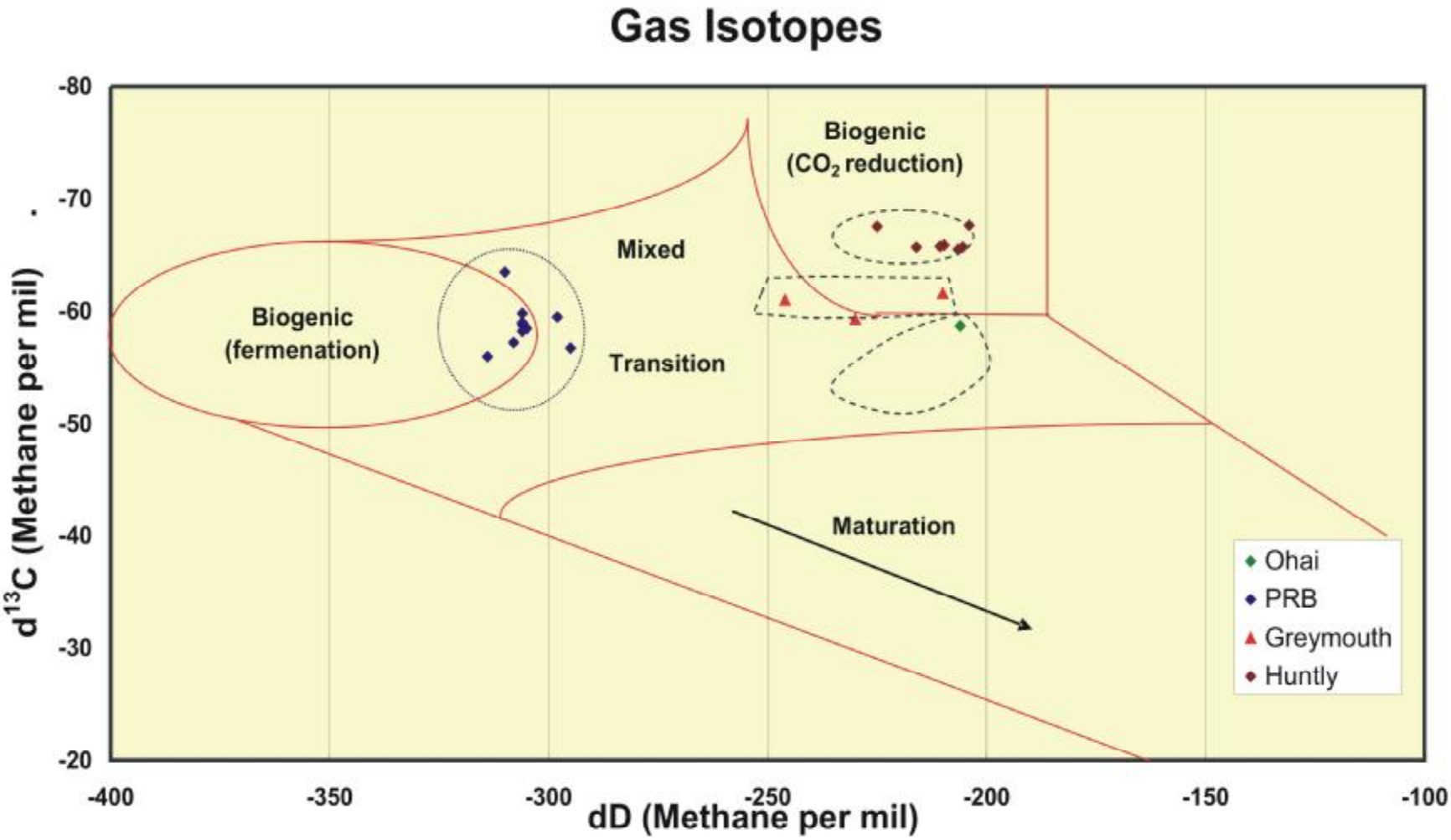

Figure 3.28: Gas isotopes of Huntly, Ohai, Greymouth and the Powder River Basin (PRB). The PRB is included as an example of a biogenic by fermentation sourced gas, which shows a different pathway of gas formation from biogenic by CO_2 reduction sourced gas. Sources of data are included in Table 3.12, except for PRB, which is sourced from Gorody (1999).

Chapter Four

Gas Associations

To determine associations and correlations of gas volume with organic and inorganic components, correlation charts were produced (Appendix J). Because of the large dataset involved, coefficients above the significant correlation coefficient at the 95% confidence limit (~ $R^2 > 0.50$) were focussed on (Table 4.1). Summary tables of variables with high correlation coefficients (~ $R^2 > 0.5$) were produced, then graphed (Appendix K). Some of the associations proved false, artefacts from clustering of data and outlying points. Table 4.2 summarises the minimum and maximum correlation coefficients, and how many coefficients were above the significant correlation coefficient.

Table 4.1: Significant levels of correlation coefficients, at the 95 % confidence level. n = number of samples, df = degrees of freedom.

Location	Analysis Type							
	Proximate		Maceral		XRF		XRD	
	n (df)	5 %	n (df)	5 %	n (df)	5 %	n (df)	5 %
Huntly	33 (31)	0.344	8 (6)	0.707	33 (31)	0.344	8 (6)	0.707
Ohai SC1	9 (7)	0.666	4 (2)	0.95	9 (7)	0.666	5 (3)	0.878
Ohai SC3	18 (16)	0.468	8 (6)	0.707	18 (16)	0.468	8 (6)	0.707
Greymouth	23 (21)	0.413	8 (6)	0.707	19 (17)	0.456	10 (8)	0.632
Average		0.47275		0.76775		0.4835		0.731

Table 4.2: Summary of correlation coefficients between proximate, XRD, XRD, maceral analyses and gas values. MG = measured gas; RG = residual gas; LG = lost gas; TG = total gas.

Analysis	Location	min R^2	min parameter	max R^2	max parameter	% above significant R^2 value
Proximate	Huntly	0.03	moisture / MG	-0.56	ash / TG	20.8
	Ohai SC1	-	VM / LG	0.90	CV / MG	29.0
	Ohai SC3	-	CV / RG	-0.80	moisture / RG	33.3
	Greymouth	-0.01	Suggate rank / LG	-0.62	ash / TG	58.0
XRD	Huntly	-0.04	ankerite / MG	-0.52	kaolinite / TG	-
	Ohai SC1	-		0.84	quartz / LG	-
	Ohai SC3	-0.11	quartz / LG	0.75	kaolinite / RG	10.0
	Greymouth	-0.04	muscovite / TG	0.97	siderite / LG	15.0
XRF	Huntly	-		0.54	Fe2O3 / TG	18.0
	Ohai SC1	0.03	SiO2 / LG	0.77	TiO2 / TG	11.4
	Ohai SC3	-	Mn3O4 / LG	-0.91	Na2O / RG	61.0
	Greymouth	0.05	Na2O / LG	0.99	P2O5 / LG	11.4
Maceral	Huntly	-	Sporinite / LG	0.86	cutinite / TG	5.2
	Ohai SC1	0.03	band telocollinite / MG	-0.99	band telocollinite / LG	4.5
	Ohai SC3	-0.01	vitrodetrinite / MG	-0.90	fusinite / LG	7.1
	Greymouth	-0.03	inertodetrinite / RG	0.82	band telocollinite / RG	7.3

4.1 Organic Correlations

4.1.1 Macroscopic

There were no correlations of gas with either the percent or size of vitrain bands (Figs. 4.1 to 4.3). However, vitrain band proportion combined with microscopic data (structured vitrinites: large telocollinite and total telocollinite) gave significant correlations in the Huntly coalfield, as discussed below.

4.1.2 Microscopic

Organic petrology data were initially treated in two ways when comparing with gas content. Firstly, as only organic material (i.e. maceral data all sums to 100%) and secondly, as a function of whole coal, where the proportion of mineral matter is also incorporated. It was found that in all cases, that there was little difference between these two data treatments. Figure 4.4 shows a typical maceral component and its relationship to gas both with and without mineral matter incorporated. Therefore, it was thought prudent to use the organic petrography results that take into account mineral matter as that best reflects the in situ conditions.

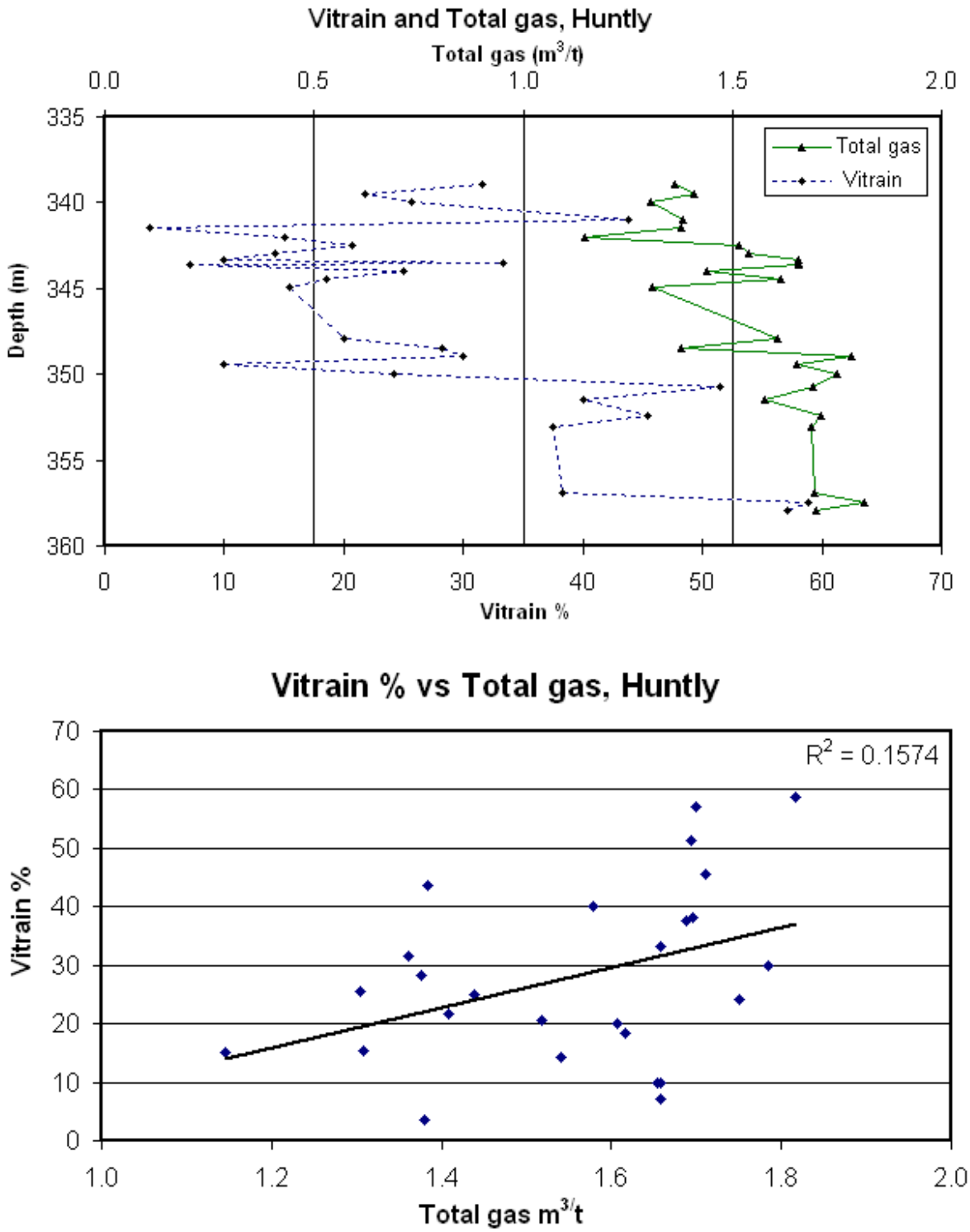

Figure 4.1: Vitrain and total gas relationships in the Huntly core. Graph A shows both the down hole variation of total gas content and vitrain content, with depth from surface. Graph B shows the association of total gas and vitrain yield.

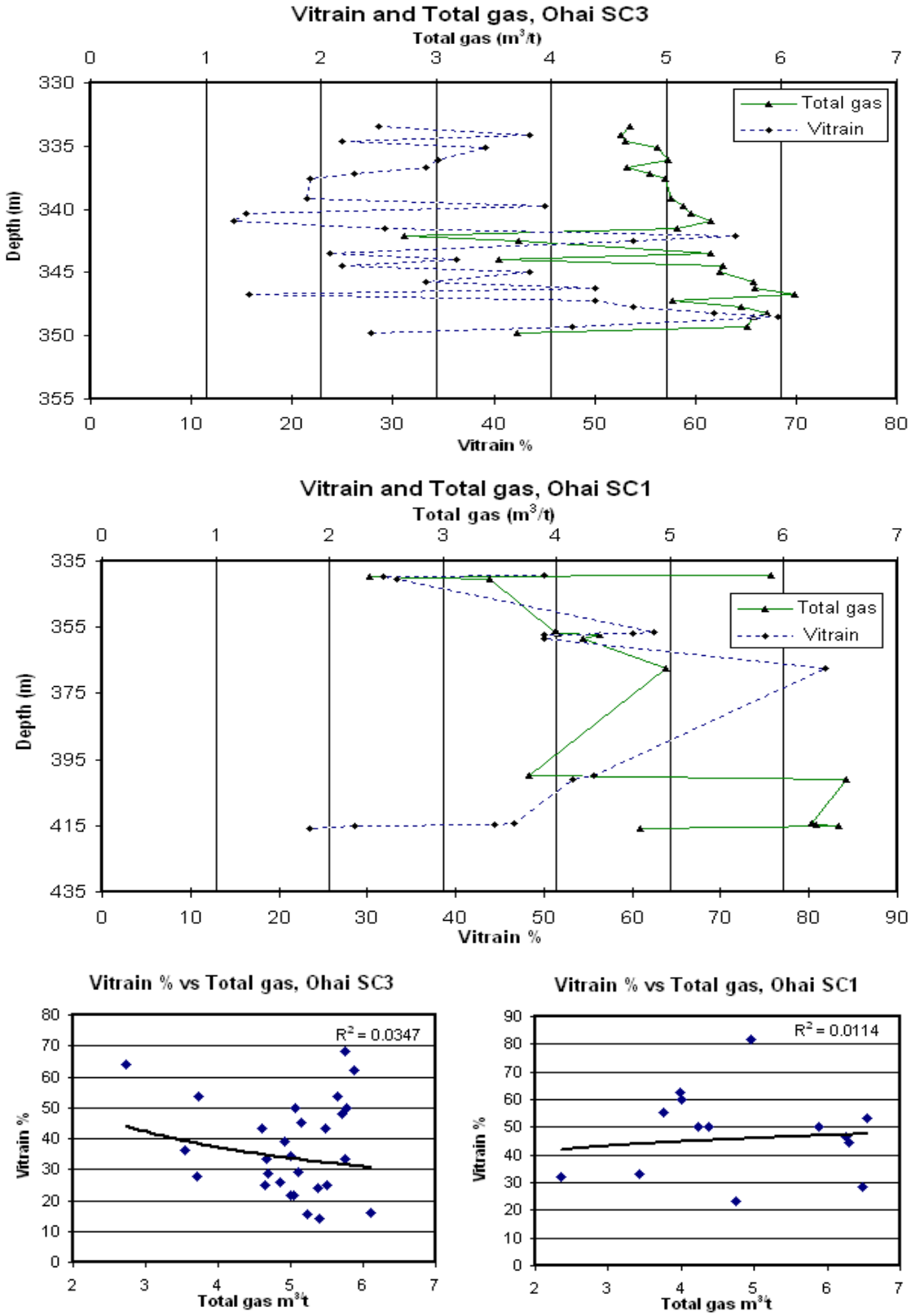

Figure 4.2: Vitrain and total gas relationships in the Ohai core. Graphs A show both the down hole variation of total gas content and vitrain content, with depth from surface. Graphs B show the association of total gas and vitrain yield.

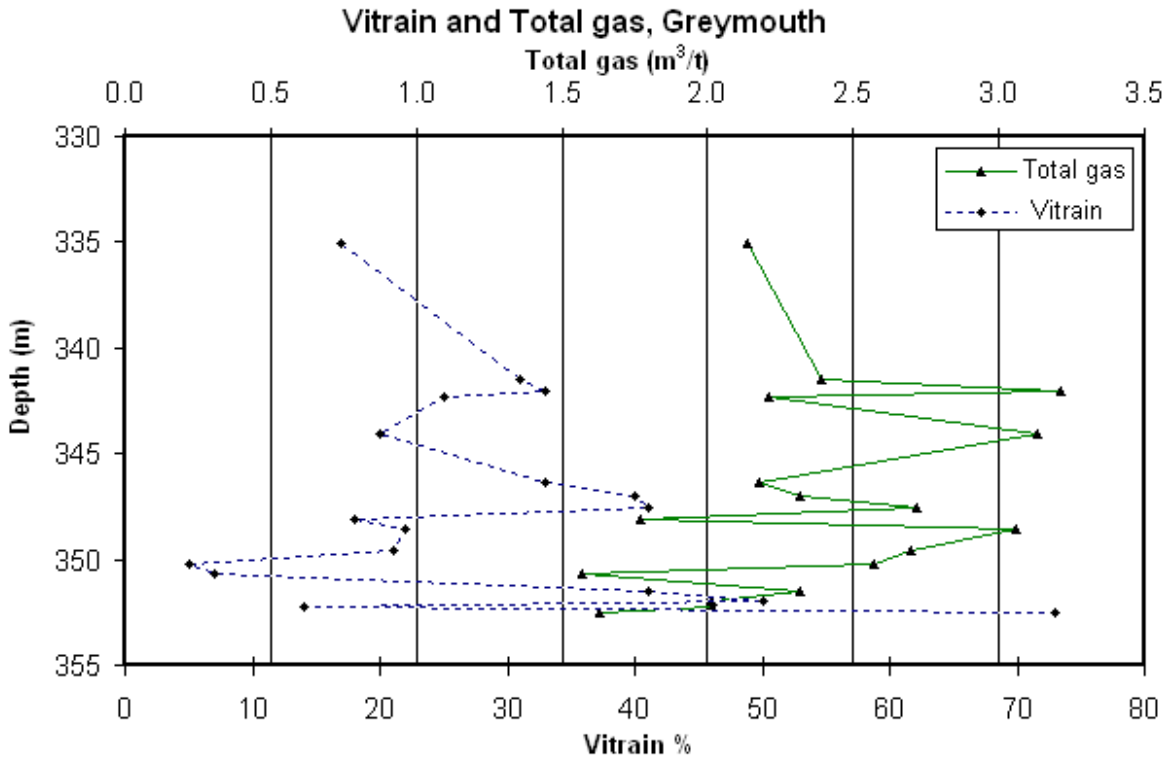

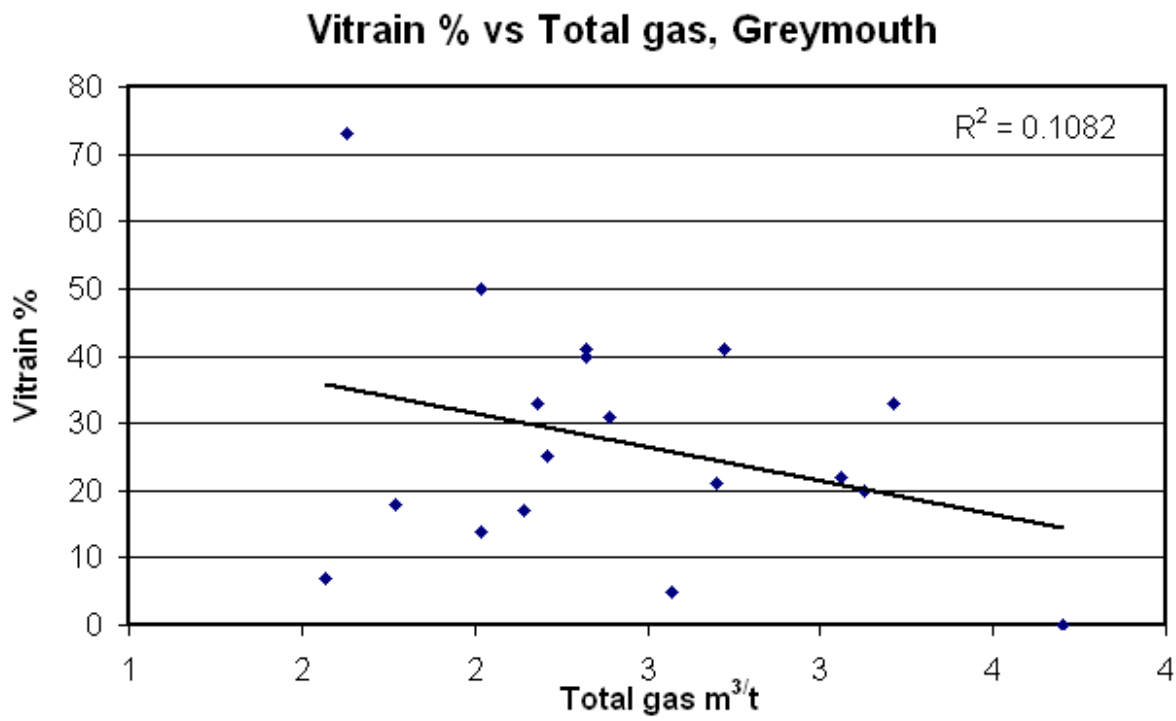

Figure 4.3: Vitrain and total gas relationships in the Greymouth core. Graph A shows both the down hole variation of total gas content and vitrain content with depth from surface. Graph B shows the association of total gas and vitrain yield.

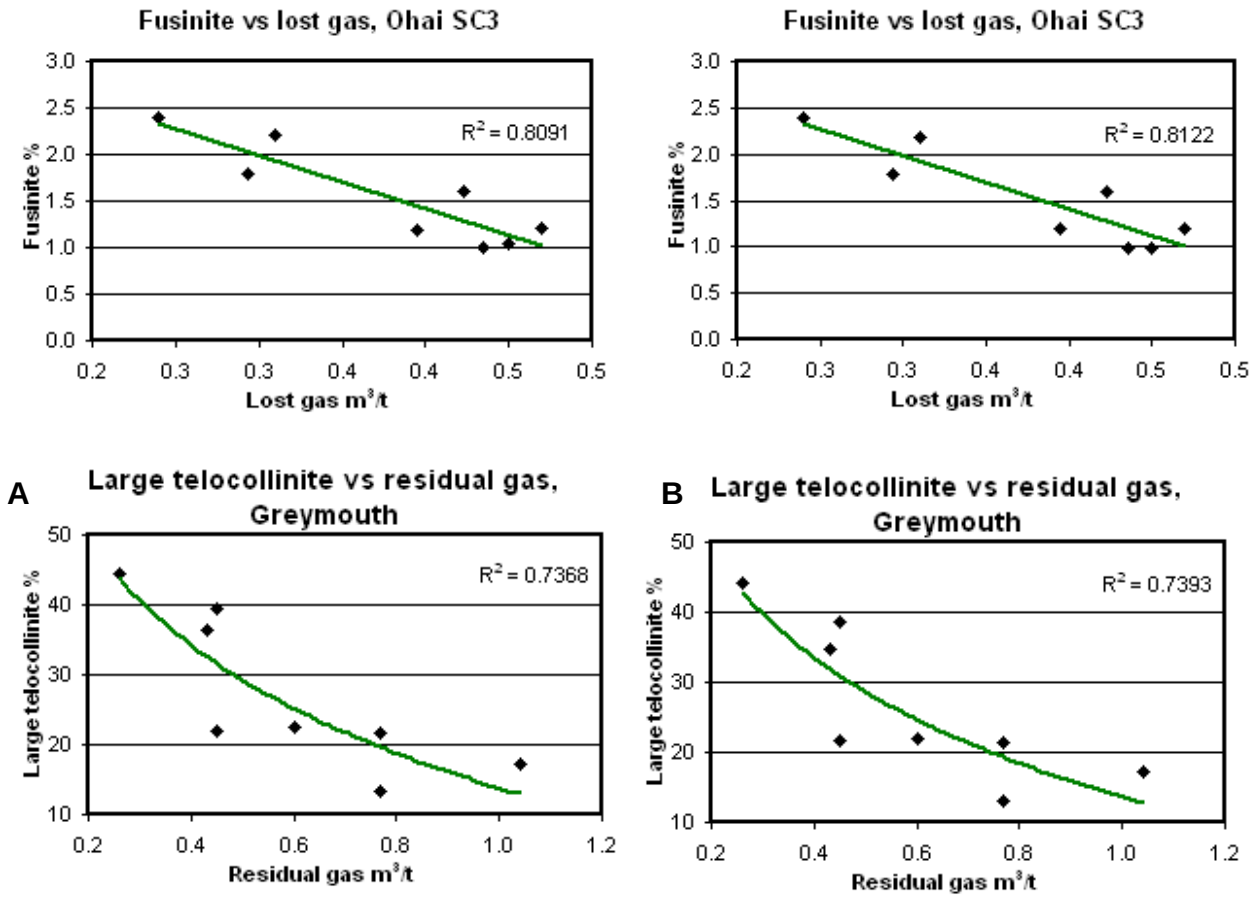

Figure 4.4: Graphs A show maceral correlations with mineral matter removed, while graphs B show maceral correlations with mineral matter incorporated into the maceral content.

In the Huntly and Ohai SC3 coal cores there were only a few correlations with maceral data., whereas in other locations had multiple correlations between macerals and gas content; for example, Ohai SC1 had strong correlations with lost gas, total gas and measured gas. Overall, however, there were only a few strong, statistically significant associations. None of the associations found in one location was found in subsequent locations; all correlations were either bound by basin or rank. A selection of significant associations are represented in Table 4.3, based on the preliminary correlation tables.

Initial analysis of the data indicate that samples from the Huntly core had only four relatively weak associations: calorific value and measured gas; ash and total gas; calorific value and total gas; and fixed carbon and total gas. However, when maceral data were combined with vitrain %, a strong positive association with structured vitrinite and total gas content is present. Both **vitrain % plus large telocollinite** and **vitrain % plus total telocollinite** yield significant correlations. Although this is not present in the other New Zealand locations, it is present in the Powder River Basin, where structured vitrain and total gas yield a very strong positive correlation, ~ $R^2 = 0.9$ (Moore et al, 2002b) (Fig. 4.5).

Table 4.3: Significant correlations between maceral data and gas data. (R^2 ~>0.50).

Location	Measured gas	Residual gas	Lost gas	Total gas
Huntly	fusinite	semi-fusinite fusinite iron-oxide total mineral matter	semi-fusinite fusinite iron-oxide	cell telocollinite desmocollinite cutinite resinite semi-fusinite quartz total mineral matter
Ohai SC3	Resinite lipto-detrinite quartz total liptinite total mineral matter	desmocollinite sporinite resinite semi-fusinite quartz clay total vitrinite total liptinite total mineral matter	cell telocollinite lipto-detrinite fusinite	cutinite resinite lipto-detrinite quartz total liptinite total mineral matter
Ohai SC1	cell telocollinite large telocollinite fusinite scelrotinite iron-oxide total inertinite	sporinite scelrotinite quartz total vitrinite	cell telocollinite band telocollinite sporinite cutinite lipto-detrinite Suberinite semi-fusinite fusinite inerto-detrinite quartz clay carbonate total vitrinite total liptinite total inertinite total mineral matter	desmocollinite fusinite scelrotinite carbonate iron-oxide
Greymouth	suberinite fusinite inerto-detrinite pyrite carbonate iron-oxide	band telocollinite large telocollinite desmocollinite vitro-detrinite cutinite suberinite pyrite iron-oxide total vitrinite total mineral matter	large telocollinite desmocollinite vitro-detrinite suberinite inerto-detrinite pyrite iron-oxide total liptinite	inerto-detrinite pyrite carbonate iron-oxide

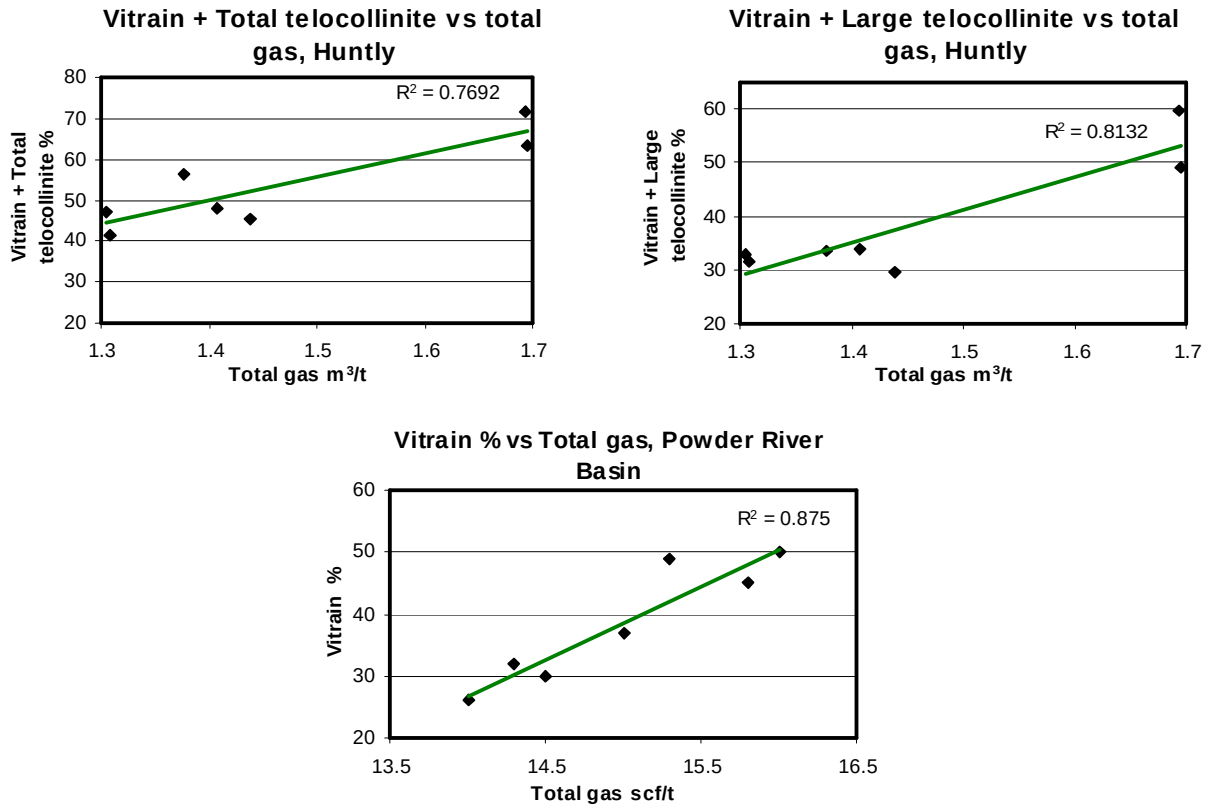

Figure 4.5: Main maceral correlation in the Huntly drill core. The Powder River basin is used to compare a similar relationship (vitrain and total gas).

Only one of the Ohai SC3 graphs proved to have any genuine correlations. All other correlation coefficients were artefacts of outliers and clustering data points. Fusinite correlated strongly with lost gas, with an R^2 = -0.8122 (Fig. 4.6). The relationship could be a result of gas being trapped in pore spaces in the fusinite maceral. Ohai SC1 also showed the majority of significant correlations from the Ohai SC1 samples were with lost gas (Fig. 4.7). Both the inertinite and liptinite groups had strong relationships with lost gas; the inertinite group increasing as lost gas increases (opposite to what was found in Ohai SC3), while the majority of the liptinites decreased with increasing lost gas values.

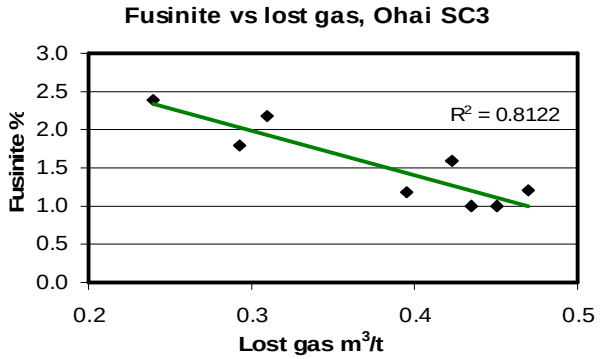

Figure 4.6: Main maceral correlation in the Ohai SC3 drill core.

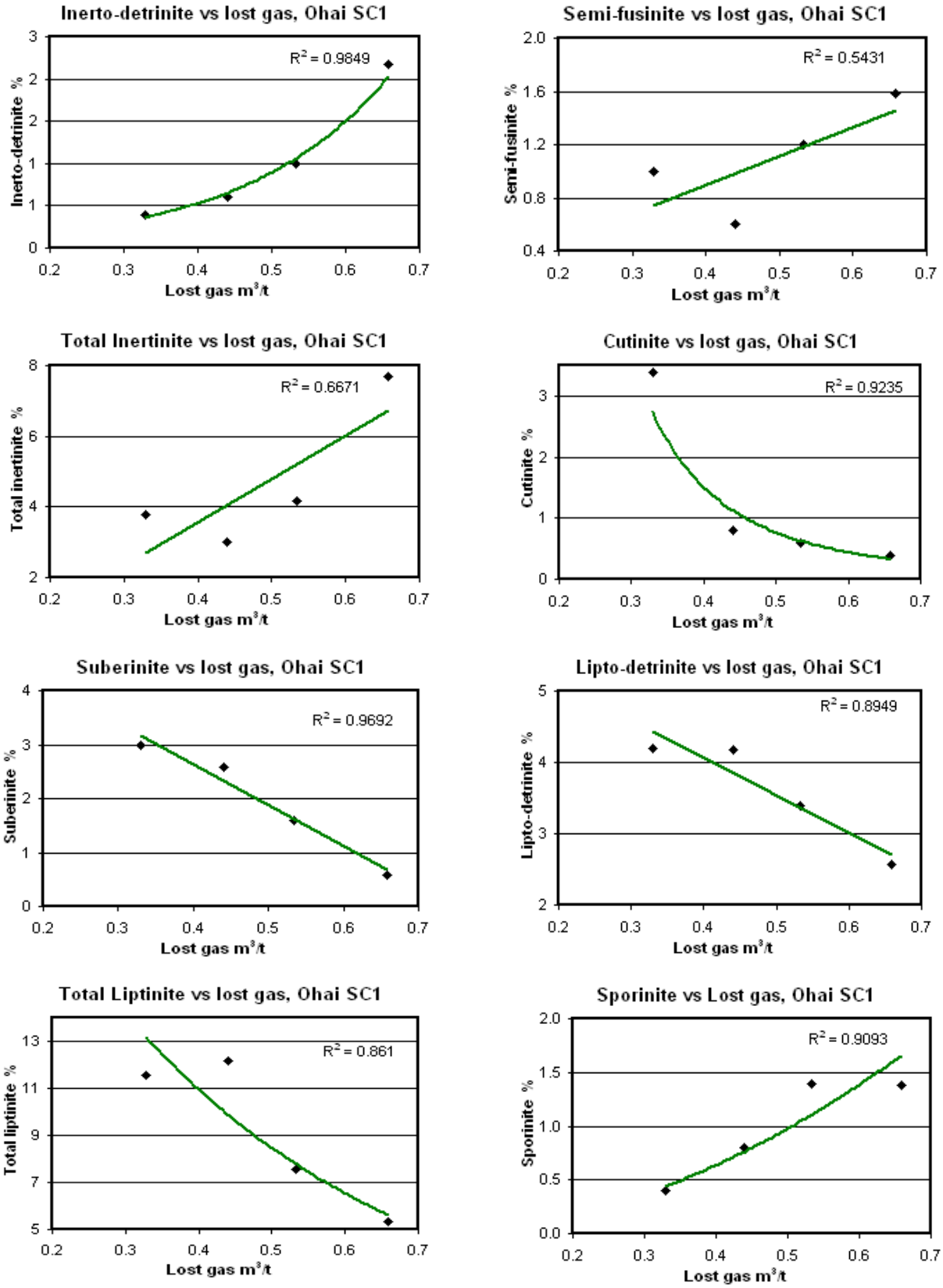

Figure 4.7: Main maceral correlation in the Ohai SC1 drill core.

Samples from the Greymouth core showed an interesting association with residual gas (Fig. 4.8). Structured vitrinite (large telocollinite) correlated positively with residual gas, whereas unstructured vitrinite (desmocollinite) had an inverse correlation. More residual gas may be trapped in the matrix material, whereas the gas may not be stored efficiently in the structured vitrinite as it can simply desorb off, if there is not a sufficient seal in the coal.

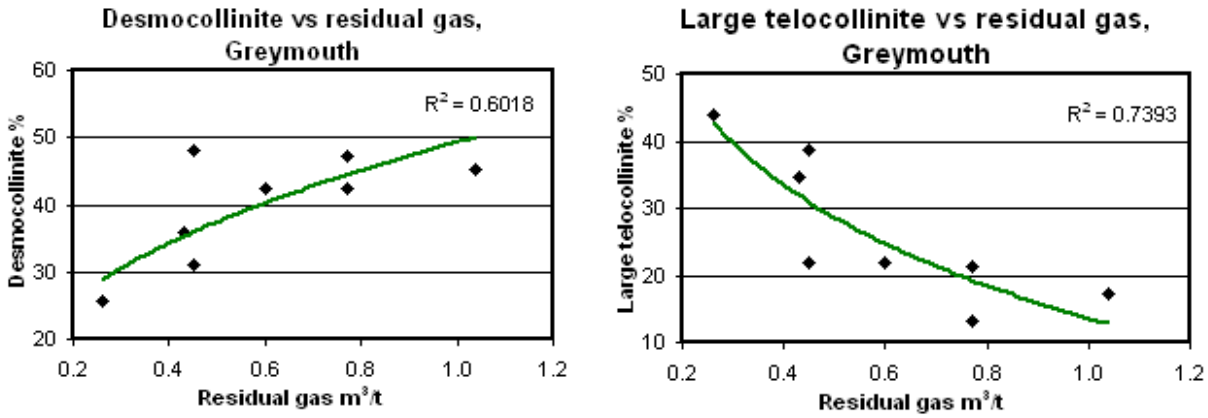

Figure 4.8: Main maceral correlation in the Greymouth drill core

4.2 Geochemical Correlations

4.2.1 Proximate analyses

Proximate and calorific value analyses are reported on a dry ash free (daf) basis, except for ash (dry basis) and inherent moisture (as analysed basis). There were no statistically significant associations between gas content and most proximate and calorific value analyses. There were some apparent relationships as indicated by correlation coefficients (Table 4.4), but under additional scrutiny these proved to be related to ash yield. Ash yield showed the most consistent association in all locations studied, when correlated with total gas volume.

Table 4.4: Significant correlations between proximate data and gas data. (R^2 ~>0.50).

Location	Measured gas	Residual gas	Lost gas	Total gas
Huntly				ash
Ohai SC3	moisture ash	ash	ash	moisture ash
Ohai SC1	ash volatile matter fixed carbon calorific value Suggate number			ash volatile matter fixed carbon calorific value Suggate number
Greymouth	moisture ash volatile matter fixed carbon calorific value	Suggate rank		moisture ash volatile matter fixed carbon calorific value Suggate rank

The inverse relationship between gas content and ash yield is shown in Figure 4.9. Although all drill cores showed strong correlations between ash yield and gas content, the relationship between ash and gas is not as clear for Ohai SC3 and Huntly cores because samples from Ohai SC3 and Huntly drill core contain a predominantly low ash yield. Ohai also showed strong negative correlations between ash yield and both measured and residual gas (Fig. 4.10).

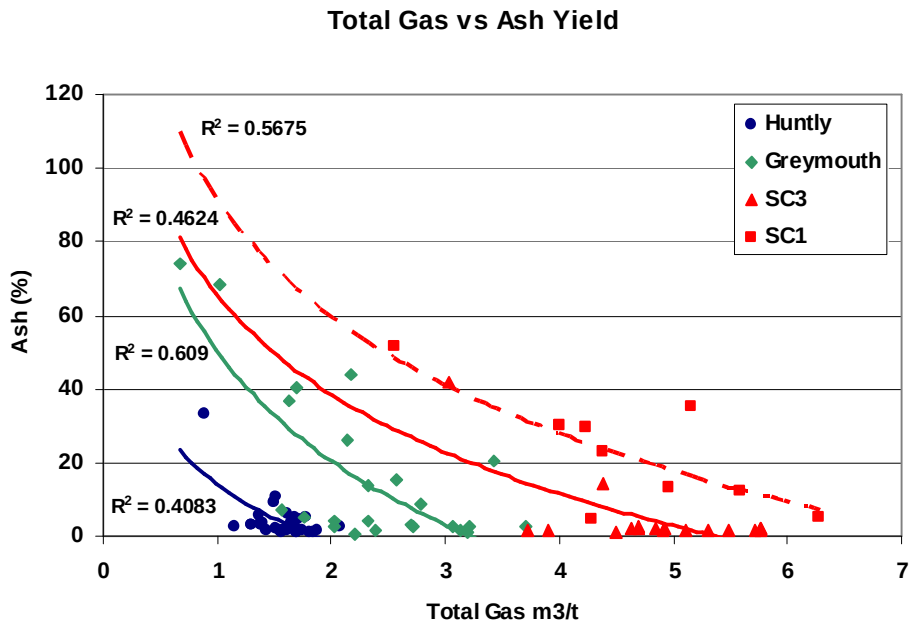

Figure 4.9: The association between ash yield and total gas volume, in all the selected cores.

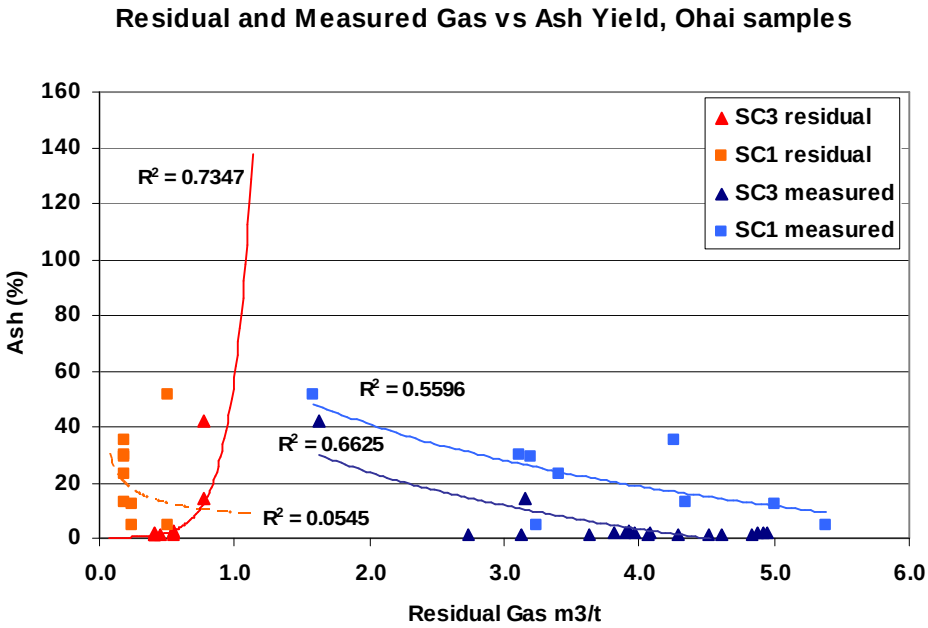

Figure 4.10: The association between ash yield and measured and residual gas volume, in the Ohai samples.

4.2.2 Ash constituents

Ash constituents had a large range of correlations with gas data (Appendix J). In some cores, especially Ohai SC3, correlations were strong. This was expected as the ash yield is the main controlling factor in the amount of gas present. However, in other locations, for example Greymouth, there were only a few correlations. Table 4.5 shows a list of all significant correlations.

Table 4.5: Significant correlations between ash constituent data and gas data. (R^2 ~>0.50).

Location	Measured gas	Residual gas	Lost gas	Total gas
Huntly				SiO_2 Al_2O_3 Fe_2O_3 MgO
Ohai SC3	SiO_2 CaO MgO K_2O Fe_2O_3	SiO_2 Na_2O SO_3 Fe_2O_3		
Ohai SC1	Al_2O_3 TiO_2			Al_2O_3 TiO_2
Greymouth			Mn_3O_4 P_2O_5	

Although correlation coefficients for the Huntly core contained low R^2 values, when plotted trends appeared real (Fig. 4.11). Genuine trends are also seen in Ohai SC3 and SC1 (Figs. 4.12 and 4.13). However, when further investigating Ohai SC3, it was observed that strong correlation coefficients are only present when analysing the whole drill core. If the Ohai SC3 rider seam is removed from the dataset, there are few significant correlations, and they are similar with Huntly correlation coefficients (Fig. 4.14). Combined data from the rider seam and the main seam in the Ohai SC3 drill core has given a false impression of correlations being stronger than they actually are for a single seam intersection. Data for the Ohai SC1 core could not be separated into a main coal seam and a rider seam, as was done in the Ohai SC3 core, because the Ohai SC1 core did not contain a single, thick seam. There were no strong correlation coefficients in the Greymouth core. Both correlation coefficients appeared strong because of a few outlying samples increasing the R^2 value.

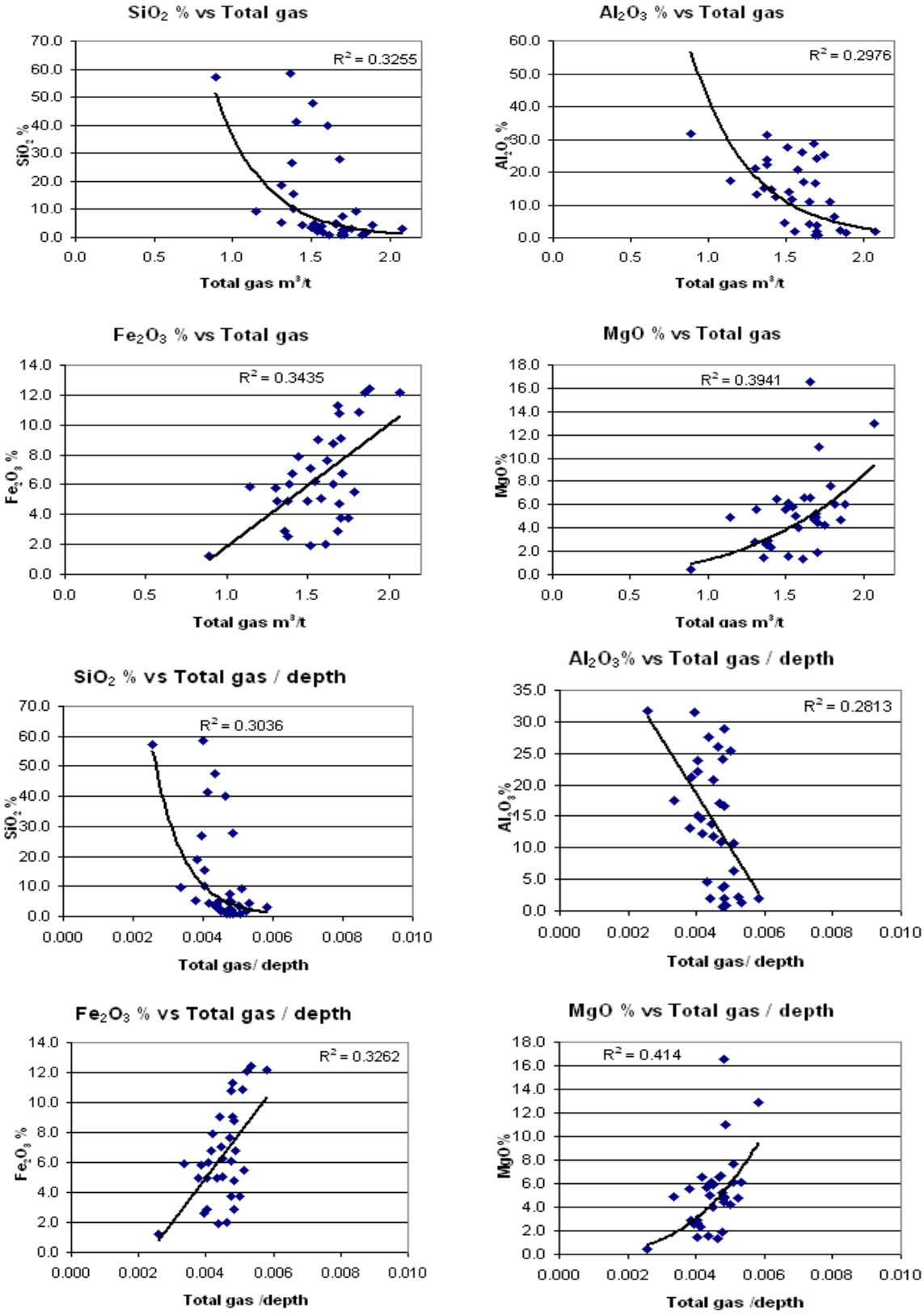

Figure 4.11: Significant correlations between gas data and ash constituents, Huntly drill core.

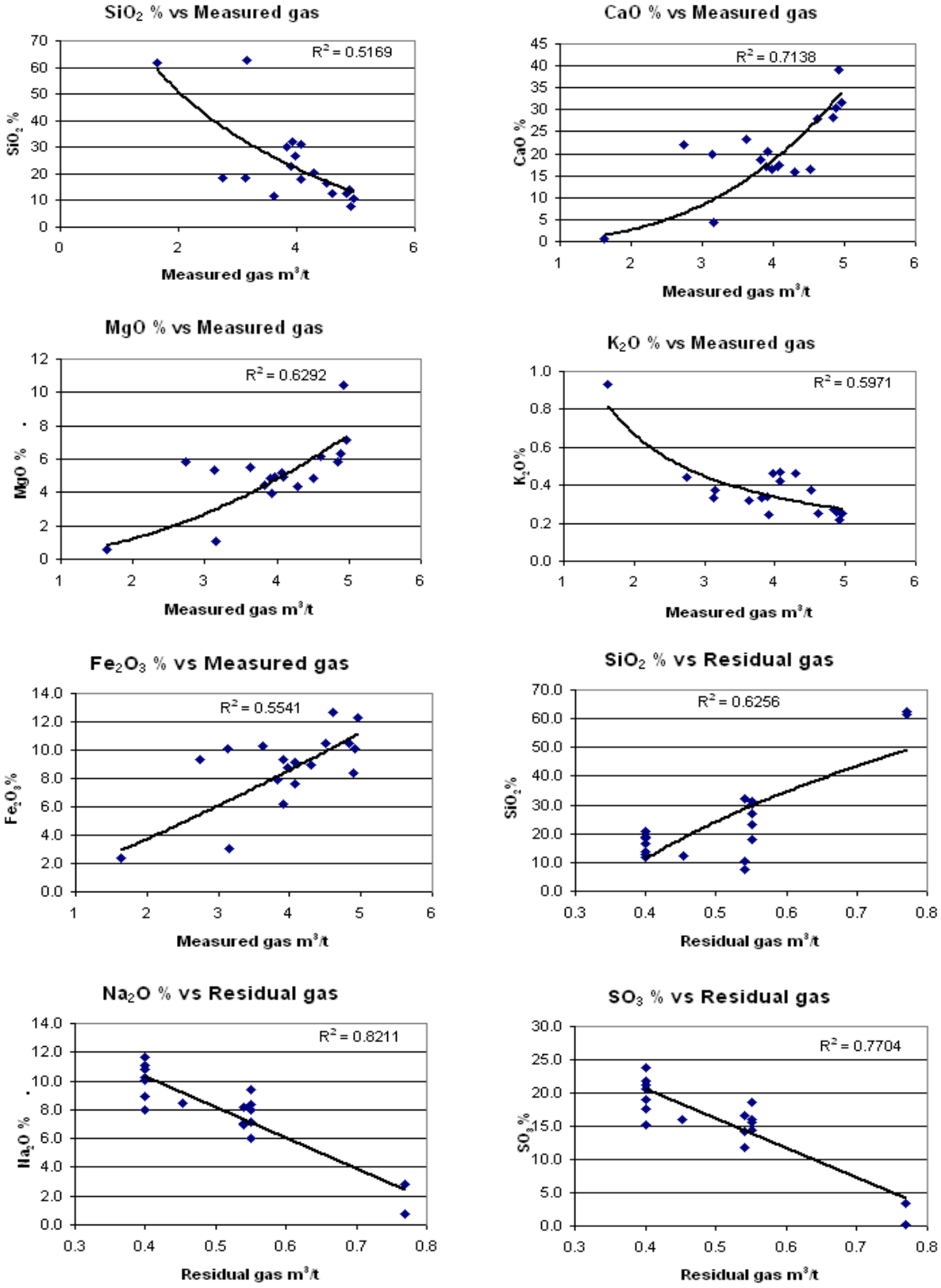

Figure 4.12: Significant correlations between gas data and ash constituents, Ohai SC3 drill core.

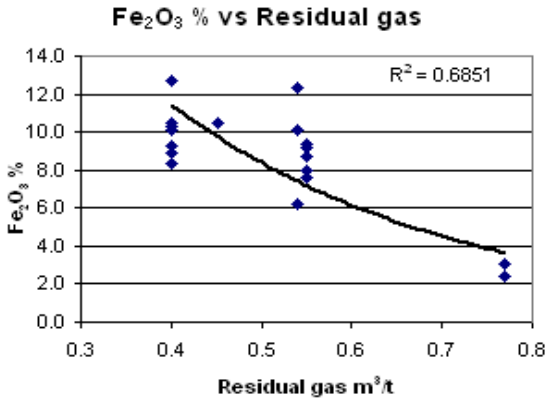

Figure 4.12 (continued): Significant correlations between gas data and ash constituents, Ohai SC3 drill core.

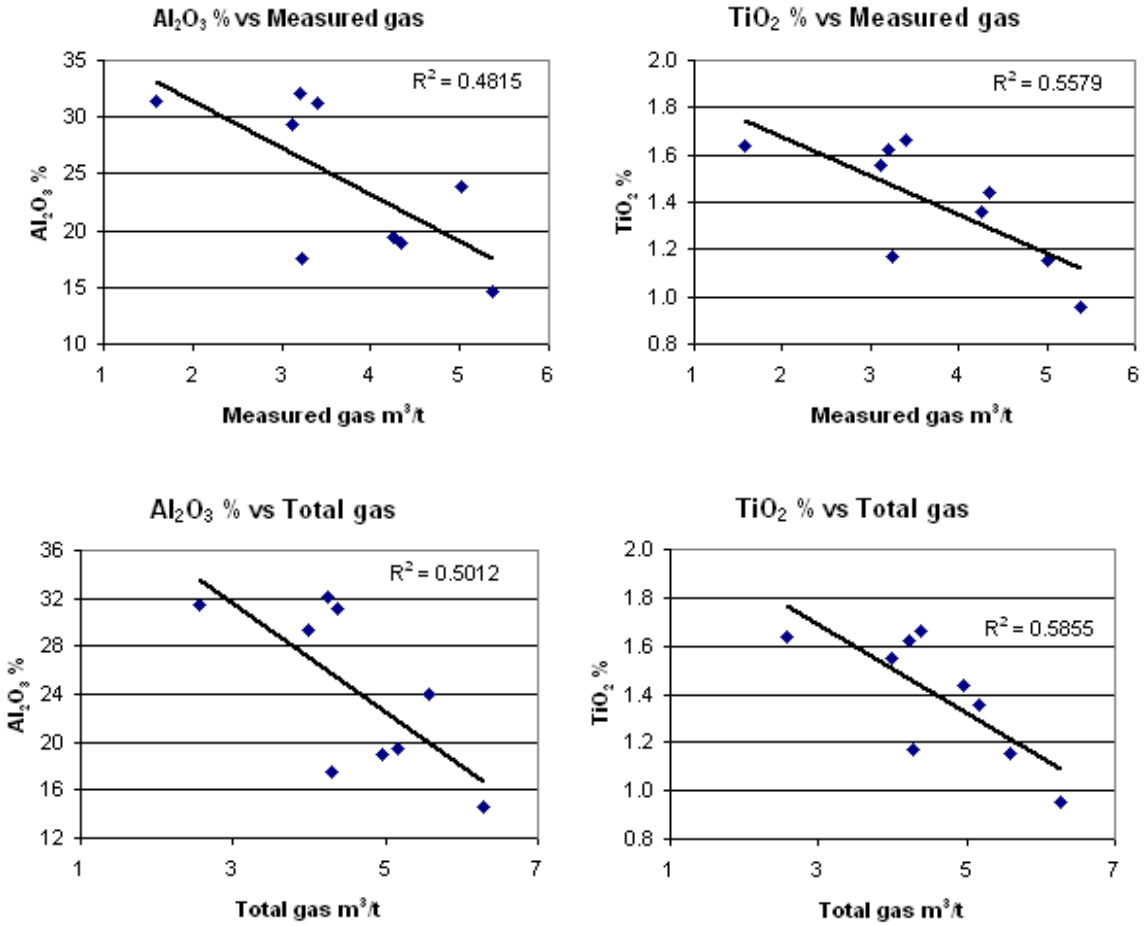

Figure 4.13: Significant correlations between gas data and ash constituents, Ohai SC1 drill core.

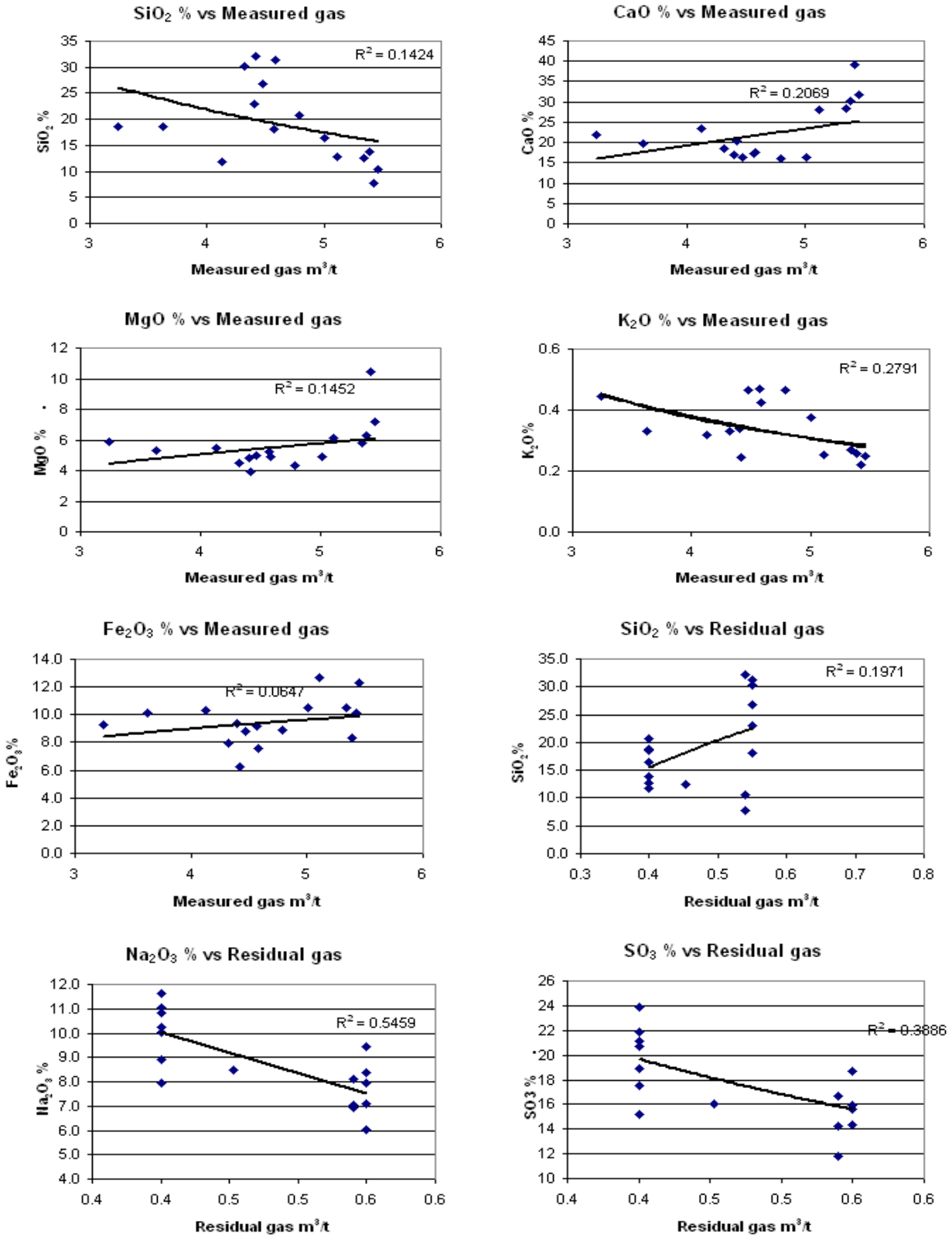

Figure 4.14: Significant correlations between gas data and ash constituents, Ohai SC3 drill core – main seam.

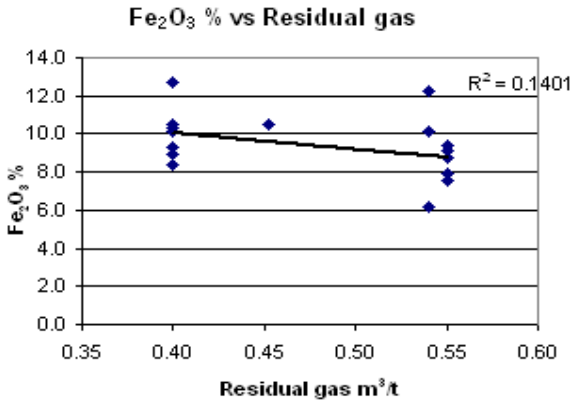

Figure 4.14 (continued): Significant correlations between gas data and ash constituents, Ohai SC3 drill core – main coal seam.

4.2.3 Mineralogy

Correlation coefficients for mineral matter and gas data ranged from very low R^2 values (0.00 ankerite and measured gas in Ohai SC1 core) to high R^2 values (0.97 siderite with lost gas in the Greymouth core) (Appendix J). Correlations would be expected to be similar to ash constituent correlations, because of the intimate relationship with ash constituents. However, as mineralogical results are less precise, as a result of analyses being on a spot basis (where the X-ray beam hits a single spot on the glass slide) not on whole coal, ash constituent correlations will be more representative of what inorganic components are in the coal. Table 4.6 shows a list of all significant correlations.

Table 4.6: Significant correlations between mineralogical data and gas data. (R^2 ~>0.50).

Location	Measured gas	Residual gas	Lost gas	Total gas
Huntly				quartz kaolinite
Ohai SC3	quartz kaolinite calcite ankerite	siderite	siderite	quartz kaolinite calcite ankerite
Ohai SC1		quartz siderite	quartz kaolinite ankerite siderite	
Greymouth	quartz siderite	pyrite	siderite	quartz siderite

Ash constituent data can be used to infer what minerals are present, and in what abundance, although certain oxides form a major part of multiple minerals. Table 4.7 summarises the oxides present, and possible minerals that may be present, based on XRD analyses for the Greymouth, Ohai and Huntly core samples (Li et al., 1999; Li, 2002; Shearer, 1992; Newman, 1988; this study).

Table 4.7: Oxides present in coal samples, and possible associated minerals, based on XRD studies (Li et al., 1999; Li, 2002; Shearer, 1992; Newman, 1998; this study.)

Oxides present	Possible minerals present (from various XRD analyses)
SiO_2	quartz; kaolinite; muscovite; illite
Al_2O_3	kaolinite; muscovite; illite
Fe_2O_3	siderite; ankerite; dolomite
CaO	calcite; ankerite; apatite; salt (gypsum)
MgO	calcite; ankerite; dolomite
Na_2O	salt (halite); "ankerite" Mg replacement
K_2O	"ankerite" Mg replacement; muscovite; illite
TiO_2	rutile; illmenite; mica
Mn_3O_4	ankerite; pyrite
SO_3	pyrite; sulphur from coal
P_2O_5	apatite

Although Huntly correlations are weak (R^2 values of -0.2272 and 0.2662), they appear to be genuine, with no clustering of samples and outliers skewing data (Fig. 4.15).

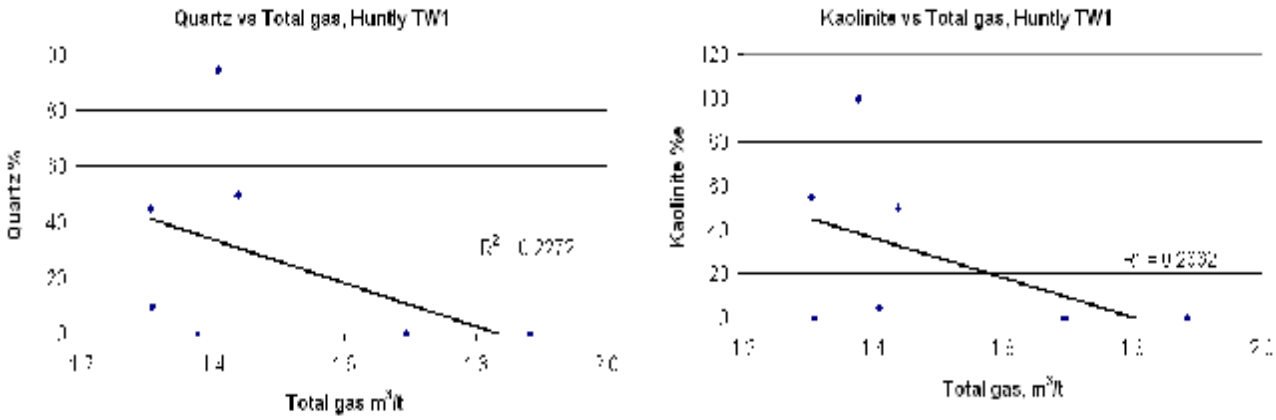

Figure 4.15: Main significant correlations with gas and mineralogical data, in the Huntly core. The main correlations were found between quartz and kaolinite and total gas volumes.

Genuine trends are also seen in Ohai SC3, where some correlation coefficients are stronger, for example calcite with total gas $R^2 = 0.5105$, showing a greater affinity between mineral matter and gas volume (Fig. 4.16). Ohai SC1 has a mixture of genuine trends with lost gas and quartz, ankerite and siderite (R^2 values 0.8411, -0.6205 and -0.7559 respectively.) However, coefficients with residual gas show a clustering of points with an outlier skewing data to create stronger R^2 values (Fig. 4.17). Samples from the Ohai SC1 core are few (n = 5), so, overall, the results are considered inconclusive. Correlation coefficients from the Greymouth samples are similar to correlations seen for the Ohai SC1 samples; that is, there are some genuine correlations, while others are an artefact of outlier samples (for example, siderite and lost gas, $R^2 = 0.9365$; siderite and total gas, $R^2 = 0.6512$; pyrite and residual gas, $R^2 = 0.3579$, Fig. 4.18). Correlations with siderite were strong, although only two samples contained siderite, indicating there may be a direct link with the occurrence of siderite with increased gas volumes. Again, a greater number of samples would yield more information to whether these correlations hold true.

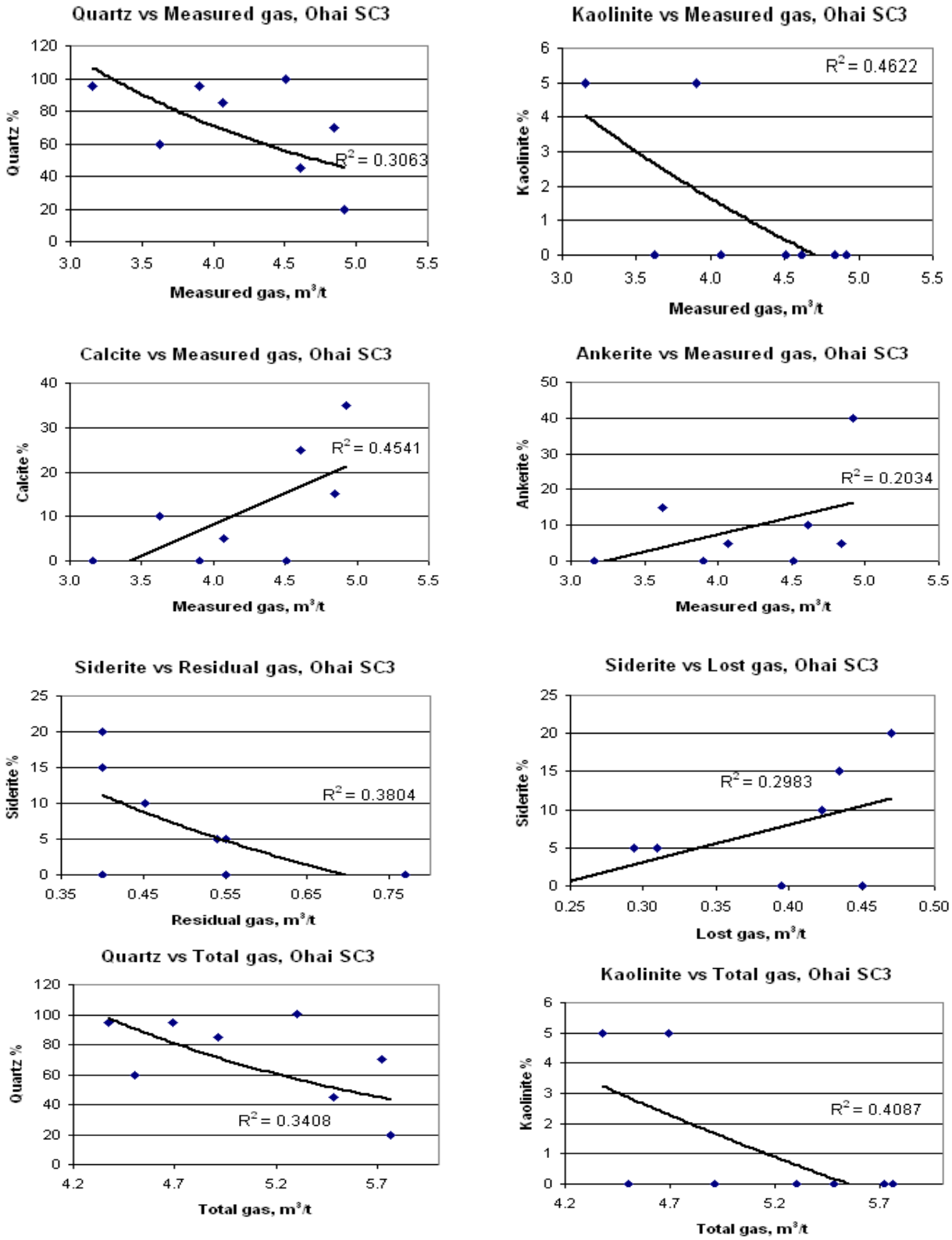

Figure 4.16: Significant correlations with gas and mineralogical data, Ohai SC3, based from correlation coefficient chart. Some correlations (for example kaolinte and total gas; siderite and lost gas; kaolinite and measured gas are a function of clustering points.

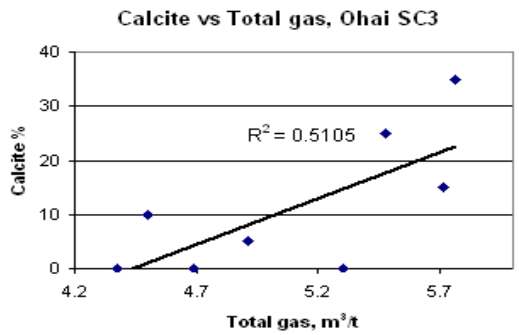

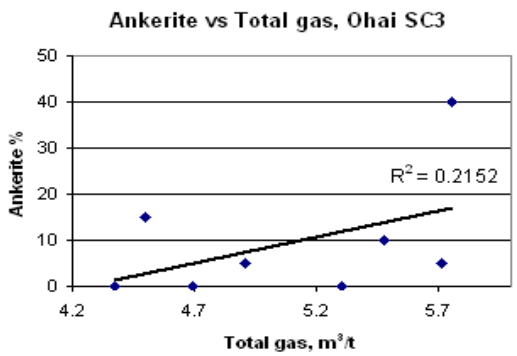

Figure 4.16 (continued): Significant correlations with gas and mineralogical data, Ohai SC3. See page 88 for full description.

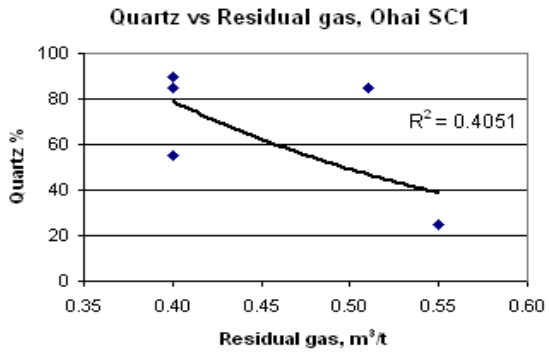

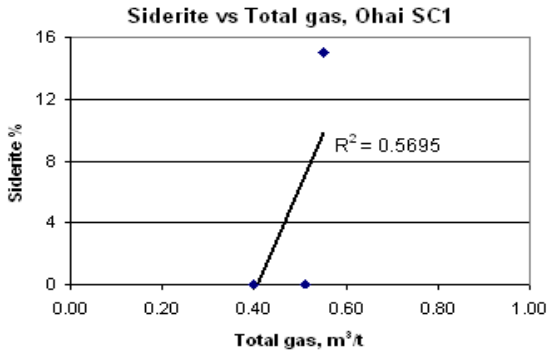

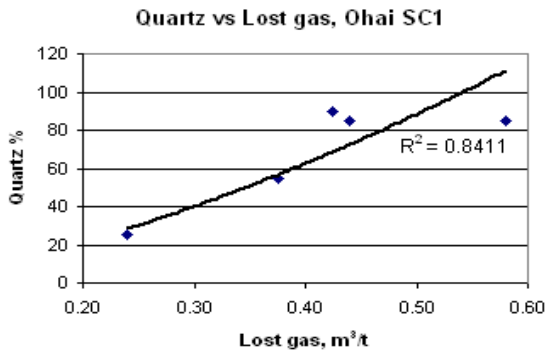

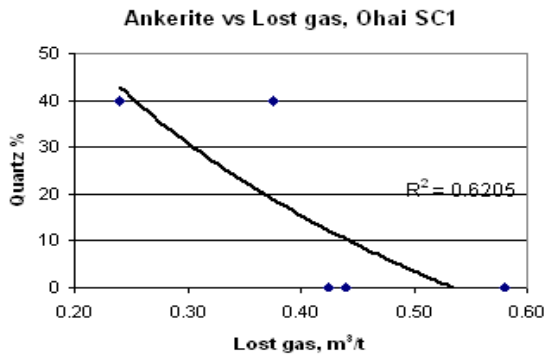

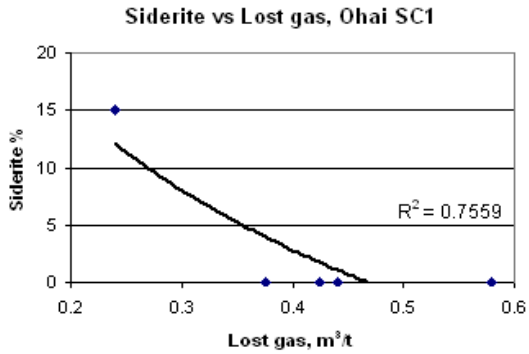

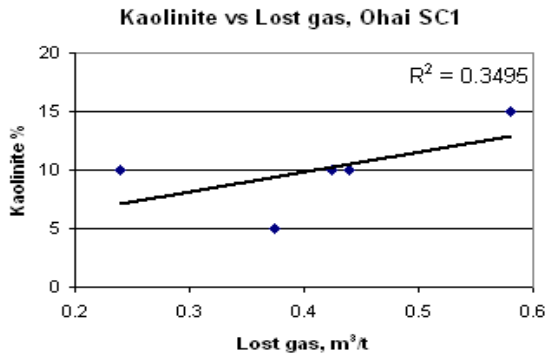

Figure 4.17: Significant correlations with gas and mineralogical data, Ohai SC1, based from correlation coefficient chart. Some correlations (for example siderite and total gas; siderite and lost gas; ankerite and lost gas are a function of clustering points.

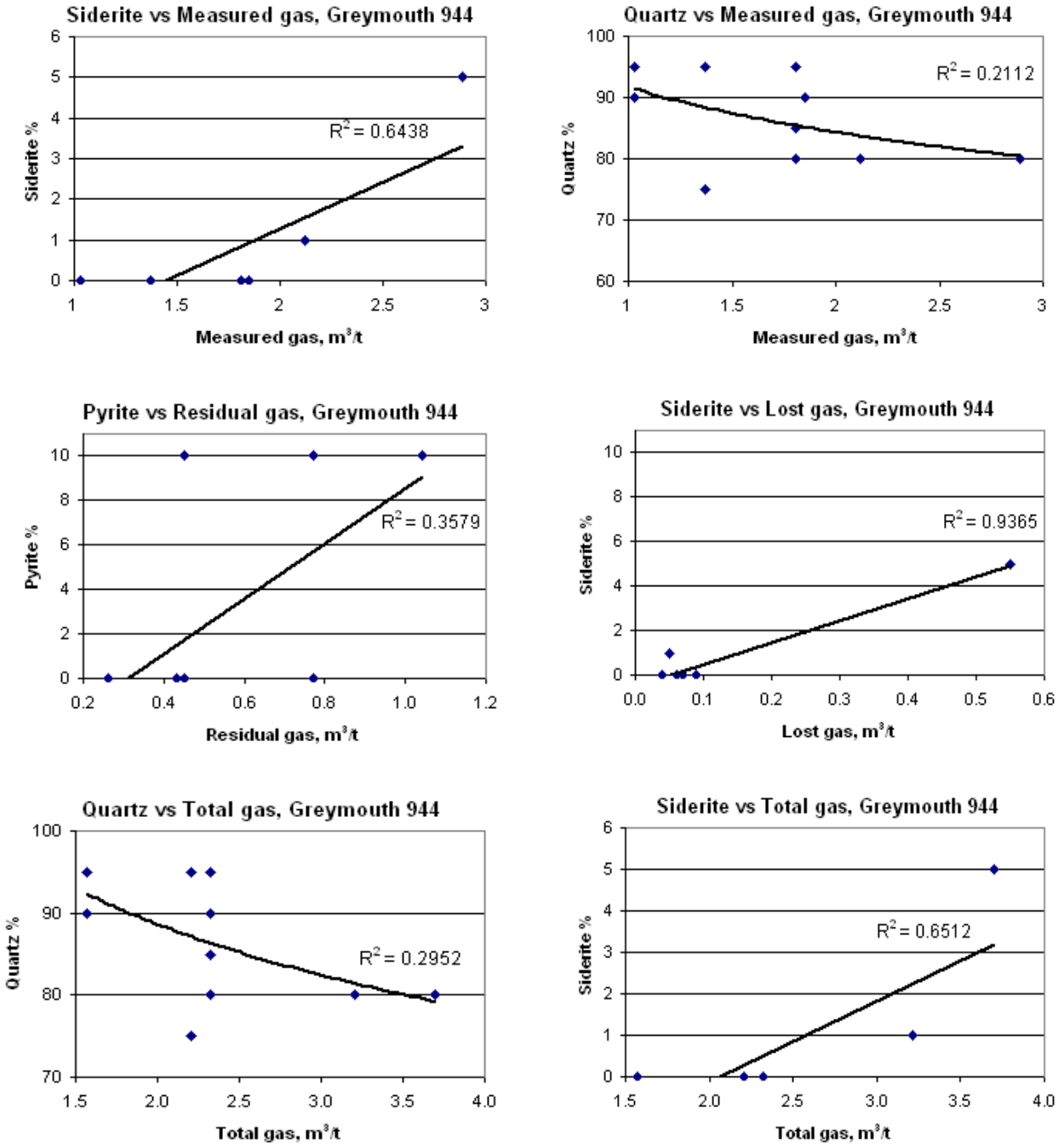

Figure 4.18: Significant correlations with gas and mineralogical data, Greymouth, based from correlation coefficient chart. Some correlations (for example siderite and measured gas; siderite and lost gas; pyrite and residual gas; siderite and total gas) are a function of clustering points.

4.3 Saturation Correlations

The degree to which coal samples were saturated with gas was compared with proximate, maceral, ash constituent, and mineralogical analyses. Proximate analyses used a dry, ash free (daf) correction, except for inherent moisture (as analysed [aa]) and ash (dry basis [db]). Table 4.8 summarises the range of correlation coefficients with each type of analysis, and the percentage of correlation coefficients that were **below** the significant correlation coefficients expressed in Table 4.1. Many of the correlations show wide scatter in the data points (the Huntly saturation data and ash constituent correlations, for example) or outlying values increasing the correlation coefficient (mineralogical correlations with Ohai SC1 and Huntly saturation data). Again, there were no consistent associations between basins.

Table 4.8: Summary of correlation coefficients between percent saturation and other parameters.

Analysis	Location	min R^2	min parameter	max R^2	max parameter	% of data under significant R^2 value
Proximate	Huntly	0.23	moisture	-0.56	ash	40
	Ohai SC1	-0.23	moisture	0.79	calorific value	60
	Ohai SC3	-0.01	calorific value	-0.62	ash	60
	Greymouth	0.63	calorific value	-0.69	ash	0
XRD	Huntly	-0.39	calcite, ankerite	-0.52	kaolinite	100
	Ohai SC1	0.01	ankerite	-0.78	siderite	100
	Ohai SC3	0.10	siderite	0.72	calcite	20
	Greymouth	0.00	muscovite	0.81	siderite	80
XRF	Huntly	0.01	Mn_3O_4	0.54	Fe_2O_3	45
	Ohai SC1	-0.08	K_2O	-0.81	TiO_2	73
	Ohai SC3	-0.02	P_2O_5	0.73	CaO	27
	Greymouth	0.14	TiO_2	-0.46	K_2O	82
Maceral	Huntly	0.00	large telocollinite	0.86	cutinite	94
	Ohai SC1	0.17	cutinite	0.94	fusinite	94
	Ohai SC3	0.02	suberinite	-0.65	cutinite	100
	Greymouth	-0.01	total inertinite	0.59	inertodetrinite	100

Samples from the Greymouth core showed a strong affiliation between proximate analyses and the saturation yield (Figs. 4.19). These samples had strong positive correlations between moisture, fixed carbon and volatile matter and % saturation, and strong negative correlations between ash and calorific value and saturation yield. Samples from the Ohai and Huntly cores also had a few significant correlations between the % saturation and ash yield (in both areas), and moisture, volatile matter, fixed carbon and calorific value (Figs. 4.19).

There were only a few correlations with % saturation and mineralogy, and these were artefacts of clustering (for example, Greymouth and Ohai SC1 samples: siderite and % saturation), or subject to wide scatter in data points (for example, Huntly and Ohai SC3 samples: Kaolinite, quartz and calcite and saturation yield).

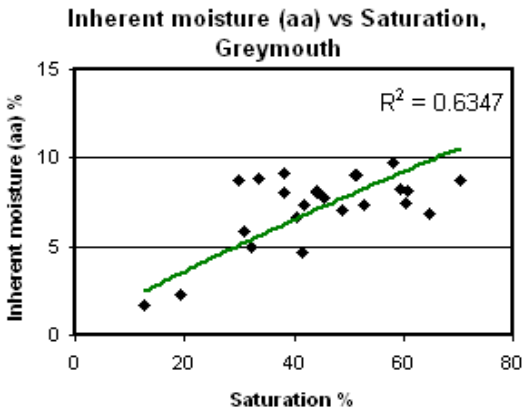

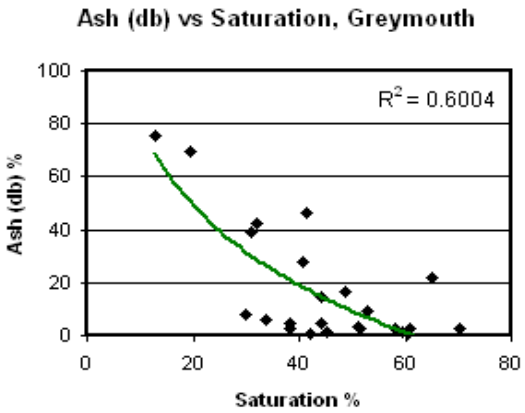

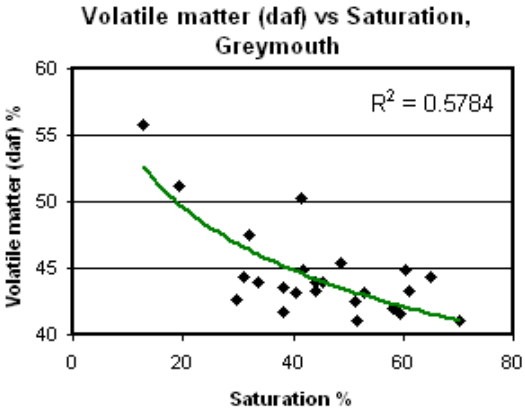

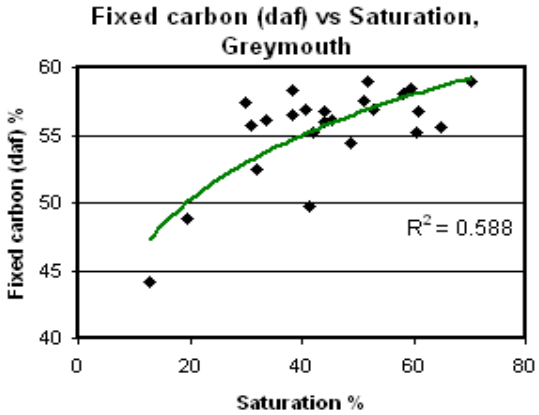

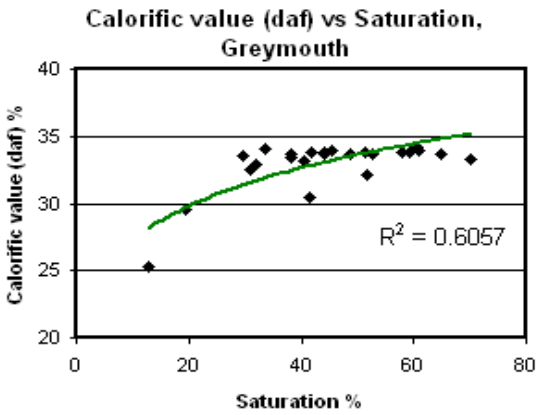

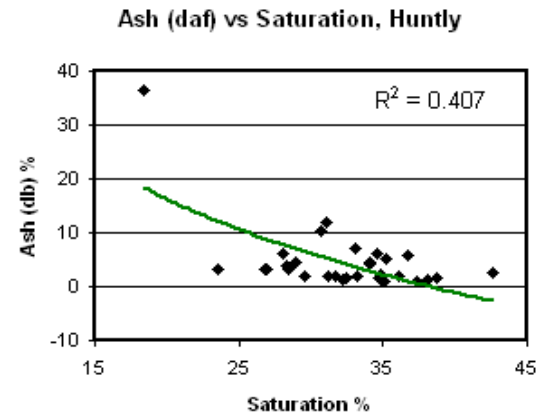

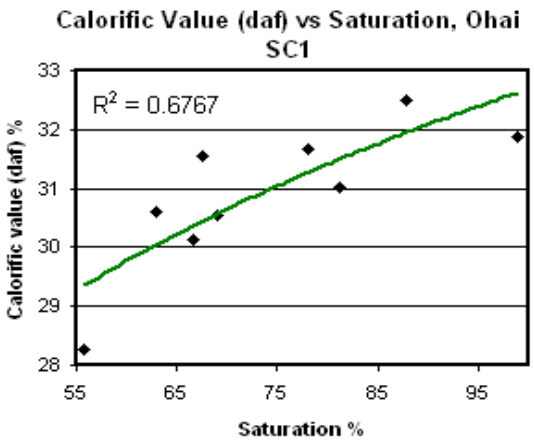

Figure 4.19: Summary of significant correlations between proximate analyses and percent saturation.

The Ohai cores contained many strong correlations between ash constituents and % saturation (Fig. 4.20). Al_2O_3 and TiO_2 had strong negative correlations with % saturation in both Ohai SC1 and SC3 samples. CaO and Na_2O_3 had strong positive correlations with saturation in Ohai SC1 samples, while Fe_2O_3, and MgO all had high positive correlation coefficients with saturation in Ohai SC3 samples. SiO_2 had a high negative correlation with saturation in Ohai SC3 samples. There were only a few correlations in the Huntly drill core, and these both had a wide scatter in data points. Samples from Greymouth did not contain any correlations between ash constituents and % saturation.

Maceral correlations were strongest with % saturation in the Huntly core (especially with the liptinites cutinite and resinite, Fig. 4.21). Desmocollinite and cell telocollinite also strongly correlated with the % saturation in Huntly samples. The Ohai SC3 core contained strong correlations between % saturation and cutinite, resinite and liptodetrinite. The Ohai SC1 core showed a strong correlation between fusinite and % saturation, (R^2 = 0.988, Fig. 4.21). Samples from Greymouth also had some strong correlations between inertinites (fusinite and inertodetrinite) and % saturation. The main trend with maceral and saturation correlations were that liptinites and inertinites were closely associated with saturation yield. However, when looking at gas data (measured, residual, lost and total) vitrinites were more closely associated with gas content.

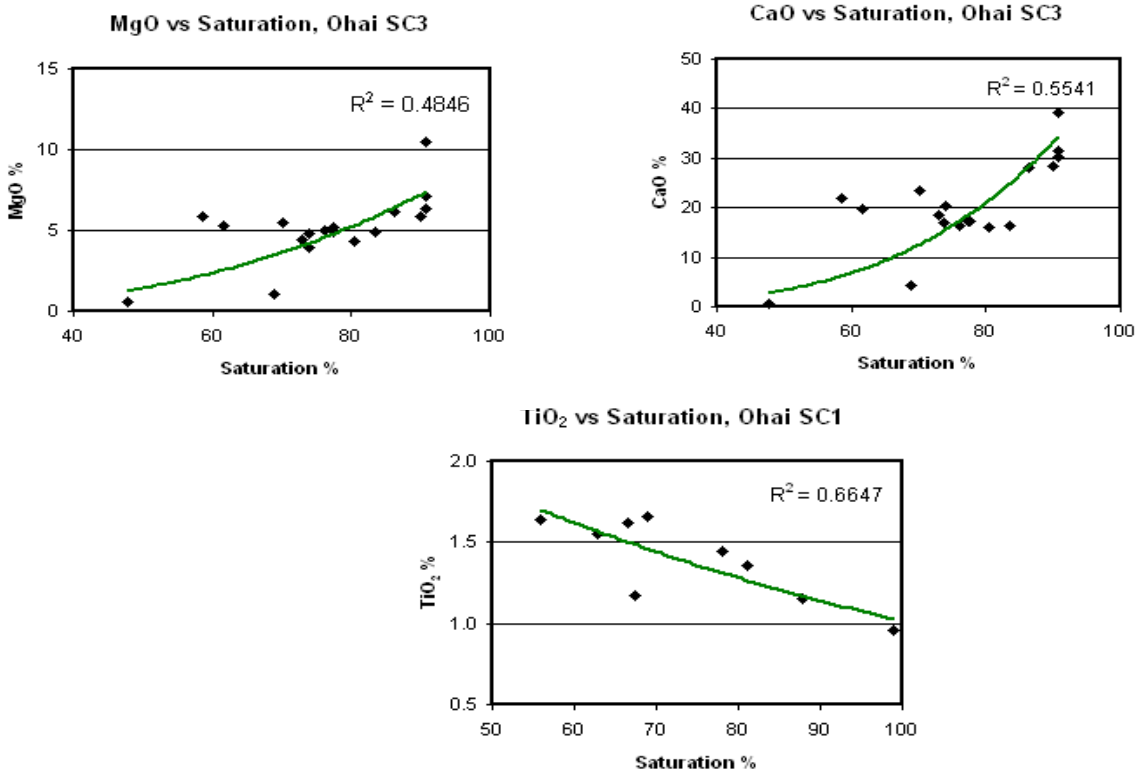

Figure 4.20: Summary of significant correlations between ash constituents and percent saturation.

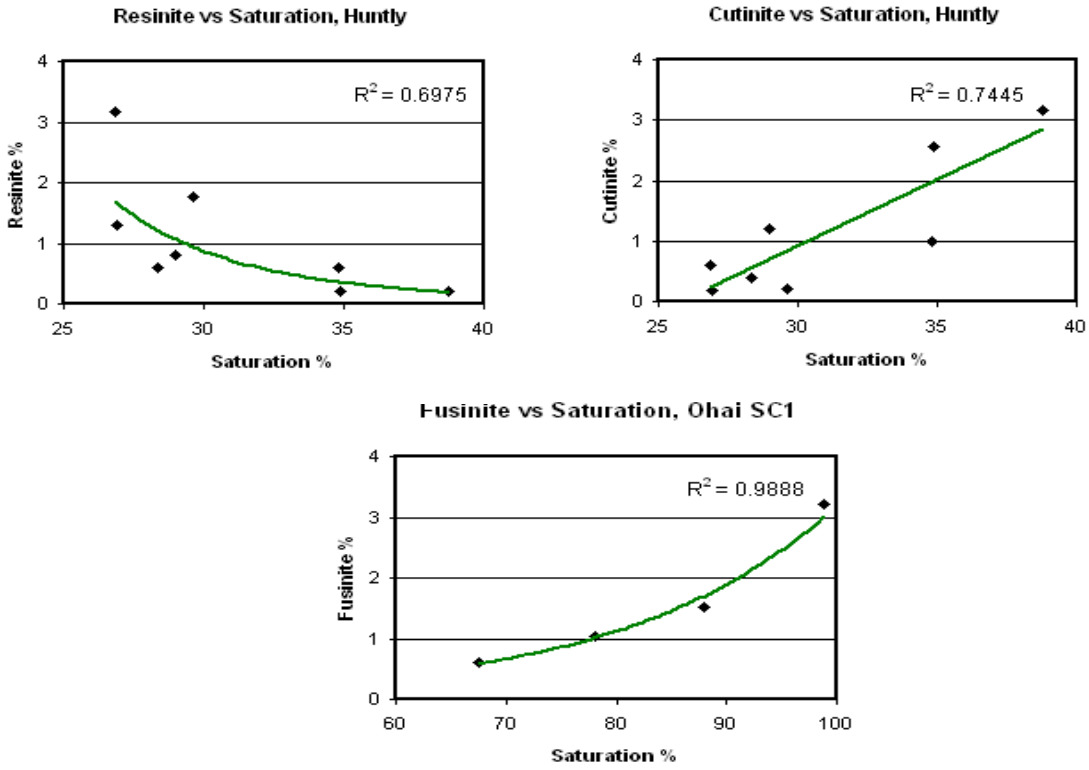

Figure 4.21: Summary of significant correlations between maceral analyses and percent saturation.

4.4 Summary by Location

A brief summary is given, by location, of all the relevant above-mentioned correlations. These are further discussed in Chapter 5. There was only one association that was found in all basins: ash yield with total gas content. Although the organic chemistry was related to gas content in each location, different macerals were associated with different types of gas volume. It is unknown if this is an effect of rank, or of a more localised nature, such as depositional environment.

Relevant gas associations found in the Huntly drill core were related to two facets: macerals and geochemistry. The following correlations were found:

- Structured vitrinite coupled with vitrain % (that is, vitrain % and large telocollinite, and vitrain % and total telocollinite) yielded strong positive correlations with the total gas content. It is thought that structured vitrinites allow gas flow through the woody material, resulting in elevated total gas readings (Moore et al., 2002b).
- The ash yield correlated negatively with the total gas volume (see Chapter 5).
- The % saturation correlated negatively with the ash yield.
- The % saturated correlated well with macerals in the Huntly drill core. Both cutinite and resinite had strong associations.

The two Ohai drill cores' contained the following relevant correlations:

- Any maceral correlations were only associated with lost gas.
- Ohai SC3 samples had a very strong negative correlation with fusinite and lost gas, possibly a result of gas being trapped in pore spaces in the fusinite maceral.
- Ohai SC1 samples also showed macerals from the inertinite group correlating with lost gas. However, in the SC1 drill core the samples correlated positively. Liptinites also correlated positively with lost gas in the SC1 drill core. The low number of samples in the SC1 drill core make it hard to assess the accuracy of the correlations, however it is clear that in both SC1 and SC3 there are associations with the inertinite group and lost gas.
- The ash yield is negatively associated with total gas volumes in both SC3 and SC1 drill cores. Ohai SC3 samples also showed the ash yield correlating with both measured (negative) and residual (positive) gas volumes.
- The minerals calcite and kaolinite also show some strong correlations in the SC3 drill core (direct and inverse, respectively). It is expected that mineral matter should be related to the gas volume, to some degree, because of the intimate relation of mineral matter and ash.
- The % saturation correlated negatively with the ash yield.
- The Ohai samples had significant correlations between ash constituents and the % saturation.
- The % saturation correlated strongly with cutinite, resinite and liptodetrinite in the SC3 samples, and with fusinite in the SC1 samples.

Correlations in the Greymouth drill core were also related to two distinct facets: organic petrology and geochemistry.

- Total vitrinite correlated with gas volume.
- Large telocollinite correlated positively with residual gas.
- Desmocollinite was associated negatively with residual gas.
- Maceral relationships with residual gas volumes in the Greymouth core may be a result of residual gas being trapped in the matrix material. In more structured vitrinite the residual gas can desorb off quickly, leading to a negative correlation.
- The ash yield is negatively correlated with total gas volume.
- The % saturation had strong positive correlations with moisture, fixed carbon, volatile matter, and negative correlations with calorific value and the ash yield.
- The % saturation correlated strongly with fusinite and inertodetrinite.

Chapter Five
Discussion

This study has identified a number of associations between gas content and coal properties in New Zealand coals. The ash yield had the strongest correlation with respect to gas variation, in all areas studied. However, when the ash yield is less than 10 %, this relationship breaks down and there is no relationship between the two parameters. Some of the variation seen in samples with less than 10% ash yield can be calculated to the organic components of coal, but these are site specific, possibly a function of the rank of the coal. The thermal maturity of the coal is known to influence methane the holding capacity (Hildenbrand et al., 2006; Levy et al., 1997; Laxminarayana and Crosdale, 2002.; Scott, 2002; Bustin and Clarkson, 1998; Hacquebard, 2002; Creedy, 1988), but the samples studied do not follow the generalised trend. This is because the Ohai samples behave as a more thermally mature coal than the higher rank (relative to Ohai) Greymouth samples, in relation to gas volume, methane adsorption capacity, and also gas composition.

This chapter is organised into six sections, the first five discuss the relationships identified above, and their importance to coal seam gas and the sixth discusses the specific 'problems' with the Ohai coal samples.

5.1 Inorganic Composition

The ash yield was the most dominant factor controlling the gas volume and there is an inverse relationship between these two parameters. Ash yield is the non-combustible inorganic residue that remains after a coal is burnt. Because it is generally accepted that gas adheres to the organic components of coal, more inorganic

matter in the coal reduces the amount of organics present, thus reducing the sites for gas to adhere (Yee et al., 1993; Crosdale et al., 1998; Scott, 2002).

All locations show relatively strong negative correlations with ash yield and total gas volume. Ohai samples also show strong negative correlations between ash yield with both measured and residual gas. The Greymouth core has the strongest correlation, whereas the Huntly core has the weakest correlation. All three locations (Fig 4.9) show that this relationship holds true when there is greater than 10 % ash. In samples with less than 10 % ash the association between total gas content and ash yield breaks down. There may be one or more parameters controlling desorbed gas volume in circumstances where the ash yield is less than 10 %.

It is interesting to note that the Huntly TW1 coal core has very few high ash layers which the above mentioned association (ash yield and total gas) is based on. By introducing higher ash layers into the coal seam one would expect to see the trend strengthened and a higher correlation coefficient produced. Recent gas exploration work in the Huntly area by Solid Energy Ltd has lead to five additional drill holes with both gas data (desorption, adsorption) and proximate analyses conducted. Initial analysis of the dataset (T. Mares, pers. comm., University of Canterbury, 2006) has shown that the relationship with ash yield and gas content does not exist in the new Huntly drill holes.

Limited general research has been conducted in terms of ash yield, mineral matter and gas content. Crosdale et al, (1998) stated that mineral matter is effectively not adsorbent to coal seam gases (in particular CH_4), and acts as a dilutant. Scott (2002) also recognised that gas is adsorbed onto the organic layers of coal, and not the ash layers. This lead to the conclusion that when comparing adsorption isotherms from different locations, the gas volume measurements should be corrected to an ash-free basis (daf) to eliminate the effects of mineral matter and ash variability. Yee et al. (1993) pointed out that as early as 1965 a French geologist, Gunther, recognised that mineral matter acted as an inert diluent with respect to gas sorption. He explained that it caused a reduction in the gas volume by displacing the organic material that can adsorb gas. Yee et al. (1993) also reports a linear relationship where gas volume increases with a reduction in the amount of ash and moisture present. Gurba et al. (2001) looked at the effect of mineralisation of gas drainage in the southern coalfield of New South Wales, Australia. They found that microcleat mineralisation may play a major role in blocking gas drainage. They observed both mylonites, or crushed, powdery zones, in cleats and siderite nodules blocking micropores in maceral cells. Clarkson and Bustin (1996) found that an increase in mineral matter also affects the CO_2 micropore adsorption capacities, as well as methane adsorption capacities.

5.2 Organic Composition

All three locations studied show similar overall maceral compositions, although they are three different ranks. When comparing the maceral composition with gas content data, very few significant correlations were actually apparent. Of the associations that are seen, they are restricted to individual basins and locations. This is most probably a function of rank. Both Hildenbrand et al (2005), and Laxminarayana and Crosdale (1999) have also found that the degree of influence of maceral composition seems to be rank dependent. Laxminarayana and Crosdale (1999) found that coal from the Bowen and Sydney basin's high volatile bituminous coals showed an increase in the adsorption capacity with an increase in vitrinite content. However, ranks higher than medium to low volatile bituminous coals showed little influence of vitrinite content over adsorption capacity.

Within locations (that is, within rank) some associations can be seen. For example, in the Greymouth drill core a strong positive association exists between residual gas and the concentration of desmocollinite. This suggests that a significant amount of gas is retained in the finer fractions of the coal. Conversely, when there is more structured vitrinites (that is, telocollinite) the residual gas volume is significantly lower. It is well known that telocollinites are more porous (Taylor et al., 1998), and thus should be able to release gas more readily. Desmocollinite is finer grained with less porosity (Taylor et al., 1998), and thus would be expected to hold more gas. The type of vitrinite has importance to CSG fields because it may relay information on gas flow rates. If coal is from an area that contains higher desmocollinite contents, rates of gas diffusion to the cleats will be slower than coals containing the more porous telocollinite maceral. The slower rates of diffusion results in lower gas flow rates.

The Ohai SC3 core showed a strong inverse relationship with lost gas and fusinite. That is, the more fusinite, the less lost gas. This suggests that when an interval of coal has higher fusinite content, which is more porous than other macerals, potential lost gas is actually stored in the pore spaces, leading to a lower proportion of lost gas. Walker et al., (2001) found that inertinite-rich coals in the northern Bowen Basin were associated with lower gas volumes, and less efficient gas drainage, retaining gas within pore spaces. This is consistent with the association seen in Ohai SC3, with lower levels of lost gas associated with high fusinite content.

In the Ohai SC1 core the inverse association was found: inertinites showed strong positive relationships with lost gas. That is, the more inertinites, the more lost gas. However, although the opposite trend is seen in Ohai SC1, because of the relatively few data points, this association is inconclusive. Another strong maceral relationship is seen in the Ohai SC1 core: liptinites showed a strong negative relationship with lost gas. Walker et al., (2001) also determined that there was a negative correlation with gas volume and liptinite content in northern Bowen Basin coals. The association was attributed to the cracking of liptinites and

bitumens, producing gas at an early stage in the coalification process. The association in Bowen Basin coals is supported by research carried out by Glickson et al., (1999) who then went on to demonstrate that up to 95% of methane in some Bowen Basin coals may have been sourced from their bitumen. This type of study has not been carried out in New Zealand and data in this study neither supports nor contradicts the relationships seen by Walker et al., (2001) and Glickson et al., (1999).

Huntly samples showed associations with gas content to both vitrain and telocollinite abundance. An increase in total gas content was synonymous with an increase in structured vitrinite. This trend, although not present in the other New Zealand basins, has been identified in the Powder River basin (Moore et al. 2002b). Vitrinite is the maceral that is readily identified with higher gas contents, as the wood structure is thought to allow better methane flow (Moore et al. 2002b).

Although maceral composition seems to exert some influence in both adsorption capacity and gas content, the degree of influence is variable between basins. Most likely, the degree of maturation (i.e. rank) is overprinting and influencing the relationships between gas and organic content. Thus, although some conclusions can be drawn between the associations of macerals and gas content, these associations have to be treated separately between different basins and certainly between different coal ranks.

5.3 Saturation

Because of the limited adsorption samples, this study could only make approximate correlations with the percent saturation, as saturation values are all estimated using the method described in Chapter 2.6.3. Many associations were seen between percent saturation and proximate, ash constituents, mineralogical and maceral analyses (see Chapter 4.3).

Coal composition correlated with the percent saturation. When looking at associations between macerals and gas content, the vitrinite group of macerals held the greatest influence on gas content. In particular, the percent saturation correlated strongly with macerals from the liptinite and inertinite groups. The majority of inertinites had a positive correlation with percent saturation, while most liptinites correlated negatively with the percent saturation, in all locations. Higher saturation, which is concordant with higher gas levels, may occur as gas stored in pore spaces in inertinite macerals. However, association between the liptinites and the percent saturation can not be explained. Previous research on the controls of coal seam gas saturation is sparse.

Bustin and Clarkson (1998) attempted to address saturation in coal seam gas reservoirs. Their study had only 11 calculated saturation values, because of a lack of adsorption samples. All other saturation data in their

study were estimated using the adsorption data. They found that their samples, from the Sydney Basin Australia, were all under-saturated, and showed variation on the order of 2 – 85 % saturated. Although Bustin and Clarkson (1998) state that the percent saturation should vary with coal composition, they give no examples of the roles maceral composition play on saturation. They do, however, relate the main cause of saturation with gas leakage as saturation was inversely correlated with permeability.

5.4 Holding capacity and rank

Previous research has demonstrated strong associations, from a number of basins, between the thermal maturity of the coal (rank) and adsorption isotherms, or holding capacity (Hildenbrand et al., 2006; Levy et al., 1997; Laxminarayana and Crosdale, 2002.; Scott, 2002; Bustin and Clarkson, 1998; Hacquebard, 2002; Creedy, 1988). However, adsorption isotherms for the Huntly, Ohai and Greymouth cores fail to follow the trend of increasing methane holding capacity with rank. At a pressure of 2 MPa the Huntly coal core has the capacity to hold 4.08 m^3/t, Ohai 12.02 m^3/t, and Greymouth 7.08 m^3/t (all daf). These data show that even with increasing pressure the Ohai coal core continues to have a substantially higher adsorption capacity than the Greymouth core which is of a higher rank.

On initial interpretation, when holding capacity is examined on an **as received** basis, the Huntly, Ohai and Greymouth samples show a weak influence of rank on the holding capacity. Nevertheless, when examined on a dry, ash free basis, to remove the influence of mineral matter and moisture (Scott, 2002), we see that rank in this case is no longer the primary control on adsorption capacity. The reason for this is unclear. However, this is not the only manner which the Ohai coal samples behave in a more thermally mature way, with respect to Greymouth coal samples (see Section 5.5).

There have been other studies which have also found that rank and adsorption capacity are not always related. Scott (2002) found that methane sorption capacity was rank dependant only after a certain thermal maturity had been met. The study showed that methane adsorption capacity initially decreased with rank until the high-volatile A bituminous rank, then subsequently increased with progressive coalification. Bustin and Clarkson (1998) state that although rank and adsorption capacity have shown strong associations together in certain basins, that there is in fact little or no actual correlation between coal rank and methane adsorption capacity as is commonly assumed.

5.5 Coal seam gas composition

Review of the isotopic gas composition in the studied New Zealand basins shows some interesting results. The role of rank plays an important part, in both terms of adsorption capacity and isotopic gas composition. Greymouth, being the highest rank coal in the study, should have both the highest adsorption capacity and the most isotopically mature gas signature. Huntly, being the lowest rank coal, should have the least capacity to hold gas and the most isotopically light $\delta^{13}C$ values. While Huntly follows this trend, when comparing the Ohai and Greymouth coals we see that Greymouth fails to hold the greatest adsorption capacity, and actual gas values are much lower than the Ohai coal cores. The gas values can be explained in terms of saturation, the Ohai coal core being many degrees more saturated than the Greymouth coal core. In terms of isotopic composition, however, things are not so straightforward. Greymouth has lighter $\delta^{13}C$ values than the Ohai coal core, that is, the Ohai coal core trends towards a mixed, or more thermogenically rich, source. As thermogenically derived gases are a function of maturity, it seems counterintuitive that the lower rank coal has the more thermally derived gas. Two important considerations arise from this situation: Why does Ohai have a more isotopically mature gas source? And is the isotopic gas composition controlling the saturation in the coals (that is, a more mature composition leads to a higher degree of saturation)? These issues are discussed below.

Boreham et al. (1998) replicated gas generation using an open system pyrolysis procedure on Bowen Basin coals. During pyrolysis of bitumen isolated from the coal in early stages of maturation, a ^{13}C depletion in CO_2 was observed (instead of the ^{13}C enrichment associated with maturation and rank). It is possible over the narrow maturation range of the Greymouth and Ohai coals that this has occurred, however, although demonstrated in a laboratory exercise, it is most unlikely to have happened in the Greymouth Coalfield as this in not often reproduced in natural environments. Another possibility is the floral differences in the organic matter. The Ohai organic matter might be heavier in carbon by a few ppm as a result of a kerogen III-like origin dominated by land plants (Whiticar, 1996). Again, this explanation does not take into account why the Ohai coal is higher saturated. Additionally, because the Ohai and Greymouth coalfields are both Cretaceous, pollen data indicate they formed from similar plant material (Moore et al., 2006; Shearer and Moore, 1994; Ward, 1996b; Ward, 1997; Ward et al., 1995; Warnes, 1988).

A better explanation for Ohai's higher saturation and more mature gas isotopes can be derived from geological/stratigraphic considerations. Coal seams can contain a variety of gas sources, from self-sourced to migrated biogenic and thermogenic gases. It is possible that thermogenic and/or slightly more isotopically mature secondary biogenic gases from down-dip of the seam migrated into the coal seam gas reservoir from where the cores SC1 and SC3 were drilled. This would be the simplest way to account for the slightly more mature isotopic signatures of the gas seen in the Ohai samples. An alternative hypothesis would be that

Greymouth has lost gas over time, and that the gas reservoir has not been replenished. Hildebrand et al., (2006) point out that present day gas content is controlled by the gas generation history. Coal seams which have lost storage capacity during geologic time will stay under-saturated if not replenished by late stage (secondary biogenic) gas. This explanation takes into account both the isotopic composition and the saturation of the coal. It is further reiterated by Scott (2002) who firstly points out that gas content can be enhanced by generation of secondary biogenic gases, or by diffusion and long distance migration of thermogenic and secondary biogenic gases. If there is an active, dynamic flow regime present, combined with high permeability, secondary biogenic gas migration can occur. Migration of gases (secondary biogenic and thermogenic) can result in abnormally high gas contents in lower rank coals, or lead to coals that are saturated or oversaturated with respect to methane (Scott, 2002). The San Juan Basin is an example of a basin that shows migration and re-saturation of coal seam gases. The San Juan Basin's lower rank coals contain a higher gas content than the higher rank coals, which indicates migration of secondary biogenic and thermogenic gases, as the coals themselves have not yet reached thermal maturity to produce thermogenic gas (Scott, 2002).

From examining previous research and case studies, it could be hypothesised that either thermogenic gas or more isotopically mature secondary biogenic gas migrated into the coal seam gas reservoir in the Ohai coalfield where SC1 and SC3 were drilled. Migrating gases may have re-saturated the coal seams in these cores, leading to greater gas contents than what is seen in the Greymouth core, although the Greymouth coalfield still has a greater capacity to hold gas (Fig. 5.1).

5.6 Modelling anomalous behaviour of Ohai coal

The Ohai coal cores have demonstrated a number of anomalous properties in relationship to gas associations, as discussed in Sections 5.4 and 5.5. To summarise these are:

1. The Ohai coal has a greater holding capacity than the Greymouth coal. It has been commonly assumed that the higher rank the coal, the greater the holding capacity, yet this is not the case.
2. The Ohai coal has heavier $\delta^{13}C$ and δD isotopes, compared with the Greymouth and Huntly coals. More mature isotopes points to a transitional-thermogenic gas origin. The common trend is that more mature coals have heavier isotopes because of the higher temperatures and pressures during coalification, creating a thermogenic derived coal gas.
3. The Ohai coal has a higher gas content, but this can be explained by it higher saturation levels.

Two hypotheses have been generated to help explain the anomalous behaviour exhibited by the Ohai coal cores:

1. The isotopic signatures can be explained by secondary biogenic / thermogenic gas migrating into the gas reservoir and re-saturating the coal, as described above. However, this does not explain why the Ohai core has a higher adsorption capacity.
2. A simpler explanation would be that the Ohai coal is **the higher rank coal.** When looking at the ASTM rank classifications, the volatile matter is very similar for the Ohai and Greymouth coals. When examining the range of volatile matter, standard deviations show large spread in the datasets, easily putting the Ohai coal as a more thermally mature coal. If the Ohai coal were of higher rank, it would explain both the higher adsorption capacity and the more mature isotopes with gas coming from a mixed origin. Contrasting with this, when looking at the Suggate plot, we can see three distinct ranks, where Huntly is the lowest and Greymouth is the highest.

To test the hypotheses, more Ohai samples would be needed. Coal samples could be tested for Ro max, to help determine another independent rank classification. Gas samples from down-dip of the Ohai core samples could be tested for gas composition; a more mature isotopic signature may indicate that thermogenic gas has migrated up into the reservoir, enriching and re-saturating the samples found at Ohai SC1 and SC3.

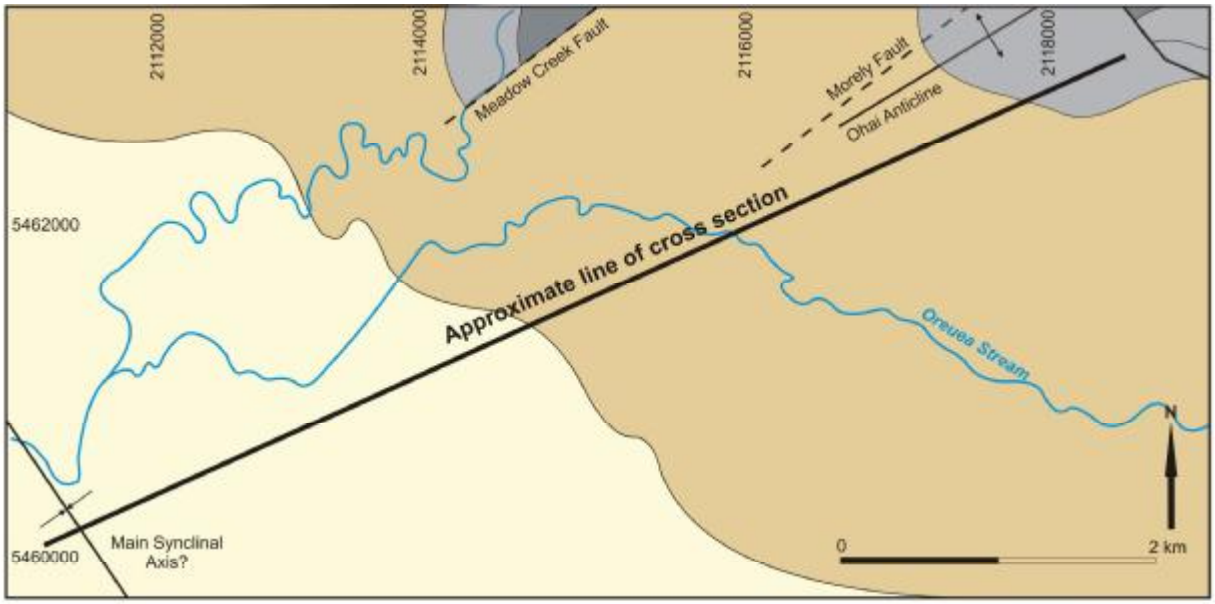

Source: Warnes, 1990

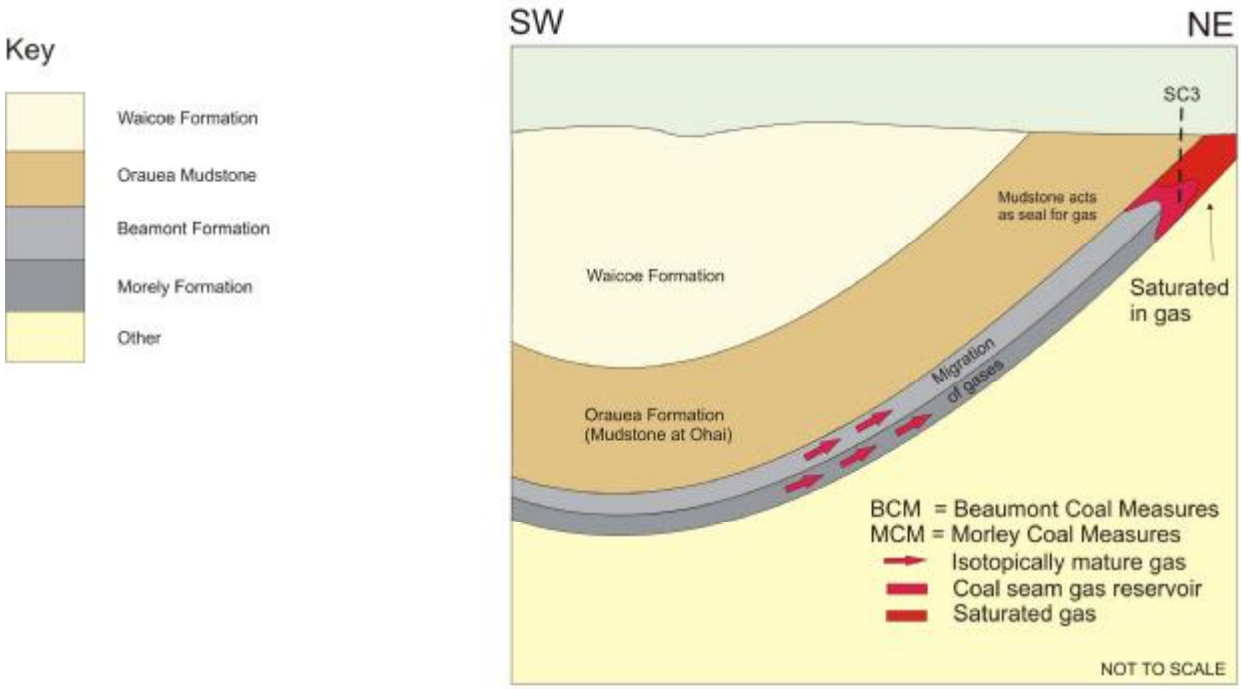

Figure 5.1: Geological map and simplified schematic diagram modelling migration of secondary biogenic and/or thermogenic gas up-dip, contributing to more mature isotopic signatures and increased saturation of coal with respect to methane, in the Ohai coalfield.

Chapter Six
Conclusions

6.1 Conclusions

In summary, the main findings of this study are:

1. The ash yield was the dominant control on the gas volume, within any single seam intersection. This relationship was strongly evident in both Ohai and Greymouth, and also weakly evident in Huntly, although further investigation is needed to confirm or deny this in the Huntly coalfield. However, this association is only valid for ash yields **above** 10 %. When the ash yield falls below 10 %, the gas variation can no longer be explained by a correlation with the ash yield.

2. Organic content has some control on gas volume, but is basin and/or rank dependant. Huntly showed a strong correlation of structured vitrinites (vitrain and telocollinite) increasing alongside an increase in the total gas volume. Ohai had a decrease of fusinite with increasing lost gas volumes, whereas Greymouth showed an increase of desmocollinite with an increase of residual gas; this was supported with the converse relationship, increasing residual gas content with decreased proportions of telocollinite. These changing relationships may be functions of many parameters, including rank, local geological conditions and local mineralisation.

3. Rank does **not** appear to control the maximum gas holding capacity in the three basins examined. In addition, actual gas present is **not** a function of rank.

4. Ohai coal has the most isotopically mature CH_4 values, trending towards a more thermogenically sourced gas, although Greymouth has the highest rank coal (therefore should be the most isotopically mature). Ohai also is the most saturated, and consequently has the highest gas volume. This could be a result of the migration of more isotopically mature secondary biogenic or thermogenic gases into the Ohai gas reservoir from down-dip, re-hydrating, or saturating the coals with respect to methane. Another possibility is that the Ohai coal is actually at a similar, or slightly higher rank than the Greymouth coal. This is seen in the large variation of volatile matter content (ASTM rank) in each location, however, it is not supported by Suggate rank.

6.2 Implications for industry

A successful CSG exploration programme involves a number of phases, as defined in Hayton et al., (2004). The assessment phase includes a preliminary appraisal, exploratory drilling and analysis and preliminary modelling all which help subsequent drilling and pilot well development. During this phase it is important to locate and define parameters that will enhance CSG development. Parameters used to model a CSG reservoir include coal seam geometry, coal thickness, coal depth and coal quality. Gas data, such as desorption, adsorption and saturation data, must also be taken into account when modelling the reservoir, as well as factors such as coal permeability; well spacing and completion type. This study has helped define some of the controlling characteristics for these key parameters. Additional information related to CSG will help isolate areas within proposed gas plays that may better meet exploration and production needs, and also help predict variations in gas volume and content.

An aspect to consider when assessing a basin for CSG is ash yield. As has been shown, low ash coals will contain higher gas volumes than their high ash counterparts. In multiple seam basins, high ash seams or layers can be avoided.

Areas of higher saturation should be targeted for their high gas volume, and pressure. Although more work has to be completed in terms of controlling factors of percent saturation, basin geology and gas isotope composition may help delineate areas of higher saturation. Areas where it is possible for secondary biogenic or thermogenic gas to migrate into the CSG reservoir may re-saturate or over-saturate the coal, relative to areas where there has been no migration of gas. Studies have also shown that there may be different origins of gas in one basin (Ayers, 2002).

This study has also shown that different basins and/or different rank coals can have different influences which control the gas content and its variation. Although structured vitrinite is strongly associated with higher total gas volumes in the Huntly coal field, other macerals have stronger influences in the other regions. Unless these macerals have been determined prior to assessment, it is important not to assume that relationships that have

worked elsewhere will also apply. However, once maceral relationships have been determined they may be a good predictor of gas volume. Another assumption that should not be relied on is that higher rank coals will have more gas, and a greater holding capacity. Again, specific differences between basins may increase gas content, as seen in the Ohai region.

It is important when planning a CSG exploration programme that proper sampling is undertaken, in order to complete a fully comprehensive model that can target the most appropriate areas to make a commercially successful resource.

6.3 Limitations and future work

This work has contributed to the basic understanding of the relationship between coal properties (proximate, maceral and mineralogical) and gas content. The biggest limitation to this study was the relatively small data per basin. A greater number of samples would have yielded a larger and more statistically valid database. Additional samples from adjacent drill holes in the basins may give more information into what factors control the gas content laterally as well as vertically. Additional adsorption samples would enable a more in depth study of the gas holding capacity of coal, and what factors control this. There is, in fact, a large scope for future work. Some key areas to address would be:

1. More in depth study of desorption: Could differences in gas volume be related to the palynology and not maceral content that are controlling the gas content? Is anything controlling the desorption rate? An attempt was made to look at this, but no associations were found with desorption rate and coal type or ash yield, as found by Laxminarayana and Crosdale (1999).
2. A fuller study of adsorption capacity: How does the holding capacity vary in a vertical section? Is this controlled by maceral composition, as many studies (see Chapter five) suggest, or another factor? Are trends bound by basin or by rank?
3. Controls of permeability and gas flow: What affects the lateral continuity of gas content?
4. Isotopic signatures of methane and carbon dioxide: Where is the gas sourced from? Does maturity of gas affect the saturation and gas volume?

References

American Society for Testing and Materials (ASTM), 2002. D3175 Standard test method for volatile matter in the analysis sample of coal and coke. Annual Book of ASTM Standards: Section 5, petroleum products, lubricants and fossil fuels, vol 05.06(Gaseous fuels; coal and coke).

American Society for Testing and Materials (ASTM), 2003. D3173 Standard test method for moisture in the analysis sample of coal and coke. Annual Book of ASTM Standards: Section 5, petroleum products, lubricants and fossil fuels, vol 05.06(Gaseous fuels; coal and coke).

American Society for Testing and Materials (ASTM), 2004a. D3174 Standard test method for ash in the analysis sample of coal and coke. Annual Book of ASTM Standards: Section 5, petroleum products, lubricants and fossil fuels, vol 05.06(Gaseous fuels; coal and coke).

American Society for Testing and Materials (ASTM), 2004b. D4239 Standard test method for sulphur in the analysis sample of coal and coke using high temperature tube furnace combustion methods. Annual Book of ASTM Standards: Section 5, petroleum products, lubricants and fossil fuels, vol 05.06(Gaseous fuels; coal and coke).

American Society for Testing and Materials (ASTM), 2004c. D5865 Standard test method for gross calorific value of coal and coke. Annual Book of ASTM Standards: Section 5, petroleum products, lubricants and fossil fuels, vol 05.06(Gaseous fuels; coal and coke).

American Society for Testing and Materials (ASTM), 2004d. D4326 Standard test method for major and minor elements in coal and coke ash by X-Ray fluorescence. Annual Book of ASTM Standards: Section 5, petroleum products, lubricants and fossil fuels, vol 05.06(Gaseous fuels; coal and coke).

American Society for Testing and Materials (ASTM), 2005a. D2799-05a Standard test method for microscopical determination of the maceral composition of coal. Annual Book of ASTM Standards: Section 5, petroleum products, lubricants and fossil fuels, vol 05.06(Gaseous fuels; coal and coke).

American Society for Testing and Materials (ASTM), 2005b. D388 Standard classification of coal by rank. Annual Book of ASTM Standards: Section 5, petroleum products, lubricants and fossil fuels, vol 05.06(Gaseous fuels; coal and coke).

Ayers, W.B., 2002. Coalbed gas systems, resources, and production and a review of contrasting cases from the San Juan and Powder River Basins. AAPG Bulletin, 86(11): 1853-1890.

Barry, J.M., Duff, S.W. and MacFarlan, D.A.B., 1994. Coal resources of New Zealand, No. 16, Energy and resources division, Ministry of Commerce.

Beamish, B.B., Crosdale, P.J. and Moore, T.A., 1996. Methane sorption capacity of upper Cretaceous coals from the Greymouth coalfield, New Zealand, Mesozoic geology of the eastern Australian plate conference, Brisbane, Australia.

Beamish, B.B., Laxminarayana, C. and Crosdale, P.J., 1998. Contrasts in methane sorption properties between New Zealand and Australian coals, 1st Australasian coal operators conference, Wollongong, Australia.

Bodden, W.R. and Ehrlich, R., 1998. Permeability of coals and characteristics of desorption tests: Implications for coalbed methane production. International Journal of Coal Geology, 35: 333-347.

Boreham, C.J., Golding, S.D. and Glikson, M., 1998. Factors controlling the origin of gas in Australian Bowen Basin coals. Organic geochemistry, 29(1-3): 347-362.

Bowen, F.E., 1964. Geology of the Ohai coalfield. New Zealand Geological Survey Bulletin 51, Wellington.

Bowman, R.G., Brodie, C.G. and Garlick, P.R., 1987. Ohai Coalfield, Coal Resource Assessment, Eastern Ohai Coalfield Area, Resource Management and Mining Group, Ministry of Energy, 127 pp.

Bromhal, G.S., Sams, W.N., Jikich, S., Ertekin, T. and Smith, D.H., 2005. Simulation of CO2 sequestration in coal beds: The effects of sorption isotherms. Chemical geology, 217: 201-211.

Busch, A., Gensterblum, Y., Krooss, B. and Littke, R., 2004. Methane and carbon dioxide adsorption - diffusion experiments on coal: upscaling and modeling. International Journal of Coal Geology, 60: 151-168.

Bustin, R.M. and Clarkson, C.R., 1998. Geological controls on coalbed methane reservoir capacity and gas content. International Journal of Coal Geology, 38: 3-26.

Cave, M., 2002. Turning a coalbed methane project into a co-producing hydrocarbon project, 2002 New Zealand Petroleum Conference Proceedings.

Clarkson, C.R. and Bustin, R.M., 1996. Variation in micropore capacity and size distribution with composition in bituminous coal of the Western Canadian Sedimentary Basin. Fuel, 75: 1483-1498.

Clarkson, C.R. and Bustin, R.M., 2000. Binary gas adsorption/desorption isotherms: effect of moisture and coal composition upon carbon dioxide selectivity over methane. International Journal of Coal Geology, 42: 241-271.

Clayton, J.L., 1998. Geochemistry of coalbed gas-A review. International Journal of Coal Geology, 35: 159-173.

Creedy, D.P., 1988. Geological controls on the formation and distribution of gas in British coal measure strata. International Journal of Coal Geology, 10(1-31).

Crosdale, Beamish and Valix, 1998. Coalbed methane sorption related to coal composition. International Journal of Coal Geology, 35: 147-158.

Crosdale, P.J., 2003a. Methane adsorption isotherms, Huntly TW1 and TW3, Coal seam gas research Institute, Townsville.

Crosdale, P.J., 2003b. Methane and Carbon dioxide adsorption isotherms, Ohai DH SC1 and Hawkdun DH H3, Coal seam gas research institute, Townsville.

Crosdale, P.J., 2004. Methane adsorption isotherm, Greymouth main seam DH944, can13, Energy resources consulting Pty, Ltd.

Davis, A., 1978. Compromise in coal seam description. In: R.R. Dutcher (Editor), Field description of coal, ASTM STP 661. American Society for Testing Materials, pp. 33-40.

Diamond, W.P. and Schatzel, S.J., 1998. Measuring the gas content of coal : A review. International Journal of Coal Geology, 35: 311-331.

Edbrooke, S.W., 1999. Mineral Commodity Report 18- Coal, Ministry of Energy, New Zealand.

Edbrooke, S.W., Sykes, R. and Pocknall, D.T., 1994. Geology of the Waikato Coal measures, Waikato Coal Region, New Zealand. Monograph Series, 6. Institute of Geological and Nuclear Sciences, Ltd.

Ferm, J.C. and Moore, T.A., 1997. Guide to cored rocks in the Greymouth coalfield, CRL Report No. 97-11189, Coal Research Ltd.

Ferm, J.C., Moore, T.A., Lindsay, P. and Campbell, R.N., 2000. A guide to cored rocks and coal in the Waikato coalfield, CRL Report no. 00-41024. CRL Energy Ltd., Lower Hutt, pp. 72.

Flores, R.M., 1998. Coalbed methane: From hazard to resource. International Journal of Coal Geology, 35: 3-26.

Gage, M., 1952. The Greymouth coalfield, New Zealand Geological Survey, Department of Scientific and Industrial Research Bulletin (N.S) 45.

Gamson, P., Beamish, B. and Johnson, D., 1996. Coal microstructure and secondary mineralisation; their effect on methane recovery. In: R. Gayer and I. Harris (Editors), Coalbed Methane and Coal Geology. Geological society special publication, pp. 165 - 179.

Gillard, G. and Trumm, D., 2002. Coalbed methane (CBM) potential of the Maramarua Coalfield, Waikato, New Zealand, CRL Energy Ltd.

Glickson, M., Boreham, C.J. and Theide, D.S., 1999. Coal composition and mode of maturation, a determining factor in the quantifying hydrocarbon species generated. In: M. Mastalerz, M. Glikson and S.D. Golding (Editors), Coalbed Methane: Scientific, Environmental and Economic Evaluation. Kluwer Academic Publishers, Dordrecht.

Gorody, A.W., 1999. The origin of natural gas in the Tertiary coal seams on the eastern margin of the Powder River Basin. In: W.R. Miller (Editor), Wyoming Geological Association Guidebook; coalbed methane and the Tertiary geology of the Powder River basin, Wyoming and Montana. Wyoming Geological Association, vol 50, pp 89-101.

Gurba, L.W. and Weber, C.R., 2001. Effects of igneous intrusions on coalbed methane potential, Gunnedah Basin, Australia. International Journal of Coal Geology, 46: 113-131.

Gurba, L.W.; Gurba, A; Ward, C.R.; Wood, J.; Filipowski, A.; and Titheridge, D, 2001. The impact of coal properties on gas drainage efficiency. In: Doyle and Moloney (Editors), Geological hazards-The impact to mining, 15-16 November 2001, pp. 215-220.

Hacquebard, P.A., 2002. Potential coalbed methane resources in Atlantic Canada. International Journal of Coal Geology, 52: 3-28.

Hall, S., 2003. Controls on deposition of coal and clastic sediment in the Waikato Coal Measures, Masters Thesis, The University of Canterbury, Christchurch, 119 pp.

Hall, S.L., Nicol, A., Moore, T.A. and Bassett, K., 2006. Timing of normal faulting in the Waikato Coal Measures, New Zealand, and its implications for coal seam geometry. New Zealand Journal of Geology and Geophysics, 49: 101-113.

Hayton, S., Manhire, D., Pope, S. and Nelson, C., 2004. Coal seam gas exploration technologies in New Zealand, 2004 New Zealand Petroleum Conference Proceedings, pp. 1-4.

Hildenbrand, A., Krooss, B., Busch, A. and Gaschnitz, R., 2006. Evolution of methane sorption capacity of coal seams as a function of burial history - a case study from the Campine Basin, NE Belgium. International Journal of Coal Geology, 66(3): 179-203.

Kamp, P.J.J., Whitehouse, I.W.S. and Newman, J., 1999. Constraints on the thermal and tectonic evolution of Greymouth coalfield. New Zealand Journal of Geology and Geophysics, 42: 447-467.

Kear, D and Schofield, J.C., 1978. Geology of the Ngaruawahia Subdivision. New Zealand Geological Survey Bulletin 88.

Kear, D. and Schofield, J.C., 1959. Te Kuiti Group. New Zealand Journal of Geology and Geophysics, 2: 685-717.

Killops, S.D., Funnell, R.H., Suggate, R.P., Sykes, R., Peters, K.E., Walters, C., Woolhouse, A.D., Weston, R.J. and Boudou, J.-P.et al., 1998. Predicting generation and expulsion of paraffinic oil from vitrinite-rich coals. Organic geochemistry, 29: 1-21.

Kirk, P.A., Sherwood, A.M. and Edbrook, S.W., 1988. Waikato Coal Region: a summary of geology and resources., New Zealand Geological Survey, 34.

Laird, M.G., 1968. The Paparoa tectonic zone. New Zealand Journal of Geology and Geophysics, 11(2): 435-454.

Laird, M.G., 1972. Sedimentology of the Greenland Group in the Paparoa Range, West Coast, South Island, New Zealand. New Zealand Journal of Geology and Geophysics, 15(3): 372-393.

Laxminarayana, L. and Crosdale, P.J., 1999. Role of coal type and rank on methane sorption characteristics of Bowen Basin, Australia coals. International Journal of Coal Geology, 40: 309-325.

Laxminarayana, L. and Crosdale, P.J., 2002. Controls of methane sorption capacity of Indian coals. AAPG Bulletin, 86(2): 201-212.

Levine, J., 1992. Oversimplifications can lead to faulty coalbed gas reservoir analysis. Oil gas journal, 90(47): 63-69.

Levy, J.H., Day, S.J. and Killingley, J.S., 1997. Methane capacities of Bowen basin coals related to coal properties. Fuel, 76(9): 813 - 819.

Li, Z. Clemens, A.H; Moore, T.A; Gong, D; Weaver, S.D. and Eby, N, 2005. Partitioning behaviour of trace elements in a stoker-fired combustion unit: An example of using bituminous coals from the Greymouth coalfield (Cretaceous), New Zealand. International Journal of Coal Geology, 63: 98-116.

Li, Z., 2002. Mineralogy and Trace Elements of the Cretaceous Greymouth Coals and their combustion products. Doctor of Philosophy Thesis, University of Canterbury, Christchurch.

Li, Z., Moore, T.A. and Weaver, S.D., 1999. Mineralogy and geochemistry of Cretaceous Main Seam coal, Greymouth, West Coast, New Zealand., Proceedings of a New Zealand Energy Road Map - Vision for 2020 and 8th New Zealand Coal Conference., Wellington, pp. 183-199.

Li, Z., Moore, T.A. and Weaver, S.D., 2001b. Leaching of inorganics in the cretaceous Greymouth coal beds, South Island, New Zealand. International Journal of Coal Geology, 47: 235-253.

Li, Z., Moore, T.A., Weaver, S.D. and Finkelman, R.B., 2001a. Crocoite: an unusual mode of occurrence for lead in coal. International Journal of Coal Geology, 45: 289-293.

Lyon, G.L. and Giggenback, W.F., 1994. The isotopic and chemical composition of natural gases from the South Island, New Zealand. 1994 New Zealand Petroleum Conference. Ministry of Commerce.: pp 361-369.

Lyon, G.L., 2004. Analysis of coal gas for Desmond Gong, CRL, Stable Isotope Laboratory, Institute of Geological and Nuclear Sciences, Lower Hutt.

Manhire, D. and Hayton, S., 2003. Coal seam gas in New Zealand: Perspective from New Zealand's most active CSG explorers. AusIMM Annual Conference Proceedings, Greymouth.

Moore, N.A., 1996. Palynology and Coal Petrography of Rewanui Member Seams in the Rapahoe Sector, Greymouth Coalfield. Masters Thesis, University of Canterbury, Christchurch.

Moore, T. A., Gillard, G.R., Boyd, R., Flores, R.M., Stricker, G.D. and Galceran, C.M. 2004. A mighty wind: Determining the methane content of New Zealand coal seams. In: T.A. Moore (Editor), The Society for Organic Petrology. The Society for Organic Petrology, 21st Annual Meeting., Sydney, Australia, pp. 114-116.

Moore, T.A. and Butland, C.I., 2005. Coal seam gas in New Zealand as a model for Indonesia. In: S. Prihatmoko, S. Digdowirogo, C. Nas, T.v. Leeuwen and H. Widjajanto (Editors), Indonesian mineral and coal discoveries. Indonesian association of geologists, Bogor, Indonesia, pp. 192-200.

Moore, T.A. and Twombly, 2006, Cracking the CSG code with the three Rs : Reasoned, rigorous and responsive development, Proc. 2006 New Zealand Petroleum Conference, 6-9 March 2006, Auckland, New Zealand.

Moore, T.A., 1995. Developing models for spatial prediction of mining and utilisation potentials in coal seams: an example from the Greymouth coalfield, Proceedings from the 6th New Zealand Coal Conference, pp. 385-402.

Moore, T.A., Flores, R.M., Stanton, R.W. and Stricker, G.D., 2002b. The role of macroscopic texture in determining coalbed methane variability in the Anderson-Wyodek coal seam, Powder River Basin, Wyoming. In: C.R. Robison (Editor), 18th Annual meeting of The Society for Organic Petrology., Houston, Texas, pp. 85-88.

Moore, T.A., Li, Z. and Moore, N.A., 2006. Controls on the formation of an anomalously thick Cretaceous-age coal mire. In: S. Greb and W. DiMichele (Editors), Wetlands through time. Geological Society of America Special Paper 399, Boulder, Colorado.

Moore, T.A., Li, Z., Nelson, C., Finkelman, R.B. and Boyd, R., 2005. Concentration of trace elements in coal beds. In: T.A. Moore, A. Black, J.S. Centeno, J.S. Harding and D.A. Trumm (Editors), Metal contaminants in New Zealand. Resolutionz press Ltd., Christchurch, pp. 81-113.

Moore, T.A., Manhire, D. and Flores, R.M., 2002a. Coalbed methane opportunities in New Zealand: Similarities with the Powder River Basin coalbed methane paradigm, AusIMM Conference, Auckland, pp. 381-385.

Moore, T.A., Shearer, J.C. and Esterle, J.S., 1993. Quantitative macroscopic textural analysis. The Society of Organic Petrology Newsletter, 9(4): 13-16.

Nathan, S., 1978. Geological map of New Zealand. 1:63360 Sheet S44 Greymouth. Wellington New Zealand Geological Survey, 36pp.

Nathan, S.; Anderson, H.J.; Cook, R.A.; Herzer, R.H.; Hoskins, R.H. and Raine, J.I, 1986. Cretaceous and Cenozoic sedimentary basins of the West Coast Region, South Island, New Zealand. New Zealand Geological Survey Basin Studies, 1.

Newman, J., 1985. Paleoenvironments, coal properties and their interrelationship between Paparoa and selected Brunner coal measures on the West coast of the South Island. Ph.D Thesis, The University of Canterbury, Christchurch.

Newman, J., 1997. New approaches to detection and correction of suppressed vitrinite reflectance. AAPEA Journal, 37(1): 524-535.

Newman, N.A., 1988. Mineral Matter in the coals of the West Coast, South Island, New Zealand. Doctor of Philosophy Thesis, University of Canterbury, Christchurch.

Newman, N.A., Moore, T.A. and Esterle, J.S., 1997. Geochemistry and petrography of the Taupiri and Kupakua coal seams, Waikato Coal Measures (Eocene), New Zealand. International Journal of Coal Geology, 33: 103-133.

Pontolillo, J. and Stanton, R.W., 1992. Coal Petrographic laboratory procedures and safety manual II, Open-file report 94-631, US Department of Interior Geological Survey.

Pope, J., 2005. CSG Analyses from specialized gas sample canisters, CRL Energy Ltd., Christchurch.

Pope, S.J., Manhire, D., Pope, J.G., Taulis, M.E. and Hayton, S., 2004. Developments in coal seam gas exploration, NZ Minerals Conference.

Rice, D.D., 1993. Composition and Origins of Coalbed Gas. AAPG Special Publication, Studies in Geology, 38(7): 159-184.

Schopf, J.M., 1960. Field Description and Sampling of Coal Beds. Geological Survey Bulletin 1111-B, Washington, 25-67 pp.

Scott, A.R., 2002. Hydrogeologic factors affecting gas content distribution in coal beds. International Journal of Coal Geology, 50: 363-387.

Shearer, J.C. and Moore, T.A., 1994. Botanical control on banding character in two New Zealand coal beds. Palaeogeography, palaeoclimatology, Palaeoecology, 110: 11 - 27.

Shearer, J.C. and Moore, T.A., 1994. Grain-size and botanical analysis of two coal beds from the South Island of New Zealand. Review of Palaeobotany and Palynology, 80: 85 - 114.

Shearer, J.C., 1992. Sedimentology, Coal Chemistry and Petrography of the Cretaceous Morley Coal Measures and Eocene Beaumont Coal Measures, Ohai Coalfield, Southland, New Zealand. Doctor of Philosophy Thesis, University of Canterbury, Christchurch.

Sherwood, A., Stagpoole, V., Funnel, R. and Darby, D., 2003. Northern Taranaki graben described as promising area in New Zealand. Oil and Gas Journal, Oct 13.

Sherwood, A.M., Lindquist, J.K., Newman, J. and Sykes, R., 1992. Depositional controls on Cretaceous coals and coal measures in New Zealand. In: P.J. McCabe and J.T. Parrish (Editors), Controls on the distribution and quality of Cretaceous coals. Geological society of America special paper, pp. 325-346.

Stach, E.; Mackowsky M-Th; Teichmuller, M; Taylor, G.H.; Chandra, D.; Teichmuller, R, 1982. Stach's Textbook of Coal Petrology. Gebrüder Borntraeger, Stuttgart, 535 pp.

Stopes, M.C., 1919. On the four visible ingredients in banded bituminous coal. Proceedings of the Royal Society, Series B, 90: 470-487.

Stopes, M.C., 1935. On the petrology of banded bituminous coals. Fuels in science and practice, 14(1): 4-13.

Suggate, R.P. and Dickinson, W.W., 2004. Carbon NMR of coals: the effect of coal type and rank. International Journal of Coal Geology, 57: 1-22.

Suggate, R.P., 1959. New Zealand Coals: Their geological setting and its influence on their properties. New Zealand department of scientific and industrial research, Bulletin 134.

Suggate, R.P., 1998. Analytical variation in Australian coals related to coal type and rank. International Journal of Coal Geology, 37: 179-206.

Suggate, R.P., 2000. The Rank (S_r) scale: its basis and applicability as a maturity index for all coals. New Zealand Journal of Geology and Geophysics, 43: 521-553.

Sykes, R., 1985. Paleoenvironmental and tectonic controls on coal measure characteristics, Ohai coalfield, Southland. Masters Thesis, University of Canterbury, Christchurch.

Sykes, R., 1988. The Morley Coal Measures, Ohai Coalfield, Southland. 170, Ministry of Energy, New Zealand Energy Research and Development committee.

Taylor, G.H. Teichmuller, M; Davis, A.; Diessel, C.F.K.; Littke, R. and Robert, P, 1998. Organic Petrology. Gebruder Borntraeger, Stuttgart, 704 pp.

Thorburn, D.F., 1983. Methane from coal - Ohai coalfield, Southland, New Zealand, 2954. Ministry of Economic Development, Wellington.

Twombly, G., Stepanek, S.H. and Moore, T.A., 2004. Coalbed methane potential in the Waikato Coalfield of New Zealand: A comparison with developed basins in the United States., 2004 New Zealand Petroleum Conference Proceedings.

Walker, R., Glikson, M. and Mastalerz, M., 2001. Relations between coal petrology and gas content in the Upper Newlands Seam, central Queensland, Australia. International Journal of Coal Geology, 46: 83-92.

Ward, C.R., 2002. Analysis and significance of mineral matter in coal seams. International Journal of Coal Geology, 50: 135-168.

Ward, C.R., Taylor, J.C., Matulis, C.E. and Dale, L.S., 2001. Quantification of mineral matter in the Argonne Premium coals using interactive Rietveld-based X-ray diffraction. International Journal of Coal Geology, 46: 67-82.

Ward, S.D., 1996b. Application of lithostratigraphic and chronostratigraphic analysis to seam modeling in the Rapahoe sector, western greymouth Coalfield., 29th Annual Conference of the Australasian Institute of Mining and Metallurgy, Greymouth, New Zealand, pp. 173-199.

Ward, S.D., 1997. Lithostratigraphy, palynostratigraphy and basin analysis of the Late Cretaceous to early Tertiary Paparoa Group, Greymouth Coalfield, New Zealand. PhD Thesis, The University of Canterbury, Christchurch, 404 pp.

Ward, S.D., Moore, T.A. and Newman, J., 1995. Floral assemblage of the "D" coal seam (Cretaceous): Implications for banding characteristics in New Zealand coal seams. New Zealand Journal of Geology and Geophysics, 38(3): 283-297.

Warnes, M.D., 1990. The Palynology of the Morley Coal Measures, Ohai Coalfield. 1, Ministry of Commerce, Energy and Resources Division.

Whiticar, M.J., 1996. Stable isotope geochemistry of coals, humic kerogens and related natural gases. International Journal of Coal Geology, 32: 191-215.

Whiticar, M.J., Faber, E. and Schoell, M., 1986. Biogenic methane formation in marine and freshwater environments, CO2 reduction vs. acetate fermentation. Geochim. Cosmochim. Acta, 50: 693-709.

Yee, D., Seidle, J.P. and Hanson, W.B., 1993. Gas Sorption on Coal and Measurement of Gas Content. AAPG Special Publication, Studies in Geology, 38(9): 203-218.

Appendix A: Common abbreviations used

Corrections

aa	as analysed
db	dry basis
daf	dry, ash free
dmmf	dry, mineral matter free
dmmSf	dry, mineral matter sulphur free

Parameters

V_A	adsorption volume
V_D	desorption volume
V_L	volume Langmuir coefficient
P_L	pressure Langmuir coefficient
P_H	hydrostatic pressure
D_S	depth (of sample)

Units

MPa	Mega pascals
m^3/t	cubic meters per tonne

Other

ISO	International Organisation for Standardisation
ASTM	American Society for Testing and Materials
DH	drillhole
CSG	coal seam gas
XRF	x-ray fluorescence
XRD	x-ray diffractometer
LTA	low temperature ash
VM	volatile matter
FC	fixed carbon
CV	calorific value
M	moisture
S	sulphur
A	ash
S_R	Suggate rank

Appendix B: Corrections

Most coal analyses are carried out and initially reported as air dried samples. These often need to be corrected to different standards using a number of different formulas. (Newman, pers. comm., 2005).

a) Air dried coal has had the adventitious moisture removed, but still contains the inherent moisture.

b) To correct to a dry basis (db), the moisture is removed from the samples:

$$X_{db} = \frac{X * 100}{100-M}$$

c) To correct to dry, ash free (daf), both ash and moisture are removed:

$$X_{daf} = \frac{X * 100}{100-A-M}$$

d) Because mineral matter and ash are not identical, we can use a general ratio of MM:A when ash constituent data is not available. Usually mineral matter is greater than the ash yield and Suggate (1959) developed a general ratio of 1.1:1 for New Zealand coals. Using this, we can correct to a dry, mineral matter free basis (dmmf):

$$X_{dmmf} = \frac{100(VM-0.1A)}{100-1.1A} \text{ (from dry basis)}$$

Where A = Ash %, M= Moisture and X = variable (such as Volatile Matter or Fixed Carbon).

e) To analyse Suggate rank, we correct to a dry, mineral matter sulphur free basis (dmmSf). Suggate's (1959) correction for sulphur assumes that sulphur is a contaminant and corrects to a sulphur free standard. However, in New Zealand coal approximately half the sulphur is organically derived. Sulphur corrections have been amended to include only sulphur lost during the analysis. These corrections are discussed in Chapter 2.4.2.

Appendix C Drill hole Coordinates

Drill hole Greymouth 944
New Zealand Map Grid: 2366952.28 E / 5868246.76 N

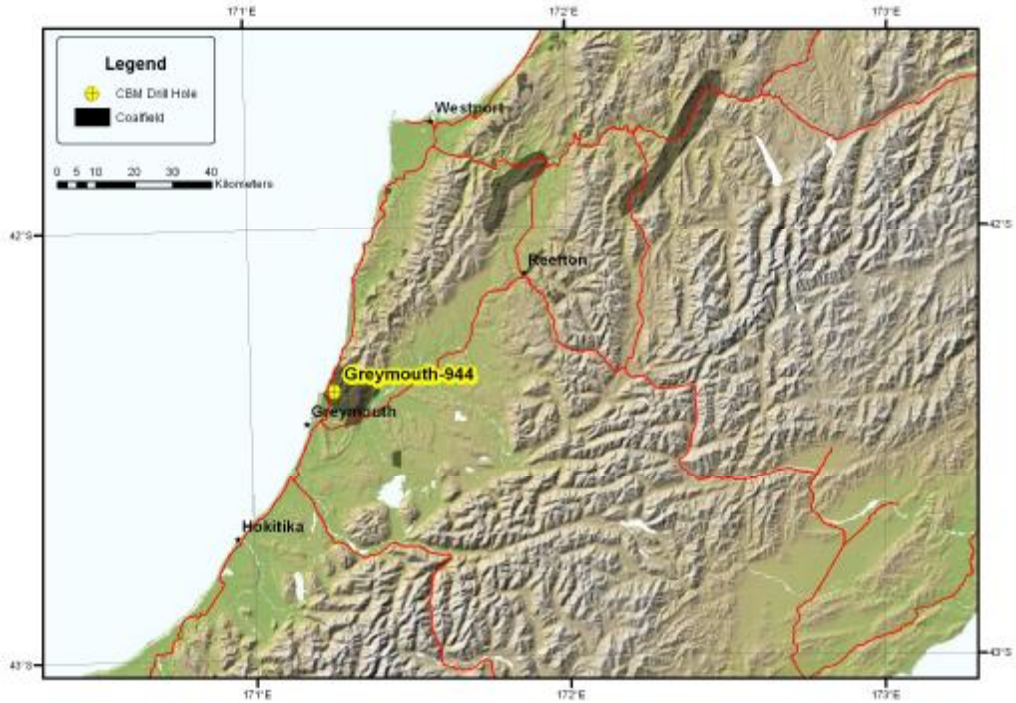

Drill hole Huntly TW1
New Zealand Map Grid: 2699554.83 E / 6407858.42 N

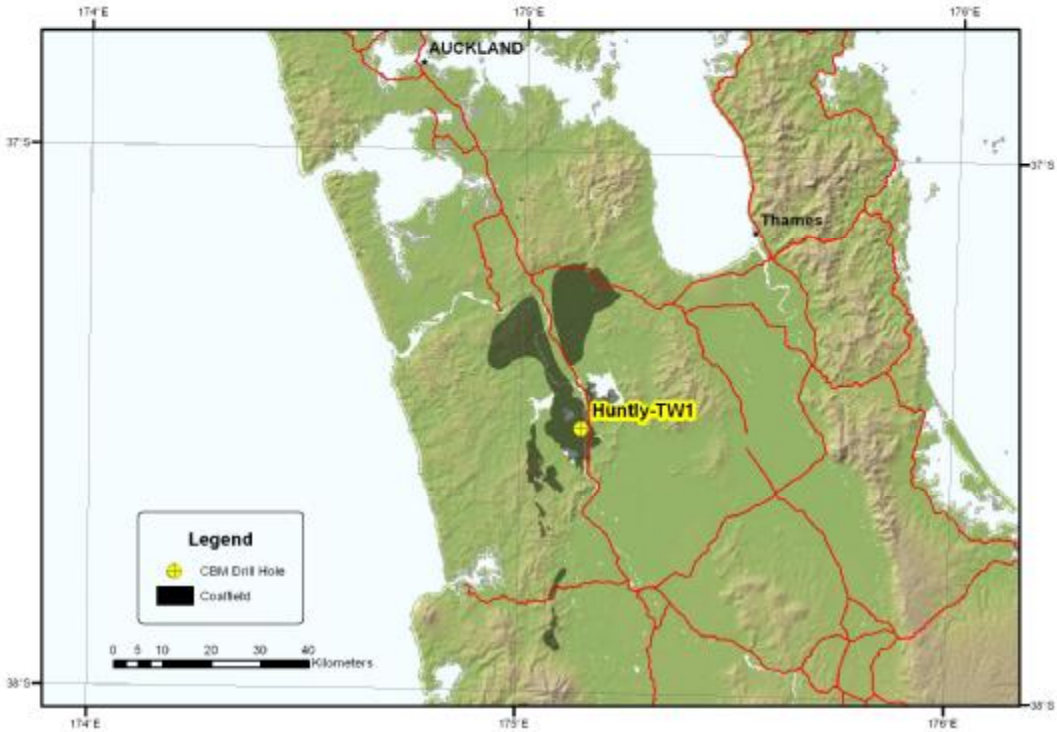

Drill holes Ohai SC1 and SC3
New Zealand map grid:
SC1 2116032.74 E / 5461962.94 N
SC3 2117238.947 E / 5462185.587 N

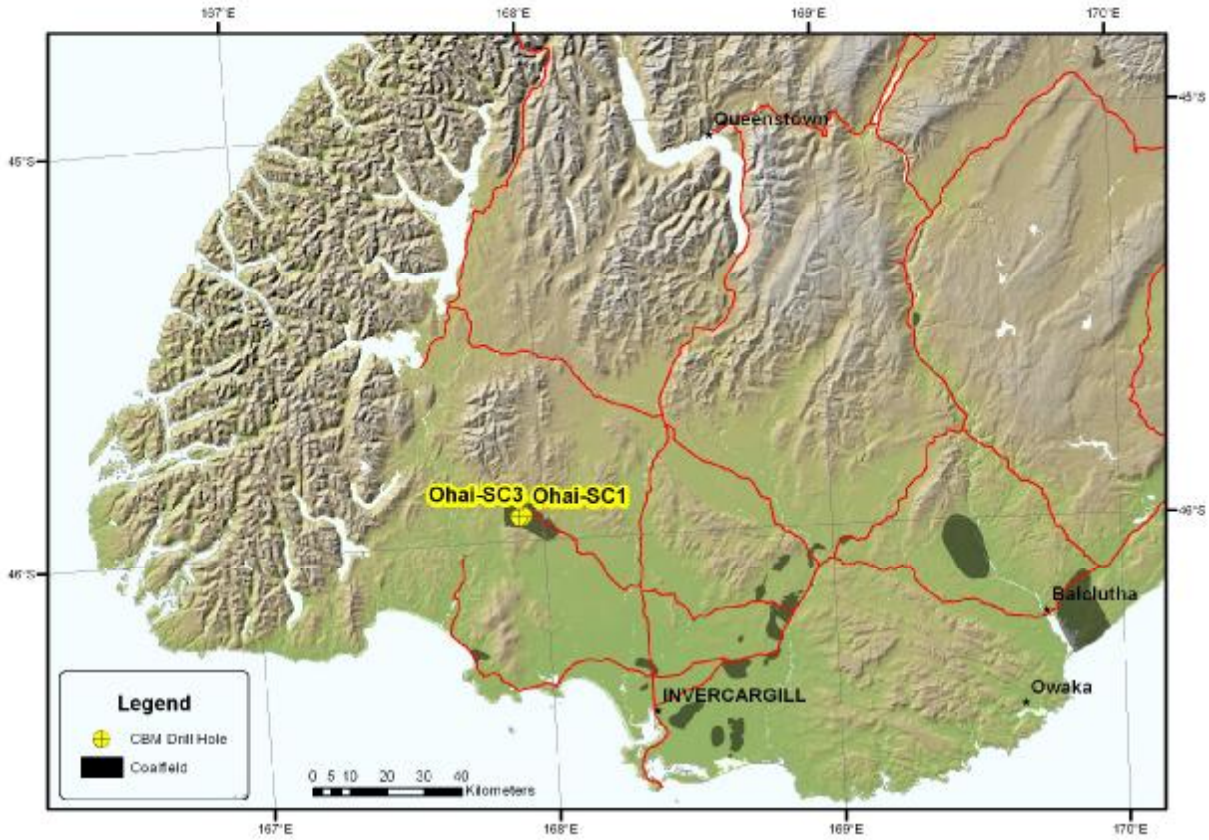

Appendix D: Macroscopic Results

Table 1 Ohai macroscopic descriptions

Canister	From (m)	To (m)	Thickness (m)	counts			percentages			Cleat (cm)	Coal Type	Comments
				attrital	fusain	vitrain	%Attrital	%Vitrain	%Fusain			
X1	319.10	319.60	0.50								BNB	broken
X2	319.60	319.85	0.25								BNB	broken
X2	319.85	320.10	0.25								Dirty Coal	semibroken
X11	320.10	320.35	0.25								Dirty Coal	semibroken
X11	320.35	320.60	0.25								CM	broken
X4	333.10	333.40	0.30	10	0	4	71%	0%	29%	1.0	B<20	
X5	333.65	334.15	0.50	13	0	10	57%	0%	43%	1.0	B<20	
X6	334.15	334.65	0.50	18	0	6	75%	0%	25%	1.5	B<20	
X7	334.65	335.15	0.50	13	1	9	57%	4%	39%	1.5	B<20	
X8	335.15	335.65	0.50	12	0	6	67%	0%	33%	1.5	B<20	
X9	335.65	336.15	0.50	19	0	10	66%	0%	34%	0.8	B<20	
X10	336.15	336.65	0.50	16	0	8	67%	0%	33%	2.0	B<20	
X12	336.65	337.15	0.50	17	0	6	74%	0%	26%	1.0	**B>20**	
X13	337.15	337.55	0.40	16	2	5	70%	9%	22%	1.5	B<20	
X14	338.85	339.15	0.30	10	1	3	71%	7%	21%	1.4	B<20	
X15	339.15	339.75	0.60	11	0	9	55%	0%	45%	2.0	B<20	
X16	339.75	340.35	0.60	11	0	2	85%	0%	15%	2.5	B<20	
X17	340.35	340.95	0.60	18	0	3	86%	0%	14%	2.0	BNB	
X18	340.95	341.55	0.60	17	0	7	71%	0%	29%	2.0	B<20	
X19	341.55	342.15	0.60	9	0	16	36%	0%	64%	1.2	**B>20**	
X20	342.15	342.50	0.35	6	0	7	46%	0%	54%	2.2	B<20	
X21	342.50	343.00	0.50	17	0	7	71%	0%	29%	3.4	B<20	
X22	343.00	343.50	0.50	16	0	5	76%	0%	24%	2.3	B<20	
X23	343.50	344.00	0.50	14	0	8	64%	0%	36%	3.5	B<20	
X24	344.00	344.50	0.50	12	0	4	75%	0%	25%	3.0	B<20	
X25	344.50	345.00	0.50	13	0	10	57%	0%	43%	1.5	**B>20**	
X26	345.36	345.70	0.34	6	0	3	67%	0%	33%	2.0	B<20	
X27	345.70	346.20	0.50	7	0	7	50%	0%	50%	1.5	**B>20**	
X28	346.20	346.70	0.50	16	0	3	84%	0%	16%	1.9	B<20	
X29	346.70	347.20	0.50	4	0	4	50%	0%	50%	1.0	B<20	
X30	347.20	347.70	0.50	12	0	14	46%	0%	54%	2.0	**B>20**	
X31	347.70	348.20	0.50	8	0	13	38%	0%	62%	-	**B>20**	
X32	348.20	348.50	0.30	7	0	15	32%	0%	68%	1.4	**B>20**	
X33	348.76	349.26	0.50	12	0	11	52%	0%	48%	1.2	**B>20**	
X34	349.26	349.76	0.50	13	0	5	72%	0%	28%	1.2	**B>20**	

Table 2 Ohai SC1 macroscopic descriptions

Canister	From (m)	To (m)	Thickness (m)	counts			percentages			Cleat (cm)	Coal Type	Comments
				attrital	fusain	vitrain	%Attrital	%Vitrain	%Fusain			
A1	254.90	255.25	0.35								CM	
A1	255.25	255.40	0.15								Dirty Coal	
A3	268.38	268.88	0.50									Isotherm sample
A5	338.95	339.55	0.60	13	0	13	50%	50%	0%	2.0	B<20	
A2	339.55	340.05	0.50	15	0	7	68%	32%	0%	0.9	B<20	
A7	340.15	340.75	0.60	4	0	2	67%	33%	0%		B<20	Residual sample?
A4	340.75	341.35	0.60									Residual sample?
A11	356.12	356.42	0.30	3	0	5	38%	63%	0%	1.0	**B>20**	
A11	356.42	356.60	0.18								Dirty Coal	
A10	356.60	356.94	0.34								Dirty Coal	
A10	356.94	357.10	0.16	2	0	3	40%	60%	0%		B<20	
A9	357.10	357.34	0.24	3	0	3	50%	50%	0%	1.0	B>20	Residual sample
A9	357.34	357.50	0.16								Dirty Coal	
A9	357.50	357.60	0.10									Residual sample
A8	358.20	358.45	0.25	4	0	4	50%	50%	0%	1.2	**B>20**	
A8	358.45	358.55	0.10								Dirty Coal	
A8	358.55	358.70	0.15								B<20	
A13	367.20	367.70	0.50	4	0	18	18%	82%	0%	1.2	**B>20**	
A15	399.73	399.96	0.23							1.5	Dirty Coal	
A15	399.96	400.06	0.10	4	0	5	44%	56%	0%		B>20	
A15	400.06	400.23	0.17								Dirty Coal	
A14	400.70	401.20	0.50	7	0	8	47%	53%	0%	1.5	**B>20**	Residual sample
A19	414.20	414.48	0.28	8	0	7	53%	47%	0%	1.5	**B>20**	
A18	414.48	414.98	0.50	10	0	8	56%	44%	0%	1.5	B<20	Residual sample
A17	414.98	415.49	0.51	20	0	8	71%	29%	0%		B<20	
A16	415.49	415.82	0.33	13	0	4	76%	24%	0%		B<20	
A16	415.82	416.04	0.22								Dirty Coal	

Table 3 Greymouth 944 macroscopic descriptions

Canister	From (m)	To (m)	Thickness (m)	counts			percentage			vitrain size (mm)	cleat (cm)	Coal Type
				attrital	fusain	vitrain	attrital	fusain	vitrain			
16	309.55	309.85	0.30	11	0	0	100%	0%	0%	-	-	Dull
1	309.85	310.35	0.50							-	-	HAC & CM
2	334.74	335.10	0.36	10	0	2	83%	0%	17%	3,2	1	B<20%
3	335.10	335.50	0.40							-	-	Dull
4	341.10	341.50	0.40	19	1	9	65%	3%	31%	5,2,1,3,7,5,3,1,3	1	B<20%
5	341.50	342.00	0.50	10	0	5	67%	0%	33%	2,3,1,1,1	0.7	B<20%
6	342.00	342.28	0.28	9	0	3	75%	0%	25%	1,3,5	-	B<20%
6	342.28	342.50	0.22							-	-	Dull
7	343.10	343.60	0.50							-	-	Dull
8	343.60	344.10	0.50	11	1	3	73%	7%	20%	1,2,5	3+	B<20%
9	344.10	344.62	0.52							-	-	Dull
9	344.62	344.70	0.08							-	-	CM
10	344.85	345.35	0.50							-	-	Dull
11	345.35	345.85	0.50							-	-	Dull
12	345.85	345.98	0.13							-	-	Dull
12	345.98	346.35	0.37	11	1	6	61%	6%	33%	2,1,2,1,1,7	3+	**B>20%**
13	346.35	347.00	0.65	12	0	8	60%	0%	40%	1,10,5,5,5,3,2,2	2	**B>20%**
14	347.10	347.60	0.50	10	0	7	59%	0%	41%	5,2,1,2,5,5,1	1	**B>20%**
15	347.60	348.10	0.50	18	0	4	82%	0%	18%	3,15,3,2	3+	B<20%
17	348.10	348.60	0.50	20	1	6	74%	4%	22%	1,2,2,1,1,1	1	B<20%
18	348.60	349.10	0.50	22	0	6	79%	0%	21%	5,1,10,2,2,2	1	B<20%
19	349.10	349.60	0.50	18	0	1	95%	0%	5%	5	3+	Dull
20	349.70	350.20	0.50	13	0	1	93%	0%	7%	2	3+	Dull
21	350.20	350.70	0.50	16	0	11	59%	0%	41%	5,2,20,2,3,10,7,12,2,1,1	3	**B>20%**
22	351.00	351.50	0.50	6	0	6	50%	0%	50%	5,1,2,1,3,2	3+	**B>20%**
23	351.50	352.00	0.50	24	0	4	86%	0%	14%	2,12,2,2	2	B<20%
24	352.00	352.27	0.27	4	0	11	27%	0%	73%	1,5,10,1,2,3,6,3,15,1,10	2	**B>20%**
24	352.27	352.50	0.23							-	-	CM & HAC

Table 4 Huntly TW1 macroscopic descriptions

Canister	From (m)	To (m)	Thickness (m)	Counts			Percentage			vitrain size (mm)	Cleat (cm)	Coal Type
				attrital	Vitrain	fusain	%Attrital	%Vitrain	% fusain			
9	338.70	339.20	0.50	13	6	0	68%	32%	0%	1,1,2,0.5,1,2	10	BNB
10	339.20	339.70	0.50	17	5	1	74%	22%	4%	1,1,1,0.5, 0.5	25	BNB
11	339.70	340.20	0.50	28	10	1	72%	26%	4%	1,1,1,1,1, 0.5,0.5, 1,1,2	20	<20
12	340.20	340.70	0.50									
13	340.70	341.20	0.50	18	14	0	56%	44%	0%	0.5, 3, 0.5, 2, 1,1,1,1,0.5, 1,1,1,0.5,30	10	<20
14	341.20	341.70	0.5	26	1	0	96%	4%	0%	1	20	BNB
15	341.70	341.87	0.17									Dirty Coal
15	341.87	342.20	0.33	17	3	0	85%	15%	0%	1,1,1	30	DNB
16	342.20	342.70	0.50	23	6	0	79%	21%	0%	1,1,1,1,2,0.5	15	BNB
17	342.70	343.20	0.50	24	4	0	86%	14%	0%	0.5,1,1,2	20	BNB
18	343.20	343.44	0.24	9	1	0	90%	10%	0%	2	15	BNB
18	343.44	343.55	0.11	6	3	0	67%	33%	0%	1,2,3		D<20
18	343.55	343.70	0.15	13	1	0	93%	7%	0%	1		BNB
19	343.70	344.20	0.50	15	5	0	75%	25%	0%	1,1,0.5, 0.5, 1	14	B<20
20	344.20	344.70	0.50	22	5	0	81%	19%	0%	2,1,1,0.5,25	15	BNB
21	344.70	345.20	0.50	11	2	0	85%	15%	0%	0.5,2		BNB
22	345.20	345.70	0.50								>25	B<20
23	345.70	346.20	0.50									
24	346.20	346.52	0.32									B<20
24	346.52	346.63	0.11									Dirty Coal
24	346.63	346.70	0.07									B<20
25	346.70	347.20	0.50								25	B<20
26	347.20	347.70	0.50								25	B<20
27	347.70	348.20	0.50	20	5	0	80%	20%	0%	3,2,3,2,3	12	B<20
28	348.20	348.70	0.50	28	11	0	72%	28%	0%	1,1,0.5,0.5,1,2,1,2,2,2,1	11	B<20
29	348.70	349.20	0.50	21	9	0	70%	30%	0%	2,3,2,3,5,0.5,2,30,1	18	B<20
30	349.20	349.70	0.50	18	2	0	90%	10%	0%	1,0.5	10	BNB
31	349.70	350.20	0.50	23	8	2	70%	24%	6%	0.5,0.5,6,30,1,4,1,2	10	B<20
32	350.20	351.20	1.00	17	18	0	49%	51%	0%	0.5,1,2,2,1,1,3,2,0.5,1,5,2,1,3,3,8,2,3	17	**B>20**
33	351.20	351.70	0.50	24	16	0	60%	40%	0%	0.5,4,0.5,7,0.5,0.5,1,0.5,0.5,0.5,4,5,0.5,3	10	**B>20**
34	351.70	352.20	0.50									
35	352.20	352.70	0.50	12	10	0	55%	45%	0%	0.5,1,2,2,1,0.5,1,0.5,0.5,2	11	B<20
36	352.70	353.39	0.69	25	15	0	63%	38%	0%	0.5,0.5,1,1,1,1,3,1,4,4,1,3,2,0.5,5	14	B<20
37	353.39	354.20	0.81								15	B<20
38	354.20	354.70	0.50								30	B<20
39	354.70	355.20	0.50								30	B<20
40	355.20	355.70	0.50									
41	355.70	356.20	0.50									B<20
42	356.20	356.70	0.50									B<20
43	356.70	357.20	0.50	21	13	0	62%	38%	0%	0.5,2,0.5,4,1,1,1,2,10,2,3,4,7	20	**B>20**
44	357.20	357.70	0.50	7	10	0	41%	59%	0%	1,4,3,3,2,4,7,2,2,1	20	**B>20**
45	357.70	358.20	0.50	9	12	0	43%	57%	0%	3,1,1,4,8,1,2,1,2,3,1,3	15	**B>20**

Tables 5 and 6 Greymouth and Huntly macroscopic comments

Greymouth				
Canister	From (m)	To (m)	Thickness (m)	comments
16	309.55	309.85	0.30	HAC in part
1	309.85	310.35	0.50	too broken to log; jointed with slickensides
2	334.74	335.10	0.36	top broken
3	335.10	335.50	0.40	too broken to log
4	341.10	341.50	0.40	rare pyrite & siderite;341.1-341.3m dull, 341.3-341.5m B>20%, but overall B<20%
5	341.50	342.00	0.50	occasional pyrite
6	342.00	342.28	0.28	rare pyrite
6	342.28	342.50	0.22	too broken to log
7	343.10	343.60	0.50	too broken to log
8	343.60	344.10	0.50	long term canister
9	344.10	344.62	0.52	too broken to log
9	344.62	344.70	0.08	
10	344.85	345.35	0.50	HAC; too broken to log
11	345.35	345.85	0.50	HAC; rare pyrite, resin and MS blebs; too broken to log
12	345.85	345.98	0.13	HAC; siderite nodule; too broken to log
12	345.98	346.35	0.37	abundant pyrite; rare siderite
13	346.35	347.00	0.65	occasional pyrite
14	347.10	347.60	0.50	long term canister
15	347.60	348.10	0.50	
17	348.10	348.60	0.50	
18	348.60	349.10	0.50	rare pyrite
19	349.10	349.60	0.50	CM band 349.21-349.26m
20	349.70	350.20	0.50	
21	350.20	350.70	0.50	rare resin & siderite nodule
22	351.00	351.50	0.50	long term canister
23	351.50	352.00	0.50	rare resin
24	352.00	352.27	0.27	rare resin
24	352.27	352.50	0.23	rare resin & MS blebs

Huntly				
Canister	From (m)	To (m)	Thickness (m)	Comments
9	338.70	339.20	0.50	
10	339.20	339.70	0.50	
11	339.70	340.20	0.50	
12	340.20	340.70	0.50	desorbing
13	340.70	341.20	0.50	
14	341.20	341.70	0.5	
15	341.70	341.87	0.17	
15	341.87	342.20	0.33	Clayey Coal
16	342.20	342.70	0.50	
17	342.70	343.20	0.50	
18	343.20	343.44	0.24	
18	343.44	343.55	0.11	Dull apperance, Possibly Fusain
18	343.55	343.70	0.15	
19	343.70	344.20	0.50	
20	344.20	344.70	0.50	0.1 - .16 weird fracture. Fusain?
21	344.70	345.20	0.50	Broken
22	345.20	345.70	0.50	Highly Broken
23	345.70	346.20	0.50	desorbing
24	346.20	346.52	0.32	Highly Broken
24	346.52	346.63	0.11	Highly Broken
24	346.63	346.70	0.07	Highly Broken
25	346.70	347.20	0.50	Highly Broken
26	347.20	347.70	0.50	Highly Broken
27	347.70	348.20	0.50	@ 0.25 - 1cm brown clay layer
28	348.20	348.70	0.50	
29	348.70	349.20	0.50	
30	349.20	349.70	0.50	Upper 5cm dull with fusain.
31	349.70	350.20	0.50	
32	350.20	351.20	1.00	Some Ca. Cleat.
33	351.20	351.70	0.50	
34	351.70	352.20	0.50	desorbing
35	352.20	352.70	0.50	Ca on cleat
36	352.70	353.39	0.69	Ca on cleat.
37	353.39	354.20	0.81	Highly broken *
38	354.20	354.70	0.50	Highly broken *
39	354.70	355.20	0.50	Highly broken *
40	355.20	355.70	0.50	desorbing
41	355.70	356.20	0.50	Highly broken *
42	356.20	356.70	0.50	Highly broken *
43	356.70	357.20	0.50	
44	357.20	357.70	0.50	Isotherm sample from base
45	357.70	358.20	0.50	

* Bedding plane fracture.

Appendix E: Proximate Results

Appendix E: Proximate and ultimate results and corrections

Sample details							Proximate Analysis, As-recieved						Proximate Analysis, Dry basis (db)					dmmSf		dry, ash free (daf)			dry, mineral matter free (dmmf)		Gas Data				
Basin	Drill hole #	Canister	From	To	Thickness	Midpoint	Inherent Moisture	Ash %	Volatile Matter %	Fixed Carbon %	Sulphur %	Calorific value	Ash (db) %	Volatile Matter (db) %	Fixed Carbon (db) %	Sulphur (db) %	Calorific value	Volatile Matter	Calorific value	Volatile Matter	Fixed carbon	Calorific value	Volatile Matter	Calorific value	Measured gas m3/t	Residual gas m3/t	Lost gas m3/t	Total gas m3/t	Suggate number
Huntly	TW1	9	338.70	339.20	0.50	338.95	11.6	5.5	36.5	46.4	0.30	24.98	6.2	41.3	52.5	0.35	28.3	43.6	30.4	44.0	56.0	30.1	43.7	30.3	1.1	0.27	0.04	1.4	6.0
Huntly	TW1	10	339.20	339.70	0.50	339.45	12.9	3.8	35.4	47.9	0.30	25.02	4.4	40.6	55.0	0.34	28.7	42.2	30.2	42.5	57.5	30.0	42.2	30.2	1.1	0.21	0.05	1.4	6.0
Huntly	TW1	11	339.70	340.20	0.50	339.95	9.2	2.9	42.0	45.9	0.30	26.90	3.2	46.3	50.5	0.33	29.6	47.7	30.8	47.8	52.2	30.6	47.7	30.7	1.0	0.22	0.05	1.3	5.6
Huntly	TW1	12	340.20	340.70	0.50	340.45						28.18					28.2		28.2	0.0	0.0	28.2		28.2	1.3	0.54	0.05	1.9	
Huntly	TW1	13	340.70	341.20	0.50	340.95	12.6	2.8	37.8	46.7	0.28	25.37	3.3	43.3	53.4	0.33	29.0	44.6	30.2	44.8	55.2	30.0	44.6	30.1	1.1	0.25	0.06	1.4	5.4
Huntly	TW1	14	341.20	341.70	0.50	341.45	11.1	3.0	41.3	44.5	0.38	26.91	3.4	46.5	50.1	0.43	30.3	47.9	31.5	48.1	51.9	31.3	47.9	31.4	1.1	0.20	0.06	1.4	5.9
Huntly	TW1	15	341.70	342.20	0.50	341.95	14.0	2.7	36.2	47.1	0.25	25.03	3.1	42.1	54.8	0.29	29.1	43.3	30.2	43.5	56.6	30.0	43.3	30.1	0.9	0.22	0.04	1.1	5.6
Huntly	TW1	16	342.20	342.70	0.50	342.45	12.0	1.8	38.3	47.9	0.23	26.34	2.1	43.5	54.4	0.26	29.9	44.3	30.7	44.4	55.5	30.6	44.3	30.6	0.7	0.74	0.03	1.5	5.9
Huntly	TW1	17	342.70	343.20	0.50	342.95	12.1	1.7	37.6	48.6	0.21	25.74	1.9	42.8	55.3	0.24	29.3	43.5	30.0	43.6	56.4	29.8	43.5	29.9	0.6	0.96	0.02	1.5	5.5
Huntly	TW1	18	343.20	343.70	0.50	343.45	12.3	3.9	35.0	48.8	0.20	24.68	4.4	39.9	55.6	0.23	28.1	41.5	29.6	41.8	58.2	29.4	41.5	29.6	0.8	0.81	0.04	1.7	5.8
Huntly	TW1	19	343.70	344.20	0.50	343.95	12.1	1.6	38.9	47.4	0.21	25.94	1.9	44.3	53.9	0.24	29.5	45.0	30.2	45.1	54.9	30.1	45.0	30.1	0.6	0.86	0.02	1.4	5.3
Huntly	TW1	20	344.20	344.70	0.50	344.45	13.9	1.7	35.9	48.5	0.22	25.30	2.0	41.7	56.3	0.25	29.4	42.4	30.1	42.6	57.5	30.0	42.4	30.0	0.8	0.78	0.03	1.6	5.7
Huntly	TW1	21	344.70	345.20	0.50	344.95	12.6	3.0	37.8	46.6	0.22	25.48	3.4	43.3	53.3	0.25	29.1	44.6	30.3	44.8	55.2	30.2	44.6	30.3	0.9	0.37	0.03	1.3	5.5
Huntly	TW1	22	345.20	345.70	0.50	345.45	12.6	9.0	37.1	41.3	0.19	21.82	10.3	42.4	47.3	0.22	25.0	46.6	28.2	47.3	52.7	27.8	46.7	28.2	1.1	0.36	0.06	1.5	3.4
Huntly	TW1	23	345.70	346.20	0.50	345.95						25.17					25.2		25.2	0.0	0.0	25.2		25.2	1.6	0.20	0.08	1.9	
Huntly	TW1	24	346.20	346.70	0.50	346.45	8.4	33.4	29.2	29.0	0.21	16.55	36.4	31.9	31.7	0.23	18.1	47.1	30.2	50.2	49.9	28.4	47.1	30.1	0.7	0.13	0.05	0.9	6.2
Huntly	TW1	25	346.70	347.20	0.50	346.95	10.9	10.7	36.0	42.4	0.29	23.49	12.0	40.4	47.6	0.32	26.4	45.2	30.5	45.9	54.1	30.0	45.2	30.4	1.0	0.45	0.06	1.5	5.9
Huntly	TW1	26	347.20	347.70	0.50	347.45	12.7	5.2	35.4	46.7	0.24	24.54	6.0	40.6	53.5	0.28	28.1	42.8	30.2	43.2	56.9	29.9	42.8	30.1	1.2	0.34	0.11	1.7	5.9
Huntly	TW1	27	347.70	348.20	0.50	347.95	12.7	6.2	35.4	45.7	0.25	24.66	7.1	40.5	52.4	0.29	28.3	43.1	30.7	43.6	56.4	30.4	43.2	30.6	0.6	0.97	0.02	1.6	6.3
Huntly	TW1	28	348.20	348.70	0.50	348.45	15.5	3.4	33.6	47.5	0.25	23.99	4.0	39.8	56.2	0.30	28.4	41.2	29.8	41.4	58.5	29.6	41.2	29.7	1.0	0.37	0.03	1.4	5.6
Huntly	TW1	29	348.70	349.20	0.50	348.95	12.8	5.0	36.1	46.1	0.23	24.17	5.7	41.4	52.9	0.26	27.7	43.6	29.6	43.9	56.1	29.4	43.6	29.6	0.9	0.88	0.02	1.8	5.2
Huntly	TW1	30	349.20	349.70	0.50	349.45	13.5	3.8	35.9	46.8	0.22	24.13	4.4	41.5	54.1	0.26	27.9	43.1	29.3	43.4	56.6	29.2	43.1	29.3	1.1	0.50	0.04	1.7	5.0
Huntly	TW1	31	349.70	350.20	0.50	349.95	13.8	1.6	36.5	48.0	0.24	25.48	1.9	42.4	55.7	0.28	29.6	43.1	30.3	43.2	56.8	30.1	43.1	30.2	0.9	0.83	0.03	1.8	5.7
Huntly	TW1	32	350.20	351.20	1.00	350.70	12.8	2.1	38.4	46.8	0.26	25.97	2.4	44.0	53.7	0.29	29.8	44.9	30.6	45.1	55.0	30.5	44.9	30.6	1.0	0.63	0.03	1.7	5.7
Huntly	TW1	33	351.20	351.70	0.50	351.45	11.2	1.4	39.7	47.7	0.27	26.75	1.6	44.7	53.7	0.31	30.1	45.3	30.7	45.4	54.6	30.6	45.3	30.7	0.7	0.84	0.02	1.6	5.8
Huntly	TW1	34	351.70	352.20	0.50	351.95						25.88					25.9		25.9	0.0	0.0	25.9		25.9	1.2	0.66	0.02	1.9	
Huntly	TW1	35	352.20	352.70	0.50	352.45	11.1	4.7	38.1	46.1	0.25	24.68	5.3	42.9	51.8	0.28	27.8	45.0	29.5	45.3	54.7	29.3	45.0	29.5	0.6	1.07	0.02	1.7	5.0
Huntly	TW1	36	352.70	353.39	0.69	353.05	12.3	1.4	36.5	49.7	0.23	26.00	1.6	41.6	56.7	0.26	29.6	42.2	30.2	42.3	57.6	30.1	42.2	30.2	0.6	1.06	0.02	1.7	6.0
Huntly	TW1	37	353.39	354.20	0.81	353.80	11.2	1.5	36.6	50.7	0.24	25.99	1.7	41.2	57.1	0.27	29.3	41.8	29.9	41.9	58.1	29.8	41.8	29.8	1.2	0.61	0.05	1.9	5.9
Huntly	TW1	38	354.20	354.70	0.50	354.45	12.1	1.0	38.0	48.9	0.29	26.81	1.2	43.2	55.6	0.33	30.5	43.6	31.0	43.7	56.3	30.9	43.7	30.9	1.3	0.54	0.05	1.9	6.3
Huntly	TW1	39	354.70	355.20	0.50	354.95	11.4	1.0	37.9	49.7	0.28	26.80	1.1	42.8	56.1	0.32	30.2	43.2	30.7	43.3	56.7	30.6	43.2	30.6	1.4	0.28	0.06	1.7	6.3
Huntly	TW1	40	355.20	355.70	0.50	355.45						26.68					26.7		26.7	0.0	0.0	26.7		26.7	1.6	0.26	0.06	1.9	
Huntly	TW1	41	355.70	356.20	0.50	355.95	12.3	1.1	36.7	49.7	0.27	26.12	1.3	41.9	56.7	0.31	29.8	42.4	30.3	42.5	57.5	30.2	42.4	30.2	1.2	0.35	0.05	1.6	6.0
Huntly	TW1	42	356.20	356.70	0.50	356.45	12.1	2.3	36.6	49.0	0.24	25.49	2.7	41.6	55.7	0.28	29.0	42.6	29.9	42.7	57.2	29.8	42.6	29.9	1.2	0.77	0.08	2.1	5.7
Huntly	TW1	43	356.70	357.20	0.50	356.95	12.2	1.2	37.8	48.9	0.25	26.94	1.3	43.0	55.7	0.28	30.7	43.5	31.2	43.6	56.4	31.1	43.5	31.1	0.5	1.13	0.02	1.7	6.5
Huntly	TW1	44	357.20	357.70	0.50	357.45	12.2	1.0	41.7	45.1	0.23	27.91	1.1	47.5	51.4	0.26	31.8	48.0	32.2	48.0	52.0	32.1	48.0	32.2	0.9	0.94	0.03	1.8	6.3
Huntly	TW1	45	357.70	358.20	0.50	357.95	12.5	1.7	37.4	48.5	0.25	26.55	1.9	42.7	55.4	0.28	30.3	43.4	31.1	43.5	56.5	30.9	43.4	31.0	0.8	0.83	0.03	1.7	6.4
Greymouth	944	16	309.55	309.85	0.30	309.70	8.7	2.3	36.5	52.5	0.23	29.7	2.5	40.0	57.5	0.25	32.5	40.8	33.5	41.0	59.0	33.3	40.9	33.4	2.89	0.26	0.55	3.70	10.6
Greymouth	944	1	309.85	310.35	0.50	310.10	1.7	74.2	13.4	10.6	0.06	6.1	75.5	13.7	10.8	0.06	6.2	36.0	36.7	55.8	44.2	25.3	36.1	36.6	0.53	0.07	0.07	0.67	13.4
Greymouth	944	2	334.74	335.10	0.36	334.92	6.7	25.9	29.1	38.3	0.22	22.4	27.8	31.2	41.1	0.24	24.0	40.9	34.6	43.2	56.8	33.2	40.9	34.5	1.83	0.26	0.05	2.14	11.5
Greymouth	944	3	335.10	335.50	0.40	335.30	7.4	8.7	36.2	47.7	0.26	28.3	9.4	39.1	51.5	0.28	30.6	42.5	34.2	43.1	56.9	33.7	42.6	34.1	2.36	0.35	0.40	2.78	10.8
Greymouth	944	4	341.00	341.50	0.50	341.25	7.7	1.3	40.0	51.0	0.41	30.9	1.4	43.3	55.3	0.44	33.4	43.8	34.1	44.0	56.0	33.9	43.9	34.0	1.79	0.58	0.02	2.39	10.4
Greymouth	944	5	341.50	342.00	0.50	341.75	8.1	2.5	38.7	50.7	0.29	30.4	2.7	42.1	55.2	0.32	33.0	43.1	34.1	43.3	56.7	34.0	43.1	34.1	2.12	1.04	0.05	3.21	10.6
Greymouth	944	6	342.00	342.50	0.50	342.25	7.4	0.7	41.2	50.7	0.33	31.1	0.8	44.5	54.7	0.36	33.6	44.8	34.0	44.8	55.2	33.9	44.8	33.9	1.37	0.77	0.07	2.21	10.1
Greymouth	944	7	343.10	343.60	0.50	343.35	7.5	0.8	41.1	50.6	0.29	31.4	0.8	44.4	54.7	0.31	34.0	44.7	34.3	44.8	55.2	34.2	44.8	34.3	2.54	0.58	0.07	3.19	10.4
Greymouth	944	8	343.60	344.10	0.50	343.85	8.2	1.3	37.6	52.9	0.36	30.6	1.4	41.0	57.6	0.39	33.4	41.4	34.0	41.5	58.5	33.8	41.5	33.9	2.85	0.20	0.08	3.13	10.9
Greymouth	944	9	344.10	344.70	0.60	344.40	6.9	20.4	32.3	40.4	0.23	24.5	21.9	34.7	43.4	0.25	26.3	42.8	34.8	44.4	55.6	33.7	42.8	34.7	2.74	0.60	0.08	3.42	11.2
Greymouth	944	10	344.85	345.35	0.50	345.10	5.0	40.3	26.0	28.7	0.17	18.0	42.4	27.4	30.2	0.18	18.9	43.3	35.6	47.5	52.5	32.9	43.4	35.5	1.47	0.19	0.03	1.69	11.6
Greymouth	944	11	345.35	345.85	0.50	345.60	2.3	68.2	15.1	14.4	0.19	8.7	69.8	15.5	14.7	0.19	8.9	36.4	38.7	51.2	48.8	29.6	36.5	38.4	0.87	0.10	0.05	1.02	13.8
Greymouth	944	12	345.85	346.35	0.50	346.10	4.6	44.0	25.8	25.5	0.35	15.7	46.2	27.1	26.8	0.37	16.4	45.6	33.5	50.3	49.7	30.5	45.6	33.4	1.44	0.67	0.07	2.18	9.5
Greymouth	944	13	346.35	347.00	0.65	346.68	8.1	4.3	37.9	49.7	0.66	29.7	4.7	41.2	54.1	0.72	32.3	42.9	34.2	43.3	56.7	33.8	43.0	34.0	1.81	0.45	0.06	2.32	10.7
Greymouth	944	14	347.10	347.60	0.50	347.35	9.0	2.5	36.3	52.2	0.28	28.4	2.7	39.9	57.4	0.31	31.2	40.8	32.3	41.0	59.0	32.1	40.8	32.2	2.42	0.22	0.08	2.72	9.5
Greymouth	944	15	347.60	348.10	0.50	347.85	8.8	5.3	37.7	48.2	0.28	29.2	5.8	41.3	52.9	0.31	32.1	43.5	34.3	43.9	56.1	34.0	43.5	34.2	1.13	0.60	0.04	1.77	10.7
Greymouth	944	17	348.10	348.60	0.50	348.35	9.7	2.5	36.8	51.0	0.28	29.6	2.8	40.8	56.5	0.31	32.8	41.7	33.9	41.9	58.1	33.8	41.7	33.9	2.58	0.41	0.07	3.06	10.8
Greymouth	944	18	348.60	349.10	0.50	348.85	9.0	3.1	37.3	50.6	0.28	29.7	3.4	41.0	55.6	0.31	32.6	42.2	34.0	42.4	57.6	33.8	42.2	33.9	2.35	0.24	0.11	2.70	10.7
Greymouth	944	19	349.10	349.60	0.50	349.35	7.1	15.6	35.2	42.2	0.25	26.1	16.8	37.8	45.4	0.27	28.1	44.3	34.5	45.5	54.5	33.7	44.3	34.4	1.96	0.54	0.07	2.57	10.6
Greymouth	944	20	349.70	350.20	0.50	349.95	8.7	7.0	35.9	48.4	0.28	28.3	7.7	39.3	53.0	0.31	31.0	42.1	34.0	42.6	57.4	33.6	42.1	33.9	1.03	0.45	0.09	1.57	10.7
Greymouth	944	21	350.20	350.70	0.50	350.45	8.0	13.6	34.5	43.9	0.27	26.4	14.8	37.5	47.7	0.29	28.7	43.0	34.3	44.0	56.0	33.6	43.0	34.2	1.85	0.43	0.04	2.32	10.8
Greymouth	944	22	351.00	351.50	0.50	351.25	9.1	2.7	36.8	51.4	0.34	29.7	3.0	40.5	56.5	0.37	32.7	41.5	33.9	41.7	58.3	33.7	41.5	33.8	2.65	0.28	0.06	2.98	10.8
Greymouth	944	23	351.50	352.00	0.50	351.75	8.0	4.0	38.3	49.7	0.33	29.5	4.3	41.6	54.0	0.36	32.0	43.2	33.7	43.5	56.5	33.5	43.3	33.6	1.56	0.41	0.05	2.02	10.2
Greymouth	944	24	352.00	352.50	0.50	352.25	5.9	36.8	25.4	31.9	0.23	18.7	39.1	27.0	33.9	0.25	19.9	40.4	34.9	44.3	55.7	32.6	40.5	34.8	1.07	0.52	0.04	1.63	11.8
Ohai	SC3	SC3-1	319.10	320.20	1.1	319.65	9.0	14.4	33.2	43.4	0.22	24.1	15.8	36.5	47.7	0.24	26.5	42.2	32.1	43.3	56.7	31.4	42.3	32.0	3.2	0.77	0.45	4.4	9.0
Ohai	SC3	SC3-2	320.15	320.75	0.6	320.45	6.2	41.9	25.0	26.9	0.18	15.1	44.7	26.7	28.7	0.19	16.1	43.6	31.7	48.2	51.8	29.1	43.6	31.6	1.6	0.77	0.64	3.0	8.3
Ohai	SC3	SC3-3	333.10	334.00	0.9	333.55	8.7	1.8	40.5	49.0	0.25	28.5	2.0	44.4	53.7	0.27	31.2	45.1	31.9	45.3	54.7	31.8	45.1	31.9	3.9	0.55	0.24	4.7	8.1
Ohai	SC3	SC3-4	333.65	334.65	1.0	334.15	9.5	1.8	39.5	49.2	0.21	28.2	2.0	43.6	54.4	0.23	31.1	44.4	31.9	44.5	55.5	31.7	44.4	31.8	3.8	0.55	0.27	4.6	8.2
Ohai	SC3	SC3-5	334.65	335.65	1.0	335.15	9.3	1.8	38.4	50.5	0.18	18.1	2.0	42.3	55.7	0.20	19.9	43.1	20.4	43.2	56.8	20.3	43.1	20.4	4.1	0.55	0.30	4.9	
Ohai	SC3	SC3-6	335.65	336.65	1.0	336.15	8.8	1.8	39.0	50.4	0.19	28.2	2.0	42.8	55.3	0.21	30.9	43.5	31.7	43.6	56.4	31.6	43.5	31.6	4.0	0.55	0.32	4.8	8.3
Ohai	SC3	SC3-7	336.65	337.55	0.9	337.10	9.2	1.6	38.5	50.7	0.20	28.2	1.8	42.4	55.8	0.22	31.0	43.0	31.7	43.2	56.8	31.6	43.1	31.6	4.1	0.55	0.29	4.9	8.4
Ohai	SC3	SC3-8	339.35	340.15	0.8	339.75	10.2	1.4	38.4	50.0	0.20	28.0	1.6	42.8	55.7	0.22	31.2	43.3	31.8	43.4	56.6	31.7	43.3	31.7	4.3	0.40	0.42	5.1	8.4
Ohai	SC3	SC3-9	340.15	341.15	1.0	340.65	10.7	1.3	37.8	50.2	0.20	27.7	1.5	42.3	56.2	0.22	31.0	42.9	31.6	43.0	57.0	31.5	42.9	31.5	4.5	0.40	0.40	5.3	8.3
Ohai	SC3	SC3-10	341.15	342.15	1.0	341.65	10.6	1.4	37.9	50.1	0.20	27.7	1.6	42.4	56.0	0.22	31.0	43.0	31.6	43.1	56.9	31.5	43.0	31.5	3.1	0.40	0.38	3.9	8.3
Ohai	SC3	SC3-11	342.15	343.00	0.9	342.58	10.7	1.5	37.0	50.8	0.17	27.6	1.7	41.4	56.9	0.19	30.9	42.0	31.5	42.1	57.9	31.4	42.0	31.4	2.7	0.40	0.58	3.7	8.5
Ohai	SC3	SC3-12	343.00	344.00	1.0	343.50	10.6	1.2	38.4	49.8	0.17	27.7	1.3	43.0	55.7	0.19	31.0	43.4	31.5	43.5	56.5	31.4	43.5	31.4	3.6	0.40	0.44	4.5	8.1
Ohai	SC3	SC3-13	344.00	345.00	1.0	344.50	10.2	1.5	38.9	49.5	0.16	27.8	1.7	43.3	55.1	0.18	31.0	43.9	31.6	44.1	56.0	31.5	44.0	31.5	4.6	0.40	0.47	5.5	8.1
Ohai	SC3	SC3-14	345.36	346.20	0.8	345.78	10.2	1.8	39.4	48.6	0.16	27.8	2.0	43.9	54.1	0.18	31.0	44.6	31.7	44.8	55.2	31.6	44.7	31.7	4.9	0.40	0.48	5.8	8.0
Ohai	SC3	SC3-15	346.20	347.00	0.8	346.60	10.3	1.5	38.9	49.3	0.17	27.7	1.7	43.4	55.0	0.19	30.9	44.0	31.5	44.1	55.9	31.5	44.0	31.5	4.8	0.45	0.42	5.7	8.0
Ohai	SC3	SC3-16	347.00	348.00	1.0	347.50	10.2	1.7	37.5	50.6	0.15	27.7	1.9	41.8	56.3	0.17	30.9	42.4	31.6	42.6	57.4	31.5	42.5	31.5	5.0	0.54	0.27	5.8	8.4
Ohai	SC3	SC3-17	348.00	348.50	0.5	348.25	10.3	2.1	37.0	50.6	0.14	27.6	2.3	41.2	56.4	0.16	30.8	42.1	31.6	42.2	57.8	31.5	42.1	31.6	4.9	0.54	0.31	5.8	8.6
Ohai	SC3	SC3-18	348.76	349.76	1.0	349.26	10.5	2.4	38.4	48.7	0.18	57.3	2.7	42.9	54.4	0.20	64.1	43.9	66.1	44.1	55.9	65.8	43.9	66.0	3.9	0.54	0.25	4.7	
Ohai	SC1	SC1-1	254.90	255.40	0.5	255.15	6.4	51.5	22.6	19.5	0.16	11.9	55.0	24.1	20.8	0.17	12.7	47.2	32.3	53.7	46.3	28.3	47.2	32.2	1.6	0.51	0.47	2.6	8.0
Ohai	SC1	SC1-2																							3.9	0.51	0.36	4.8	
Ohai	SC1	SC1-3	338.95	340.05	1.1	339.50	9.4	4.5	37.7	48.4	0.40	27.2	5.0	41.6	53.4	0.44	30.0	43.5	31.8	43.8	56.2	31.5	43.5	31.7	3.2	0.51	0.53	4.3	8.4
Ohai	SC1	SC1-4																							3.7	0.51	0.44	4.6	
Ohai	SC1	SC1-5	356.12	357.10	1.0	356.61	6.8	29.9	30.1	33.2	0.19	19.4	32.1	32.3	35.6	0.20	20.8	44.9	32.2	47.6	52.4	30.6	45.0	32.1	3.1	0.18	0.70	4.0	8.4
Ohai	SC1	SC1-6	357.10	357.60	0.5	357.35	6.9	22.9	33.1	37.1	0.20	21.4	24.6	35.6	39.8	0.21	23.0	45.4	31.6	47.2	52.8	30.5	45.4	31.6	3.4	0.18	0.79	4.4	7.8
Ohai	SC1	SC1-7	358.20	358.70	0.5	358.45	6.7	29.4	31.1	32.8	0.20	19.3	31.5	33.3	35.2	0.21	20.6	46.2	31.7	48.7	51.3	30.1	46.2	31.6	3.2	0.18	0.85	4.2	7.6
Ohai	SC1	SC1-8	367.20	367.70	0.5	367.45	9.0	13.1	32.9	45.0	0.22	24.7	14.4	36.2	49.5	0.24	27.1	41.2	32.3	42.2	57.8	31.7	41.2	32.2	4.3	0.18	0.44	5.0	9.4
Ohai	SC1	SC1-9	399.73	401.20	1.5	400.47	5.1	35.4	26.8	32.7	0.22	18.5	37.3	28.2	34.5	0.23	19.5	41.5	33.1	45.0	55.0	31.0	41.6	33.0	4.3	0.18	0.72	5.2	10.1
Ohai	SC1	SC1-10	414.20	414.98	0.8	414.59	6.6	4.9	38.8	49.7	0.24	28.2	5.2	41.5	53.2	0.26	30.2	43.5	32.1	43.8	56.2	31.9	43.5	32.1	5.4	0.24	0.66	6.3	8.7
Ohai	SC1	SC1-11	414.98	416.14	1.2	415.56	5.6	12.4	39.3	42.7	0.27	26.6	13.1	41.6	45.2	0.29	28.2	47.1	33.1	47.9	52.1	32.5	47.1	33.0	5.0	0.24	0.33	5.6	8.7

Appendix F: Ash Constituent Results

Table 1 Huntly ash constituent data

Interval	Midpoint	SiO_2	Al_2O_3	Fe_2O_3	CaO	MgO	Na_2O	K_2O	TiO_2	Mn_3O_4	SO_3	P_2O_5	Loss on Ignition	Total	Total with loss of Ignition
		%	%	%	%	%	%	%	%	%	%	%	%	%	
TW1 C9	338.95	58.70	15.07	2.90	8.23	1.43	2.85	0.78	0.90	0.01	6.05	0.05	0.42	96.97	97.39
TW1 C10	339.45	41.23	14.75	6.74	13.24	2.31	4.30	0.44	2.45	0.01	11.64	0.04	0.61	97.15	97.76
TW1 C11	339.95	18.82	21.25	5.80	21.37	2.84	5.56	0.26	5.17	0.01	15.08	0.05	1.04	96.21	97.25
TW1 C12	340.45	7.61	25.86	7.12	27.31	3.86	6.81	0.25	1.55	0.01	14.65	0.06	1.13	95.09	96.22
TW1 C13	340.95	10.23	23.75	6.03	29.22	2.94	5.46	0.22	2.93	0.01	14.80	0.09	2.58	95.68	98.26
TW1 C14	341.45	15.36	22.08	4.94	22.39	2.63	4.93	0.58	6.91	0.01	16.23	0.07	1.38	96.13	97.51
TW1 C15	341.95	9.51	17.47	5.89	34.45	4.89	6.39	0.25	0.24	0.01	15.56	0.07	2.09	94.73	96.82
TW1 C16	342.45	4.71	13.89	7.05	33.89	6.13	8.41	0.31	0.35	0.01	19.80	0.04	1.60	94.59	96.19
TW1 C17	342.95	2.39	11.83	6.22	34.91	5.86	9.19	0.28	0.30	0.01	21.14	0.03	1.99	92.16	94.15
TW1 C18	343.45	4.78	3.98	8.76	51.90	16.58	3.37	0.24	0.31	0.01	8.40	0.01	4.95	98.34	103.29
TW1 C19	343.95	4.28	12.34	7.88	35.25	6.52	7.92	0.73	0.47	0.01	19.20	0.06	2.19	94.66	96.85
TW1 C20	344.45	1.03	17.04	7.64	33.22	6.58	8.08	0.21	0.28	<0.01	19.29	0.03	1.80	93.40	95.20
TW1 C21	344.95	5.20	13.22	4.94	46.54	5.57	5.79	0.21	0.47	0.02	13.63	0.03	2.19	95.62	97.81
TW1 C22	345.45	3.68	4.68	4.94	74.69	5.64	1.24	0.17	0.12	0.05	4.69	0.03	4.38	99.93	104.31
TW1 C23	345.95	17.83	22.63	4.48	31.86	3.67	4.42	0.21	0.53	0.01	9.80	0.37	1.13	95.81	96.94
TW1 C24	346.45	57.10	31.79	1.23	1.60	0.47	0.62	0.48	3.47	<0.01	0.92	0.06	0.86	97.74	98.60
TW1 C25	346.95	47.73	27.55	1.94	7.29	1.57	1.98	0.32	4.66	<0.01	4.44	0.22	0.52	97.70	98.22
TW1 C26	347.45	27.95	28.85	2.88	18.41	4.74	3.50	0.37	0.69	<0.01	9.02	0.41	0.97	96.82	97.79
TW1 C27	347.95	39.96	25.95	1.98	7.83	1.38	2.45	0.33	11.20	<0.01	5.71	0.26	0.60	97.05	97.65
TW1 C28	348.45	26.73	31.51	2.58	14.01	2.55	4.70	0.17	1.95	<0.01	12.47	0.33	0.74	97.01	97.75
TW1 C29	348.95	9.30	10.76	5.48	52.83	7.64	2.06	0.14	1.51	0.02	7.84	1.29	2.03	98.87	100.90
TW1 C30	349.45	5.01	10.92	6.06	57.72	6.64	2.56	0.22	0.59	0.02	9.49	0.03	2.29	99.26	101.55
TW1 C31	349.95	3.31	25.43	3.78	27.84	4.24	7.07	0.21	1.40	<0.01	20.12	0.05	1.50	93.45	94.95
TW1 C32	350.70	1.75	16.65	4.75	30.41	4.88	5.65	0.21	12.45	0.01	18.47	0.06	1.63	95.29	96.92
TW1 C33	351.45	1.74	20.81	5.08	28.42	3.98	7.74	1.01	1.88	<0.01	23.31	0.02	1.04	94.00	95.04
TW1 C34	351.95	0.79	10.30	6.61	33.83	4.67	8.11	0.38	0.32	0.01	26.52	0.04	1.79	91.58	93.37
TW1 C35	352.45	0.96	0.94	6.77	71.01	10.99	1.00	0.09	0.06	0.03	6.54	0.01	3.72	98.40	102.12
TW1 C36	353.05	0.79	0.68	11.31	42.00	4.77	7.53	0.25	0.22	0.02	25.38	0.03	0.54	92.98	93.52
TW1 C37	353.80	4.27	1.40	12.42	33.86	6.07	7.90	0.44	0.17	0.01	25.49	0.04	0.72	92.07	92.79
TW1 C38	354.45	1.65	2.18	12.13	29.68	4.74	9.11	0.32	0.38	0.01	30.11	0.03	0.56	90.34	90.90
TW1 C39	354.95	2.37	1.86	9.08	31.54	4.46	9.13	0.33	0.29	0.01	31.82	0.03	0.49	90.92	91.41
TW1 C40	355.45	3.35	3.63	17.29	36.82	11.94	3.85	0.15	0.17	0.02	18.49	0.08	0.93	95.79	96.72
TW1 C41	355.95	3.80	2.02	9.05	32.05	5.02	8.49	0.37	0.18	0.01	30.89	0.04	0.66	91.92	92.58
TW1 C42	356.45	3.15	1.98	12.18	46.21	12.94	3.57	0.36	0.13	0.01	16.71	0.03	2.99	97.27	100.26
TW1 C43	356.95	2.54	3.79	10.80	31.45	5.20	8.52	0.35	0.49	0.01	27.01	0.05	0.71	90.21	90.92
TW1 C44	357.45	0.78	6.32	10.89	31.39	6.08	7.48	0.50	0.67	0.01	25.75	0.04	0.96	89.91	90.87
TW1 C45	357.95	7.35	24.14	3.75	22.46	1.88	6.36	0.33	10.70	0.01	15.53	0.08	0.98	92.60	93.58
	mean	**12.37**	**14.31**	**6.74**	**32.08**	**5.25**	**5.52**	**0.34**	**2.07**	**0.01**	**16.27**	**0.12**	**1.53**	**95.07**	**96.61**
	Std	*16.36*	*9.84*	*3.50*	*16.09*	*3.33*	*2.58*	*0.19*	*3.24*	*0.01*	*8.16*	*0.22*	*1.09*	*2.72*	*3.36*

Table 2 Ohai ash constituent data

Interval	Midpoint	SiO_2	Al_2O_3	Fe_2O_3	CaO	MgO	Na_2O	K_2O	TiO_2	Mn_3O_4	SO_3	P_2O_5	Loss on Ignition	Total	Total with Loss of Ignition
		%	%	%	%	%	%	%	%	%	%	%	%	%	
SC1															
SC1-1	255.15	59.56	31.47	3.49	0.67	0.95	0.72	0.74	1.64	<0.01	0.14	0.03	0.67	99.41	100.08
SC1-3	339.50	32.74	17.59	11.17	12.63	6.39	4.03	0.25	1.17	0.06	10.40	0.81	0.45	97.24	97.70
SC1-4	340.60	40.45	24.46	2.05	4.95	1.11	7.24	0.35	5.16	<0.01	4.40	4.96	0.59	95.13	95.72
SC1-5	356.61	63.15	29.36	2.67	0.37	0.45	0.93	0.50	1.55	0.01	0.06	0.05	1.02	99.09	100.11
SC1-6	357.35	52.16	31.17	4.75	4.28	2.39	1.11	0.38	1.66	0.01	1.22	0.05	0.73	99.18	99.91
SC1-7	358.45	56.56	32.09	5.68	0.61	1.28	1.00	0.43	1.62	0.01	0.30	0.04	1.63	99.62	101.25
SC1-8	367.45	72.97	18.98	1.23	0.46	0.30	1.86	0.25	1.44	<0.01	0.07	0.02	0.67	97.58	98.25
SC1-9	400.47	71.36	19.48	1.72	0.43	0.47	1.45	1.09	1.36	<0.01	0.16	0.02	1.57	97.51	99.08
SC1-10	414.59	40.43	14.54	5.43	15.82	6.23	3.98	0.21	0.96	<0.01	8.55	0.27	0.39	96.40	96.79
SC1-11	415.51	51.77	23.92	4.21	3.83	1.43	4.16	0.73	1.15	0.01	5.44	0.19	0.55	96.84	97.39
	mean	**54.12**	**24.31**	**4.24**	**4.40**	**2.10**	**2.65**	**0.49**	**1.77**	**0.02**	**3.07**	**0.64**	**0.83**	**97.80**	**98.63**
	Std	*13.38*	*6.47*	*2.89*	*5.52*	*2.30*	*2.13*	*0.28*	*1.21*	*0.02*	*3.91*	*1.54*	*0.44*	*1.49*	*1.74*
SC3															
SC3-1	319.60	62.64	18.42	3.07	4.19	1.06	2.79	0.38	1.11	0.01	3.44	0.03	1.05	97.10	98.14
SC3-2	320.45	61.54	29.91	2.37	0.77	0.57	0.78	0.93	1.61	<0.01	0.27	0.02	2.15	98.77	100.92
SC3-3	333.55	23.00	13.72	9.37	17.05	4.84	7.12	0.34	0.70	0.01	18.65	0.03	0.66	94.83	95.49
SC3-4	333.90	30.26	6.41	7.95	18.51	4.46	6.05	0.33	0.66	0.01	14.39	0.02	0.30	95.45	95.75
SC3-5	335.15	31.33	9.62	7.58	17.42	4.94	7.96	0.43	0.50	0.01	15.67	0.03	0.66	95.45	96.11
SC3-6	336.15	26.89	12.71	8.76	16.39	4.96	8.36	0.47	0.62	0.01	15.97	0.03	0.95	95.15	96.10
SC3-7	337.10	18.19	15.62	9.14	17.17	5.20	9.42	0.47	0.66	0.01	18.66	0.03	1.02	94.58	95.60
SC3-8	339.75	20.66	12.29	8.93	15.98	4.36	10.80	0.47	0.64	0.01	20.67	0.03	0.92	94.83	95.74
SC3-9	340.65	16.53	10.89	10.51	16.45	4.88	11.05	0.38	0.57	0.01	23.84	0.03	0.84	95.10	95.94
SC3-10	341.65	18.70	9.34	10.09	19.82	5.32	10.24	0.33	0.50	0.01	21.18	0.03	0.67	95.53	96.20
SC3-11	342.58	18.51	10.38	9.31	21.98	5.85	10.04	0.44	0.55	0.04	18.93	0.05	0.98	96.09	97.07
SC3-12	343.50	11.85	11.01	10.31	23.42	5.47	11.61	0.32	0.48	0.04	21.85	0.03	0.88	96.39	97.27
SC3-13	344.50	12.68	9.71	12.68	28.02	6.14	8.91	0.26	0.51	0.12	17.58	0.03	1.08	96.61	97.69
SC3-14	345.60	13.87	13.09	8.35	30.31	6.32	7.96	0.26	1.04	0.04	15.21	0.03	1.30	96.48	97.78
SC3-15	346.60	12.52	13.95	10.52	28.28	5.83	8.47	0.27	0.63	0.11	16.09	0.04	1.63	96.70	98.33
SC3-16	347.50	10.48	9.63	12.29	31.60	7.15	8.13	0.25	0.49	0.16	16.64	0.04	1.46	96.84	98.30
SC3-17	348.25	7.77	8.42	10.10	39.10	10.44	6.93	0.22	0.37	0.06	14.20	0.03	2.21	97.64	99.85
SC3-18	349.26	32.19	14.38	6.21	20.38	3.95	7.06	0.25	0.93	0.03	11.76	0.13	1.49	97.23	98.72
	mean	**23.87**	**12.75**	**8.75**	**20.38**	**5.09**	**7.98**	**0.38**	**0.70**	**0.04**	**15.83**	**0.04**	**1.12**	**96.15**	**97.28**
	Std	*15.69*	*5.16*	*2.69*	*9.20*	*2.11*	*2.75*	*0.16*	*0.30*	*0.04*	*5.94*	*0.02*	*0.51*	*1.13*	*1.57*

Table 3 Greymouth ash constituent data

Canister	Midpoint	SiO_2	Al_2O_3	Fe_2O_3	CaO	MgO	Na_2O	K_2O	TiO_2	Mn_3O_4	SO_3	P_2O_5	Loss on Ignition	Total	Total with loss of Ignition
		%	%	%	%	%	%	%	%	%	%	%	%	%	
Seam 1															
16	309.70	56.96	21.78	13.00	2.45	0.44	1.09	0.68	1.03	0.11	0.38	1.34	0.29	99.26	99.55
1	309.97	67.81	21.84	2.68	0.14	1.24	0.15	4.49	0.98	0.01	<0.01	0.10	0.26	99.44	99.70
Seam 2															
2	334.92	75.92	15.68	1.10	0.19	0.71	0.23	2.83	1.14	<0.01	<0.01	0.08	0.53	97.88	98.41
3	335.30	75.21	15.52	0.92	0.72	0.46	0.48	1.70	1.30	<0.01	<0.01	1.03	0.64	97.34	97.98
4	341.25	58.72	16.23	16.53	1.22	0.64	1.72	1.26	1.18	0.02	0.46	0.07	0.89	98.06	98.95
5	341.75	75.90	14.23	2.63	0.78	0.36	0.83	0.77	1.43	<0.01	0.40	0.03	2.02	97.34	99.36
6	342.25	47.23	20.72	18.76	2.66	0.84	3.54	0.72	1.09	0.02	0.06	0.06	0.73	95.70	96.43
7	343.35	*Insufficient sample*													
8	343.85	*Long Term Desorption*													
9	344.36	66.29	23.97	1.54	0.30	1.09	0.37	4.13	0.95	<0.01	0.00	0.02	0.37	98.68	99.05
10	345.10	70.58	19.99	1.34	0.12	1.07	0.15	4.22	1.04	<0.01	<0.01	0.01	0.61	98.53	99.14
11	345.60	71.17	18.84	1.92	0.12	1.09	0.13	4.17	0.98	<0.01	<0.01	0.01	1.04	98.43	99.47
12	345.92	69.86	12.74	9.48	0.94	1.83	0.12	2.82	0.86	0.04	0.84	0.01	1.69	99.54	101.23
13	346.55	71.31	11.39	11.83	1.54	0.37	0.70	1.64	0.98	0.01	0.03	0.06	2.09	99.86	101.95
14	347.35	*Long Term Desorption*													
15	347.85	83.46	10.48	0.94	0.44	0.16	0.56	0.22	1.60	<0.01	0.06	0.01	1.60	97.92	99.52
17	348.35	74.71	18.58	1.44	1.66	0.20	1.09	0.50	1.33	<0.01	<0.01	0.07	1.99	99.57	101.56
18	348.85	64.66	29.02	1.22	1.63	0.24	0.98	0.29	0.78	<0.01	<0.01	0.08	4.95	98.89	103.84
19	349.43	65.41	26.33	1.36	1.74	0.20	1.32	0.27	2.76	<0.01	<0.01	0.10	2.19	99.49	101.68
20	349.95	81.22	13.71	0.98	1.48	0.13	0.45	0.24	1.20	<0.01	<0.01	0.11	1.80	99.51	101.31
21	350.45	84.40	10.62	1.10	1.28	0.15	0.32	0.68	1.12	<0.01	<0.01	0.08	2.19	99.74	101.93
22	351.25	*Long Term Desorption*													
23	351.50	*Sample omitted from XRF run in error will be analysed in next run*													
24	352.39	73.17	18.46	1.46	1.29	0.87	0.17	3.37	0.98	<0.01	<0.01	0.07	4.38	99.84	104.22
	mean	**70.21**	**17.90**	**4.75**	**1.09**	**0.64**	**0.76**	**1.84**	**1.20**	**0.04**	**0.28**	**0.18**	**1.59**	**98.69**	**100.28**
	Std	*9.22*	*5.26*	*5.92*	*0.77*	*0.47*	*0.82*	*1.58*	*0.43*	*0.04*	*0.29*	*0.36*	*1.29*	*1.10*	*1.98*

*** NOTE** In some canisters, the full interval was not sampled. This is the case for canisters 19 and 24, and the depths that were sampled are noted down. In canisters 7, 23, and the three samples that were held in long term desorption (8, 14, 22) no XRF analysis was performed.

Appendix G: Microscopic Results

Table 1 Petrological data for Huntly, Ohai and Greymouth point counts

	Vitrinite					Liptinite						Inertinite				Mineral matter					Total Counts
Sample	C Tell	B Tell	L Tell	Des	V-d	Spor	Cu	Res	L-d	Sub	Fl	S-Fus	Fus	I-d	Scel	Pyr	Qtz	clay	Cbn	Fe-O	
944 c5	16	87	88	230	23	4	14	7	8	2	0	7	5	12	5	0	1	0	0	0	509
944 c6 p8 A	30	61	110	218	16	6	18	2	12	2	0	10	7	8	10	0	3	0	0	0	513
944 c6 p8 B	16	89	66	237	32	2	8	0	22	1	0	8	6	9	4	0	1	2	0	0	503
944 c13	7	65	123	272	25	3	2	5	21	2	0	11	4	15	2	1	6	1	0	0	565
944 c15	7	69	112	217	21	7	9	9	11	14	0	4	6	9	2	0	12	3	1	0	513
944 c16	14	51	226	131	6	5	5	5	15	25	0	4	4	15	2	1	2	1	0	1	513
944 c20	16	44	196	158	11	6	4	10	16	6	0	4	11	7	7	0	8	2	2	0	508
944 c21	11	46	182	189	21	8	6	7	8	11	1	4	1	2	5	0	18	5	1	0	526
TW1 c10	33	64	81	209	42	4	6	4	24	1	1	5	0	16	7	0	1	3	2	1	504
TW1 c11	23	78	50	226	25	6	3	16	50	4	0	7	0	7	10	1	0	0	0	5	511
TW1 c19	46	62	32	222	45	6	1	9	45	1	1	3	1	15	17	1	1	2	3	0	513
TW1 c21	29	34	108	294	20	4	1	7	17	4	0	2	0	17	7	0	1	0	4	0	549
TW1 c28	62	96	39	222	43	3	2	3	11	2	0	0	1	9	2	0	1	6	0	0	502
TW1 c32	60	64	91	202	29	5	5	3	23	2	1	0	0	13	8	0	0	2	2	0	510
TW1 c37	99	41	39	209	49	4	16	1	18	1	0	0	0	20	7	0	0	1	0	1	506
TW1 c43	29	85	92	194	41	4	13	1	21	5	0	0	1	10	9	0	0	1	0	0	506
SC3-1	18	119	114	138	6	11	12	5	17	15	0	16	5	4	2	0	15	5	0	0	502
SC3-3	16	119	76	206	29	2	12	1	9	7	0	5	12	6	1	0	0	0	0	0	501
SC3-7	8	99	108	194	15	4	16	1	6	9	0	8	9	17	6	0	1	0	1	0	502
SC3-9	15	127	80	221	15	1	8	0	7	3	0	5	6	10	3	0	0	1	1	0	503
SC3-12	14	97	82	226	22	6	6	1	13	3	0	4	5	13	8	0	1	0	1	0	502
SC3-13	17	105	101	191	18	1	3	2	14	22	0	5	6	7	8	0	1	0	1	0	502
SC3-15	12	107	115	184	14	10	6	0	5	7	0	13	8	13	2	0	1	3	0	0	500
SC3-17	7	89	110	214	12	6	1	0	8	6	0	15	11	13	7	0	0	1	2	0	502
SC1-3	6	76	194	151	13	7	3	3	17	8	0	6	3	5	7	0	2	0	1	0	502
SC1-8	4	89	249	64	4	4	4	19	21	13	0	3	5	3	4	0	9	7	0	0	502
SC1-10	10	58	149	202	14	7	2	2	13	3	0	8	16	11	4	0	1	1	4	1	506
SC1-11	20	115	44	189	14	2	17	3	21	15	0	5	7	2	5	0	8	33	0	1	501

Appendix H: Gas Results

Table 1 Huntly gas data

Sample details					Gas Data			
Basin	Drill hole #	Canister	From	To	Measured gas m3/t	Residual gas m3/t	Lost gas m3/t	Total gas m3/t
Huntly	TW1	9	338.70	339.20	1.1	0.27	0.04	1.4
Huntly	TW1	10	339.20	339.70	1.1	0.21	0.05	1.4
Huntly	TW1	11	339.70	340.20	1.0	0.22	0.05	1.3
Huntly	TW1	12	340.20	340.70	1.3	0.54	0.05	1.9
Huntly	TW1	13	340.70	341.20	1.1	0.25	0.06	1.4
Huntly	TW1	14	341.20	341.70	1.1	0.20	0.06	1.4
Huntly	TW1	15	341.70	342.20	0.9	0.22	0.04	1.1
Huntly	TW1	16	342.20	342.70	0.7	0.74	0.03	1.5
Huntly	TW1	17	342.70	343.20	0.6	0.96	0.02	1.5
Huntly	TW1	18	343.20	343.70	0.8	0.81	0.04	1.7
Huntly	TW1	19	343.70	344.20	0.6	0.86	0.02	1.4
Huntly	TW1	20	344.20	344.70	0.8	0.78	0.03	1.6
Huntly	TW1	21	344.70	345.20	0.9	0.37	0.03	1.3
Huntly	TW1	22	345.20	345.70	1.1	0.36	0.06	1.5
Huntly	TW1	23	345.70	346.20	1.6	0.20	0.08	1.9
Huntly	TW1	24	346.20	346.70	0.7	0.13	0.05	0.9
Huntly	TW1	25	346.70	347.20	1.0	0.45	0.06	1.5
Huntly	TW1	26	347.20	347.70	1.2	0.34	0.11	1.7
Huntly	TW1	27	347.70	348.20	0.6	0.97	0.02	1.6
Huntly	TW1	28	348.20	348.70	1.0	0.37	0.03	1.4
Huntly	TW1	29	348.70	349.20	0.9	0.88	0.02	1.8
Huntly	TW1	30	349.20	349.70	1.1	0.50	0.04	1.7
Huntly	TW1	31	349.70	350.20	0.9	0.83	0.03	1.8
Huntly	TW1	32	350.20	351.20	1.0	0.63	0.03	1.7
Huntly	TW1	33	351.20	351.70	0.7	0.84	0.02	1.6
Huntly	TW1	34	351.70	352.20	1.2	0.66	0.02	1.9
Huntly	TW1	35	352.20	352.70	0.6	1.07	0.02	1.7
Huntly	TW1	36	352.70	353.39	0.6	1.06	0.02	1.7
Huntly	TW1	37	353.39	354.20	1.2	0.61	0.05	1.9
Huntly	TW1	38	354.20	354.70	1.3	0.54	0.05	1.9
Huntly	TW1	39	354.70	355.20	1.4	0.28	0.06	1.7
Huntly	TW1	40	355.20	355.70	1.6	0.26	0.06	1.9
Huntly	TW1	41	355.70	356.20	1.2	0.35	0.05	1.6
Huntly	TW1	42	356.20	356.70	1.2	0.77	0.08	2.1
Huntly	TW1	43	356.70	357.20	0.5	1.13	0.02	1.7
Huntly	TW1	44	357.20	357.70	0.9	0.94	0.03	1.8
Huntly	TW1	45	357.70	358.20	0.8	0.83	0.03	1.7
				mean	**1.0**	**0.6**	**0.0**	**1.6**
				Std	*0.3*	*0.3*	*0.0*	*0.2*

Table 2 Ohai gas data

Sample details					Gas Data			
Basin	Drill hole #	Canister	From	To	Measured gas m3/t	Residual gas m3/t	Lost gas m3/t	Total gas m3/t
Ohai	SC3	SC3-1	319.10	320.20	3.2	0.77	0.45	4.4
Ohai	SC3	SC3-2	320.15	320.75	1.6	0.77	0.64	3.0
Ohai	SC3	SC3-3	333.10	334.00	3.9	0.55	0.24	4.7
Ohai	SC3	SC3-4	333.65	334.65	3.8	0.55	0.27	4.6
Ohai	SC3	SC3-5	334.65	335.65	4.1	0.55	0.30	4.9
Ohai	SC3	SC3-6	335.65	336.65	4.0	0.55	0.32	4.8
Ohai	SC3	SC3-7	336.65	337.55	4.1	0.55	0.29	4.9
Ohai	SC3	SC3-8	339.35	340.15	4.3	0.40	0.42	5.1
Ohai	SC3	SC3-9	340.15	341.15	4.5	0.40	0.40	5.3
Ohai	SC3	SC3-10	341.15	342.15	3.1	0.40	0.38	3.9
Ohai	SC3	SC3-11	342.15	343.00	2.7	0.40	0.58	3.7
Ohai	SC3	SC3-12	343.00	344.00	3.6	0.40	0.44	4.5
Ohai	SC3	SC3-13	344.00	345.00	4.6	0.40	0.47	5.5
Ohai	SC3	SC3-14	345.36	346.20	4.9	0.40	0.48	5.8
Ohai	SC3	SC3-15	346.20	347.00	4.8	0.45	0.42	5.7
Ohai	SC3	SC3-16	347.00	348.00	5.0	0.54	0.27	5.8
Ohai	SC3	SC3-17	348.00	348.50	4.9	0.54	0.31	5.8
Ohai	SC3	SC3-18	348.76	349.76	3.9	0.54	0.25	4.7
				mean	**3.9**	**0.5**	**0.4**	**4.8**
				Std	*0.9*	*0.1*	*0.1*	*0.8*
Ohai	SC1	SC1-1	254.90	255.40	1.6	0.51	0.47	2.6
Ohai	SC1	SC1-2			3.9	0.51	0.36	4.8
Ohai	SC1	SC1-3	338.95	340.05	3.2	0.51	0.53	4.3
Ohai	SC1	SC1-4			3.7	0.51	0.44	4.6
Ohai	SC1	SC1-5	356.12	357.10	3.1	0.18	0.70	4.0
Ohai	SC1	SC1-6	357.10	357.60	3.4	0.18	0.79	4.4
Ohai	SC1	SC1-7	358.20	358.70	3.2	0.18	0.85	4.2
Ohai	SC1	SC1-8	367.20	367.70	4.3	0.18	0.44	5.0
Ohai	SC1	SC1-9	399.73	401.20	4.3	0.18	0.72	5.2
Ohai	SC1	SC1-10	414.20	414.98	5.4	0.24	0.66	6.3
Ohai	SC1	SC1-11	414.98	416.14	5.0	0.24	0.33	5.6
				mean	**3.7**	**0.3**	**0.6**	**4.6**
				Std	*1.0*	*0.2*	*0.2*	*1.0*

Table 3 Greymouth gas data

Sample details					Gas Data			
Basin	Drill hole #	Canister	From	To	Measured gas m3/t	Residual gas m3/t	Lost gas m3/t	Total gas m3/t
Greymouth	944	16	309.55	309.85	2.89	0.26	0.55	3.70
Greymouth	944	1	309.85	310.35	0.53	0.07	0.07	0.67
Greymouth	944	2	334.74	335.10	1.83	0.26	0.05	2.14
Greymouth	944	3	335.10	335.50	2.36	0.35	0.40	2.78
Greymouth	944	4	341.00	341.50	1.79	0.58	0.02	2.39
Greymouth	944	5	341.50	342.00	2.12	1.04	0.05	3.21
Greymouth	944	6	342.00	342.50	1.37	0.77	0.07	2.21
Greymouth	944	7	343.10	343.60	2.54	0.58	0.07	3.19
Greymouth	944	8	343.60	344.10	2.85	0.20	0.08	3.13
Greymouth	944	9	344.10	344.70	2.74	0.60	0.08	3.42
Greymouth	944	10	344.85	345.35	1.47	0.19	0.03	1.69
Greymouth	944	11	345.35	345.85	0.87	0.10	0.05	1.02
Greymouth	944	12	345.85	346.35	1.44	0.67	0.07	2.18
Greymouth	944	13	346.35	347.00	1.81	0.45	0.06	2.32
Greymouth	944	14	347.10	347.60	2.42	0.22	0.08	2.72
Greymouth	944	15	347.60	348.10	1.13	0.60	0.04	1.77
Greymouth	944	17	348.10	348.60	2.58	0.41	0.07	3.06
Greymouth	944	18	348.60	349.10	2.35	0.24	0.11	2.70
Greymouth	944	19	349.10	349.60	1.96	0.54	0.07	2.57
Greymouth	944	20	349.70	350.20	1.03	0.45	0.09	1.57
Greymouth	944	21	350.20	350.70	1.85	0.43	0.04	2.32
Greymouth	944	22	351.00	351.50	2.65	0.28	0.06	2.98
Greymouth	944	23	351.50	352.00	1.56	0.41	0.05	2.02
Greymouth	944	24	352.00	352.50	1.07	0.52	0.04	1.63
				mean	**1.9**	**0.4**	**0.1**	**2.4**
				Std	*0.7*	*0.2*	*0.1*	*0.8*

Appendix I: Saturation Results

Huntly		Ohai SC1		Ohai SC3		Greymouth	
Interval	Sat^n %	Interval	Sat^n %	Interval	Sat^n %	Interval	Sat^n %
9	28.0	SC1-1	55.8	SC3-1	68.9	16	70.2
10	29.0	SC1-2	75.0	SC3-2	47.7	1	12.7
11	26.9	SC1-3	67.5	SC3-3	73.9	2	40.6
12	39.1	SC1-4	72.5	SC3-4	72.8	3	52.8
13	28.5	SC1-5	62.9	SC3-5	77.5	4	45.4
14	28.4	SC1-6	69.0	SC3-6	76.1	5	60.9
15	23.6	SC1-7	66.6	SC3-7	77.4	6	41.9
16	31.2	SC1-8	78.1	SC3-8	80.5	7	60.5
17	31.7	SC1-9	81.2	SC3-9	83.5	8	59.4
18	34.1	SC1-10	98.8	SC3-10	61.6	9	64.9
19	29.6	SC1-11	87.9	SC3-11	58.6	10	32.1
20	33.3	-	-	SC3-12	70.2	11	19.4
21	26.9	-	-	SC3-13	86.3	12	41.4
22	30.7	-	-	SC3-14	90.7	13	44.0
23	39.2	-	-	SC3-15	90.0	14	51.6
24	18.3	-	-	SC3-16	90.8	15	33.6
25	31.1	-	-	SC3-17	90.7	17	58.1
26	34.6	-	-	SC3-18	74.0	18	51.2
27	33.1	-	-	-	-	19	48.8
28	28.3	-	-	-	-	20	29.8
29	36.7	-	-	-	-	21	44.0
30	34.0	-	-	-	-	22	38.3
31	36.0	-	-	-	-	23	38.3
32	34.8	-	-	-	-	24	30.9
33	32.5	-	-	-	-	-	-
34	38.4	-	-	-	-	-	-
35	35.2	-	-	-	-	-	-
36	34.8	-	-	-	-	-	-
37	38.8	-	-	-	-	-	-
38	38.1	-	-	-	-	-	-
39	35.1	-	-	-	-	-	-
40	38.6	-	-	-	-	-	-
41	32.1	-	-	-	-	-	-
42	42.7	-	-	-	-	-	-
43	34.9	-	-	-	-	-	-
44	37.4	-	-	-	-	-	-
45	35.0	-	-	-	-	-	-

Appendix J: Correlation Charts

Table 1 Charts showing correlation coefficients for vitrain % and gas volume

Huntly	**Vitrain %**	**Measured gas**	**Residual gas**	**Lost gas**	**Total gas**
Vitrain %	1.00				
Measured gas	-0.11	1.00			
Residual gas	0.30	-0.85	1.00		
Lost gas	-0.28	0.81	-0.81	1.00	
Total gas	0.40	-0.37	0.81	-0.50	1.00

Greymouth	**Vitrain %**	**Measured gas**	**Residual gas**	**Lost gas**	**Total gas**
Vitrain %	1.00				
Measured gas	-0.30	1.00			
Residual gas	0.17	-0.45	1.00		
Lost gas	-0.44	0.49	-0.30	1.00	
Total gas	-0.33	0.93	-0.14	0.58	1.00

Ohai SC3	**Vitrain %**	**Measured gas**	**Residual gas**	**Lost gas**	**Total gas**
Vitrain %	1.00				
Measured gas	-0.12	1.00			
Residual gas	0.19	0.02	1.00		
Lost gas	-0.11	0.08	-0.85	1.00	
Total gas	-0.11	1.00	0.00	0.12	1.00

Ohai SC1	**Vitrain %**	**Measured gas**	**Residual gas**	**Lost gas**	**Total gas**
Vitrain %	1.00				
Measured gas	0.02	1.00			
Residual gas	-0.46	-0.31	1.00		
Lost gas	0.40	-0.22	-0.44	1.00	
Total gas	0.03	0.99	-0.28	-0.14	1.00

Table 2 Charts showing correlation coefficients for proximate and ultimate analyses and gas volume

Huntly TW1	Inherent Moisture (aa)	Ash (db) %	Volatile Matter (daf)	Fixed carbon (daf)	Calorific value (daf)	Suggate number	Measured gas m3/t	Residual gas m3/t	Lost gas m3/t	Total gas m3/t
Moisture (aa)	1.00									
Ash (db) %	-0.49	1.00								
Volatile Matter (daf)	-0.65	0.55	1.00							
Fixed carbon (daf)	0.66	-0.55	-1.00	1.00						
Calorific value (daf)	-0.01	-0.55	0.02	-0.02	1.00					
Suggate number	-0.19	-0.05	-0.16	0.16	0.68	1.00				
Measured gas m3/t	0.03	-0.12	-0.12	0.12	-0.48	-0.04	1.00			
Residual gas m3/t	0.16	-0.35	-0.26	0.26	0.28	0.10	-0.66	1.00		
Lost gas m3/t	-0.13	0.20	0.04	-0.04	-0.27	-0.04	0.72	-0.64	1.00	
Total gas m3/t	0.23	-0.56	-0.46	0.46	-0.22	0.10	0.37	0.45	0.11	1.00

Greymouth	Inherent Moisture (aa)	Ash (db) %	Volatile Matter (daf)	Fixed carbon (daf)	Calorific value (daf)	Suggate number	Measured gas m3/t	Residual gas m3/t	Lost gas m3/t	Total gas m3/t
Moisture (aa)	1.00									
Ash (db) %	-0.95	1.00								
Volatile Matter (daf)	-0.94	0.89	1.00							
Fixed carbon (daf)	0.94	-0.89	-1.00	1.00						
Calorific value (daf)	0.83	-0.85	-0.86	0.86	1.00					
Suggate number	-0.73	0.77	0.63	-0.63	-0.63	1.00				
Measured gas m3/t	0.59	-0.62	-0.64	0.64	0.56	-0.48	1.00			
Residual gas m3/t	0.30	-0.39	-0.19	0.19	0.45	-0.50	0.05	1.00		
Lost gas m3/t	0.17	-0.18	-0.25	0.25	0.08	-0.11	0.43	-0.20	1.00	
Total gas m3/t	0.64	-0.69	-0.66	0.66	0.63	-0.59	0.95	0.32	0.43	1.00

Ohai SC3	Inherent Moisture (aa)	Ash (db) %	Volatile Matter (daf)	Fixed carbon (daf)	Calorific value (daf)	Suggate number	Measured gas m3/t	Residual gas m3/t	Lost gas m3/t	Total gas m3/t
Moisture (aa)	1.00									
Ash (db) %	-0.82	1.00								
Volatile Matter (daf)	-0.77	0.75	1.00							
Fixed carbon (daf)	0.77	-0.75	-1.00	1.00						
Calorific value (daf)	0.24	-0.09	0.04	-0.04	1.00					
Suggate number	-0.08	0.19	-0.39	0.39	0.00	1.00				
Measured gas m3/t	0.58	-0.71	-0.46	0.47	0.03	-0.23	1.00			
Residual gas m3/t	-0.80	0.72	0.45	-0.46	0.00	0.53	-0.47	1.00		
Lost gas m3/t	-0.22	0.57	0.34	-0.33	-0.27	-0.01	-0.52	0.00	1.00	
Total gas m3/t	0.51	-0.62	-0.41	0.41	-0.01	-0.19	0.99	-0.39	-0.44	1.00

Ohai SC1	Inherent Moisture (aa)	Ash (db) %	Volatile Matter (daf)	Fixed carbon (daf)	Calorific value (daf)	Suggate number	Measured gas m3/t	Residual gas m3/t	Lost gas m3/t	Total gas m3/t
Moisture (aa)	1.00									
Ash (db) %	-0.48	1.00								
Volatile Matter (daf)	-0.47	0.78	1.00							
Fixed carbon (daf)	0.47	-0.78	-1.00	1.00						
Calorific value (daf)	0.15	-0.88	-0.78	0.78	1.00					
Suggate number	-0.12	-0.16	-0.58	0.58	0.48	1.00				
Measured gas m3/t	-0.14	-0.72	-0.70	0.70	0.90	0.54	1.00			
Residual gas m3/t	0.33	0.11	0.33	-0.33	-0.36	-0.26	-0.41	1.00		
Lost gas m3/t	-0.19	0.21	0.00	0.00	-0.27	-0.27	-0.14	-0.59	1.00	
Total gas m3/t	-0.14	-0.74	-0.71	0.71	0.88	0.51	0.99	-0.39	-0.06	1.00

Table 3 Charts showing correlation coefficients for ash constituents and gas volume

Huntly	SiO_2 %	Al_2O_3 %	Fe_2O_3 %	CaO %	MgO %	Na_2O %	K_2O %	TiO_2 %	Mn_3O_4 %	SO_3 %	P_2O_5 %	Measured gas m^3/t	Residual gas m^3/t	Lost gas m^3/t	Total gas m^3/t
SiO_2 %	1.00														
Al_2O_3 %	0.57	1.00													
Fe_2O_3 %	-0.59	-0.79	1.00												
CaO %	-0.70	-0.66	0.37	1.00											
MgO %	-0.54	-0.63	0.60	0.69	1.00										
Na_2O %	-0.56	-0.25	0.41	-0.08	-0.08	1.00									
K_2O %	0.26	0.10	-0.09	-0.41	-0.29	0.19	1.00								
TiO_2 %	0.28	0.48	-0.45	-0.43	-0.43	-0.20	0.03	1.00							
Mn_3O_4 %	-0.21	-0.35	0.04	0.72	0.25	-0.44	-0.37	-0.20	1.00						
SO_3 %	-0.64	-0.49	0.62	0.04	0.07	0.91	0.16	-0.24	-0.32	1.00					
P_2O_5 %	0.17	0.21	-0.25	0.01	-0.03	-0.33	-0.21	0.06	0.05	-0.32	1.00				
Measured gas m^3/t	0.02	-0.04	0.23	-0.04	0.02	-0.07	-0.16	-0.13	-0.02	0.07	0.06	1.00			
Residual gas m^3/t	-0.45	-0.33	0.22	0.32	0.35	0.26	0.00	0.00	0.03	0.25	0.04	-0.66	1.00		
Lost gas m^3/t	0.26	0.16	0.01	-0.15	0.00	-0.28	-0.09	-0.11	-0.02	-0.20	0.08	0.72	-0.64	1.00	
Total gas m^3/t	-0.52	-0.44	0.54	0.34	0.46	0.22	-0.20	-0.15	0.01	0.38	0.12	0.37	0.45	0.11	1.00

Ohai SC3	SiO_2 %	Al_2O_3 %	Fe_2O_3 %	CaO %	MgO %	Na_2O %	K_2O %	TiO_2 %	Mn_3O_4 %	SO_3 %	P_2O_5 %	Measured gas m^3/t	Residual gas m^3/t	Lost gas m^3/t	Total gas m^3/t
SiO_2 %	1.00														
Al_2O_3 %	0.72	1.00													
Fe_2O_3 %	-0.93	-0.74	1.00												
CaO %	-0.86	-0.67	0.76	1.00											
MgO %	-0.88	-0.71	0.78	0.94	1.00										
Na_2O %	-0.82	-0.68	0.79	0.48	0.53	1.00									
K_2O %	0.64	0.77	-0.62	-0.76	-0.66	-0.46	1.00								
TiO_2 %	0.79	0.89	-0.84	-0.65	-0.75	-0.78	0.64	1.00							
Mn_3O_4 %	-0.49	-0.26	0.59	0.68	0.52	0.13	-0.46	-0.32	1.00						
SO_3 %	-0.83	-0.73	0.83	0.48	0.56	0.96	-0.48	-0.81	0.10	1.00					
P_2O_5 %	-0.01	0.00	-0.12	0.12	-0.01	0.06	-0.25	0.08	0.06	-0.05	1.00				
Measured gas m^3/t	-0.71	-0.61	0.68	0.76	0.71	0.46	-0.76	-0.57	0.52	0.49	0.02	1.00			
Residual gas m^3/t	0.84	0.67	-0.78	-0.60	-0.57	-0.91	0.51	0.65	-0.23	-0.88	-0.07	-0.47	1.00		
Lost gas m^3/t	0.28	0.51	-0.29	-0.28	-0.34	-0.18	0.53	0.47	0.00	-0.30	-0.22	-0.52	0.00	1.00	
Total gas m^3/t	-0.48	-0.42	0.47	0.60	0.56	0.18	-0.58	-0.35	0.47	0.22	0.00	0.89	-0.24	-0.42	1.00

Ohai SC1	SiO_2 %	Al_2O_3 %	Fe_2O_3 %	CaO %	MgO %	Na_2O %	K_2O %	TiO_2 %	Mn_3O_4 %	SO_3 %	P_2O_5 %	Measured gas m^3/t	Residual gas m^3/t	Lost gas m^3/t	Total gas m^3/t
SiO_2 %	1.00														
Al_2O_3 %	0.25	1.00													
Fe_2O_3 %	-0.91	-0.18	1.00												
CaO %	-0.87	-0.63	0.70	1.00											
MgO %	-0.92	-0.55	0.82	0.98	1.00										
Na_2O %	-0.68	-0.73	0.53	0.78	0.71	1.00									
K_2O %	0.50	0.20	-0.46	-0.55	-0.57	-0.29	1.00								
TiO_2 %	0.54	0.86	-0.35	-0.78	-0.67	-0.93	0.18	1.00							
Mn_3O_4 %	-0.65	-0.35	0.85	0.53	0.65	0.47	-0.33	-0.32	1.00						
SO_3 %	-0.89	-0.64	0.78	0.93	0.92	0.91	-0.43	-0.84	0.68	1.00					
P_2O_5 %	-0.82	-0.51	0.90	0.75	0.83	0.72	-0.40	-0.59	0.94	0.89	1.00				
Measured gas m^3/t	-0.10	-0.69	-0.11	0.41	0.26	0.65	-0.13	-0.75	-0.16	0.40	0.08	1.00			
Residual gas m^3/t	-0.50	-0.06	0.58	0.33	0.43	0.24	-0.04	-0.12	0.65	0.44	0.61	-0.54	1.00		
Lost gas m^3/t	0.03	0.32	0.04	-0.05	0.02	-0.49	-0.07	0.38	-0.15	-0.28	-0.23	-0.14	-0.43	1.00	
Total gas m^3/t	-0.17	-0.71	-0.03	0.48	0.34	0.66	-0.16	-0.77	-0.12	0.45	0.13	0.99	-0.52	-0.05	1.00

Greymouth	SiO_2 %	Al_2O_3 %	Fe_2O_3 %	CaO %	MgO %	Na_2O %	K_2O %	TiO_2 %	Mn_3O_4 %	SO_3 %	P_2O_5 %	Measured gas m^3/t	Residual gas m^3/t	Lost gas m^3/t	Total gas m^3/t
SiO_2 %	1.00														
Al_2O_3 %	-0.60	1.00													
Fe_2O_3 %	-0.74	-0.06	1.00												
CaO %	-0.50	0.19	0.57	1.00											
MgO %	-0.30	0.09	0.19	-0.41	1.00										
Na_2O %	-0.72	0.25	0.70	0.72	-0.22	1.00									
K_2O %	-0.03	0.13	-0.18	-0.69	0.80	-0.51	1.00								
TiO_2 %	0.09	0.11	-0.20	0.14	-0.44	0.20	-0.42	1.00							
Mn_3O_4 %	-0.45	0.11	0.51	0.46	0.11	0.16	-0.15	-0.16	1.00						
SO_3 %	-0.23	-0.25	0.50	0.12	0.41	0.06	-0.07	-0.14	0.53	1.00					
P_2O_5 %	-0.21	0.10	0.18	0.31	-0.18	0.05	-0.19	-0.02	0.71	0.12	1.00				
Measured gas m^3/t	-0.19	0.27	0.06	0.33	-0.35	0.17	-0.36	0.08	0.36	0.10	0.48	1.00			
Residual gas m^3/t	-0.06	-0.29	0.29	0.28	-0.10	0.41	-0.41	0.27	-0.07	0.43	-0.24	0.16	1.00		
Lost gas m^3/t	-0.24	0.16	0.17	0.34	-0.15	0.05	-0.19	-0.06	0.74	0.13	0.99	0.51	-0.23	1.00	
Total gas m^3/t	-0.23	0.18	0.18	0.44	-0.34	0.29	-0.46	0.14	0.41	0.25	0.45	0.96	0.41	0.48	1.00

Table 4 Charts showing correlation coefficients for mineralogy and gas volume

Huntly	Quartz	Kaolinite	Calicite	Ankerite	Siderite	Pyrite	Muscavite	Measured gas	Residual gas	Lost gas	Total gas
Quartz	1.00										
Kaolinite	0.02	1.00									
Calicite	-0.17	-0.28	1.00								
Ankerite	-0.17	-0.28	1.00	1.00							
Siderite	-	-	-	-	1.00						
Pyrite	-	-	-	-	-	1.00					
Muscavite	-	-	-	-	-	-	1.00				
Measured gas	0.11	-0.10	-0.04	-0.04	-	-	-	1.00			
Residual gas	-0.42	-0.26	-0.22	-0.22	-	-	-	-0.74	1.00		
Lost gas	0.50	-0.10	-0.13	-0.13	-	-	-	0.90	-0.79	1.00	
Total gas	-0.48	-0.52	-0.39	-0.39	-	-	-	0.10	0.59	-0.07	1.00

Ohai SC3	Quartz	Kaolinite	Calicite	Ankerite	Siderite	Pyrite	Muscavite	Measured gas	Residual gas	Lost gas	Total gas
Quartz	1.00										
Kaolinite	0.52	1.00									
Calicite	-0.98	-0.53	1.00								
Ankerite	-0.91	-0.43	0.86	1.00							
Siderite	-0.60	-0.56	0.56	0.26	1.00						
Pyrite	-	-	-	-	-	1.00					
Muscavite	-	-	-	-	-	-	1.00				
Measured gas	-0.54	-0.67	0.67	0.45	0.27	-	-	1.00			
Residual gas	0.29	0.75	-0.28	-0.12	-0.60	-	-	-0.58	1.00		
Lost gas	-0.11	-0.23	0.11	-0.13	0.55	-	-	-0.09	-0.18	1.00	
Total gas	-0.57	-0.63	0.71	0.46	0.26	-	-	0.98	-0.47	0.02	1.00

Greymouth	Quartz	Kaolinite	Calicite	Ankerite	Siderite	Pyrite	Muscavite	Measured gas	Residual gas	Lost gas	Total gas
Quartz	1.00										
Kaolinite	-0.78	1.00									
Calicite	-	-	1.00								
Ankerite	-	-	-	1.00							
Siderite	-0.37	0.33	-	-	1.00						
Pyrite	-0.60	0.00	-	-	-0.12	1.00					
Muscavite	0.07	-0.25	-	-	-0.20	0.22	1.00				
Measured gas	-0.45	0.35	-	-	0.80	0.07	0.12	1.00			
Residual gas	-0.23	-0.09	-	-	-0.29	0.60	-0.25	-0.17	1.00		
Lost gas	-0.28	0.31	-	-	0.97	-0.24	-0.22	0.68	-0.46	1.00	
Total gas	-0.53	0.34	-	-	0.81	0.22	-0.04	0.95	0.10	0.65	1.00

Ohai SC1	Quartz	Kaolinite	Calicite	Ankerite	Siderite	Pyrite	Muscavite	Measured gas	Residual gas	Lost gas	Total gas
Quartz	1.00										
Kaolinite	0.41	1.00									
Calicite	-	-	1.00								
Ankerite	-0.91	-0.71	-	1.00							
Siderite	-0.86	0.00	-	0.58	1.00						
Pyrite	-	-	-	-	-	1.00					
Muscavite	-	-	-	-	-	-	1.00				
Measured gas	-0.12	-0.23	-	0.00	0.36	-	-	1.00			
Residual gas	-0.86	0.00	-	0.58	1.00	-	-	0.36	1.00		
Lost gas	0.86	0.60	-	-0.80	-0.78	-	-	-0.58	-0.78	1.00	
Total gas	-0.05	-0.12	-	-0.10	0.34	-	-	0.99	0.34	-0.50	1.00

Table 5 Charts showing correlation coefficients for organic petrology and gas volume

Greymouth	Cell Tel	Band Tel	Large Tel	Des	V-d	Spor	Cu	Res	L-d	Sub	Fl	S-Fus	Fus	l-d	Scel	S	Qtz
Cell Tel	1.00																
Band Tel	0.10	1.00															
Large Tel	-0.11	-0.85	1.00														
Des	-0.04	0.70	-0.96	1.00													
V-d	-0.17	0.74	-0.87	0.86	1.00												
Spor	0.03	-0.62	0.51	-0.51	-0.49	1.00											
Cu	0.75	0.46	-0.48	0.32	0.14	0.12	1.00										
Res	-0.44	-0.44	0.47	-0.41	-0.42	0.60	-0.28	1.00									
L-d	-0.07	0.17	-0.16	0.17	0.24	-0.73	-0.44	-0.51	1.00								
Sub	-0.30	-0.46	0.73	-0.78	-0.66	0.44	-0.32	0.32	-0.21	1.00							
Fl	-0.21	-0.42	0.29	-0.19	0.07	0.54	-0.18	0.15	-0.48	0.14	1.00						
S-Fus	0.39	0.43	-0.68	0.74	0.45	-0.63	0.36	-0.70	0.37	-0.73	-0.37	1.00					
Fus	0.41	0.03	0.00	-0.11	-0.21	-0.03	0.15	0.21	0.30	-0.26	-0.62	0.00	1.00				
l-d	-0.13	0.30	-0.07	0.05	-0.16	-0.63	-0.10	-0.19	0.36	0.18	-0.74	0.29	0.01	1.00			
Scel	0.88	-0.11	-0.06	-0.01	-0.14	0.27	0.63	-0.13	-0.22	-0.46	0.04	0.27	0.48	-0.48	1.00		
S	-0.35	-0.30	0.38	-0.26	-0.39	-0.35	-0.54	-0.14	0.36	0.45	-0.22	0.10	-0.35	0.72	-0.58	1.00	
Qtz	-0.46	-0.56	0.33	-0.20	-0.05	0.76	-0.33	0.55	-0.45	0.23	0.77	-0.55	-0.29	-0.73	-0.09	-0.27	1.00
clay	-0.50	-0.36	0.27	-0.21	0.14	0.54	-0.44	0.33	-0.19	0.28	0.77	-0.62	-0.32	-0.73	-0.24	-0.29	0.88
Cbn	-0.21	-0.54	0.47	-0.43	-0.30	0.61	-0.35	0.76	-0.16	0.12	0.25	-0.66	0.48	-0.58	0.17	-0.41	0.64
Fe-O	-0.03	-0.28	0.64	-0.71	-0.65	-0.02	-0.24	-0.07	0.08	0.83	-0.14	-0.35	-0.20	0.54	-0.37	0.70	-0.29
Total Vit	0.00	0.61	-0.67	0.73	0.76	-0.73	0.09	-0.54	0.27	-0.72	0.02	0.67	-0.30	0.13	-0.03	-0.03	-0.38
Total Lip	-0.04	-0.40	0.65	-0.77	-0.71	0.57	-0.04	0.38	-0.28	0.91	-0.04	-0.72	0.08	0.08	-0.18	0.17	0.18
Total Int	0.60	0.31	-0.33	0.27	-0.06	-0.52	0.40	-0.35	0.40	-0.47	-0.82	0.67	0.62	0.51	0.43	0.08	-0.81
Total MM	-0.50	-0.59	0.41	-0.29	-0.09	0.74	-0.42	0.56	-0.38	0.31	0.76	-0.63	-0.28	-0.71	-0.16	-0.22	0.99
Measured gas	-0.12	-0.09	0.39	-0.38	-0.36	-0.17	-0.14	-0.13	-0.16	0.54	0.10	-0.12	-0.60	0.54	-0.41	0.68	-0.29
Residual gas	0.42	0.82	-0.81	0.68	0.59	-0.29	0.77	-0.24	-0.21	-0.67	-0.27	0.47	0.17	0.00	0.38	-0.60	-0.42
Lost gas	0.02	-0.29	0.65	-0.72	-0.67	-0.05	-0.25	-0.08	0.14	0.79	-0.19	-0.33	-0.13	0.55	-0.32	0.69	-0.33
Total gas	0.05	0.14	0.21	-0.27	-0.26	-0.26	0.09	-0.22	-0.18	0.43	-0.05	-0.02	-0.49	0.60	-0.29	0.55	-0.48

Huntly	Cell Tel	Band Tel	Large Tel	Des	V-d	Spor	Cu	Res	L-d	Sub	Fl	S-Fus	Fus	l-d	Scel	S	Qtz
Cell Tel	1.00																
Band Tel	-0.19	1.00															
Large Tel	-0.48	-0.22	1.00														
Des	-0.30	-0.49	0.12	1.00													
V-d	0.58	0.27	-0.55	-0.61	1.00												
Spor	-0.25	-0.04	-0.27	-0.17	-0.20	1.00											
Cu	0.49	-0.08	0.04	-0.59	0.52	-0.25	1.00										
Res	-0.53	0.03	-0.27	0.37	-0.51	0.72	-0.59	1.00									
L-d	-0.39	0.09	-0.37	-0.09	-0.15	0.94	-0.30	0.84	1.00								
Sub	-0.62	0.24	0.49	0.16	-0.55	-0.03	0.03	0.21	0.04	1.00							
Fl	-0.04	-0.08	0.07	-0.32	0.15	0.40	-0.27	-0.02	0.27	-0.60	1.00						
S-Fus	-0.59	0.02	-0.13	0.19	-0.30	0.56	-0.40	0.83	0.74	0.04	0.18	1.00					
Fus	-0.05	0.61	-0.32	-0.23	0.48	-0.11	-0.08	-0.19	-0.03	0.12	-0.08	-0.35	1.00				
l-d	0.52	-0.81	0.01	0.10	0.31	-0.19	0.36	-0.44	-0.30	-0.62	0.27	-0.24	-0.37	1.00			
Scel	-0.24	-0.16	-0.23	-0.15	0.07	0.84	-0.13	0.44	0.79	-0.08	0.46	0.35	0.19	0.08	1.00		
S	-0.32	0.12	-0.54	0.07	-0.11	0.87	-0.42	0.86	0.95	0.01	0.14	0.66	0.14	-0.33	0.75	1.00	
Qtz	-0.21	-0.05	-0.12	0.51	0.09	-0.28	-0.63	0.03	-0.15	-0.39	0.27	0.15	0.28	0.17	-0.05	0.00	1.00
clay	0.29	0.58	-0.32	-0.21	0.50	-0.47	-0.21	-0.37	-0.40	-0.45	0.19	-0.28	0.48	-0.17	-0.45	-0.28	0.51
Cbn	-0.31	-0.61	0.36	0.55	-0.40	0.15	-0.56	0.12	0.06	-0.22	0.54	0.12	-0.19	0.42	0.35	0.06	0.56
Fe-O	-0.27	0.14	-0.26	0.02	-0.30	0.52	-0.06	0.77	0.65	0.24	-0.26	0.77	-0.42	-0.41	0.11	0.58	-0.38
Total Vit	0.32	0.09	0.35	0.09	0.07	-0.92	0.16	-0.76	-0.97	0.04	-0.29	-0.75	0.12	0.09	-0.83	-0.90	0.15
Total Lip	-0.36	0.07	-0.31	-0.16	-0.15	0.91	-0.10	0.79	0.97	0.16	0.12	0.71	-0.09	-0.30	0.74	0.89	-0.35
Total Int	-0.05	-0.55	-0.21	0.03	0.15	0.60	-0.02	0.30	0.58	-0.42	0.51	0.43	-0.18	0.56	0.81	0.52	0.15
Total MM	-0.26	0.21	-0.36	0.32	-0.06	0.19	-0.81	0.51	0.33	-0.43	0.41	0.56	0.06	-0.19	0.06	0.42	0.74
Measured gas	0.43	-0.26	-0.07	0.05	-0.06	-0.23	0.17	-0.04	-0.24	-0.39	-0.06	0.16	-0.77	0.30	-0.57	-0.31	-0.14
Residual gas	0.12	0.11	0.06	-0.47	0.37	0.10	0.44	-0.42	-0.02	0.21	0.04	-0.57	0.60	0.05	0.45	-0.03	-0.32
Lost gas	0.18	-0.23	-0.12	0.02	-0.01	0.00	0.11	0.20	0.08	-0.40	0.08	0.52	-0.76	0.27	-0.30	-0.04	-0.04
Total gas	0.70	-0.16	0.01	-0.65	0.49	-0.11	0.86	-0.67	-0.31	-0.17	0.00	-0.64	-0.04	0.44	0.00	-0.41	-0.64

Ohai SC3	Cell Tel	Band Tel	Large Tel	Des	V-d	Spor	Cu	Res	L-d	Sub	Fl	S-Fus	Fus	l-d	Scel	S	Qtz
Cell Tel	1.00																
Band Tel	0.71	1.00															
Large Tel	-0.36	-0.38	1.00														
Des	-0.36	-0.27	-0.66	1.00													
V-d	0.16	0.05	-0.77	0.60	1.00												
Spor	-0.07	-0.15	0.67	-0.61	-0.59	1.00											
Cu	0.10	0.41	-0.08	-0.35	0.06	0.04	1.00										
Res	0.59	0.28	0.29	-0.83	-0.40	0.39	0.34	1.00									
L-d	0.67	0.11	0.00	-0.47	-0.15	0.18	-0.07	0.84	1.00								
Sub	0.42	0.03	0.42	-0.63	-0.24	-0.03	-0.05	0.63	0.58	1.00							
Fl	-	-	-	-	-	-	-	-	-	-	1.00						
S-Fus	-0.28	-0.18	0.82	-0.62	-0.77	0.80	-0.09	0.31	0.04	0.11	-	1.00					
Fus	-0.52	-0.21	-0.03	0.26	0.38	-0.20	0.07	-0.46	-0.57	-0.25	-	0.11	1.00				
l-d	-0.86	-0.64	0.18	0.48	-0.03	0.02	-0.01	-0.66	-0.68	-0.50	-	-0.03	0.19	1.00			
Scel	-0.35	-0.77	0.06	0.40	0.01	-0.26	-0.48	-0.15	0.19	0.17	-	-0.25	-0.21	0.43	1.00		
S	-	-	-	-	-	-	-	-	-	-	-	-	-	-	-	1.00	
Qtz	0.46	0.31	0.42	-0.87	-0.62	0.64	0.33	0.92	0.68	0.41	-	0.56	-0.45	-0.55	-0.32	-	1.00
clay	0.27	0.33	0.59	-0.81	-0.73	0.82	0.11	0.58	0.29	0.18	-	0.78	-0.33	-0.38	-0.54	-	0.82
Cbn	-0.61	-0.64	0.01	0.57	-0.13	-0.35	-0.52	-0.42	-0.15	-0.16	-	-0.05	0.11	0.49	0.78	-	-0.44
Fe-O	-	-	-	-	-	-	-	-	-	-	-	-	-	-	-	-	-
Total Vit	-0.09	0.12	-0.74	0.89	0.67	-0.69	-0.27	-0.82	-0.54	-0.55	-	-0.70	0.25	0.24	0.05	-	-0.86
Total Lip	0.52	0.20	0.41	-0.88	-0.37	0.40	0.39	0.96	0.75	0.73	-	0.31	-0.40	-0.55	-0.13	-	0.86
Total Int	-0.93	-0.80	0.61	0.11	-0.36	0.34	-0.21	-0.37	-0.46	-0.22	-	0.54	0.43	0.73	0.37	-	-0.22
Total MM	0.38	0.27	0.51	-0.87	-0.72	0.70	0.23	0.86	0.61	0.36	-	0.67	-0.45	-0.50	-0.33	-	0.99
Measured gas	-0.49	-0.30	0.18	0.42	-0.01	-0.28	-0.62	-0.75	-0.65	-0.08	-	0.04	0.36	0.40	0.21	-	-0.69
Residual gas	0.09	0.17	0.45	-0.77	-0.48	0.56	0.49	0.73	0.37	0.24	-	0.68	0.12	-0.39	-0.43	-	0.82
Lost gas	0.50	0.09	0.24	-0.33	-0.43	0.31	-0.38	0.39	0.54	0.41	-	0.06	-0.90	-0.25	0.23	-	0.40
Total gas	-0.45	-0.28	0.34	0.25	-0.19	-0.14	-0.64	-0.62	-0.56	0.03	-	0.21	0.29	0.32	0.17	-	-0.53

Ohai SC1	Cell Tel	Band Tel	Large Tel	Des	V-d	Spor	Cu	Res	L-d	Sub	Fl	S-Fus	Fus	l-d	Scel	S	Qtz
Cell Tel	1.00																
Band Tel	0.61	1.00															
Large Tel	-0.99	-0.49	1.00														
Des	0.68	-0.12	-0.79	1.00													
V-d	0.62	-0.09	-0.74	0.97	1.00												
Spor	-0.62	-0.94	0.48	0.15	0.21	1.00											
Cu	0.89	0.90	-0.82	0.30	0.29	-0.87	1.00										
Res	-0.55	0.17	0.68	-0.95	-1.00	-0.30	-0.20	1.00									
L-d	0.20	0.90	-0.06	-0.55	-0.51	-0.85	0.62	0.56	1.00								
Sub	0.36	0.95	-0.21	-0.41	-0.38	-0.91	0.74	0.44	0.99	1.00							
Fl	-	-	-	-	-	-	-	-	-	-	1.00						
S-Fus	0.18	-0.64	-0.33	0.84	0.81	0.65	-0.27	-0.84	-0.92	-0.84	-	1.00					
Fus	0.23	-0.52	-0.28	0.58	0.38	0.27	-0.17	-0.37	-0.71	-0.65	-	0.70	1.00				
l-d	-0.22	-0.90	0.09	0.47	0.38	0.77	-0.63	-0.42	-0.97	-0.97	-	0.85	0.82	1.00			
Scel	-0.06	0.06	-0.03	0.14	0.39	0.29	0.01	-0.43	0.02	0.01	-	0.11	-0.63	-0.24	1.00		
S	-	-	-	-	-	-	-	-	-	-	-	-	-	-	-	1.00	
Qtz	0.21	0.82	-0.04	-0.57	-0.61	-0.90	0.58	0.68	0.94	0.93	-	-0.90	-0.45	-0.83	-0.33	-	1.00
clay	0.87	0.91	-0.78	0.24	0.20	-0.92	0.99	-0.11	0.65	0.76	-	-0.32	-0.13	-0.63	-0.11	-	0.65
Cbn	-0.11	-0.84	-0.02	0.56	0.45	0.71	-0.54	-0.49	-0.97	-0.94	-	0.88	0.86	0.99	-0.26	-	-0.82
Fe-O	0.81	0.10	-0.84	0.82	0.65	-0.25	0.50	-0.60	-0.30	-0.15	-	0.55	0.75	0.35	-0.41	-	-0.14
Total Vit	-0.73	-0.88	0.60	-0.02	0.08	0.98	-0.90	-0.17	-0.72	-0.81	-	0.49	0.09	0.64	0.37	-	-0.81
Total Lip	0.19	0.86	-0.03	-0.59	-0.59	-0.88	0.59	0.65	0.98	0.97	-	-0.93	-0.60	-0.92	-0.16	-	0.98
Total Int	0.07	-0.74	-0.19	0.68	0.56	0.61	-0.39	-0.59	-0.93	-0.88	-	0.92	0.91	0.96	-0.27	-	-0.78
Total MM	0.84	0.90	-0.73	0.17	0.10	-0.95	0.97	-0.01	0.68	0.78	-	-0.38	-0.10	-0.63	-0.22	-	0.71
Measured gas	0.55	0.03	-0.52	0.44	0.20	-0.32	0.31	-0.14	-0.20	-0.10	-	0.29	0.82	0.36	-0.82	-	0.10
Residual gas	-0.23	-0.24	0.11	0.19	0.42	0.56	-0.25	-0.48	-0.26	-0.28	-	0.32	-0.44	0.04	0.95	-	-0.58
Lost gas	-0.50	-0.99	0.38	0.25	0.21	0.93	-0.84	-0.28	-0.95	-0.98	-	0.74	0.59	0.94	-0.06	-	-0.87
Total gas	0.49	-0.17	-0.49	0.56	0.33	-0.10	0.16	-0.29	-0.42	-0.32	-	0.49	0.93	0.55	-0.74	-	-0.13

Appendix K: Graphs of correlations (from correlation charts)

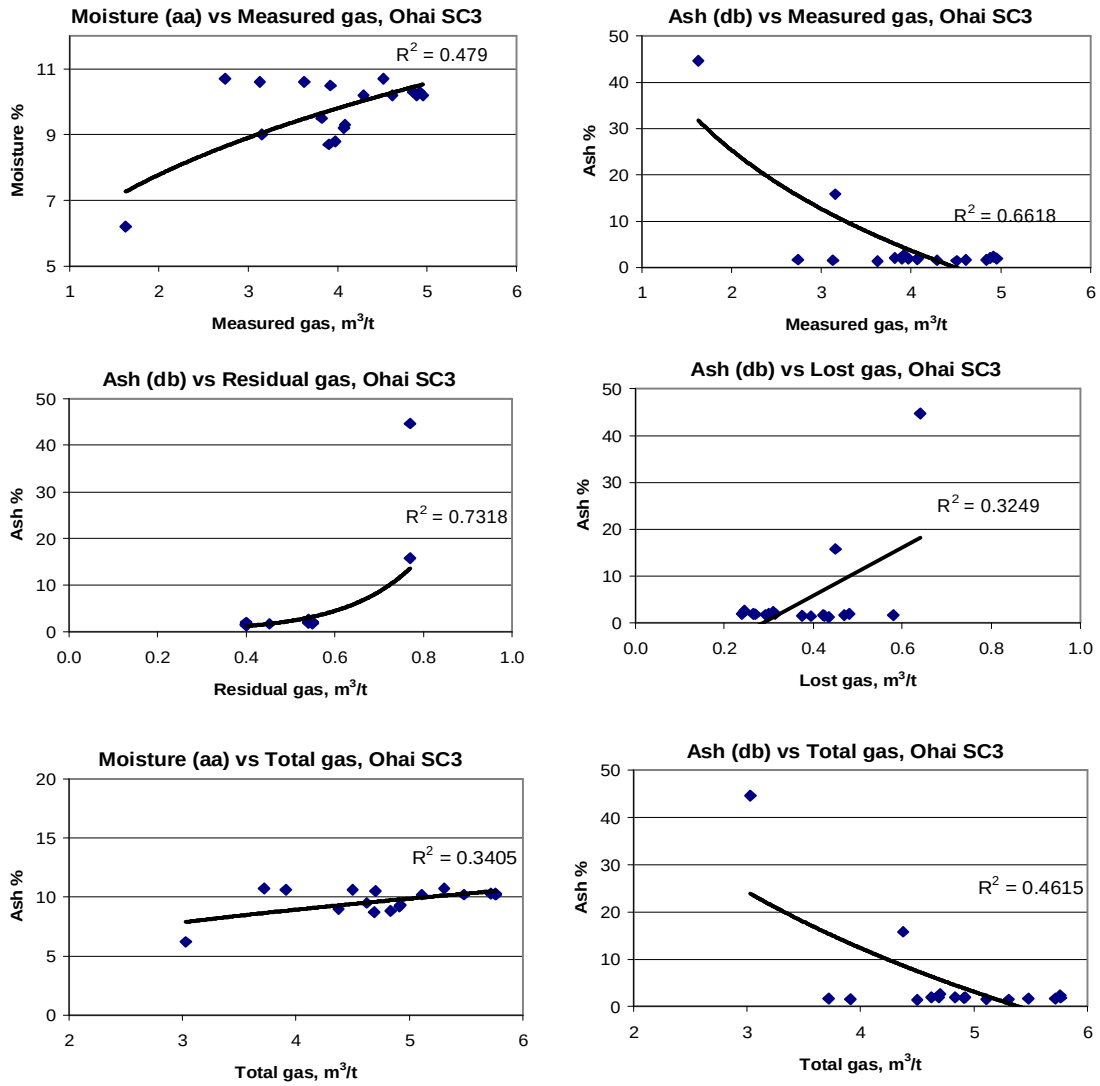

Figure 1: Ohai SC3 significant correlations with gas and proximate data, based on correlation chart.

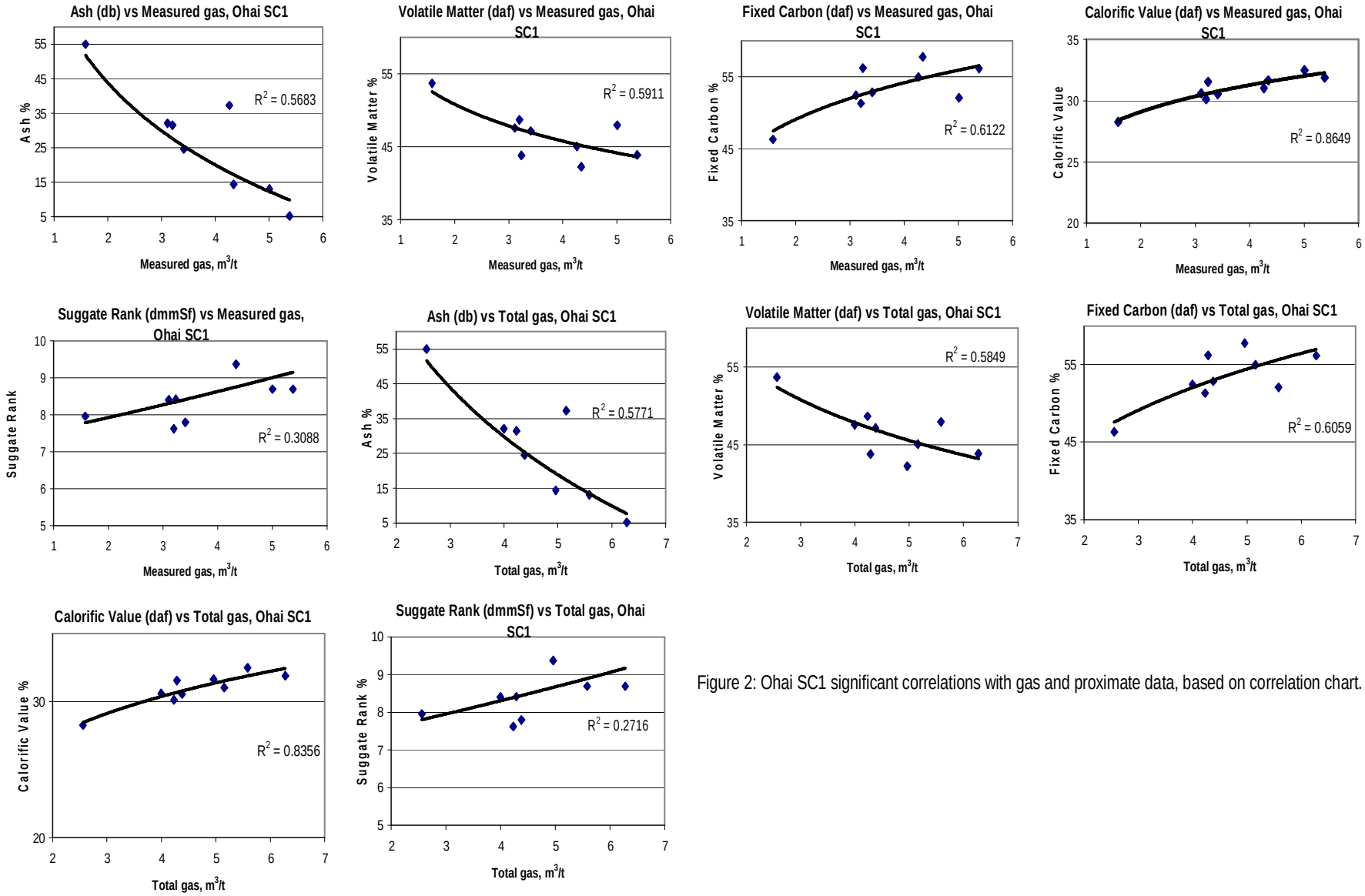

Figure 2: Ohai SC1 significant correlations with gas and proximate data, based on correlation chart.

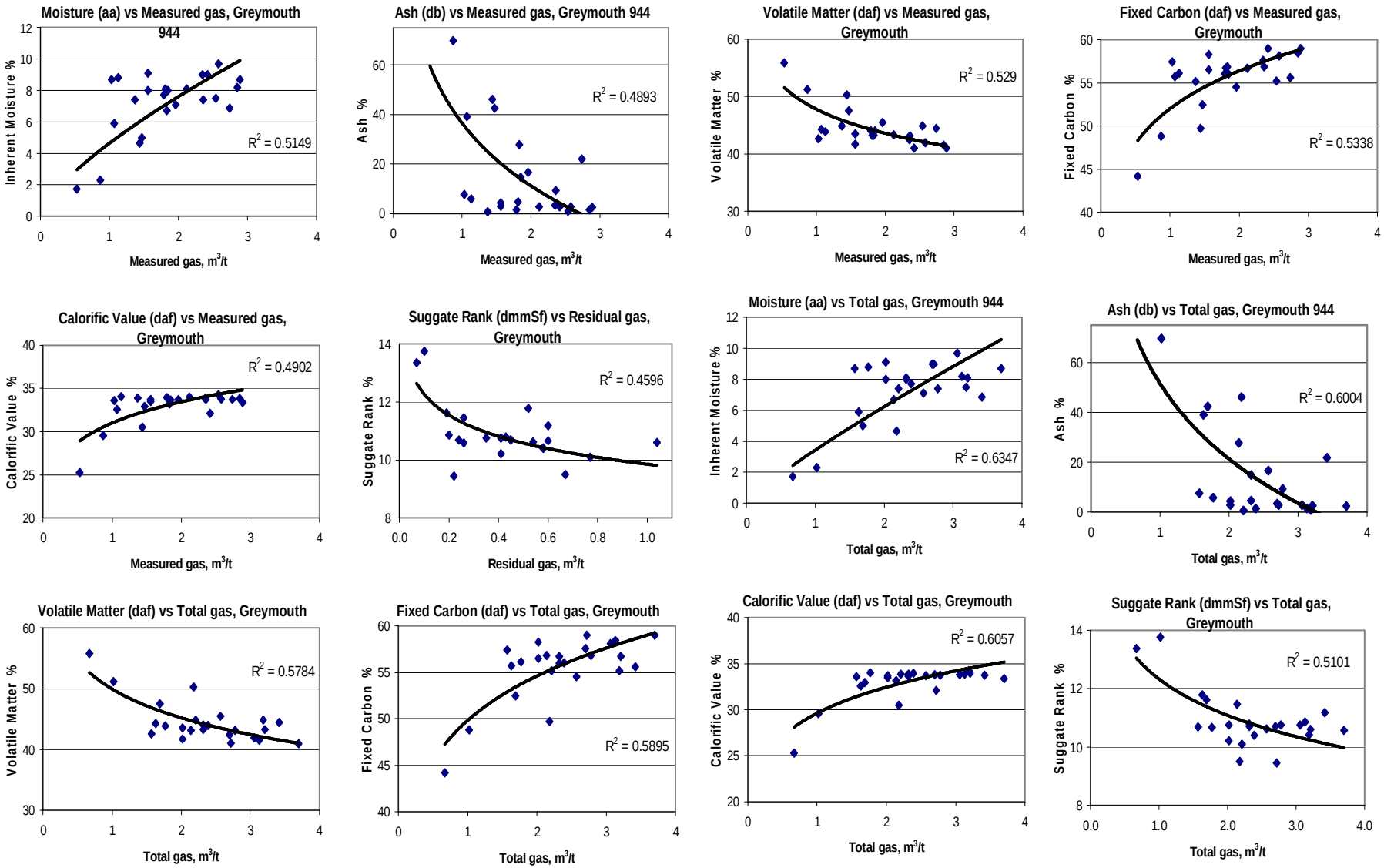

Figure 3: Greymouth 944 significant correlations with gas and proximate data, based on correlation chart.

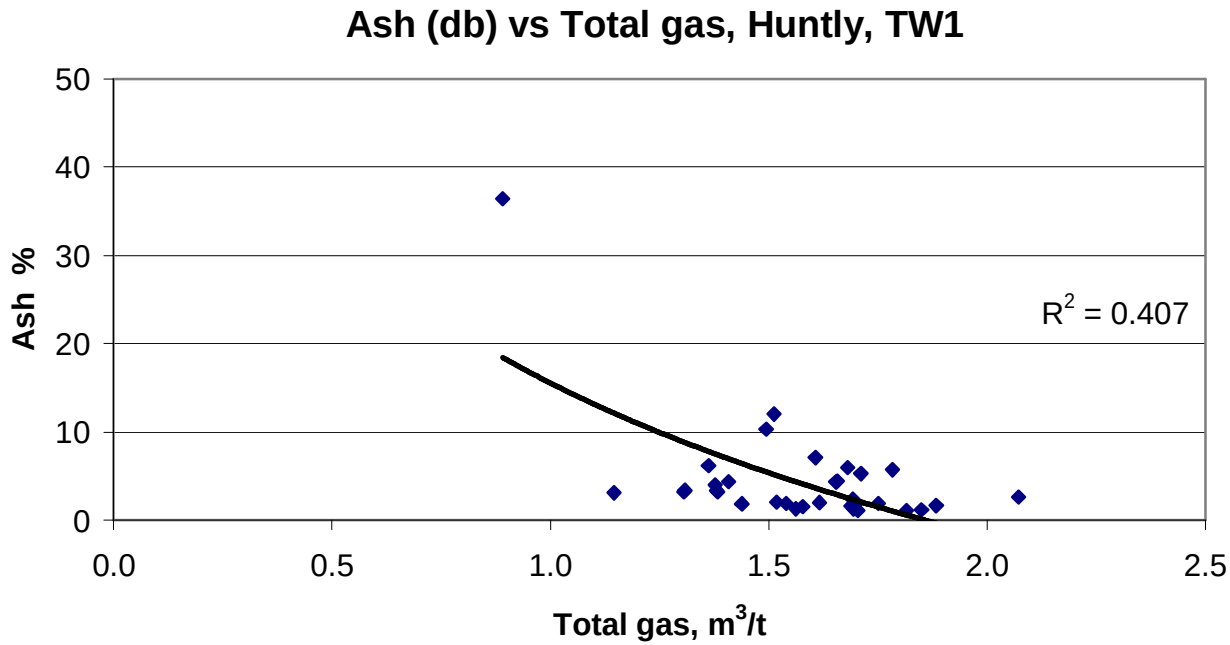

Figure 4: Huntly TW1 significant correlations with gas and proximate data, based on correlation chart.

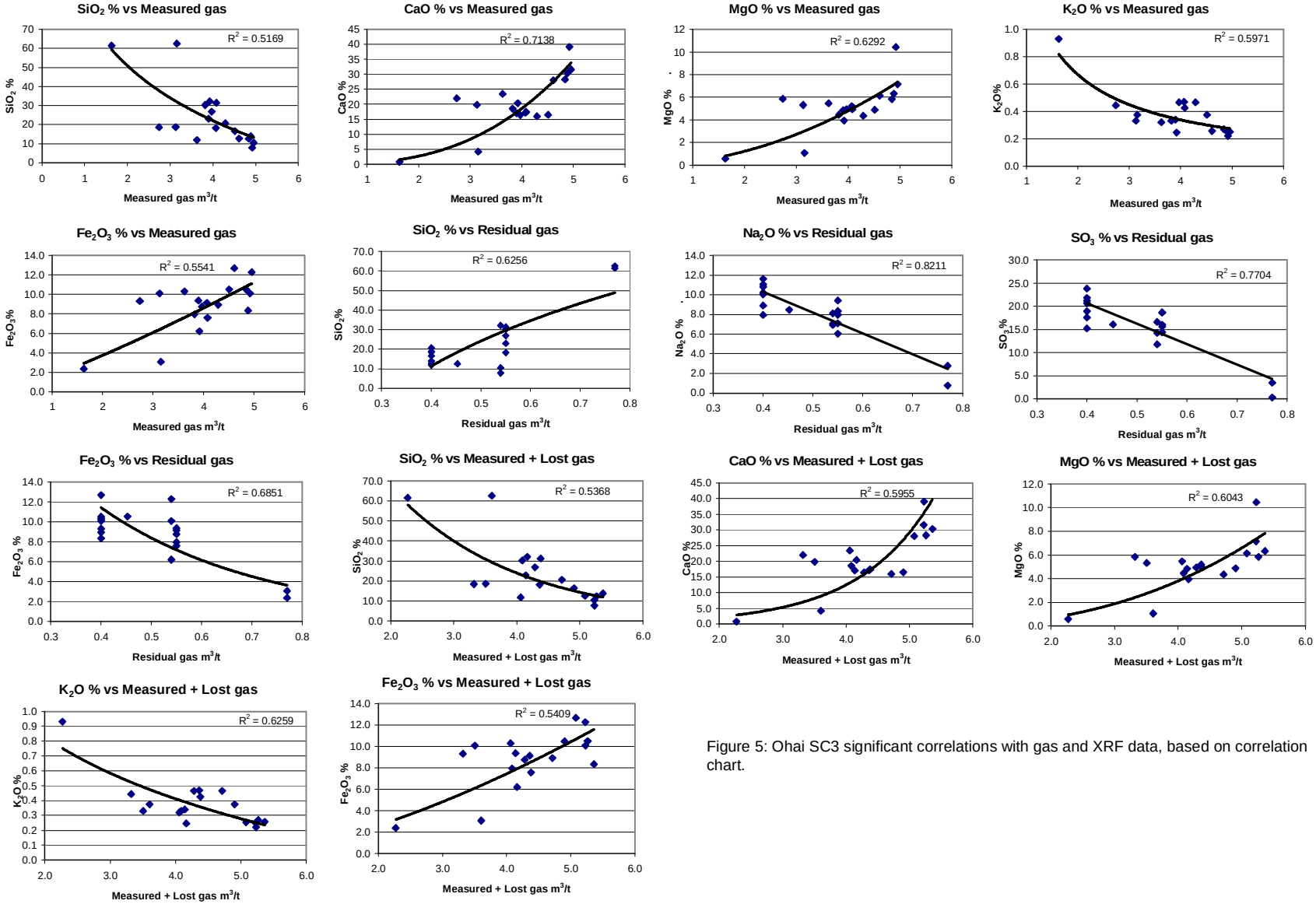

Figure 5: Ohai SC3 significant correlations with gas and XRF data, based on correlation chart.

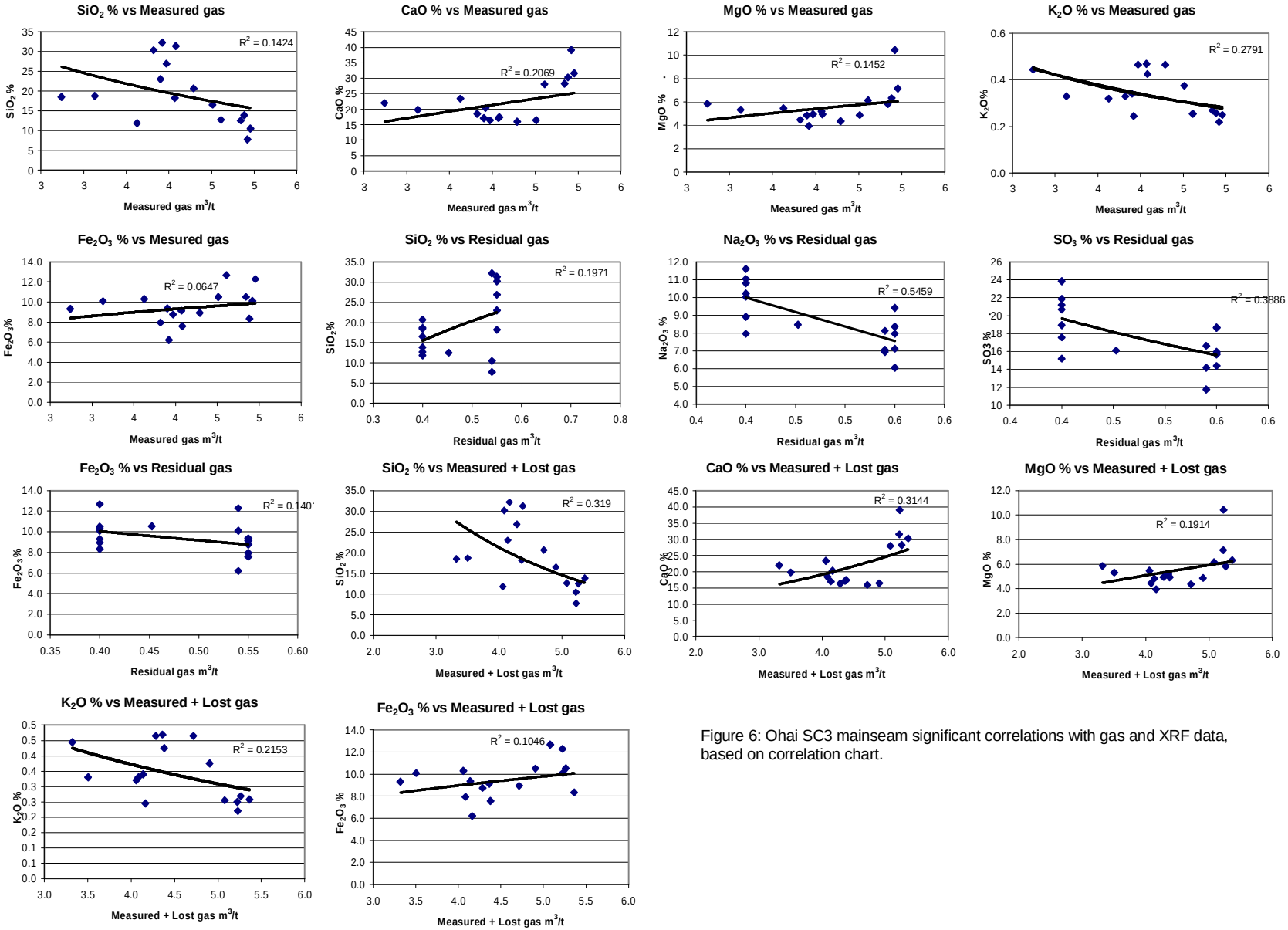

Figure 6: Ohai SC3 mainseam significant correlations with gas and XRF data, based on correlation chart.

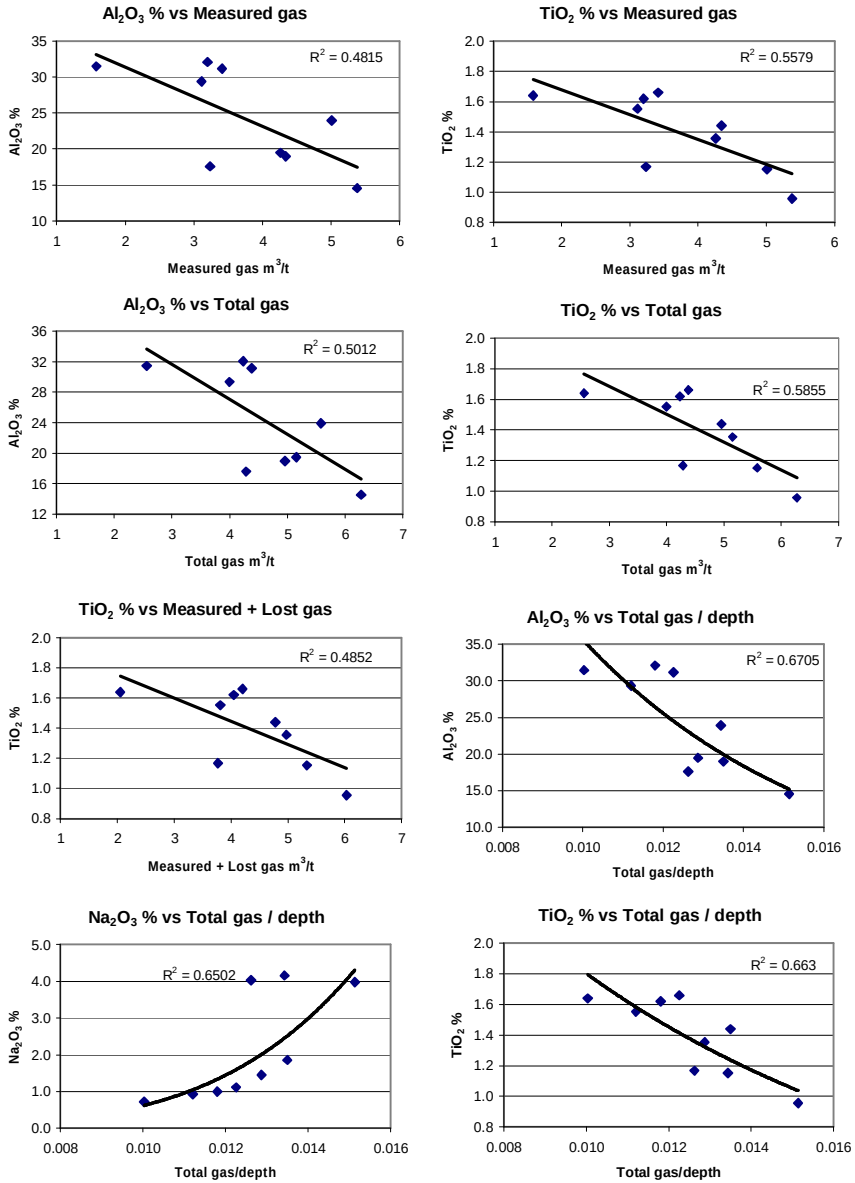

Figure 7: Ohai SC1 significant correlations with gas and XRF data, based on correlation chart.

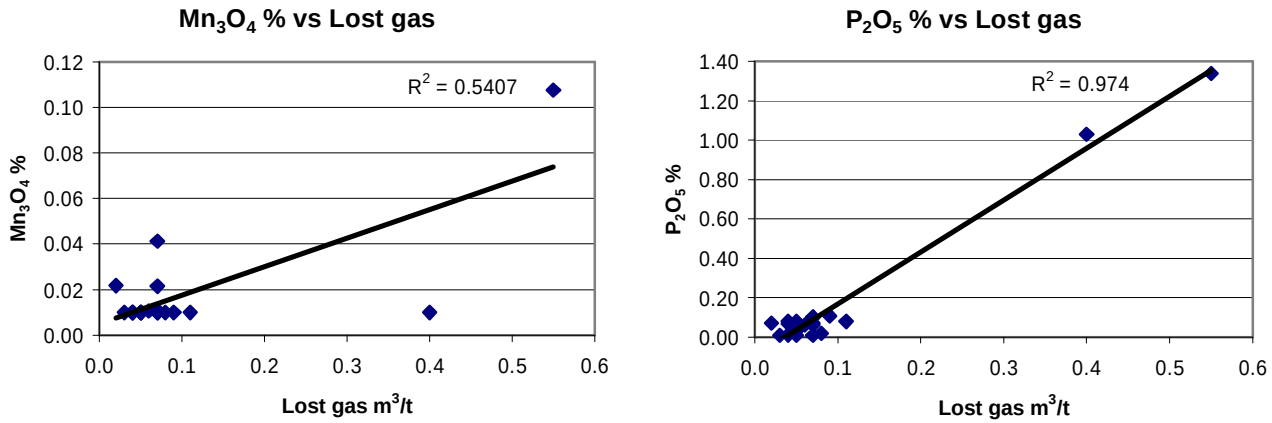

Figure 8: Greymouth 944 significant correlations with gas and XRF data, based on correlation chart.

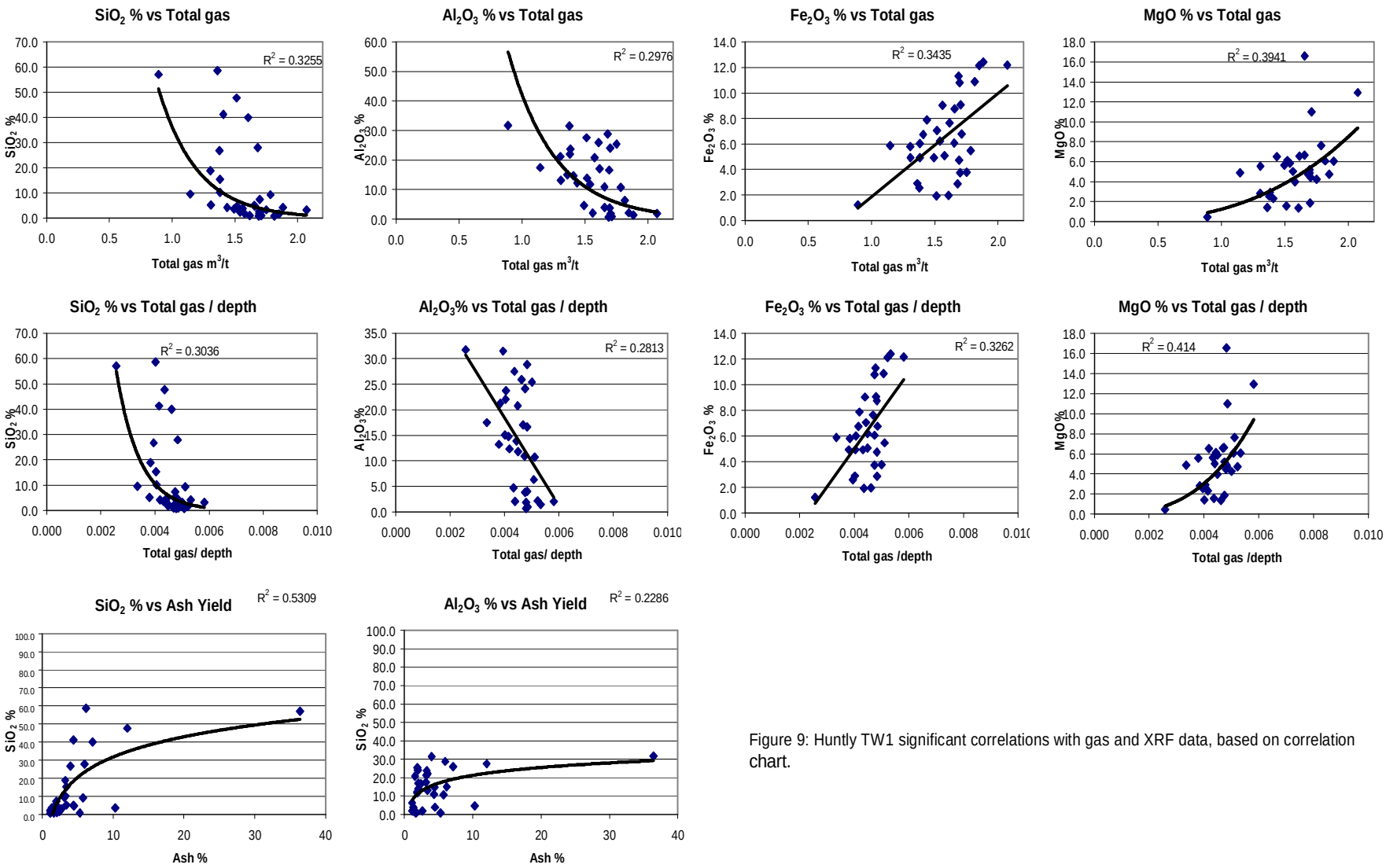

Figure 9: Huntly TW1 significant correlations with gas and XRF data, based on correlation chart.

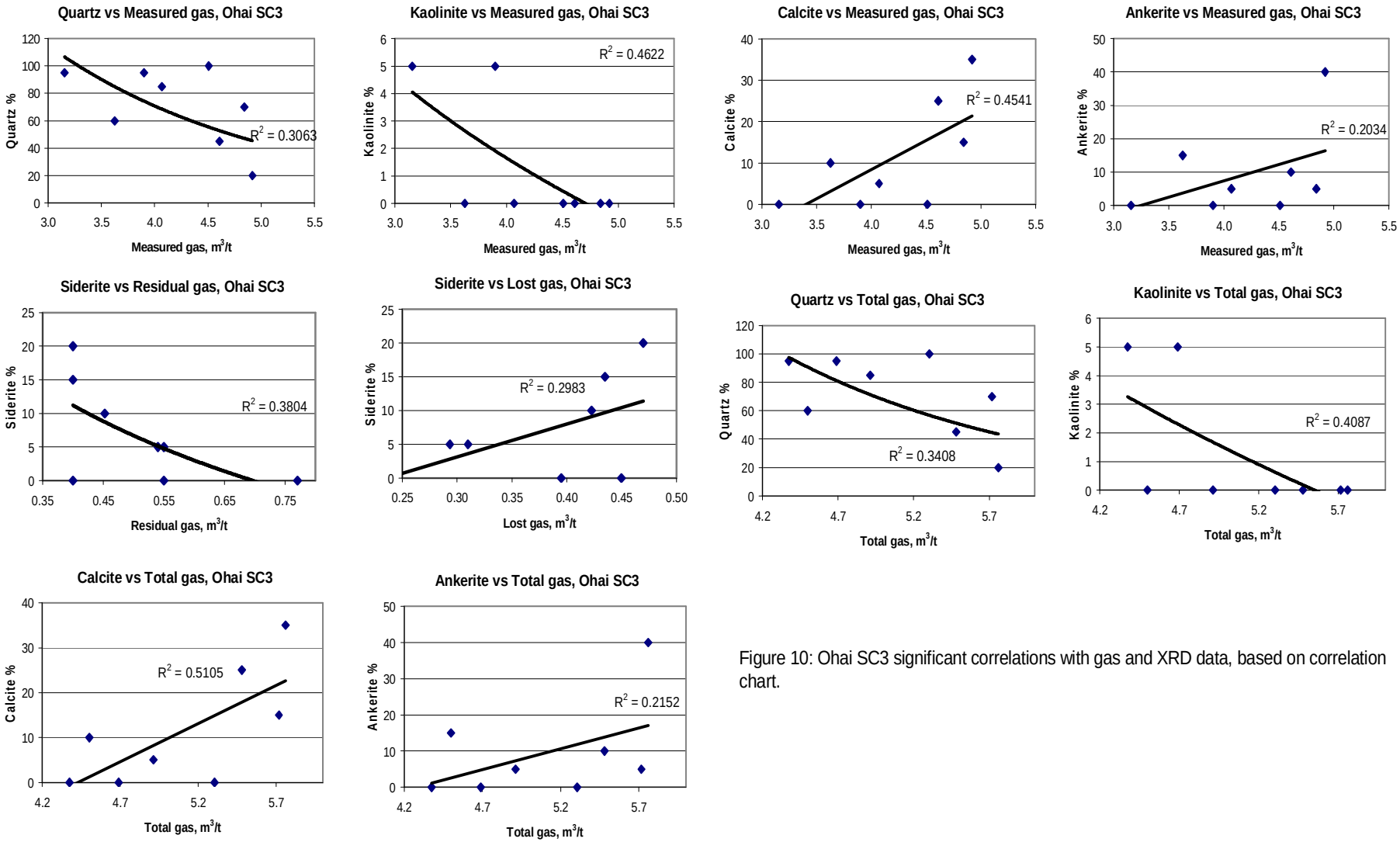

Figure 10: Ohai SC3 significant correlations with gas and XRD data, based on correlation chart.

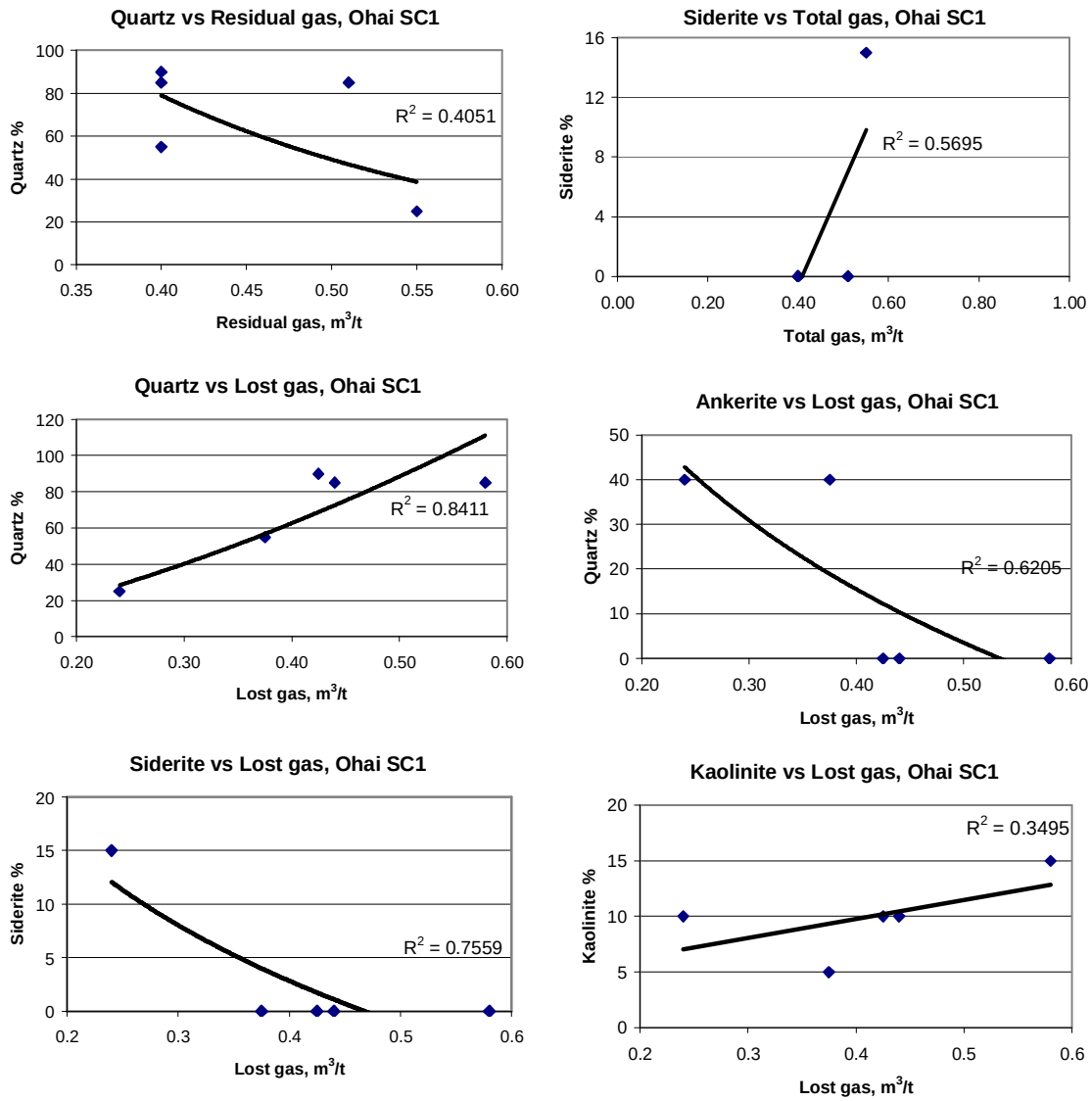

Figure 11: Ohai SC1 significant correlations with gas and XRD data, based on correlation chart.

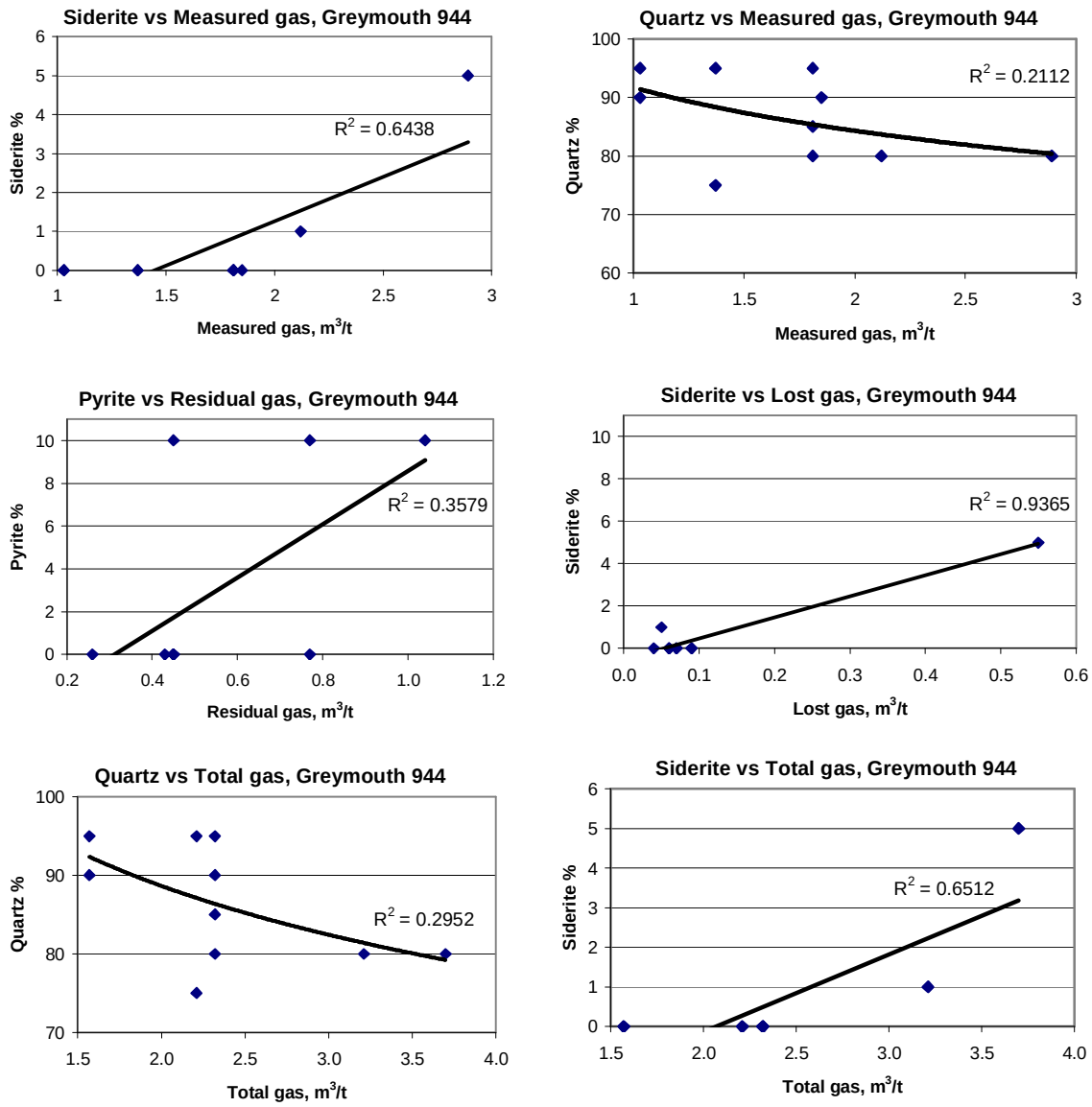

Figure 12: Greymouth 944 significant correlations with gas and XRD data, based on correlation chart.

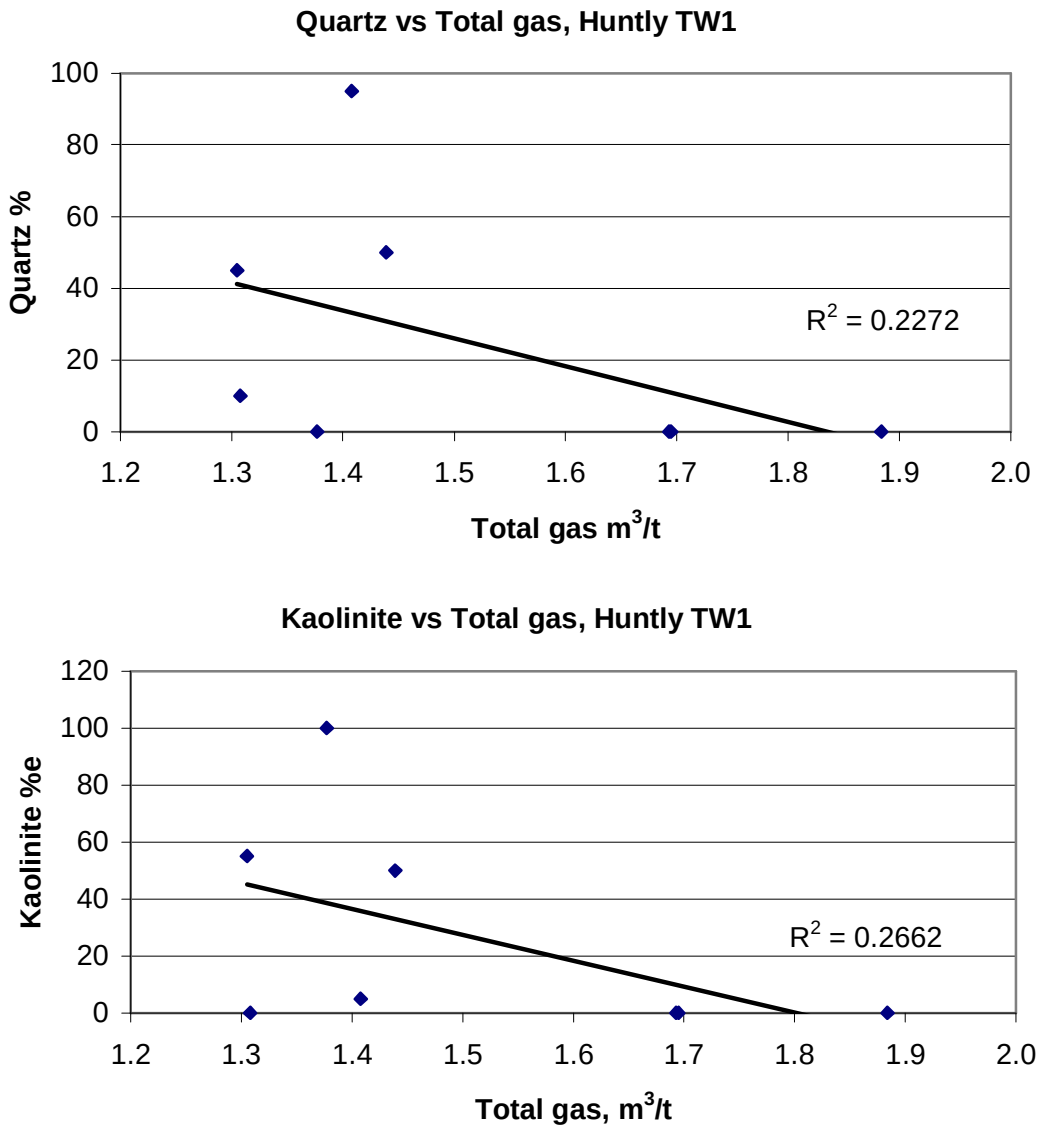

Figure 13: Huntly TW1 significant correlations with gas and XRD data, based on correlation chart.

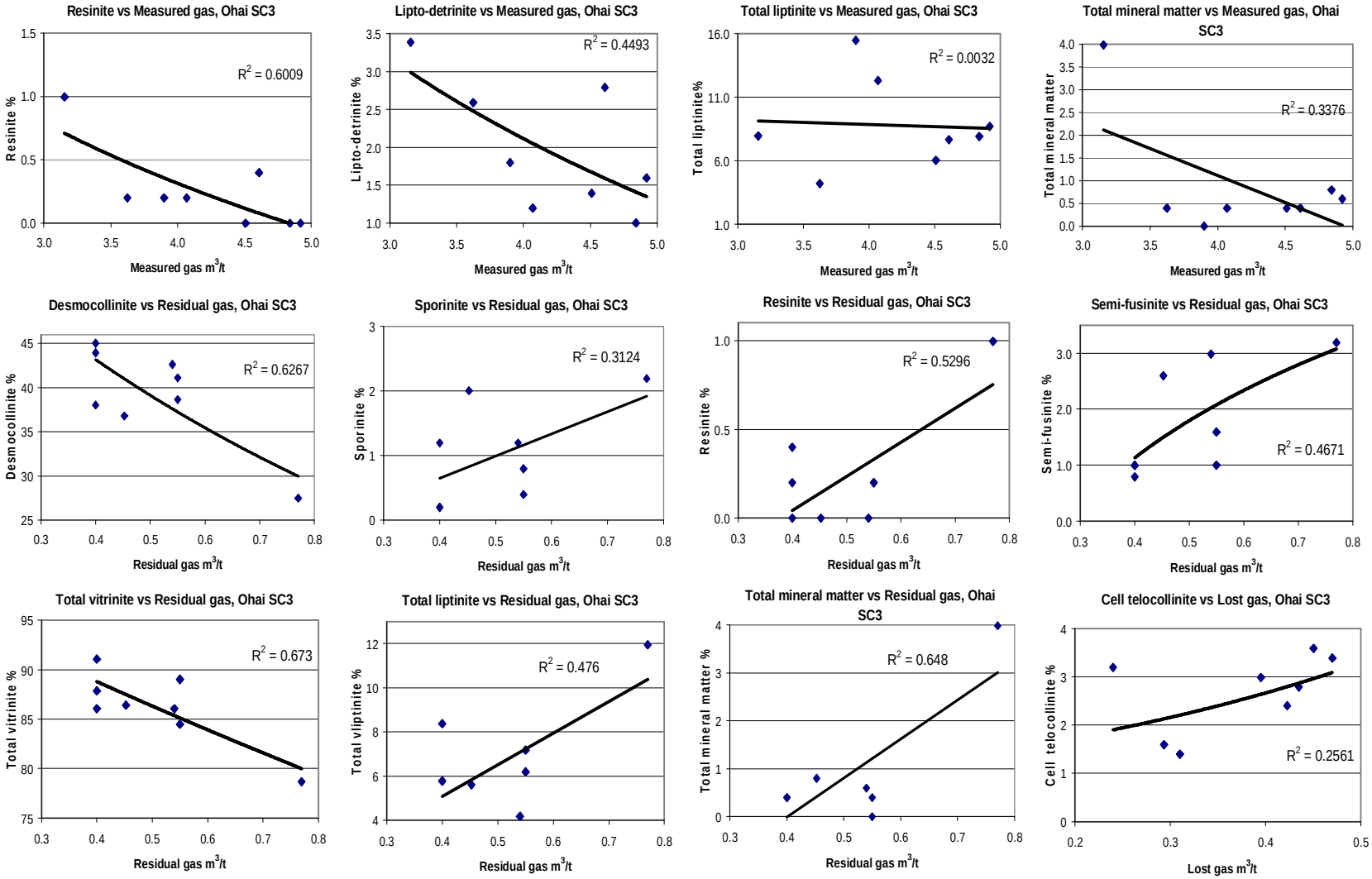

Figure 14: Ohai SC3 significant correlations with gas and maceral data, based on correlation charts.

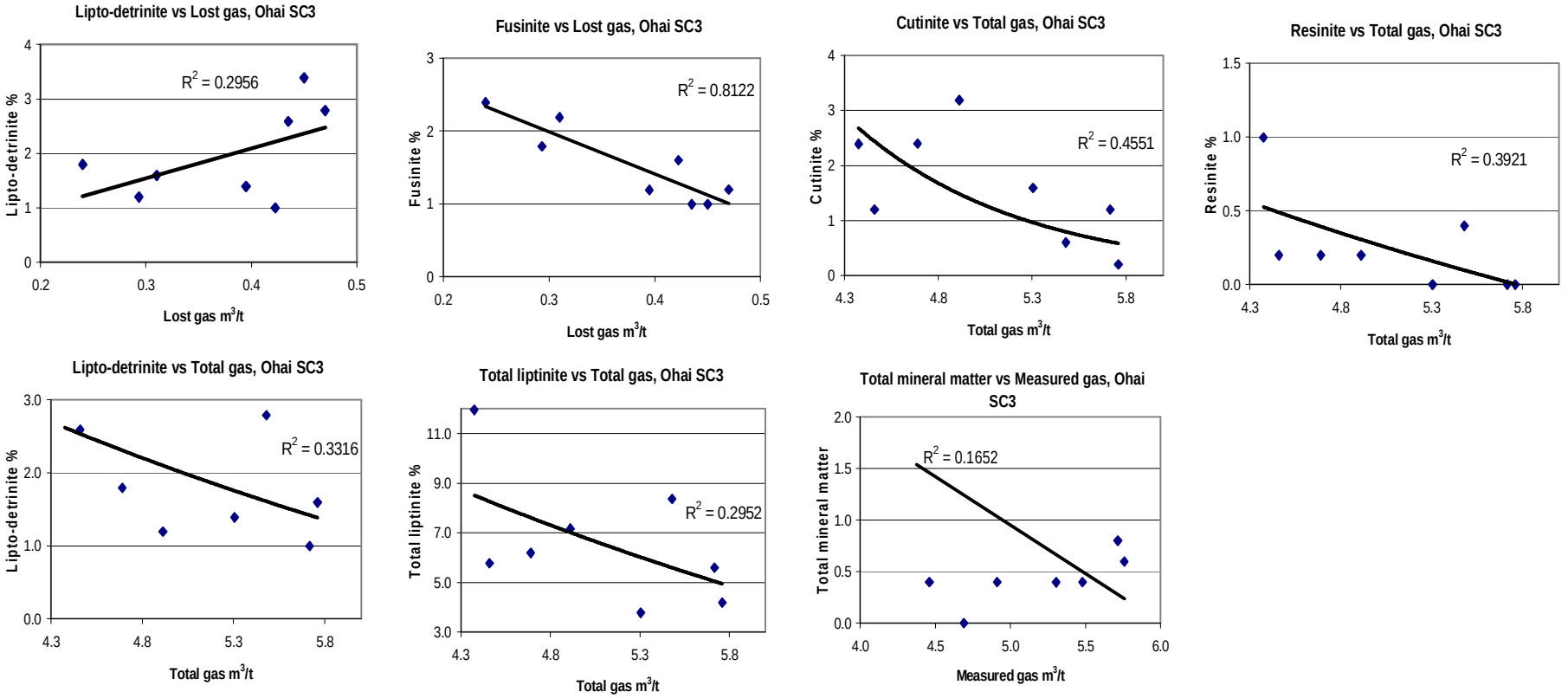

Figure 15: Ohai SC3 significant correlations with gas and maceral data, based on correlation charts., continued.

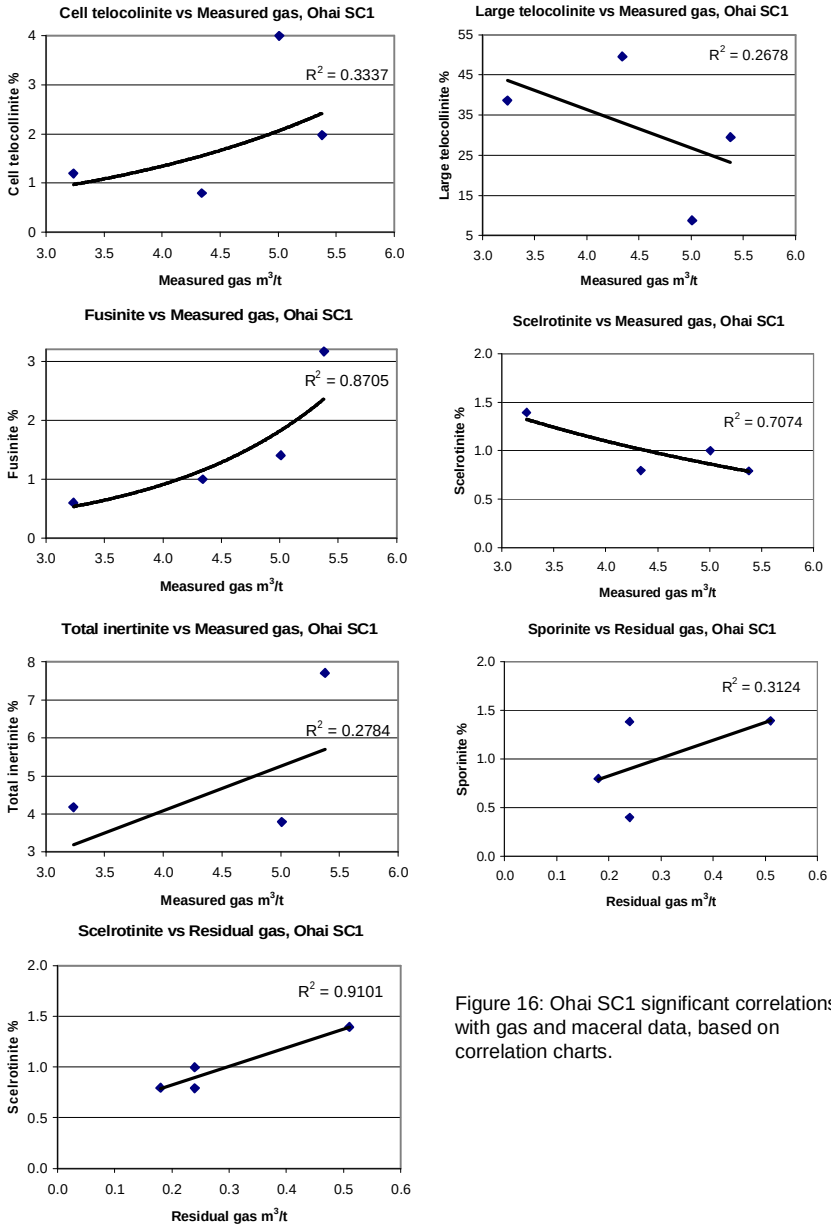

Figure 16: Ohai SC1 significant correlations with gas and maceral data, based on correlation charts.

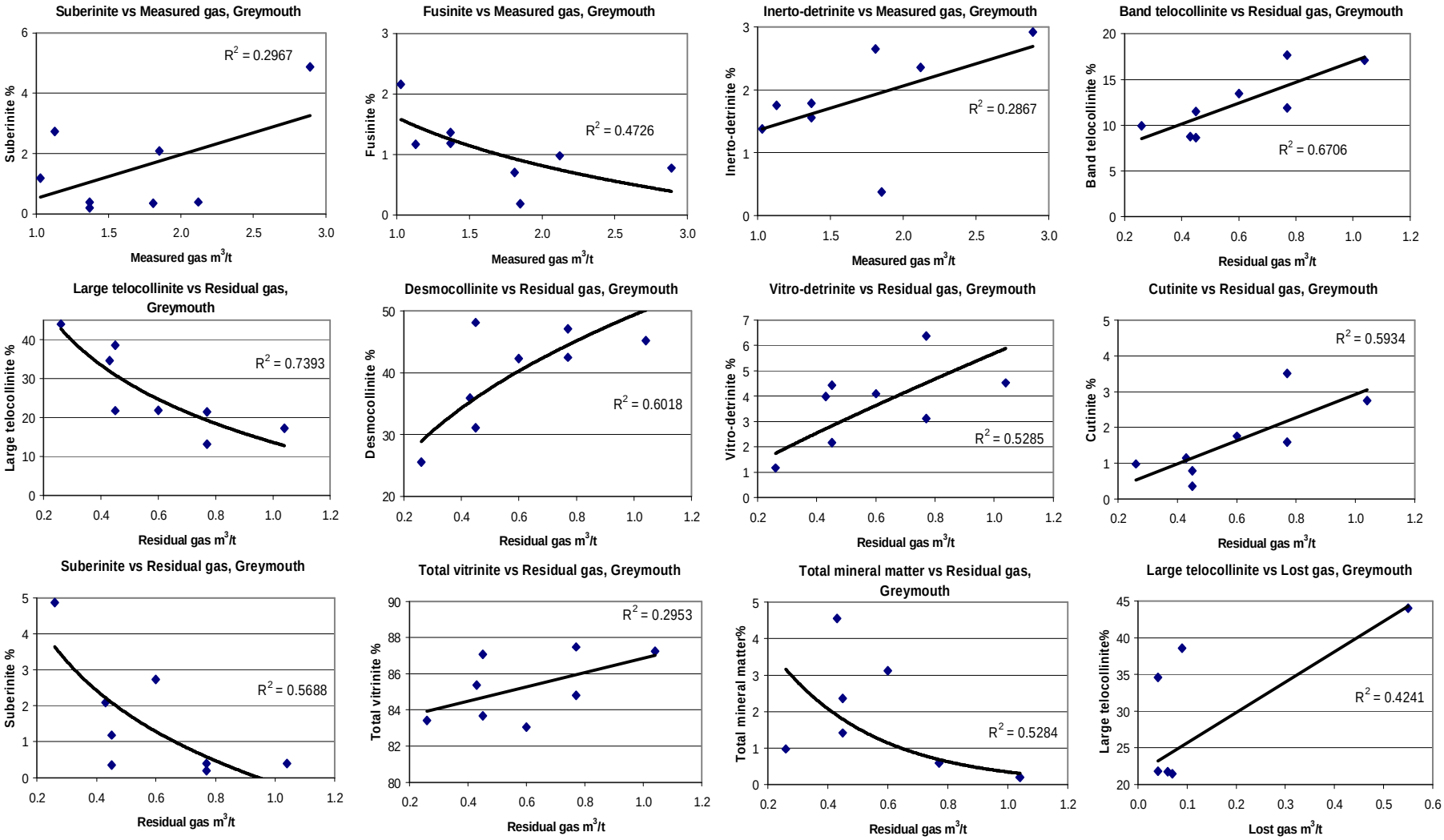

Figure 17:Greymouth 944 significant correlations with gas and maceral data, based on correlation chart.

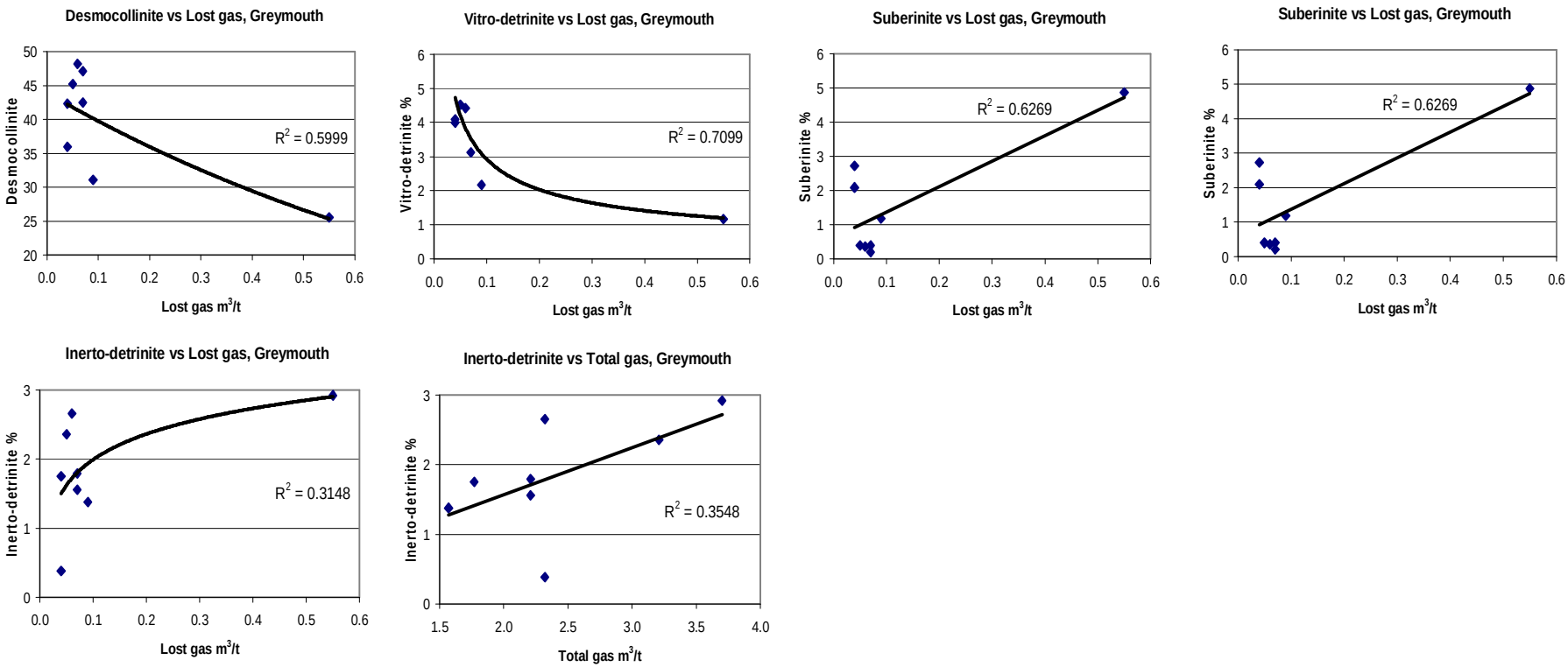

Figure 18:Greymouth 944 significant correlations with gas and maceral data, based on correlation chart, continued.

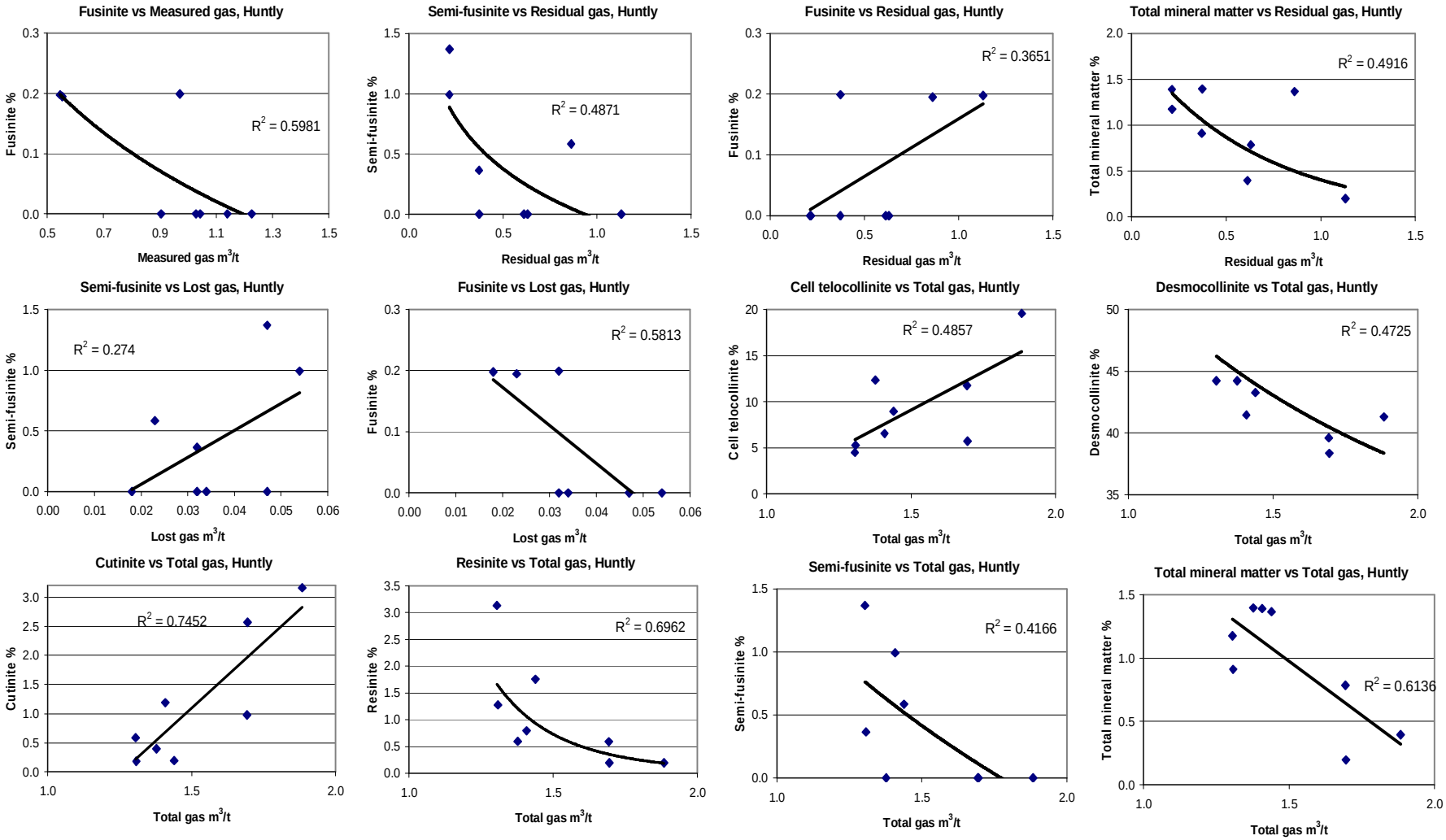

Figure 19: Huntly significant correlations with gas and maceral data, based on correlation charts.